



years of publishing!

Green Chemistry...



- The most highly cited *Green Chemistry* journal, Impact factor = 4.192*
- Fast publication, typically <90 days for full papers
- Full variety of research including reviews, communications, full papers and perspectives.

Celebrating 10 years of publishing, *Green Chemistry* offers the latest research that reduces the environmental impact of the chemical enterprise by developing alternative sustainable technologies, and provides a unique forum for the rapid publication of cutting-edge and innovative research for a greener, sustainable future

...for a sustainable future!

* 2006 Thomson Scientific (ISI) Journal Citation Reports®

Green Chemistry

Cutting-edge research for a greener sustainable future

www.rsc.org/greenchem

RSC Publishing is a not-for-profit publisher and a division of the Royal Society of Chemistry. Any surplus made is used to support charitable activities aimed at advancing the chemical sciences. Full details are available from www.rsc.org

IN THIS ISSUE

ISSN 1463-9262 CODEN GRCHFJ 10(4) 349–472 (2008)



Cover

See Tao *et al.*, pp. 361–372. A ribbon image of *Pseudomonas cepacia* lipase represents the use of biocatalysts in developing green industrial chemical syntheses of pharmaceuticals, fine chemicals and polymers. Image reproduced from the protein data bank ID 3lip (J. D. Schrag *et al.*, The open conformation of a *Pseudomonas* lipase, *Structure*, 1997, **5**, 187–202) using VMD software (W. Humphrey *et al.*, VMD - Visual Molecular Dynamics, *J. Mol. Graphics*, 1996, **14**, 33–38). Design by Junhua Tao from *Green Chem.*, 2008, **10**, 361.

CHEMICAL TECHNOLOGY

T25

Drawing together research highlights and news from all RSC publications, *Chemical Technology* provides a 'snapshot' of the latest applications and technological aspects of research across the chemical sciences, showcasing newsworthy articles and significant scientific advances.

Chemical Technology

April 2008/Volume 5/Issue 4

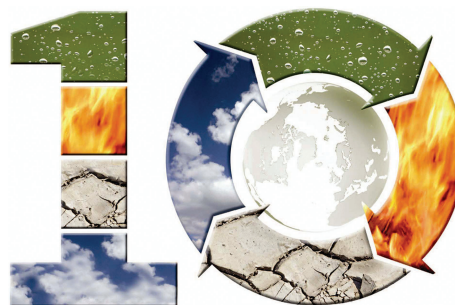
www.rsc.org/chemicaltechnology

EDITORIAL

359

Green and sustainable chemistry: challenges and perspectives

Roger Sheldon, former Chair of the *Green Chemistry* Editorial Board, comments on green chemistry over the last 10 years, and introduces the papers published in this issue that were presented at the 3rd International Conference on Green and Sustainable Chemistry.



EDITORIAL STAFF

Editor

Sarah Ruthven

Assistant editor

Sarah Dixon

Publishing assistant

Ruth Bircham

Team leader, serials production

Stephen Wilkes

Technical editor

Edward Morgan

Production administration coordinator

Sonya Spring

Administration assistantsClare Davies, Donna Fordham, Kirsty Lunnon,
Julie Thompson**Publisher**

Emma Wilson

Green Chemistry (print: ISSN 1463-9262; electronic: ISSN 1463-9270) is published 12 times a year by the Royal Society of Chemistry, Thomas Graham House, Science Park, Milton Road, Cambridge, UK CB4 0WF.

All orders, with cheques made payable to the Royal Society of Chemistry, should be sent to RSC Distribution Services, c/o Portland Customer Services, Commerce Way, Colchester, Essex, UK CO2 8HP. Tel +44 (0) 1206 226050; E-mail sales@rscdistribution.org

2008 Annual (print + electronic) subscription price: £947; US\$1799. 2008 Annual (electronic) subscription price: £852; US\$1695. Customers in Canada will be subject to a surcharge to cover GST. Customers in the EU subscribing to the electronic version only will be charged VAT.

If you take an institutional subscription to any RSC journal you are entitled to free, site-wide web access to that journal. You can arrange access via Internet Protocol (IP) address at www.rsc.org/ip. Customers should make payments by cheque in sterling payable on a UK clearing bank or in US dollars payable on a US clearing bank. Periodicals postage paid at Rahway, NJ, USA and at additional mailing offices. Airfreight and mailing in the USA by Mercury Airfreight International Ltd, 365 Blair Road, Avenel, NJ 07001, USA.

US Postmaster: send address changes to Green Chemistry, c/o Mercury Airfreight International Ltd., 365 Blair Road, Avenel, NJ 07001. All despatches outside the UK by Consolidated Airfreight.

PRINTED IN THE UK

Advertisement sales: Tel +44 (0) 1223 432246; Fax +44 (0) 1223 426017; E-mail advertising@rsc.org

Green Chemistry

Cutting-edge research for a greener sustainable future

www.rsc.org/greenchem

Green Chemistry focuses on cutting-edge research that attempts to reduce the environmental impact of the chemical enterprise by developing a technology base that is inherently non-toxic to living things and the environment.

EDITORIAL BOARD

Chair

Professor Martyn Poliakoff
Nottingham, UK

Scientific Editor

Professor Walter Leitner
RWTH-Aachen, Germany

Associate Editors

Professor C. J. Li
McGill University, Canada

Members

Professor Paul Anastas
Yale University, USA
Professor Joan Brennecke
University of Notre Dame, USA
Professor Mike Green
Sasol, South Africa
Professor Buxing Han
Chinese Academy of Sciences,
China

Dr Alexei Lapkin
Bath University, UK
Professor Steven Ley
Cambridge, UK
Dr Janet Scott
Unilever, UK
Professor Tom Welton
Imperial College, UK

ADVISORY BOARD

James Clark, York, UK
Avelino Corma, Universidad
Politécnica de Valencia, Spain
Mark Harmer, DuPont Central
R&D, USA
Herbert Hugl, Lanxess Fine
Chemicals, Germany
Roshan Jachuck,
Clarkson University, USA
Makato Misono, nite,
Japan

Colin Raston,
University of Western Australia,
Australia
Robin D. Rogers, Centre for Green
Manufacturing, USA
Kenneth Seddon, Queen's
University, Belfast, UK
Roger Sheldon, Delft University of
Technology, The Netherlands
Gary Sheldrake, Queen's
University, Belfast, UK

Pietro Tundo, Università ca
Foscari di Venezia, Italy

INFORMATION FOR AUTHORS

Full details of how to submit material for publication in Green Chemistry are given in the Instructions for Authors (available from <http://www.rsc.org/authors>). Submissions should be sent via ReSource: <http://www.rsc.org/resource>.

Authors may reproduce/republish portions of their published contribution without seeking permission from the RSC, provided that any such republication is accompanied by an acknowledgement in the form: (Original citation) – Reproduced by permission of the Royal Society of Chemistry.

© The Royal Society of Chemistry 2008. Apart from fair dealing for the purposes of research or private study for non-commercial purposes, or criticism or review, as permitted under the Copyright, Designs and Patents Act 1988 and the Copyright and Related Rights Regulations 2003, this publication may only be reproduced, stored or transmitted, in any form or by any means, with the prior permission in writing of the Publishers or in the case of reprographic reproduction in accordance with the terms of licences issued by the Copyright Licensing Agency in the UK. US copyright law is applicable to users in the USA.

The Royal Society of Chemistry takes reasonable care in the preparation of this publication but does not accept liability for the consequences of any errors or omissions.

The paper used in this publication meets the requirements of ANSI/NISO Z39.48-1992 (Permanence of Paper).

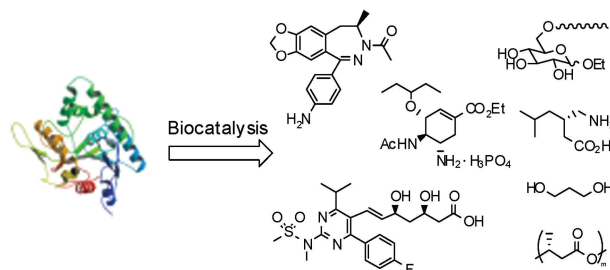
Royal Society of Chemistry: Registered Charity No. 207890

361

Recent applications of biocatalysis in developing green chemistry for chemical synthesis at the industrial scale

Ningqing Ran, Lishan Zhao, Zhenming Chen and Junhua Tao*

Enzymes catalyze molecular transformations with exquisite regio- and stereoselectivity under mild conditions. As a result, they are uniquely suited for the development of green industrial chemical processes.



THEMED ISSUE ARTICLES

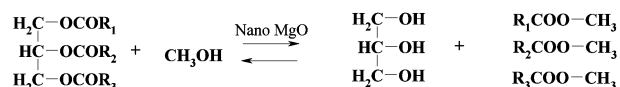
PAPERS

373

Sunflower and rapeseed oil transesterification to biodiesel over different nanocrystalline MgO catalysts

Marian Verziu, Bogdan Cojocaru, Juncheng Hu, Ryan Richards,* Crinu Ciuculescu, Petru Filip and Vasile I. Parvulescu*

The catalytic activity for the production of biodiesel for three morphologically different nanocrystalline MgO materials prepared using simple, green and reproducible methods was investigated.

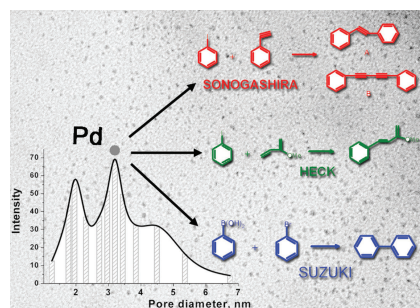


382

Palladium nanoparticles on polysaccharide-derived mesoporous materials and their catalytic performance in C–C coupling reactions

Vitaly L. Budarin, James H. Clark,* Rafael Luque, Duncan J. Macquarrie and Robin J. White

Palladium nanoparticles were successfully prepared using porous materials derived from starch, with a controllable nanoparticle size by selection of the preparation solvent.

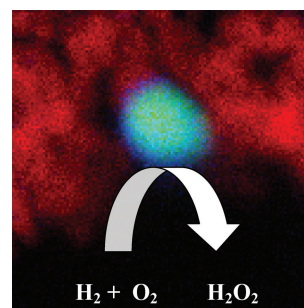


388

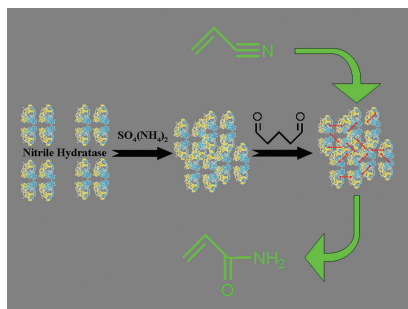
Au–Pd supported nanocrystals as catalysts for the direct synthesis of hydrogen peroxide from H₂ and O₂

Jennifer K. Edwards, Adrian Thomas, Albert F. Carley, Andrew A. Herzing, Christopher J. Kiely and Graham J. Hutchings*

Supported Au–Pd nanoparticles are found effective for the direct synthesis of H₂O₂ and bromide and phosphate additives are shown to be inhibitors, whereas CO₂ as diluent acts as an *in situ* acid promoter.



395

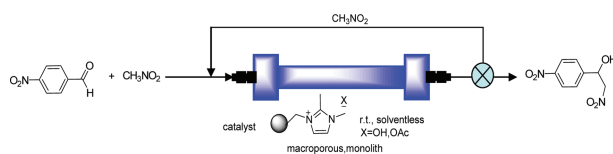


Nitrile hydratase CLEAs: The immobilization and stabilization of an industrially important enzyme

Sander van Pelt, Sandrine Quignard, David Kubáč, Dmitry Y. Sorokin, Fred van Rantwijk and Roger A. Sheldon*

The first successful attempt to immobilize cell-free nitrile hydratase is described. Nitrile hydratase cross-linked enzyme aggregates (CLEAs[®]) are easy to separate and recover from the reaction medium and have a higher operational and storage stability than cell-free and whole cell nitrile hydratase.

401

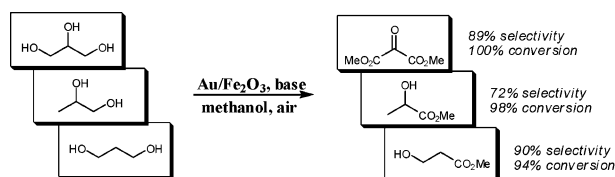


Base supported ionic liquid-like phases as catalysts for the batch and continuous-flow Henry reaction

M. Isabel Burguete, Hanno Erythropel, Eduardo Garcia-Verdugo,* Santiago V. Luis* and Victor Sans

New solid basic catalysts immobilised onto supported ionic liquid-like phases have been prepared, having suitable mechanical stability for their use for the continuous-flow Henry reaction.

408

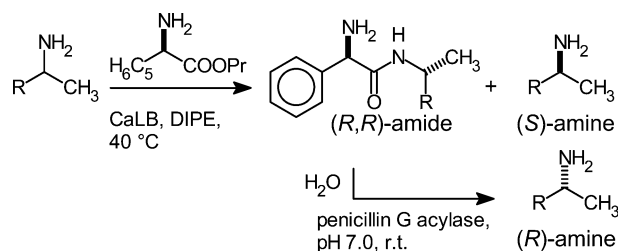


Oxidation of glycerol and propanediols in methanol over heterogeneous gold catalysts

Esben Taarning, Anders Theilgaard Madsen, Jorge Mario Marchetti, Kresten Egeblad and Claus Hviid Christensen*

Gold catalyzed oxidative esterification of glycerol, 1,2-propanediol and 1,3-propanediol has been examined and is found to be a possible route to important large scale chemicals such as methyl lactate and methyl acrylate.

415



A green, fully enzymatic procedure for amine resolution, using a lipase and a penicillin G acylase

Hilda Ismail, Rute Madeira Lau, Luuk M. van Langen, Fred van Rantwijk, Vytas K. Švedas and Roger A. Sheldon*

A green, fully enzymatic kinetic resolution of chiral amines has been demonstrated. The methodology obviates the common, waste-generating deacylation under strongly alkaline conditions.

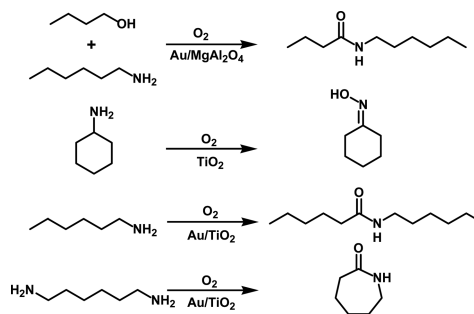
PAPERS

419

Oxidations of amines with molecular oxygen using bifunctional gold–titania catalysts

Søren K. Klitgaard, Kresten Egeblad, Uffe V. Mentzel, Andrey G. Popov, Thomas Jensen, Esben Taarning, Inger S. Nielsen and Claus Hviid Christensen*

New green protocols for the synthesis of amides and green pathways to cyclohexanone oxime and caprolactam are developed using aerobic oxidations with different heterogeneous gold catalysts and pure TiO₂ (anatase).

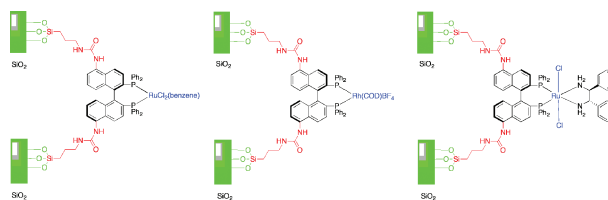


424

BINAP-Ru and -Rh catalysts covalently immobilised on silica and their repeated application in asymmetric hydrogenation

Aidan R. McDonald, Christian Müller, Dieter Vogt, Gerard P.M. van Klink and Gerard van Koten*

BINAP-Ru and -Rh complexes have been functionalised and immobilised on a high density, low porosity silica, and subsequently applied in asymmetric hydrogenation catalysis followed by catalytic material recycling, demonstrating the expected high yields and selectivity levels of BINAP ligand systems.



REGULAR RESEARCH ARTICLES

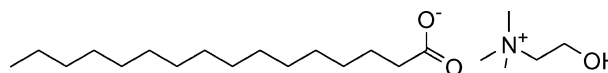
COMMUNICATIONS

433

**Choline carboxylate surfactants: biocompatible and highly soluble in water**

Regina Klein, Didier Touraud and Werner Kunz*

By the replacement of alkali ions in common soaps with choline as a counterion of biological origin, even long chain carboxylate surfactants can be used at ambient temperature, and biocompatibility can be ensured as well.

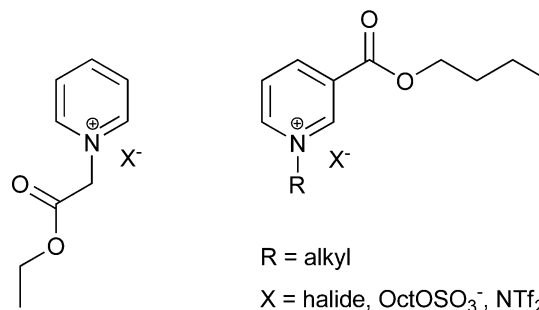


436

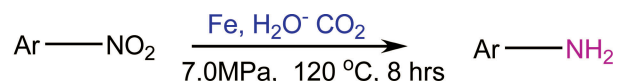
**The design and synthesis of biodegradable pyridinium ionic liquids**

Jitendra R. Harjani, Robert D. Singer, M. Teresa Garcia and Peter J. Scammells*

Ionic liquids with a pyridinium cation bearing an ester side chain moiety were prepared from either pyridine or nicotinic acid and their biodegradability was evaluated using the CO₂ Headspace test (ISO 14593). ILs of this type showed exceptionally high levels of biodegradation under aerobic conditions and can be classified as 'readily biodegradable'.



439



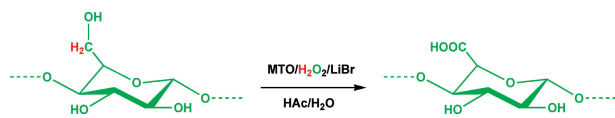
Ar = p-ClC₆H₄-, o-ClC₆H₄-, p-CH₃COC₆H₄- etc.,

Environmentally benign and selective reduction of nitroarenes with Fe in pressurized CO₂-H₂O medium

Ge Gao, Yuan Tao and Jingyang Jiang*

Substituted nitroarenes can be reduced to corresponding anilines with high efficiency and high chemoselectivity using iron in a pressurized CO₂-H₂O system.

442

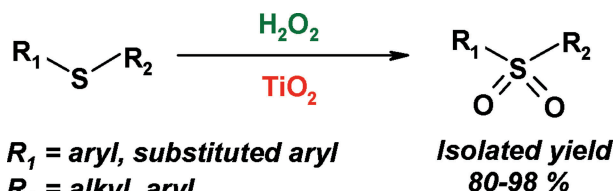


Super absorbers from renewable feedstock by catalytic oxidation

Wolfgang A. Herrmann,* Alexandra M. J. Rost, Evangeline Tosh, Herbert Riepl and Fritz E. Kühn*

An environmentally benign, catalytic oxidation process applying the three-component system MTO/H₂O₂/LiBr to prepare biodegradable oxidized starch super absorbers with high water absorption capacity has been developed.

447

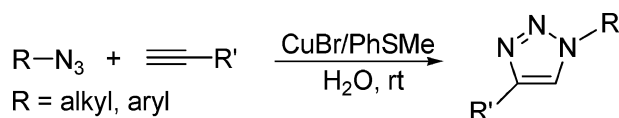


Practical oxidation of sulfides to sulfones by H₂O₂ catalysed by titanium catalyst

Walid Al-Maksoud, Stéphane Daniele* and Alexander B. Sorokin*

An efficient and simple protocol for the selective oxidation of sulfides to sulfones, which can be easily isolated from the reaction mixture in the pure form.

452



Quick and highly efficient copper-catalyzed cycloaddition of aliphatic and aryl azides with terminal alkynes "on water"

Feng Wang, Hua Fu,* Yuyang Jiang and Yufen Zhao

We have developed a quick and highly efficient method for CuBr/PhSMe-catalyzed cycloaddition of water-insoluble aliphatic/aryl azides and alkynes to synthesize various triazoles "on water" at room temperature.

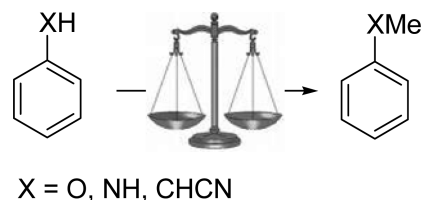
PAPERS

457

Green chemistry metrics: a comparative evaluation of dimethyl carbonate, methyl iodide, dimethyl sulfate and methanol as methylating agents

Maurizio Selva* and Alvise Perosa

Green chemistry metrics (atom economy and mass index) have been applied to compare a total of 33 procedures for the synthesis of anisole, 2-phenylpropionitrile, and N-methylaniline, carried out with four methylating agents such as dimethyl carbonate, dimethyl sulfate, methyl iodide and methanol. The non toxic DMC proved to be the best reagent among those considered.

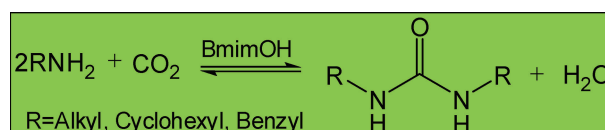


465

Solvent-free synthesis of substituted ureas from CO₂ and amines with a functional ionic liquid as the catalyst

Tao Jiang,* Xiumin Ma, Yinxi Zhou, Shuguang Liang, Jicheng Zhang and Buxing Han*

The synthesis of disubstituted ureas from amines and CO₂ were carried out using a basic ionic liquid (IL) 1-*n*-butyl-3-methyl imidazolium hydroxide ([Bmim]OH) as the catalyst.




AUTHOR INDEX

- | | | | |
|------------------------------------|--------------------------------|-----------------------------|------------------------------|
| Al-Maksoud, Walid, 447 | Herzing, Andrew A., 388 | Marchetti, Jorge Mario, 408 | Taarning, Esben, 408, 419 |
| Budarin, Vitaly L., 382 | Hu, Juncheng, 373 | McDonald, Aidan R., 424 | Tao, Junhua, 361 |
| Burguete, M. Isabel, 401 | Hutchings, Graham J., 388 | Mentzel, Uffe V., 419 | Tao, Yuan, 439 |
| Carley, Albert F., 388 | Ismail, Hilda, 415 | Müller, Christian, 424 | Thomas, Adrian, 388 |
| Chen, Zhenming, 361 | Jensen, Thomas, 419 | Nielsen, Inger S., 419 | Tosh, Evangeline, 442 |
| Christensen, Claus Hviid, 408, 419 | Jiang, Jingyang, 439 | Parvulescu, Vasile I., 373 | Touraud, Didier, 433 |
| Ciuculescu, Crinu, 373 | Jiang, Tao, 465 | Perosa, Alvise, 457 | van Klink, Gerard P.M., 424 |
| Clark, James H., 382 | Jiang, Yuyang, 452 | Popov, Andrey G., 419 | van Koten, Gerard, 424 |
| Cojocar, Bogdan, 373 | Kiely, Christopher J., 388 | Quignard, Sandrine, 395 | van Langen, Luuk M., 415 |
| Daniele, Stéphane, 447 | Klein, Regina, 433 | Ran, Ningqing, 361 | van Pelt, Sander, 395 |
| Edwards, Jennifer K., 388 | Klitgaard, Søren K., 419 | Richards, Ryan, 373 | van Rantwijk, Fred, 395, 415 |
| Egeblad, Kresten, 408, 419 | Kubáč, David, 395 | Riepl, Herbert, 442 | Verziu, Marian, 373 |
| Erythropel, Hanno, 401 | Kühn, Fritz E., 442 | Rost, Alexandra M. J., 442 | Vogt, Dieter, 424 |
| Filip, Petru, 373 | Kunz, Werner, 433 | Sans, Victor, 401 | Wang, Feng, 452 |
| Fu, Hua, 452 | Lau, Rute Madeira, 415 | Scammells, Peter J., 436 | White, Robin J., 382 |
| Gao, Ge, 439 | Liang, Shuguang, 465 | Selva, Maurizio, 457 | Zhang, Jicheng, 465 |
| Garcia, M. Teresa, 436 | Luis, Santiago V., 401 | Sheldon, Roger A., 395, 415 | Zhao, Lishan, 361 |
| Garcia-Verdugo, Eduardo, 401 | Luque, Rafael, 382 | Singer, Robert D., 436 | Zhao, Yufen, 452 |
| Han, Buxing, 465 | Ma, Xiumin, 465 | Sorokin, Alexander B., 447 | Zhou, Yinxi, 465 |
| Harjani, Jitendra R., 436 | Macquarrie, Duncan J., 382 | Sorokin, Dmitry Y., 395 | |
| Herrmann, Wolfgang A., 442 | Madsen, Anders Theilgaard, 408 | Švedas, Vytas K., 415 | |

FREE E-MAIL ALERTS AND RSS FEEDS


Contents lists in advance of publication are available on the web *via* www.rsc.org/greenchem – or take advantage of our free e-mail alerting service (www.rsc.org/ej.alert) to receive notification each time a new list becomes available.

 Try our RSS feeds for up-to-the-minute news of the latest research. By setting up RSS feeds, preferably using feed reader software, you can be alerted to the latest Advance Articles published on the RSC web site. Visit www.rsc.org/publishing/technology/rss.asp for details.

ADVANCE ARTICLES AND ELECTRONIC JOURNAL

Free site-wide access to Advance Articles and the electronic form of this journal is provided with a full-rate institutional subscription. See www.rsc.org/ejs for more information.

* Indicates the author for correspondence: see article for details.

 Electronic supplementary information (ESI) is available *via* the online article (see <http://www.rsc.org/esi>) for general information about ESI.

Call for Papers

Energy & Environmental Science

'Energy is the most important scientific and technological challenge facing humanity in the twenty-first century. Energy security and environmental security have come to the forefront of both global and national priorities. This journal aims to bridge the various disciplines involved with energy and the environment, providing a forum for disclosing research results and discourse on this critical field.' Professor Nathan Lewis



Launching Summer 2008

Energy & Environmental Science will publish high quality research from aspects of the chemical sciences relating to energy conversion and storage, alternative fuel technologies and environmental science. It will contain a full mix of primary articles, communications and reviews.

The current issue in 2008/9 will be free online. Institutional access to all 2008/9 content will be available following registration at www.rsc.org/ees_registration

Contact the Editor, Philip Earis, at ees@rsc.org or visit the website for more details.



International Editorial Board members include:

Professor Nathan Lewis, Caltech, USA (*Editorial Board Chair*)

Professor Michael R Wasielewski, Northwestern, IL, USA

Professor Arthur Nozik, National Renewable Energy Laboratory, USA

Professor Jefferson W Tester, MIT, MA, USA

Professor Steven E Koonin, BP, London, UK

Submit your work today!

RSC Publishing

www.rsc.org/ees

Registered Charity Number 207890

Chemical Technology

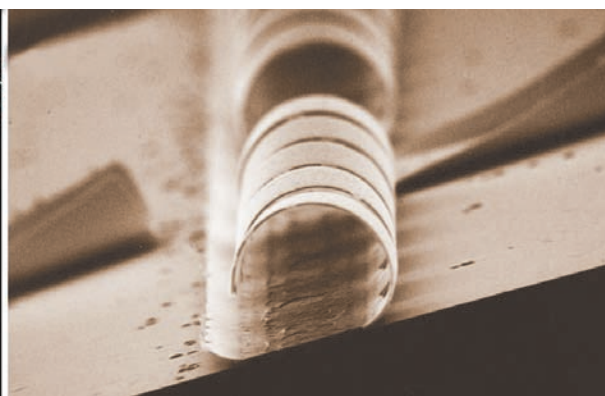
Layered polyimide and chromium curl and uncurl by applying a voltage

Miniature mixing inspired by nature

Dutch scientists have copied nature to develop a faster and more efficient method for mixing small volumes of liquid. They were inspired by micro-organisms that use tiny oscillating hairs (called cilia) to move through liquid, and made artificial cilia to use in microfluidics.

Microfluidics is the study of fluid flow in structures with dimensions smaller than a millimetre, with devices as small as a credit card. Key applications for these devices include biochips, especially the immediate point-of-care diagnosis of diseases. The problem with such a small device is that good mixing is almost impossible. Usually, mixing is done by etching grooves into the fluid channels or applying an electrical pulse or sound wave. However, there is no real control over the mixing in these cases, according to Jaap den Toonder of the Philips Research Laboratory in Eindhoven.

Toonder and colleagues have therefore made artificial cilia from a double layer of thin polymer, called polyimide, and a thin conductive



layer of chromium. The artificial cilia looks a lot like a curled-up leaf.

These tiny mixers are activated by applying a voltage. When applied, the rolled-up cilia uncurl. When the voltage is turned off, the cilia roll back up by elastic recovery. In this way, the mixing can be turned on or off by demand and in any location in the device, an advantage over other mixing methods.

Andreas Manz, head of the Institute for Analytical Sciences in Dortmund, Germany, commented

Artificial cilia (right) mimic real cilia such as those on a Paramecium micro-organism (left)

that the use of the artificial cilia for mixing was intriguing, as 'in biological systems cilia are used for transport'.

When questioned about the future, den Toonder said the next steps were to find alternative ways to activate the artificial cilia, such as magnetically-driven systems. The team's final goal is to develop artificial cilia 'into a versatile method for medical diagnostic lab-on-a-chip devices'.

Rebecca Brodie

Reference
J den Toonder *et al*, *Lab Chip*, 2008, DOI: 10.1039/b717681c

In this issue

Detecting a microbe among millions

Piezoelectric cantilever picks out anthrax in real time

Metals without the meltdown

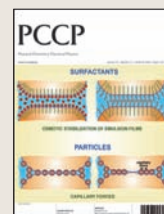
An environmentally friendly alternative to pyrometallurgical processes

Instant insight: Organic field-effect transistors

Marta Mas-Torrent and Concepció Rovira look at how small molecules could be used as processable semiconductors

Interview: Flying high with nanomedicine

Jinwoo Cheon explains how nanoparticles can be used in medical diagnostics



The latest applications and technological aspects of research across the chemical sciences

Application highlights

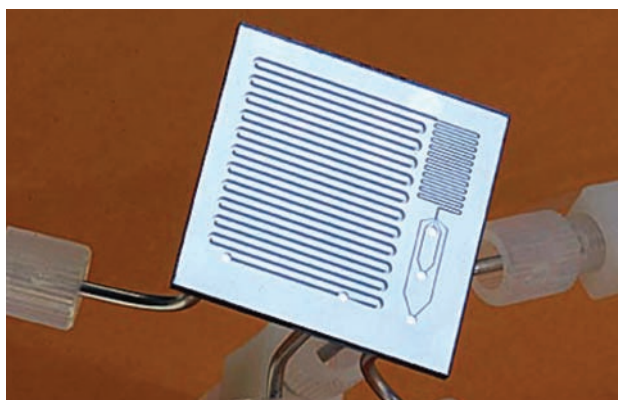
Amides in minutes using continuous flow microreactor

Big impact for small reactors

Microreactors can be a powerful tool for product synthesis in the pharmaceutical industry, say Swiss and Swedish scientists. Their application of microreactor technology to an amide bond formation reaction illustrates this.

Peter Seeberger from the Swiss Federal Institute of Technology, Zurich, and colleagues showed that their method can cope with a range of substrates, and applied it to the synthesis of two pharmaceutically active compounds. They claim that the microreactor-based technique is faster and safer than traditional methods, and that scale-up to bulk synthesis level is not a problem.

‘One can think of a microreactor as a small pipe,’ explained Seeberger. ‘Chemicals are pumped through the pipe and additional inlets can be used to add reagents.’ Microreactors allow fast mixing, quick and even heating, and the generation of high pressures. Together this



makes for short reaction times; Seeberger’s amide bond formation was completed within two minutes, compared to four to sixteen hours using conventional methods. In addition, microreactor systems are safer because the small reaction volumes mean that any hazardous intermediates are formed only in small amounts.

Safe, efficient and versatile: microreactors could become the method of choice for industry

Reference
T Gustafsson *et al*, *Chem. Commun.*, 2008, 1100 (DOI: 10.1039/b719603b)

Steve Haswell, an expert in microreactor chemistry from the University of Hull, UK, said that microreactor technology has great potential for industry. Possible applications are reaction optimisation, library building, and safe and efficient product production, he said. The type of work performed by Seeberger ‘should make medicinal chemists sit up and look seriously at the contribution microreactor technology has to offer,’ said Haswell.

To illustrate the technique’s versatility, Seeberger’s group is working on applying microreactors for fluorinations and in radical and photochemistry. The group also has close collaborations with industry to look at real-life problems that microreactors could be used to solve. ‘Industry is getting into this technology big-time,’ said Seeberger.
Danièle Gibney

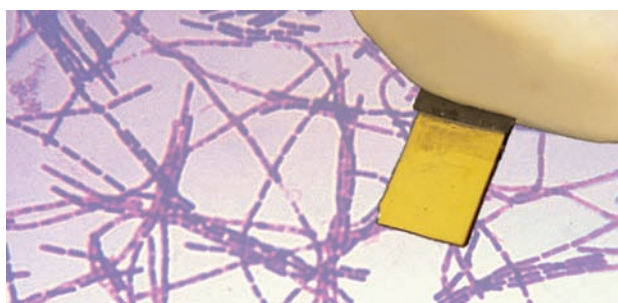
Piezoelectric cantilever picks out anthrax in real time

Detecting a microbe among millions

A sensor that can discriminate between closely related bacteria has been developed by materials scientists in the US.

Wan Shih and colleagues at Drexel University in Philadelphia immobilised a rabbit antibody to *Bacillus anthracis* (anthrax) on a piezoelectromicrocantilever sensor (PEMS). They then exposed the sensor to suspensions of anthrax spores and some of its close relatives. Because the chemical structures in the spore coats of these bacteria are similar, they all bind to the anthrax antibody to some extent. However, the binding interactions of the ‘close relatives’ are weaker than that of anthrax itself.

PEMS uses antibodies, which have high affinity and specificity for different microbes, attached to tiny cantilevers. ‘These can be thought of as tiny diving boards made from piezoelectric material that can detect small particles, like



deadly *Bacillus anthracis* spores, by vibrating,’ explained Wei-Heng Shih, a member of the US team. The cantilevers’ combination of specific antibody and sensitivity enables the sensor to accurately detect any micro-organism (depending on the antibody used) in real time, with no added chemicals, radioactive tags or external manipulation. ‘The sensor can detect its preferred microbe in the presence of a million of its closely related cousins. It can detect a needle in a haystack!’ said Wei-

The PEMS cantilever vibrates when anthrax spores bind to an attached antibody

Reference
J-P McGovern *et al*, *Analyst*, 2008, DOI:10.1039/b715948j

Heng Shih.

To test if the PEMS could preferentially detect anthrax spores, the team flowed suspensions of the different bacteria across the sensor. The team observed that, at first, increasing the flow speed of the bacterial suspensions across the sensor led to increased binding of all four species because the sensor surface was exposed to more spores. But at higher flow rates, preferential anthrax-antibody binding was increased and binding to close relatives was suppressed.

‘This result means that flow can be used to enhance the specificity of antibody-based detection,’ said Wan Shih. ‘With the right antibodies or receptors our sensor can detect air or food-borne pathogens and blood or urinary biomarkers for human diseases like cancer or AIDS...and it will make detection possible in minutes instead of days,’ she added.
Janet Crombie

X-ray fluorescence reveals metals diffusing from paint into glass

Watching paint die

A new analytical technique from German scientists may help restore decaying glass paintings.

Birgit Kanngiesser led researchers from Berlin's Federal Institute for Materials Research and Testing, and the Technical University of Berlin, in studying reverse glass paintings – made by painting onto the back of a glass sheet. Unlike stained glass, these paintings are not fired and the contact between glass and paint is fragile.

The team used a technique called 3D micro x-ray fluorescence (3D micro XRF) to identify the elements in the corroded areas of the glass of a 19th century painting and compare them to healthy areas, without further damaging the artwork.

As with any XRF technique, micro XRF involves firing an x-ray beam at the sample to eject electrons. Higher-



orbital electrons fall down to fill the gaps left by removed electrons, and in doing so emit photons of radiation characteristic to a particular element. In micro XRF, though, the beam can be focused onto a very small area. By using a powerful x-ray source and applying their recently-discovered calibration improvements to the

Reverse glass paintings: beautiful but fragile

Reference
B Kanngiesser *et al.*, *J. Anal. At. Spectrom.*, 2008, DOI: 10.1039/b717286a

technique, the researchers were able to study the composition of layers buried under the surface.

Kanngiesser's team identified the paints used and found that lead and mercury had diffused into the glass. The information should help conservators find the best way to protect and restore reverse glass artworks.

Kanngiesser hopes the non-destructive technique will extend to other fields, such as environmental science or archaeometry. 'Unlike other elemental imaging methods, there is no principal size restriction of the objects investigated,' she explains. 'And for life sciences the possibility of obtaining elemental distribution in virtual cross sections without having to cut the sample might open up new ways of in vivo measurements.' *Clare Boothby*

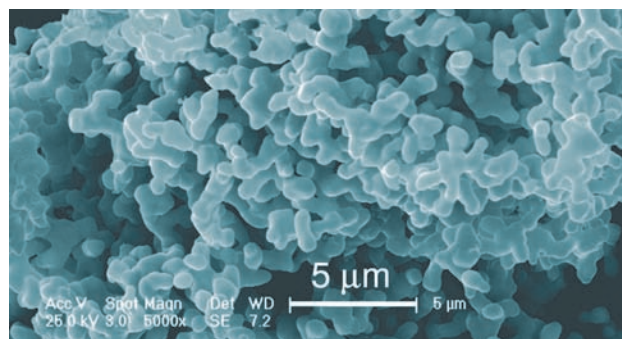
An environmentally friendly alternative to pyrometallurgical processes

Metals without the meltdown

Scientists have found a practical, cheap and environmentally friendly way of producing the industrially important metal niobium.

Niobium is used in a variety of applications, from superalloys to optics. Total world production is nearly 23 000 tonnes per year. But like many industrially important metals, it is extracted from metal ores and minerals using high temperatures – a relatively costly process. 'Alternative processes are essential to provide environmentally acceptable and energy efficient routes to metal extraction,' explains Frank Walsh, an expert on industrial electrochemistry from the University of Southampton, UK. 'In particular, minimising the number of steps in a production route and achieving direct transformation of minerals to metals is a critical subject area.'

George Zheng Chen from the University of Nottingham, UK, and colleagues at Wuhan University, China, have now cut the energy



consumption of niobium extraction by a third, by improving on the already green FFC Cambridge process, named for its inventors Fray, Farthing and Chen, and originating in the late 1990s. In the FFC process, which is carbon-emission free, metals and alloys are extracted directly from their solid oxides using electrolysis in molten calcium chloride.

Chen and co-workers found that electrolysis of niobium oxide in a three-electrode cell using a variable voltage uses significantly less energy

Niobium oxide pellets after electrolysis in calcium chloride

Reference
T Wu *et al.*, *Phys. Chem. Chem. Phys.*, 2008, **10**, 1809 (DOI: 10.1039/b719369f)

than the FFC's constant voltage two-electrode system. However, the set-up is more complicated and so impractical in large scale operations. To get around this problem the scientists mimicked variable voltage with computer-aided control (CAC) of the two-electrode cell. Modifying the FFC process in this way results in a 'more than 37 per cent saving in energy consumption,' the team says. Chen says the energy-saving modification shouldn't require any changes to the FFC cells.

'CAC is demonstrated in principle for niobium extraction, but it is perfectly suitable for other reactive metals such as tantalum, titanium, zirconium and many rare earths,' says Chen. Also, adds Walsh, 'the system described provides an attractive and direct route to the formation of speciality alloys.'

The FFC Cambridge Process is being commercialised by a spin-out company – Metalysis, which has formed strategic partnerships with industry, including BHP Billiton and Rolls-Royce. *Freya Mearns*

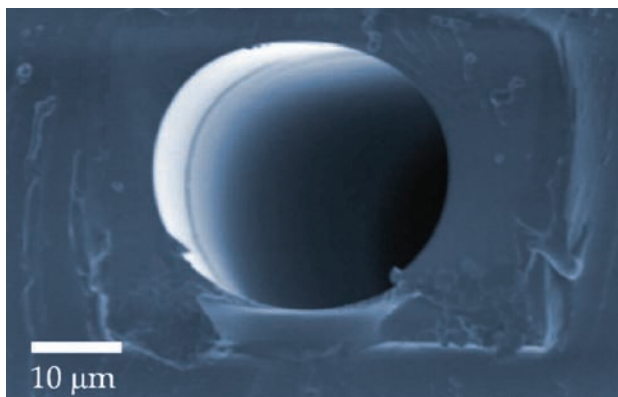
Coating improves chemical resistance of channels in microfluidic devices

Glass-coated microchannels

Scientists in the US have developed a simple method of coating the channels of microfluidic devices to make them more resistant to chemicals. David Weitz and colleagues from Harvard University, Cambridge, used a sol-gel method to create a glass coating on polydimethylsiloxane (PDMS) microchannels.

PDMS, a type of silicone rubber, is easy to make into microfluidic devices using soft lithography, where the material is 'stamped' with a channel pattern. This makes it ideal for large-scale use. However, PDMS is permeable to liquids and gases, which can affect reactions occurring in the channels. Additionally, organic solvents make the PDMS channels swell, degrading device performance. Glass is far more chemically robust but is much more difficult to make into microfluidic devices.

The glass coating developed by Weitz's group is easily deposited on PDMS channels and acts as a barrier,



providing resistance to chemicals and solvents. Weitz said that this coating method would make device production easier as it 'combines the chemical robustness of glass with the ease of fabrication of PDMS.'

To form the coating, Weitz's group used a sol-gel mixture that begins as a fluid and hardens into a glass. They filled the channels with the mixture, initiated a gelation reaction and

The best of both worlds: glass-coatings for PDMS channels mean robustness and easy device fabrication

Reference
A R Abate *et al*, *Lab Chip*, 2008, DOI: 10.1039/b800001h

then used air to flush out most of the material, leaving the glass coating.

The scientists discovered that the coated channels were resistant to the fluorescent chemical Rhodamine B. After an hour of exposure to the organic solvent toluene the channels changed very little. By contrast, uncoated channels swelled upon exposure to toluene.

Stephen Haswell, who develops microfluidic devices at the University of Hull, UK, said that although there would be issues with performing reactions at high temperatures, the work represented a step towards merging the advantages of PDMS and glass. 'Lack of chemical resistance is a big problem, and it will be something of a breakthrough to extend the fabrication benefits of PDMS to give more glass-type robustness,' he said.

Weitz's group is working on refining the technique so that the thickness of the coating can be more finely controlled.
Fay Riordan

Tuneable system picks out particles of the required size

To sort, simply stretch

Researchers in Sweden have come up with a straightforward method for sorting particles in microfluidics – simply stretching the microchannel.

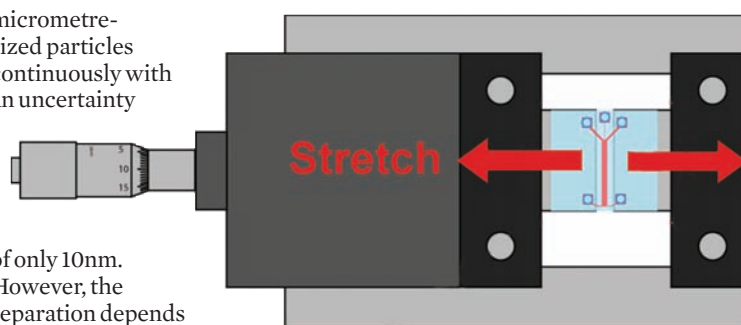
Sorting particles by size, anything from cells to plastic beads, is very useful in both analytical and preparative chemistry, but it is not always easy to achieve. In particular, a tuneable system, so that particles of different sizes can be sorted by the same device, is a major challenge. Jason Beech and Jonas Tegenfeldt of Lund University have struck upon a solution that makes use of the fact that the material used to make many microfluidic devices is very elastic.

Several methods have been proposed to sort particles in microfluidic devices, and one of the most promising is 'deterministic lateral displacement'. Originally reported by Huang and co-workers,¹ the technique is able to separate

micrometre-sized particles continuously with an uncertainty

of only 10nm. However, the separation depends on distances between obstacles in a narrow channel and so the channel has to be designed to separate only the particle of desired size. Beech and Tegenfeldt realised that simply stretching the microchip changes the separation parameters. This gives a tuneable sorting device.

'The concept of macroscopic stretching to change the dimensions of fluidics devices on the nanometre to micrometre scale is something



Stretching a microchip changes its separation parameters giving a tuneable sorting system

References
J P Beech and J O Tegenfeldt, *Lab Chip*, 2008, DOI: 10.039/b719449h
1 L R Huang *et al*, *Science*, 2004, **304**, 987

that has not been exploited fully in the microfluidics community and could, with a little imagination, lead to promising applications,' explained Beech 'Having had the idea that stretching the devices would tune them, we began to realise the wealth of

interesting applications that this could lead to.'

Beech hopes the idea will spread. 'It will be interesting to see if others put the concept of stretching fluidics devices to use,' he said, 'but the challenges are those of engineering and materials science, namely making more stretchable, more robust and more homogenous devices.' *Edward Morgan*

Instant insight

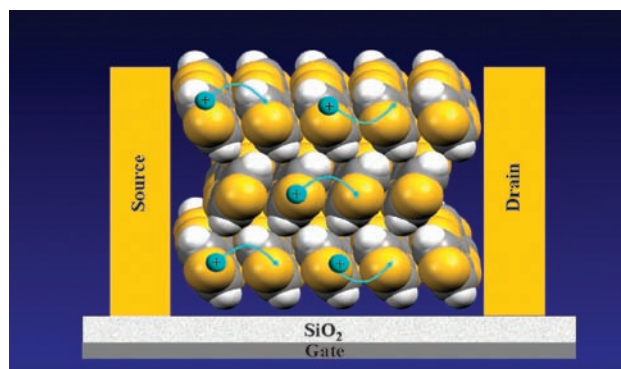
Organic field-effect transistors

Marta Mas-Torrent and Concepció Rovira of the Institute of Science of Materials (CSIC) in Barcelona, Spain, look at how small molecules can be used as processable semiconductors

Our daily life involves the continuous use of field-effect transistors: they are the main logic units, functioning as either switches or amplifiers, controlling current flow in electronic circuits. A field-effect transistor is a three-terminal device in which current flows through a semiconductor from the 'source' terminal to the 'drain'. This flow is controlled at the third 'gate' terminal by a voltage that creates an electric field through the insulator (dielectric) on which the semiconductor is deposited. Since the invention of the first transistor in 1947 by John Bardeen, William Shockley and Walter Brattain, the vast majority of electronic devices have been based on inorganic semiconductors and, in particular, on silicon.

Over the past few years, however, organic field-effect transistors (OFETs) have attracted a great deal of interest due to their unique processing characteristics. Organic materials offer the benefit that they can be printed over large areas on plastic, flexible substrates at low temperature by solution-based techniques, which would result in a dramatic reduction of manufacturing costs. Though the first OFETs did not transport charge as well as inorganic materials, the best ones nowadays are achieving charge carrier mobilities of the same order as amorphous silicon. Organic-based electronics will not replace high density and high speed silicon circuits, but might play an important role in applications such as identification tags, electronic bar codes or active matrix elements for displays.

OFETs have been mainly based on two types of semiconductors that feature π - π interactions: conjugated polymers and small conjugated



molecules. Polymers are deposited from solution, allowing for low cost electronics. However, the higher molecular disorder in polymers limits their charge transport, typically resulting in lower mobilities compared to devices based on small molecules. On the other hand, devices prepared with small conjugated molecules have to be prepared more expensively by evaporating organic materials, due to their low solubility in common organic solvents. Therefore, to promote the development and use of organic semiconductors, there is a clear need to find materials that can be processed in solution and that simultaneously achieve a high OFET mobility.

One way of imparting solubility to organic semiconductors is to prepare a precursor compound that can be converted into the parent semiconductor by heat or irradiation. An alternative strategy is to structurally modify organic semiconductors to impart solubility and, if possible, also achieve higher stability and increase π - π interactions. Semiconductors such as acenes and oligothiophenes (classified as p-type, since the charge carriers are mainly holes) have been processed by techniques such as spin coating and drop or zone

casting, and very high performances have been achieved.

Currently, there is a growing interest in developing n-type semiconductors (where charge carriers are electrons) and ambipolar devices (which conduct both electrons and holes) in order to fabricate complementary circuits. The development in these devices is still far from the performance achieved with p-type materials, because transport in n-channel conductors is easily degraded by air and finding suitable metals for contacts is difficult.

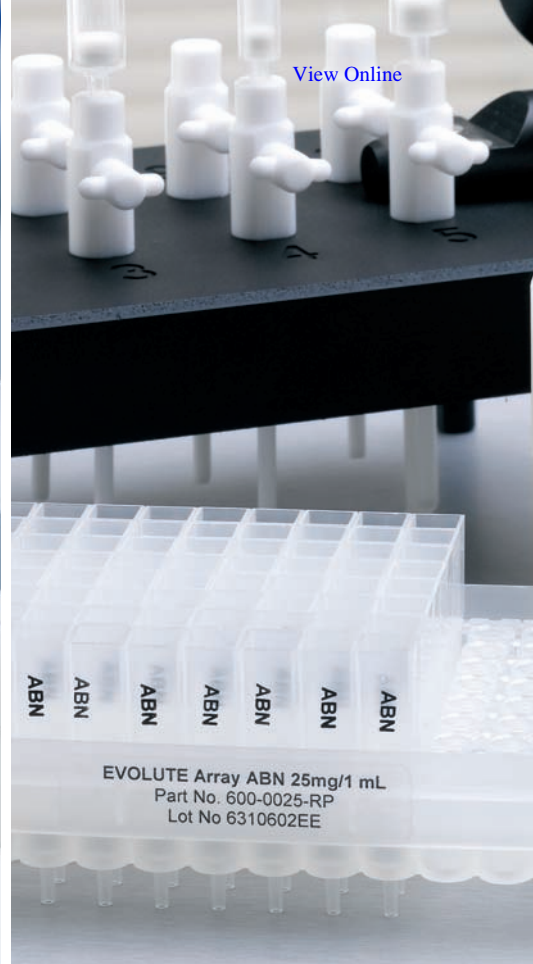
Circuits based on organic transistors are being extensively investigated for a range of applications. One of the first emerging devices realised with OFETs is flexible electronic paper (see *Chemistry World*, April 2007, p15), where organic transistors switch pixels formed by charged pigments. OFETs also offer great promise for applications in chemical and biological sensing: organic semiconductors can interact with different analytes and it is possible to transduce the chemical information to electronic information, creating an 'electronic nose'. And the electrical switching of an OFET has been combined with an organic semiconductor's ability to generate light, to create organic light-emitting transistors (OLETs).

OFETs promise to be important in applications ranging from sophisticated medical diagnostics to 'smart' clothes that can display changing images. New markets will undoubtedly appear in areas where electronics meets with information technology, biomedicine or optics.

Read *Concepció Rovira and Marta Mas-Torrent's critical review in issue 4, 2008, of Chemical Society Reviews.*

Reference

M Mas-Torrent and C Rovira, *Chem. Soc. Rev.*, 2008, **37**, 827 (DOI: 10.1039/b614393h)



IST Sample Preparation • Bioanalysis • Clinical • Environmental • Forensic • Agrochemical • Food • Doping Control

EVOLUTE® CX **NEW!**

Mixed-mode selectivity, generic methodology and efficient extraction

EVOLUTE® CX mixed-mode resin-based SPE sorbent extracts a wide range of **basic drugs** from biological fluid samples. EVOLUTE CX removes matrix components such as proteins, salts, non-ionizable interferences and phospholipids, delivering cleaner extracts with reproducible recoveries for accurate quantitation.

EVOLUTE® ABN

Minimize matrix effects, reduce ion suppression and concentrate analytes of interest

EVOLUTE®ABN (Acid, Base, Neutral) is a water-wettable polymeric sorbent optimized for fast generic reversed phase SPE. Available in 30 μm columns and 96-well plates for bioanalysis and **NEW 50 μm columns** – ideally suited for environmental, food/agrochemical and industrial analysis as well as forensic and doping control applications.

Come by **Booth #1611 at ACS** or contact your local Biotage representative to request a **FREE** sample.

Interview

Flying high with nanomedicine

Jinwoo Cheon tells Stephen Davey how nanoparticles can be used in medical diagnostics



Jinwoo Cheon

Jinwoo Cheon is professor of chemistry at Yonsei University, Korea, and head of the nanomaterials division of the Nano-Medical National Core Research Center of Korea. His research areas include the fabrication and shape control of inorganic nanocrystals, nanoscale biomagnetics, and the applications of nanocrystals for biomedical sciences. Jinwoo is on the editorial board of *Journal of Materials Chemistry*.

What inspired you to become a scientist?

I have always loved the arts, and art is what I saw in my first chemistry classes. The representation of molecules and the systematic formation or cleavage of bonds to give different molecules with different properties fascinated me. I found it easy to comprehend what was happening in this molecular world and I viewed it as if playing a game of Lego.

Can you tell me a little about your background?

My training is in the area of synthetic inorganic chemistry. I studied organometallic and materials chemistry under the guidance of some wonderful mentors including Gregory Girolami at the University of Illinois, John Arnold at Berkeley, and Jeffrey Zink at UCLA. The areas of molecular precursor chemistry for materials synthesis and their transformations from a mechanistic point of view are of particular interest. I have extended these concepts to nanoparticle synthesis in which the size, shape, and composition are of significant importance to their material properties. I hope to make major contributions towards solving today's health issues, such as cancer, and energy storage concerns by using nanoscale materials.

One of the applications of your research into magnetic nanomaterials is in medical diagnostics. Can you explain how this works?

Nanoparticles are important in biomedical applications due to their small size and wonderful properties. Magnetic nanoparticles are especially useful for biological separation, diagnostics and treatment of diseases. By tuning their magnetism by varying their size or composition, we have been able to fabricate extremely sensitive magnetic resonance imaging (MRI) probes. They selectively target biological species with strong enhancement of detection sensitivity for the diagnosis of smaller cancers. We are also developing biocompatible nanoparticles which are free of potential toxicity without losing their materials properties.

What's the trickiest problem that you've faced, and how did you solve it?

Interdisciplinary research topics such as nanomedicine require collaboration between different research fields. This is not always easy as it is difficult to get people to buy into concepts that they are not familiar with.

I often have to be persistent and an advocate for our nanomaterials. However, synergistic results between research groups are the most important outcome. As scientists, researchers and educators, we should try to understand each other's language and to overcome the boundaries between different disciplines.

As chemists, we are in a good position to be translators of these different languages since chemistry plays a pivotal role in interfacial problem solving and bridges interdisciplinary subjects.

What is the secret to running a successful research group?

Highly motivated and enthusiastic students are the most important assets. A research group's goals cannot be realised without open communication and ownership. Members must share the group's vision but also be willing to take a chance with new ideas and bring their own insight to the table. There has to be an atmosphere of trust and mutual respect in order to nurture the growth of all involved.

What is the most rewarding aspect of your work?

Working with next generation chemists who will be the leaders in our global community through our research efforts is the most rewarding part. Hopefully, in the future, new nanomaterials that are developed as a result of our work can contribute towards enhancing the quality of human life in terms of medical sciences or energy-related technologies.

Do you have a message for young scientists?

Try to develop your own interpretation of science. In your pursuit of becoming a scientist, be persistent and enjoy the ride and you will be rewarded in the future, regardless of where the road takes you.

Which scientist, current or historic, do you most admire and why?

Marie Curie. She was not only a great chemist but she was successful despite being in adverse surroundings, which included gender and racial discrimination and extremely poor research environments.

If you weren't a scientist, what would you be?

A pilot, if wearing glasses did not matter!

Essential elements

A winning combination!

Visit the RSC stand, booth 411, at the ACS Spring National Meeting & Exposition in New Orleans, US, 6–10th April 2008 and you could be a winner! To celebrate the success of their monthly podcast and the launch of their new mini-podcast 'Chemistry in its element – a tour of the periodic table' the award-winning *Chemistry World* is offering an iPod to one lucky listener.

Or give your energy levels a boost with our cookies and cakes event in anticipation of the summer launch of our brand new journal - *Energy & Environmental Science*, linking all aspects of the chemical sciences relating to energy conversion and storage, alternative fuel technologies and environmental science. Sign up to e-alerts to secure your entry into a prize draw for a solar-powered charger for your mobile phone, MP3 player and other mobile devices.

Meet the editors of our



journals, pick up some free copies and make the most of the RSC books sale – offering up to

20% off selected titles

Celebrate with us as four titles from our successful journal portfolio mark their 10th year of publication. *CrystEngComm*, *Green Chemistry*, *Journal of Environmental Monitoring* (*JEM*), and *Physical Chemistry Chemical Physics* (*PCCP*) have all made huge advances in their first decade. Check out the *RSC eBook Collection*, a fully searchable online reference library covering more than 750 titles, or discuss with us the award-winning *RSC Prospect* enhanced HTML articles.

Plus, why not take this opportunity join over 44 000 people worldwide by becoming a member of the RSC and benefit from the wealth of knowledge that we contribute to the chemical science community.

We look forward to seeing you there!

Visit www.rsc.org/rscatacs

Hot off the press



The μ TAS 2008 conference in San Diego, US, is featuring a new award sponsored by *Lab on a Chip* titled 'Under the Looking Glass: Art from the World of Small Science.' Applications are encouraged from any person attending the conference and the winner will be selected by a panel of senior scientists in the field of μ TAS.

Applications must show a photograph, micrograph or other accurate representation of a system that would be of interest to the μ TAS community. They must also contain a brief caption that describes the illustration's content and its scientific merit. The winner will be selected on the basis of aesthetic appeal, artistic allure and scientific merit. In addition to having the image featured on the cover of *Lab on a Chip*, the winner will also receive a financial award at the conference.

For more information email loc@rsc.org

April free access

Do you have online access to one or more journals from RSC Publishing? Would you like to have access to even more content?

From April 1st to April 30th 2008, you can!

Like any organisation, we are keen to reward our loyal customers. So, to show our appreciation for your continued support of RSC journals, we are providing you with free

online access to all of our online journals – completely free!

All you need is a current institutional subscription (or rights to access online) for one or more RSC journal titles. Then, for the whole of April 2008, you and your colleagues will be able to read all content, published between 1997 and the present day, in all RSC journals.

A complete list of all journals

included in this offer is listed on the website. The list includes all our established titles, such as *ChemComm*, *The Analyst*, *Green Chemistry*, *Lab on a Chip* and *Journal of Materials Chemistry*, as well as more recent additions *Soft Matter* and *Molecular BioSystems*.

Visit www.rsc.org/april_access for full details

Chemical Technology (ISSN: 1744-1560) is published monthly by the Royal Society of Chemistry, Thomas Graham House, Science Park, Milton Road, Cambridge UK CB4 0WE. It is distributed free with *Chemical Communications*, *Journal of Materials Chemistry*, *The Analyst*, *Lab on a Chip*, *Journal of Atomic Absorption Spectrometry*, *Green Chemistry*, *CrystEngComm*, *Physical Chemistry Chemical Physics* and *Analytical Abstracts*.

Chemical Technology can also be purchased separately. 2008 annual subscription rate: £199; US \$396. All orders accompanied by payment should be sent to Sales and Customer Services, RSC (address above). Tel +44 (0) 1223 432360, Fax +44 (0) 1223 426017 Email: sales@rsc.org

Editor: Neil Withers

Associate editors: Nina Notman, Celia Clarke

Interviews editor: Joanne Thomson

Web editors: Michael Spenceleyah, Debora Giovanelli

Essential Elements: Daniel Bradnam, Valerie Simpson and Kathryn Lees

Publishing assistant: Ruth Bircham

Publisher: Graham McCann

Apart from fair dealing for the purposes of research or private study for non-commercial purposes, or criticism or review, as permitted under the Copyright, Designs and Patents Act 1988 and the copyright and Related Rights Regulations 2003, this publication may only be reproduced, stored or transmitted, in any form or by any means, with the prior permission of the Publisher or in the case of reprographic reproduction in accordance with the terms of licences issued by the Copyright Licensing Agency in the UK. US copyright law is applicable to users in the USA.

The Royal Society of Chemistry takes reasonable care in the preparation of this publication but does not accept liability for the consequences of any errors or omissions.

Royal Society of Chemistry: Registered Charity No. 207890.

RSC Publishing

Green and sustainable chemistry: challenges and perspectives

DOI: 10.1039/b804163f

In the last ten years, following the appearance of the first issue of the journal *Green Chemistry*, the attention devoted worldwide to the concepts of green chemistry and sustainability, both in industry and academia, has undergone an explosive growth. The design of greener, more sustainable products and processes has become a top priority item in annual reports and many chemical and pharmaceutical companies have appointed global green chemistry managers. I stress the words “greener” and “more sustainable” rather than “green” and “sustainable” because there are many shades of green as well as degrees of sustainability.

Green chemistry and sustainability essentially go hand in hand. Sustainable development is meeting the needs of the present generation without compromising the ability of future generations to meet their own needs. We need greener chemistry—chemistry that efficiently utilises (preferably renewable) raw materials, eliminates waste and avoids the use of toxic and/or hazardous solvents and reagents in both products and processes—in order to achieve this noble and lofty goal. Green chemistry embodies two main components. First, it addresses the problem of efficient utilisation of raw materials and the concomitant elimination of waste. Second, it deals with the health, safety and environmental issues associated with the manufacture, use and disposal or re-use of chemicals.

The waste problem in the fine and specialty chemical industries is being dramatically reduced by replacing antiquated technologies employing stoichiometric reagents by greener, catalytic alternatives—homogeneous, heterogeneous and enzymatic. It is now widely accepted that the use of organic solvents is a major source of waste in the fine and specialty chemical industries and, in the case of many traditional organic solvents, is associated with serious health hazards and/or environmental problems. Hence, the need for alternative reaction

media is now widely acknowledged and has become a major focus of research in industry and academia. Research on ionic liquids, for example, has undergone exponential growth in the last decade. More recently, the petrochemical and oil refining industries have focused their attention on the third aspect of green chemistry (after catalysis and alternative reaction media): the use of renewable raw materials as alternatives to fossil resources—oil, coal and natural gas—as feedstocks for liquid fuels and commodity chemicals. It is becoming increasingly clear that in the longer term biorefineries will utilise waste and/or inedible biomass as feedstocks for the manufacture of a broad spectrum of products, from biofuels to biodegradable plastics and platform commodity chemicals. This will inevitably lead to the development of greener products such as polymers that are recyclable and/or biodegradable.

It is no mere coincidence that the industrial applications of biocatalysis, what has become known as white biotechnology (to distinguish it from red and green biotechnology for medical and agricultural applications, respectively), has also undergone explosive growth in the same period. In addition to being green catalytic processes that are performed at ambient temperature and pressure, often in water as solvent, the catalysts themselves (enzymes) are biocompatible, have low ecotoxicity and are produced from natural, renewable raw materials. What more could you want? It is appropriate, therefore, that this part-themed issue of *Green Chemistry*, in its tenth year, contains a review, by Junhua Tao, on recent applications of biocatalysis in the industrial scale synthesis of pharmaceuticals, fine chemicals, commodity chemicals and polymers.

In addition to this timely review, this issue contains a selection of papers based on lectures presented at the 3rd International Conference on Green and Sustainable Chemistry (GSC-3) which was held in Delft, The Netherlands in July

2007. The major themes of GSC-3 reflected the multifaceted, interdisciplinary nature of research on green and sustainable chemistry at the academic/industrial interface. They included homogeneous, heterogeneous and enzymatic catalysis, multicatalytic cascade processes, alternative reagents and reaction media, renewable raw materials and sustainable energy, and life cycle analysis. Graham Hutchings, a pioneer in catalysis by gold, presented the *Green Chemistry* Lecture, entitled “Selective oxidation using supported gold and gold palladium nanoparticles”. This issue contains a contribution, based on this lecture, devoted to the direct synthesis of hydrogen peroxide from hydrogen and oxygen over Au–Pd supported nanocrystals. An effective and inexpensive method for the direct synthesis of hydrogen peroxide from its elements paves the way for the broad application of this green oxidant in a multitude of processes. The growing importance of gold as a catalyst is further underscored by two more contributions, from the group of Christensen, that deal with supported gold-catalysed oxidations, of amines, and glycerol and propane diols, respectively. Two contributions concerned with renewable raw materials are the production of biodiesel by transesterification over nanocrystalline magnesia catalysts (Parvelescu *et al.*) and the use of palladium nanoparticles supported on polysaccharide-based mesoporous materials as catalysts in C–C coupling reactions (Clark *et al.*). Further contributions deal with the immobilization of homogeneous catalysts, on silica (van Koten *et al.*) or in a supported ionic liquid phase (Luis *et al.*), the biocatalytic resolution of amines and the immobilisation of the industrially important group of enzymes, the nitrile hydratases.

Finally, I note that many current developments have a familiar ring to readers of Ernest Callenbach's book, *Ecotopia*, published in 1975. The setting was a future, ecologically sustainable society formed by the creation, in 1999, of an independent

country, Ecotopia, comprising Northern California, Oregon and Washington State, with a woman as president. The disposition of Ecotopians to modern technology was not one of rejection but rather one of careful selection on the basis of sustainability. Only fully recyclable plastics were permitted, for example, and the

word “consumer” was not used in polite company. Ecotopia was clearly based on the concepts of green and sustainable chemistry *avant la lettre*.

The journal *Green Chemistry* continues, in its tenth year, to play a pivotal role in promoting green and sustainable chemistry by publishing papers that combine

excellent science with practical and social relevance. I wish the journal continued success in the future and hope that the reader will enjoy the papers in this part-themed issue.

Roger A. Sheldon

Recent applications of biocatalysis in developing green chemistry for chemical synthesis at the industrial scale

Ningqing Ran,^a Lishan Zhao,^a Zhenming Chen^b and Junhua Tao^{*a}

Received 17th October 2007, Accepted 22nd November 2007

First published as an Advance Article on the web 4th December 2007

DOI: 10.1039/b716045c

Application of the twelve principles of green chemistry can deliver higher efficiency and reduce the environmental burden during chemical synthesis. As a result of recent advances in genomics, proteomics and pathway engineering, biocatalysis is emerging as one of the greenest technologies. Enzymes are highly efficient with excellent regioselectivity and stereoselectivity. By conducting reactions in water under ambient reaction conditions, both the use of organic solvents and energy input are minimized.

1. Introduction

A number of green chemistry performance metrics, such as atom economy, raw material efficiency (RME) and E-factor, have been developed to guide the development of new reactions and technologies to reduce waste generation and solvent usage, minimize energy input, improve safety, material and cost efficiency.^{1–6} As the green chemistry movement gains momentum,^{1,7} a fresh landscape of research and development opportunities has been opened up to improve the efficiency of chemical processes while simultaneously reducing production costs. For example, 54% of drug molecules are chiral and resolution remains an important and cost-effective approach to chiral molecules.⁸

^aBioVerdant Inc., 7330 Carroll Road, San Diego, CA 92121, USA.

E-mail: junhua_tao@yahoo.com; Fax: +1 858 368 6005

^bZhejiang University of Technology, Hangzhou 310032, P. R. China



Junhua Tao

Junhua (Alex) Tao is currently the Chief Scientific Officer of BioVerdant, Inc. Prior to co-founding BioVerdant, he was the creator and Head of the Biotransformations Group at La Jolla, a Center of Emphasis of Pfizer Global R&D. He was also a member of the API Review Team and API Development Team of Pfizer Global Manufacturing, and the Pfizer Biotask Force steering committee. He has a BSc in analytical

chemistry, an MSc in quantum chemistry, and a PhD in organic chemistry, which was followed by a postdoctoral position in biochemistry at Harvard Medical School. Alex is the recipient of the 2004 Pfizer Achievement Award, and a 2005 Pfizer Green Chemistry Award, and a contributor to a green chemistry manufacturing process for Pregabalin, which won the 2006 IChemE–AstraZeneca Award for Excellence in Green Chemistry and Engineering.

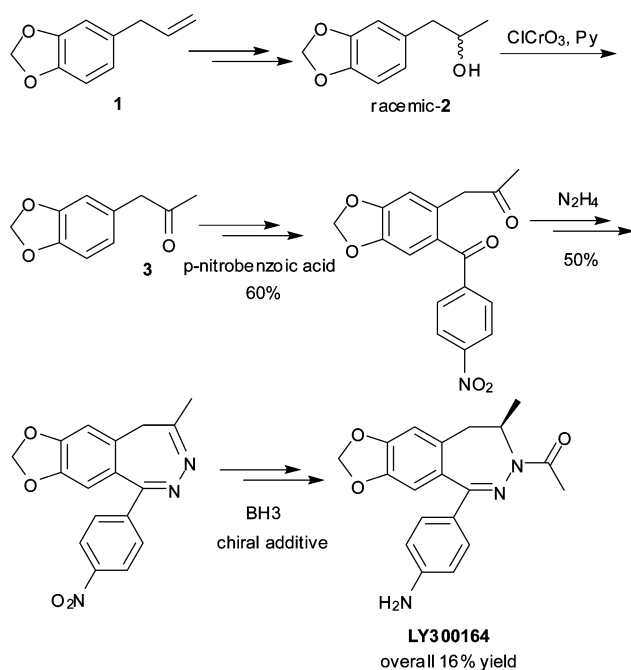
In order to achieve a typical enantiomeric purity of 99.5%, resolution is often accomplished at the price of restricting the overall maximum yield of a process to 50% at most. While metal-catalyzed reactions have become prevalent in recent years, their use in manufacturing requires great effort to identify appropriate catalysts, solvents and reaction conditions. Reproducibility and robustness can remain a problem, especially with regard to sensitivity to substrate quality and small variation in reaction parameters. There is a clear need for new methodologies to produce chiral molecules. As a result of recent advances in large scale DNA sequencing, structural biology, protein expression, high throughput screening, directed enzyme evolution and metabolic engineering, biocatalysis is becoming a transformational technology for chemical synthesis.^{9,10} Due to the high chemical and energy efficiency of enzymatic transformation in water, biocatalysis is one of the greenest technologies for chemical syntheses. Specifically, biocatalysis can prevent waste generation by performing catalytic processes with high stereo- and regio-selectivity, and by preventing or limiting the use of hazardous organic reagents. Furthermore, one can design processes with high energy efficiency and safe chemistry by conducting reactions at ambient temperature under ambient atmosphere, and atom economy can be increased by avoiding extensive protection and deprotection sequences. In this review, examples involving strategic use of biocatalysis were selected to illustrate the status of this technology to develop green processes for the production of pharmaceuticals, fine chemicals and polymers.

2. Results and discussions

2.1 Pharmaceuticals

The synthesis of a pharmaceutical agent is frequently accompanied by the use and generation of large quantities of hazardous substances. This should not be surprising as numerous steps are commonly necessary, each of which may require feedstocks, reagents, solvents, and separation. An example of the reduction of these hazards is the use of a chemoenzymatic synthesis for the production of LY300164 (Talampanol) for treating epilepsy and neurodegenerative diseases. The first generation synthesis,

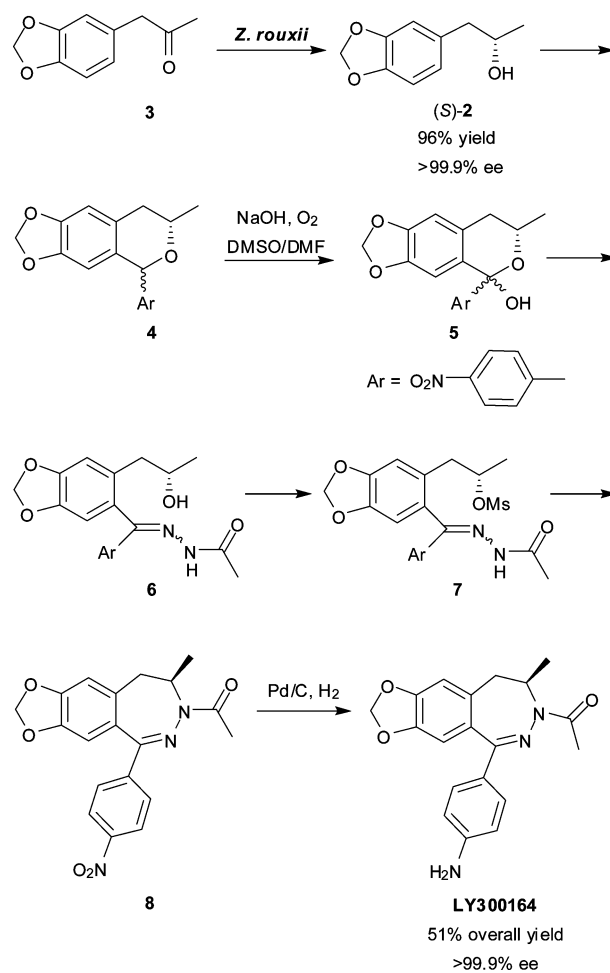
which starts from 5-allyl-1,3-benzodioxole **1**, suffers from a low yield of 16%, and requires the use of a large amount of organic solvents and chromium oxide, a cancer-suspect agent, to oxidize racemic alcohol **2** to ketone **3** (Scheme 1).¹¹



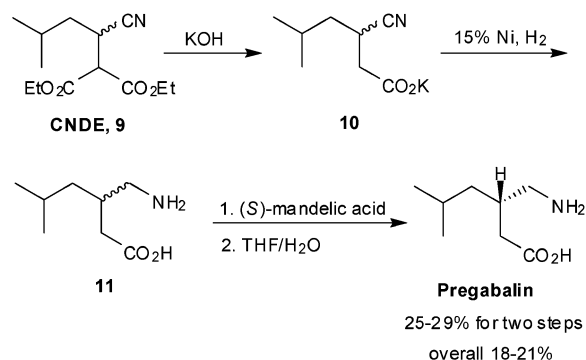
Scheme 1

In order to improve its synthesis, a second generation route was developed involving a biocatalytic ketone reduction of **3** by *Zygosaccharomyces rouxii* to give (*S*)-**2** with a yield of 96% and >99.9% ee (Scheme 2).¹² Acid-catalyzed reaction with 4-nitrobenzaldehyde led to 1-arylisochroman **4**, which was subsequently oxidized to ketal **5** in the presence of oxygen. The final product LY300164 was obtained after formation of hydrazone **6**, and cyclization *via* mesylate **7** to give **8** followed by Pd-catalyzed nitro group reduction. By using a chemoenzymatic approach, not only was the overall yield improved to 51% from 16% in the old route, the new synthetic pathway eliminated the use of transition metal oxidants and a large volume of organic solvents by judicious adjustment of oxidation states and integration of a biotransformation. For example, using the biocatalytic process, approximately 340 000 L of solvents and 3000 kg of chromium waste were eliminated for the production of every 1000 kg of LY300164.¹³

Most enzymatic catalysis achieves high regio- and stereo-selectivity under mild conditions, allowing new and more efficient processes to be designed with significant advantages over chemical approaches. For example, in the first generation route for the production of pregabalin, chemical resolution of the racemic γ -amino acid **11**, which was prepared from the racemic cyanodiester **9** (CNDE) after hydrolysis and decarboxylation, took place at the end of the process (Scheme 3).¹⁴ To obtain a high optical purity (99.5%) of the final API, (*S*)-mandelic acid resolution was followed by another step of recrystallization in THF/H₂O with a combined two-step yield of 25–29%. As a result, the overall yield for the route is only 18–21% and over 70% of all process materials before the resolution step including



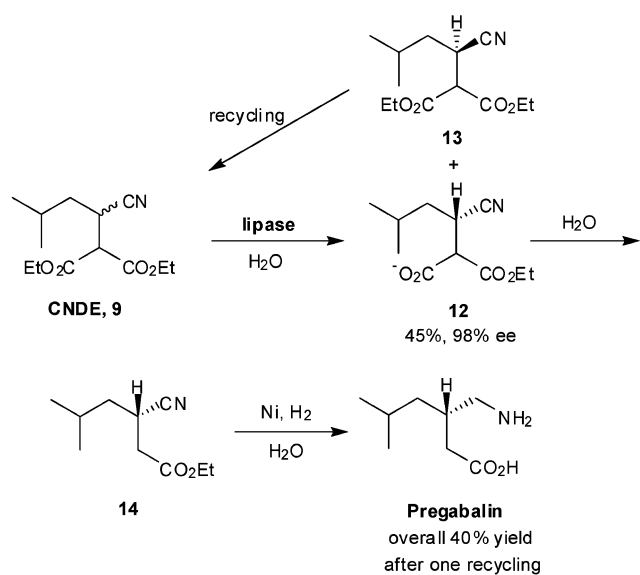
Scheme 2



Scheme 3

nickel were ultimately turned into wastes. Since the undesired enantiomer could not be recycled, this modest efficiency leads to a large amount of wastes and excessive reactor capacity requirements.

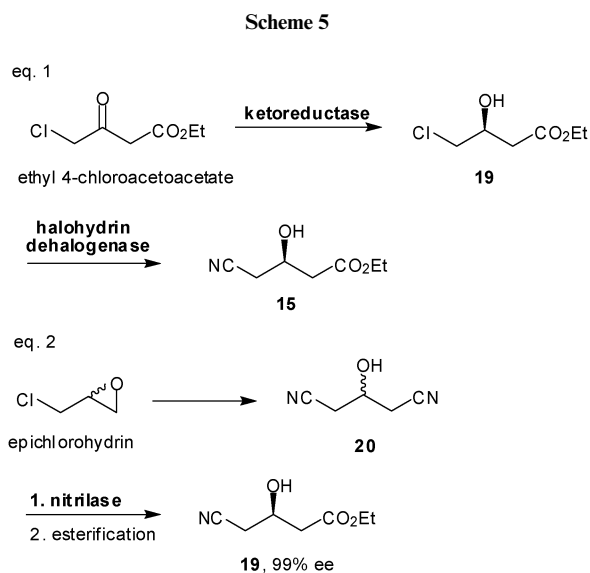
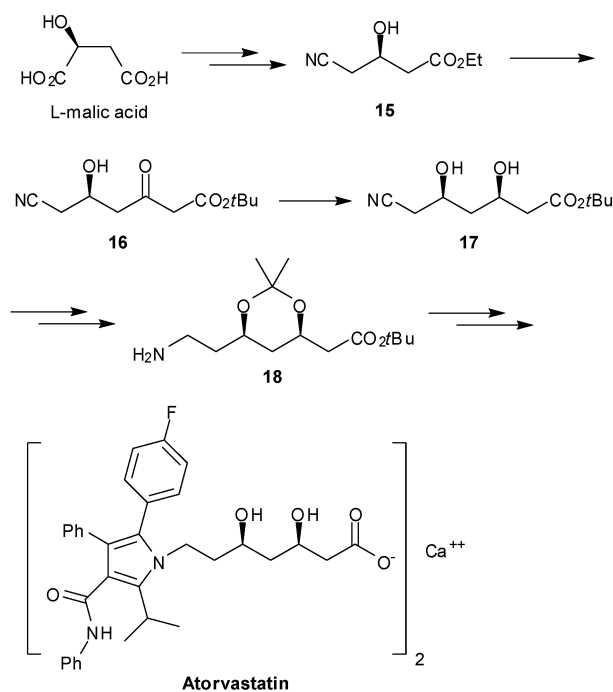
To overcome these issues, a second generation process using a fungal lipase was developed, where enzymatic resolution occurred at the first step and the undesired enantiomer **13** could be easily recycled (Scheme 4).¹⁵ Regio- and stereospecific hydrolysis of **9** led to the mono acid **12** with 45% conversion and >98% ee. After decarboxylation of **12** and phase splitting, mono ester **14** was telescopically subjected to basic hydrolysis



and hydrogenation to give the final product. Simple operation as a result of using water as the solvent significantly improved process efficiency. Comparing with the first generation synthesis, not only are a large amount of (*S*)-mandelic acid completely eliminated, the biocatalytic process also rendered it unnecessary to use most organic solvents. This stands in contrast to a typical process for the production of an API, where 80% of all wastes are solvents.¹⁶ If spent solvents are incinerated instead of being recovered, the life-cycle profile and impacts are considerably increased. Moreover, recycling of the undesired enantiomer **13** doubled both the yield (40% vs. <21%) and throughput. Overall, it was projected that at the peak of manufacturing, the biocatalytic aqueous process would annually eliminate the usage of over thousands of metric tons of raw materials including mandelic acid, CNDE and nickel, and tens millions of gallons of alcoholic solvents and THF associated with the classic resolution route.

Enzymes catalyze a wide range of reactions and a target molecule can often be approached by a number of chemoenzymatic syntheses.¹⁷ For example, atorvastatin calcium is the active ingredient of Lipitor[®], the first drug with annual sales exceeding \$10B. In the current process, the key chiral building block in the synthesis of atorvastatin is ethyl (*R*)-4-cyano-3-hydroxybutyrate (**15**) with an annual demand estimated to be about £440 000,¹⁸ which was then converted to atorvastatin side chain **18** upon Claisen condensation (**16**), borane-chelation controlled reduction (**17**), both under cryogenic conditions, followed by protection of the two hydroxy groups and Ni-catalyzed nitrile group hydrogenation. The final API atorvastatin was produced after Paal–Knorr condensation of **18** with a diketone (Scheme 5).¹⁹

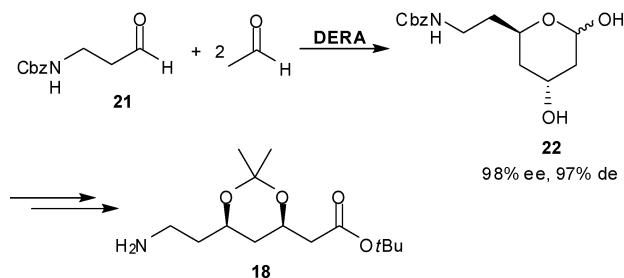
A number of biocatalytic approaches have been reported for the synthesis of (*R*)-4-cyano-3-hydroxybutyrate **15**. For example, a green process has recently been reported using a two-enzyme system under neutral conditions in water (eq. 1, Scheme 6).^{18–21} In this process, the first step involves enantioselective enzymatic reduction of ethyl 4-chloroacetoacetate to give **19** followed by a biocatalytic cyanation of the chlorohydrin to produce **15**.



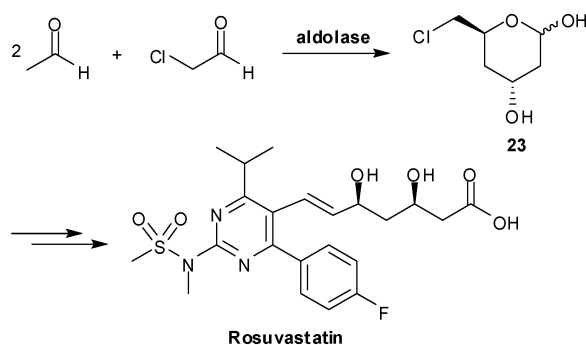
Alternatively, **15** was synthesized from inexpensive racemic epichlorohydrin *via* nitrilase-catalyzed desymmetrization of *meso*-3-hydroxyglutaronitrile **20** (eq. 2, Scheme 6).²² By applying gene site saturation mutagenesis to improve the stereoselectivity of the biocatalyst, the ee of the desired product reached 99% under a 3 M loading of the substrate. The synthesis is short and utilizes an inexpensive starting material. Both the ketoreductase (eq. 1, Scheme 6) and nitrilase processes (eq. 2, Scheme 6) led to significant reduction of byproducts, wastes and organic solvents associated with existing chemical routes.

Recently, a more concise approach to install the atorvastatin side chain was reported by using a microbial deoxyribose-5-phosphate aldolase (DERA). This enzyme catalyzes the sequential aldol condensation between one equivalent of amino aldehyde **21** and two equivalents of acetaldehyde to form lactol

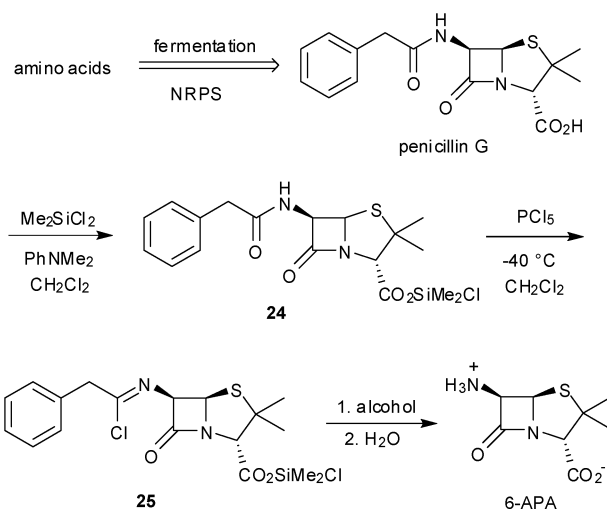
22 with excellent ee (98%) and de (97%), which was then converted to the statin side chain **18** upon oxidation, protection and esterification.²³ Using this method, the overall process to atorvastatin was shortened significantly and two cryogenic steps in the existing process were eliminated (Scheme 7). It is estimated that hundreds of metric tons of raw materials and solvents will be reduced each year by using the chemoenzymatic route in concomitant with significant reduction in energy consumption.



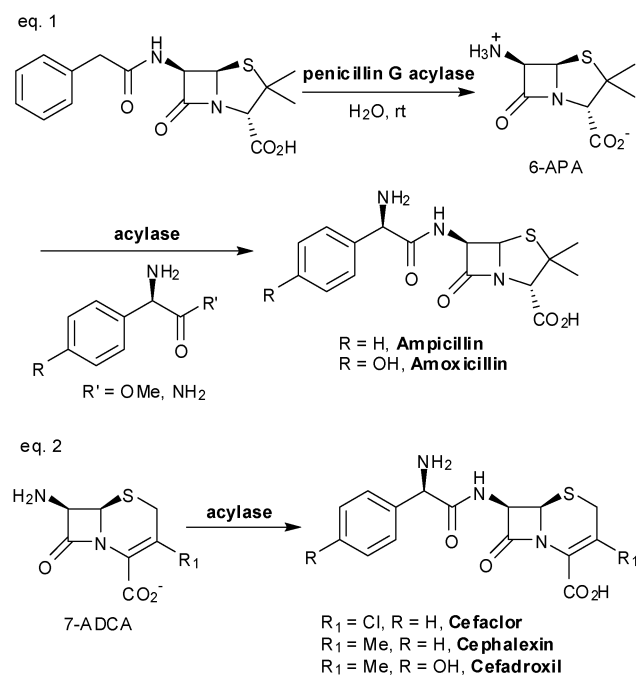
Similar approaches have been applied to the synthesis of the side chain of rosuvastatin, the API of Crestor^(R) (Scheme 8).²⁴ By a combination of activity- and sequence-based screening, a novel DERA was discovered from environmental DNA libraries leading to an enzymatic process to obtain lactol **23** with volumetric productivity of 720 g L⁻¹ day⁻¹ under an enzyme loading of 2% wt/wt.²⁵



Biocatalysis is uniquely suited to the development of green chemistry routes for complex molecules, which are often labile and densely functionalized. As a result of high selectivity and mild conditions, enzymatic catalysis has been applied to the industrial production of β -lactam antibiotics, which are mostly derived from 6-aminopenicillanic acid (6-APA) or 7-aminodesacetoxycephalosporanic acid (7-ADCA). The annual world production of 6-APA and 7-ADCA were estimated to be over 8000 and 600 t, respectively. Until recently, they were prepared from penicillin G, a fermentation product derived from non-ribosomal peptide synthase (NRPS), by chemical deacylation, where the carboxy group of the penicillin G is first protected by silylation (**24**), followed by selective deacylation *via* the imidoyl chloride (**25**), and removal of the protecting group (Scheme 9).²⁶ The method uses stoichiometric amounts of the silylating agent, and a large amount of hazardous chemicals and solvents such as phosphorus pentachloride and dichloromethane.

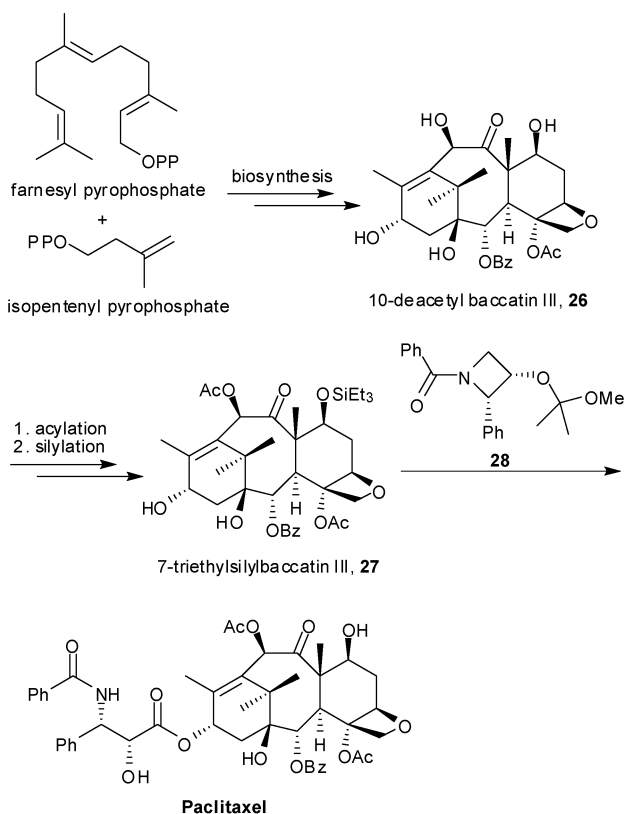


In contrast, enzymatic deacylation of penicillin G by penicillin G acylase was accomplished in water at room temperature requiring no protection and deprotection of other functional groups (Scheme 10). Moreover, under kinetic control, an immobilized penicillin acylase was also able to catalyze the acylation of 6-APA and 7-ADCA with either D-phenylglycine methyl ester (PGA), D-phenylglycine amides (PGA) or their *para*-hydroxylated analogs to produce a wide range of semi-synthetic β -lactam antibiotics such as ampicillin, amoxicillin, cefaclor, cephalexin and cefadroxil (Scheme 10).²⁷ As a result of the bio-transformation, raw material efficiency and E-factor were significantly improved from the first generation of chemical processes.



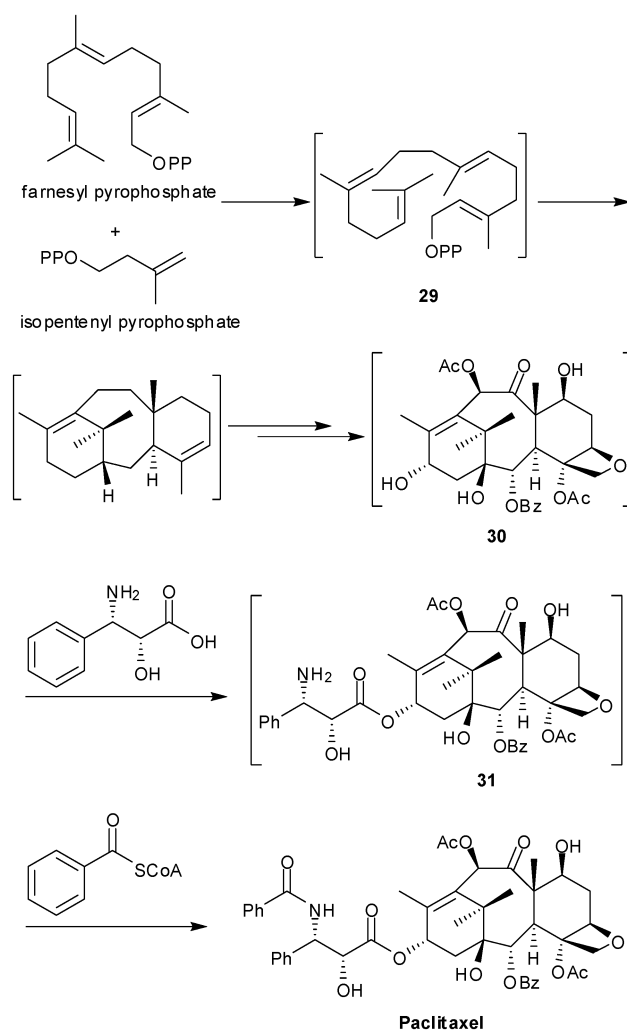
Plant secondary metabolites have provided a rich and renewable resource of natural products for drug development. However, establishing a stable supply of the active compounds

from plants is often difficult. A prominent example is Paclitaxel (Taxol[®]), a complex diterpenoid alkaloid originally isolated from the bark of the pacific yew tree *Taxus brevifolia* with a yield of 0.014%.^{28,29} In addition, isolating Paclitaxel required stripping the bark from the yew trees, thus killing a slow-growing tree in the process, which takes about 200 years to mature. On the other hand, the complexity of the Paclitaxel molecule makes commercial production by chemical synthesis from simple compounds impractical. As a result, a semisynthetic process was developed starting from 10-deacetylbaccatin III (26) (Scheme 11), a more abundant taxoid biosynthesized from isoprenyl diphosphate and farnesyl diphosphate in the needles of the European yew tree *Taxus baccata*,³⁰ which could be isolated with a yield of 0.1% without harm to the trees. In this route, 10-deacetylbaccatin III was first acetylated and silylated. The resulting 7-triethylsilyl baccatin III (27) was then coupled to an *N*-acyl- β -lactam (28) to install a phenylisoserine side chain at the C-13 position followed by deprotection to afford Paclitaxel. Overall, however, the semisynthetic process is still complex requiring eleven chemical transformations including the preparation of 28 and seven isolations.³⁰



Scheme 11

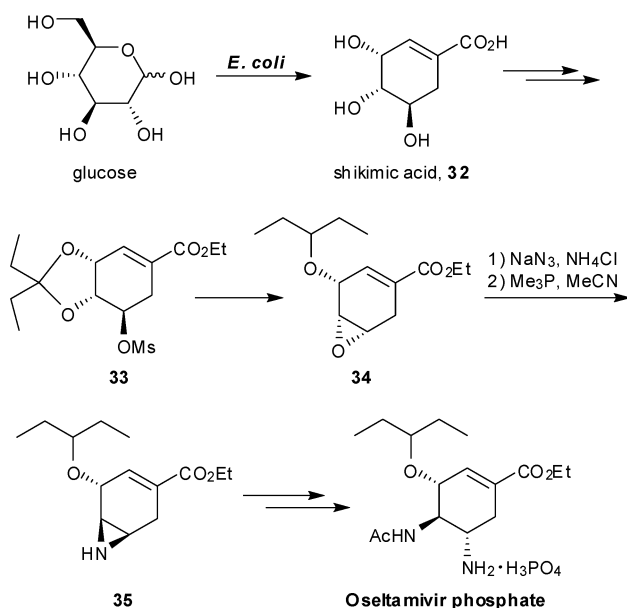
Consequently, an alternative process to Paclitaxel was developed using *Taxus* cell fermentation and extraction from culture medium, followed by recrystallization. Starting from the two isoprenoid precursors, isoprenyl diphosphate and farnesyl diphosphate (Scheme 12),^{31,32} geranylgeranyl pyrophosphate catalyzes the coupling to give geranylgeranyl pyrophosphate, 29, which is then cyclized and then converted to baccatin III 30 through a series of enzymatic transformations



Scheme 12

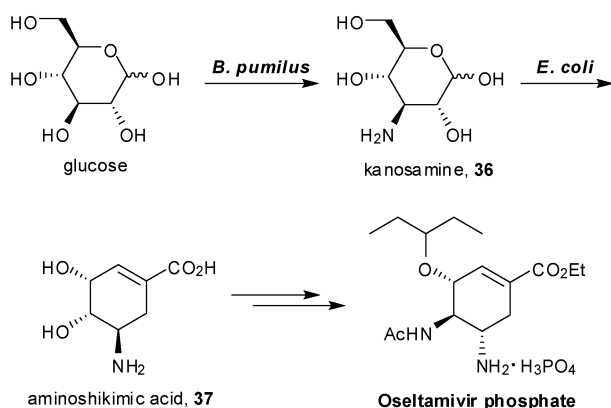
including hydroxylation, acylation, oxidation and generation of the oxetane ring. The side chain in 31 was installed by enzymatic transfer of phenylisoserine. To achieve a high titer of Paclitaxel production, cell cultures from various species of *Taxus* and different elicitors to induce Paclitaxel production have been examined.³³ For example, methyl jasmonate was able to enhance Paclitaxel production to 110 mg L⁻¹ every 2 weeks in cell suspension culture of *T. media*. The plant cell fermentation process led to an elimination of the eleven chemical transformations and a large amount of hazardous solvents and wastes, which came with the semi-synthesis route.³⁴

Recent advances in metabolic engineering have created another opportunity to develop green processes for relatively complex molecules. An example is the production of shikimic acid for the synthesis of oseltamivir phosphate (Tamiflu[®]) for treatment and prevention of influenza virus infections. In the current ten-step commercial synthesis (Scheme 13),³⁵ the key intermediate is shikimic acid 32, which was produced by a genetically engineered *E. coli* strain deficient in both shikimate kinase isozymes or isolated from the star anise.³⁶ The metabolic engineering efforts have led to the development of an *E. coli* strain capable of producing the molecule with a titer of 84 g L⁻¹ and a yield of 33% from glucose.³⁷ This acid was subsequently



converted into a diethyl ketal **33**, which was then transformed to the oseltamivir phosphate after side chain installation, reductive opening of the ketal, base-catalyzed epoxide ring closure (**34**) followed by aziridination (**35**).

One drawback of the above process is the use of the hazardous azide reagent to prepare the aziridine intermediate **35**. To eliminate the use of azides, an azide-free chemoenzymatic synthesis of oseltamivir phosphate was recently reported that comprised fewer synthetic steps than the commercial process.^{38,39} In this method, the key intermediate is aminoshikimic acid (**37**) that was produced from glucose by a two-step microbial process using *Bacillus pumilus* to generate kanosamine **36** followed by an engineered *E. coli* to give **37** (Scheme 14).^{38,39} The new route has an overall yield of 22% from aminoshikimic acid and holds great potential if the biosynthesis of aminoshikimic acid can be further improved.



2.2 Fine chemicals

Due to the exquisite regioselectivity under mild conditions, biotransformations often offer great advantages over chemical

synthesis in large-scale production of fine chemicals, which is usually energy intensive and generates a large amount of wastes and gas emissions.

The first example of enzymatic manufacture of a bulk chemical involves the conversion of acrylonitrile to acrylamide, which is the monomer of widely used polyacrylamide. The chemical manufacturing process involves hydration of acrylonitrile at 70–120 °C by Raney copper resulting in a large volume of toxic wastes and HCN. In addition, the acrylamide produced by this fashion requires considerable purification as it tends to polymerize under the harsh reaction conditions. Acrylic acid is also a byproduct of chemical hydration.⁴⁰ Many nitrile hydratases catalyze the conversion of acrylonitrile into acrylamide. For example, immobilized *Rhodococcus rhodochrous* J1 was able to produce acrylamide at a concentration of 400 g L⁻¹ in a fed batch process under 10 °C.^{40–43} There is no need to recover residual acrylonitrile because the yield of the enzymatic conversion is almost 100%. Currently the microbial process is operated at a scale of >40 000 t year⁻¹. It is much greener and more economical than the chemical process. In addition to acrylamide, *Rhodococcus rhodochrous* J1 was also used to prepare a variety of amides in high concentration and throughput in water (Fig. 1).^{40–43}

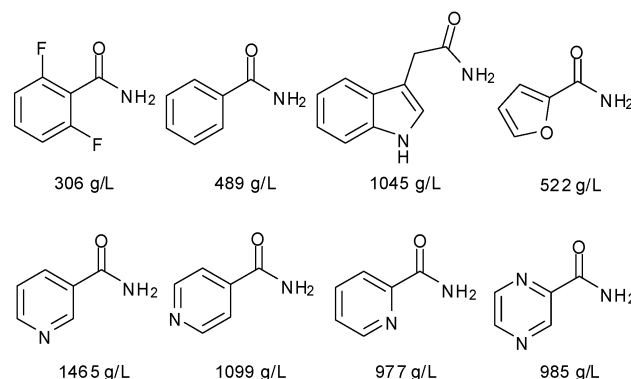
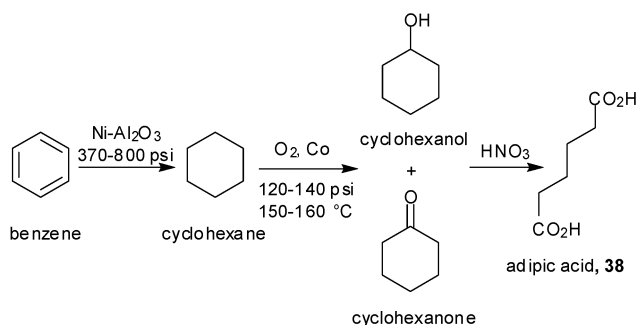


Fig. 1 Products and concentrations catalyzed by *Rhodococcus rhodochrous* J1.

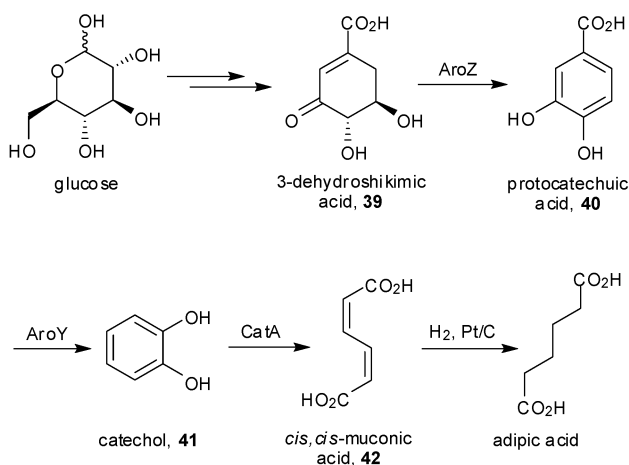
The drive toward environmentally benign synthesis and sustainable development in the chemical industry is contributing to a growing interest in the use of renewable feed stocks and reduction of hazardous wastes in manufacturing. Consequently, carbohydrates such as glucose derived from corn starch or cellulosic biomass provide an intriguing alternative to the current use of nonrenewable petroleum as starting materials. The keys to the success of this transition are the elaboration of new synthetic routes, as well as the design and engineering of robust microbial biocatalysts. Two examples are the development of biocatalytic syntheses of adipic acid and catechol from glucose.⁴⁴ Adipic acid (**38**), one of the monomers used in the manufacture of nylon 6,6, is currently produced at 2.2 million metric tons per year.⁴⁵ The existing route to adipic acid first entails oxidation of cyclohexane, mostly derived from benzene, to a mixture of cyclohexanol and cyclohexanone by oxygen with a cobalt catalyst at a temperature of 150–160 °C. This mixture was then converted to adipic acid by oxidation in nitric acid (Scheme 15). Due to its massive scale, adipic acid manufacture has been estimated to account for some 10% of the annual increase in



Scheme 15

atmospheric nitrous oxide levels. Benzene is a carcinogen and volatile chemical that must derive from nonrenewable fossil fuels.

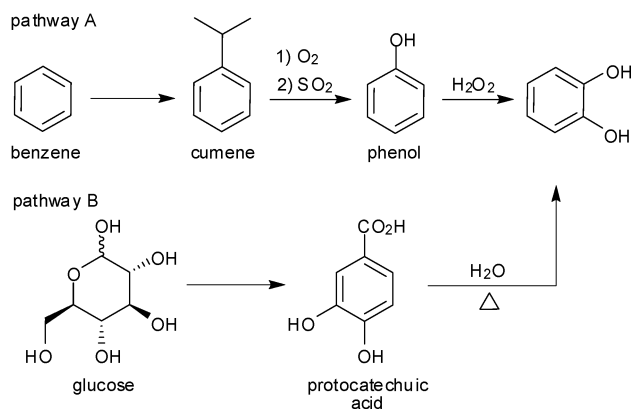
Biocatalytic routes to adipic acid have been reported in which glucose was converted to *cis,cis*-muconic acid followed by hydrogenation (Scheme 16).^{44b} The biosynthetic pathway leading to the production of *cis,cis*-muconic acid was assembled by expressing *Klebsiella pneumoniae* *aroZ*-encoded 3-dehydroshikimate dehydratase, *aroY*-encoded protocatechuate decarboxylase,^{44c} and *Acinetobacter calcoaceticus* *catA*-encoded catechol 1,2-dioxygenase in a 3-dehydroshikimate-synthesizing *E. coli* strain.⁴⁶ The resulting heterologous biocatalyst *E. coli* WN1/pWN2.248 was able to produce 37 g L⁻¹ of *cis,cis*-muconic acid (**42**) in 22% yield from glucose in one-pot *via* intermediates **39**, **40** and **41** (Scheme 16). Catalytic hydrogenation of *cis,cis*-muconic acid affords adipic acid in 97% yield.



Scheme 16

In the above metabolic pathway, catechol is an intermediate in the route to *cis,cis*-muconic acid. As a result, this technology may also be applied to the production of catechol, which is manufactured at an annual volume of 25 000 metric tons as an important chemical building block for flavors, pharmaceuticals, agrochemicals, polymerization inhibitors and antioxidants. Although some catechol is distilled from coal tar, phenol is the starting material for the production of the majority of catechol, and was obtained by Hock-type air oxidation of benzene-derived cumene (pathway A, Scheme 17).⁴⁷

Direct microbial synthesis of catechol from glucose resulted in only 5% yield due to its high toxicity to the production host.^{44b} The issue was circumvented by microbial production

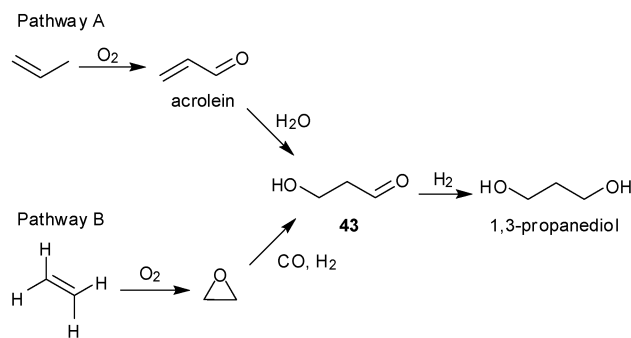


Scheme 17

of a less toxic intermediate protocatechuate using *E. coli* KL3/pWL2.46B followed by chemical decarboxylation in water (pathway B, Scheme 17). By this strategy, the overall yield of catechol from glucose was improved to 43%.^{44b}

As illustrated in microbial syntheses of adipic acid and catechol, manufacture of chemicals of major industrial importance from renewable feedstocks offer significant environmental advantages and economic opportunities. A single genetically engineered microbe is able to catalyze the conversion of glucose in water at near-ambient pressure and temperature.⁴⁸ The spectrum of chemicals that could be synthesized from glucose can be further expanded by the construction of heterologous biocatalysts and integration of microbial and chemical transformations. Research aimed at increasing synthetic efficiency and overcoming product toxicity and isolation problems are critical to move biocatalytic syntheses from proof-of-concept into practical routes to compete with existing chemical routes based on petroleum.

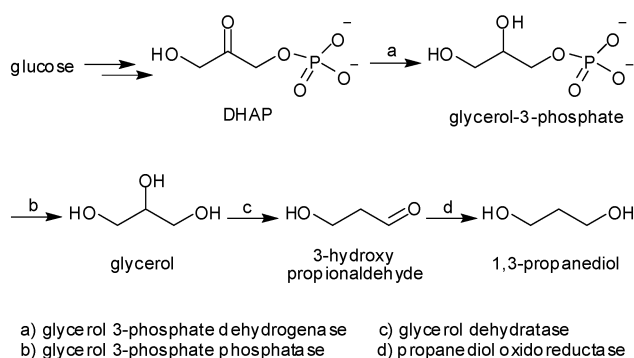
Another example using metabolic engineering is microbial production of 1,3-propanediol. The emergence of a new 1,3-propanediol (PDO)-based polyester has dramatically increased the demand for PDO in recent years. Once a fine chemical, PDO is now becoming a bulk chemical as its production volume will increase to a level of one million tons annually.⁴⁹ Historically, PDO was produced from petroleum chemicals from two different chemical processes. One uses propylene as the starting material, which was catalytically oxidized to acrolein, followed by hydration to 3-hydroxypropionaldehyde (**43**) (pathway A, Scheme 18).⁵⁰ An alternative process starts from ethylene oxide obtained from oxidation of ethylene



Scheme 18

(pathway B, Scheme 18). Ethylene oxide was then converted to 3-hydroxypropionaldehyde by hydroformylation under high pressure.⁵¹ The conversion of **43** to PDO requires hydrogenation over a rubidium or nickel catalyst under high-pressure.

To lower the cost of PDO and reduce the negative environmental impact of its production, a recombinant *E. coli* strain was developed to produce PDO from glucose.⁵² The *E. coli* strain was modified to contain genes from *Saccharomyces cerevisiae*, which is capable of producing glycerol from glucose, and *Klebsiella pneumoniae*, which contains the metabolic pathway of glycerol to PDO (Scheme 19). The engineered strain relies on a predominantly heterologous carbon pathway that diverts carbon from dihydroxyacetone phosphate (DHAP) to PDO. Two genes from yeast encoding glycerol 3-phosphate dehydrogenase (*dar1*) and glycerol 3-phosphate phosphatase (*gpp2*) directs glycolysis pathway to glycerol. Two genes from *K. pneumoniae* encoding glycerol dehydratase (*dhaB1-3*) and 1,3-propanediol oxidoreductase (*dhaT*) then transform glycerol to PDO. Significant modifications were then made to the base strain by extensive metabolic engineering to improve the fermentation productivity.⁵³ Additional genes from *dha* operon were incorporated into the engineered strain to stabilize glycerol dehydratase *via* reactivation. Moreover, an *E. coli* endogenous oxidoreductase (*yqhD*) was found to be superior to *dhaT* in providing high PDO titer ($\sim 130 \text{ g L}^{-1}$). As a result, the yield of PDO production in one-pot from glucose was eventually improved to 51% (g g^{-1}).



Scheme 19

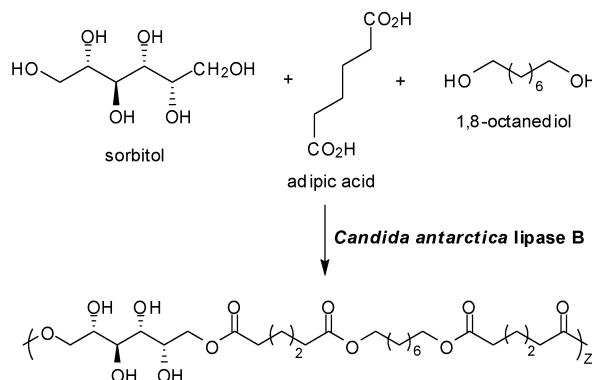
In contrast to the chemical processes to PDO, the biocatalytic process uses a renewable resource and was run at close to room temperature without added pressure. The bioprocess to PDO also reduces the energy consumption by 40% and green gas emissions by 20%. As of December 2006, shipments of corn sugar-derived PDO have been initiated from a 100 million-lb-per-year plant.⁵⁴ The successful development of a bio-based PDO process showed that it is possible to produce bulk chemicals in a more cost-effective way than the chemical processes while adhering to the principles of green chemistry.

2.3 Polymers

Another recent application of biocatalysis for green chemistry development is the production of polymeric materials. Enzymatic polymerization, *i.e.*, *in vitro* synthesis of polymers using isolated enzymes, offers a number of advantages over conventional chemical methods that often require harsh conditions

and the use of toxic reagents. Benefiting from high regio- and enantioselectivities under mild conditions, an enzymatic approach provides a new synthetic strategy for the production of novel polymers, which are otherwise difficult to get by chemical transformations.⁵⁵ Enzymatic polymerization has been applied to the synthesis of a number of polymers such as polyesters, polycarbonates, polysaccharides, polyurethanes, polyaromatics and vinyl polymers using oxidoreductases, transferases and hydrolases.⁵⁶

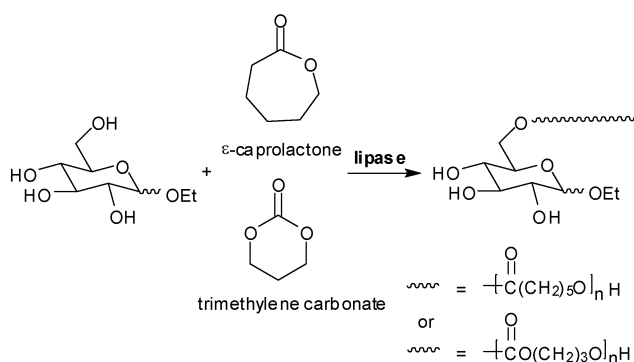
For example, a simple, environmentally-friendly, and versatile method was recently developed to produce polyol-containing polyesters through selective lipase-catalyzed condensation polymerization between diacids and reduced sugar polyols such as sorbitol (Scheme 20).⁵³ Instead of using organic solvents, the monomers adipic acid, glycerol and sorbitol were solubilized within binary or ternary mixtures, and no preactivation of adipic acid was needed. The direct condensation of adipic acid and sorbitol was performed in bulk at 90 °C for 48 h using immobilized lipase B from *Candida Antartica* (Scheme 20). The product, poly(sorbityl adipate), had an average molecular weight of 10 880 (M_n) and 17 030 (M_w) respectively. By replacing a fraction of sorbitol with 1,8-octanediol, copolyesters of adipic acid, 1,8-octanediol, and sorbitol were obtained in the molar ratio of 50 : 35 : 15 with an M_w of > 100 000. Similar results were also obtained with glycerol in place of sorbitol as the natural polyol (not shown). The condensation reactions with glycerol and sorbitol building blocks proceeded with high regioselectivity without protection-deprotection of functional groups. Although the polyol monomers contain three or more hydroxy groups, only two are highly reactive in enzymatic polymerization. Therefore instead of obtaining highly cross-linked products, the high regioselectivity leads to lightly branched polymers where the degree of branching varies with the reaction time and monomer stoichiometry. The mild reaction conditions also facilitate the polymerization of chemically and thermally sensitive molecules. Alternative chemical polymerization would necessitate the usage of stoichiometric amount of coupling agents. The biocatalytic approach is also versatile for simultaneous polymerization of lactones, hydroxyacids, cyclic carbonates, cyclic anhydrides, amino alcohols, and hydroxythiols as a result of high regioselectivity.⁵⁷



Scheme 20

Another example is enzyme-catalyzed ring-opening polymerizations of lactones and cyclic carbonates, which offers a number of advantages over chemical methods including mild

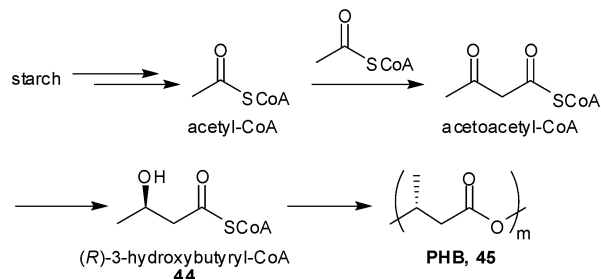
reaction conditions and improved propagation kinetics and/or molecular weights. The ring-opening polymerization of ω -pentadecalactone and trimethylene carbonate catalyzed by the lipase PS-30 and Novozyme-435 in bulk at 70 °C afforded high average molecular weight and moderate dispersity products (not shown).⁵⁸ Enzymatic polymerization also allows structural control by regioselective incorporation of multifunctional initiators such as carbohydrates. In the ring-opening polymerization of ϵ -caprolactone or trimethylene carbonate with ethyl glucopyranoside as an initiator catalyzed by porcine pancreatic lipase, the polymerization occurred selectively from the 6-hydroxyl position (Scheme 21).⁵⁹ Since both ethyl glucopyranoside and the monomers are liquids, the reaction could be carried out in the absence of solvents. The novel amphiphilic product was prepared in one-pot without the need of protection and deprotection chemistry.



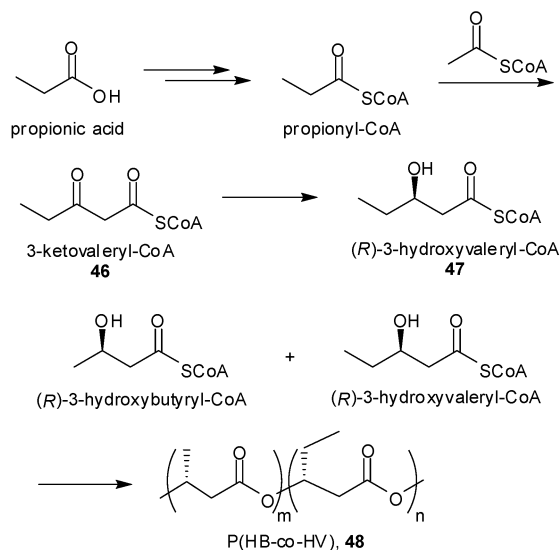
Hydrolases were also able to catalyze transesterification reactions between a monomer and a polymer or between two homopolyesters that differ in main chain structure.⁶⁰ For example, Novozym-435 catalyzed transesterification between polypentadecalactone (4300 g mol⁻¹) and polycaprolactone (9200 g mol⁻¹) resulted in random copolymers within only one hour. In addition to catalyzing metal-free transesterification under mild conditions, lipases endow transesterification reactions with remarkable selectivity, allowing the preparation of block copolymers that have selected block lengths.

Recent advances in biocatalysis have also made an inroad in the manufacture of biodegradable plastics such as polyhydroxyalkanoates (PHA)⁶¹ and polylactides (PLA).⁶² Polyhydroxyalkanoates are a class of natural polyesters produced by many bacteria in the form of intracellular granulates as a carbon and energy reserve. Since the initial discovery of poly-3-hydroxybutyrate (PHB) (**45**), more than 130 hydroxyacid monomer compositions have been identified that have been classified as short-chain and medium-chain hydroxyalkanoates.⁶³ Once extracted from bacterial cells, the biobased polymers display diverse material properties that range from thermoplastics to elastomers depending upon their monomer unit composition. The environmental benefit of using biodegradable PHA and the utilization of abundant, renewable starch as a starting material for its synthesis provide an appealing alternative to the commonly used petroleum-derived plastics. Of all the PHAs, PHB copolymers are the most extensively studied. The biosynthetic pathway of polyhydroxybutyrate consists of three

enzymatic reactions (Scheme 22).⁶⁴ A thiolase catalyzes the condensation of two molecules of acetyl-CoA to form one molecule of acetoacetyl-CoA, which is then reduced to (*R*)-3-hydroxybutyryl-CoA (**44**) by a NADPH-dependent acetoacetyl-CoA dehydrogenase. The crucial polymerization of **44** is catalyzed by a PHB synthase with concomitant regeneration of coenzyme A (Scheme 22).



PHB homopolymer is a stiff and brittle material. The high melting temperature of PHB limits the ability to process the biopolymer.⁶¹ Incorporation of 3-hydroxyvalerate into PHB renders a poly(3-hydroxybutyrate-co-3-hydroxyvalerate) block copolymer **48**, which can be processed at a lower temperature while still retaining excellent mechanical properties. The monomer (*R*)-3-hydroxyvaleryl-CoA **47** is produced from condensation of acetyl-CoA and propionyl-CoA to 3-ketovaleryl-CoA (**46**) followed by reduction catalyzed by acetoacetyl-CoA dehydrogenase (Scheme 23).



With the advances in genome sequencing projects, novel PHA synthases with different activities and substrate specificities have been identified.⁶⁵ Together with metabolic engineering of diverse, heterologous pathways for efficient biosynthesis of the monomer substrates from renewable starting materials, high yielding production of polyhydroxyalkanoates has been achieved *via* microbial fermentation. Accumulation of PHA in genetically engineered *Pseudomonas* reached 90% of the

cell weight.⁶⁶ Typical molecular weight of the polymer ranges from 50 000 to 1 000 000 Da. Recent research efforts have been devoted to the production of PHA in transgenic plants.⁶⁷ Direct production of PHA in plants has the potential to dramatically lower the manufacturing cost, and reduce the burden of plastic wastes as a result of biodegradability to environmentally friendly products.^{68,69}

3. Conclusions

Green chemistry principles have created a new landscape of opportunities to develop new technologies to improve chemical processes. A recent study shows that among the 1039 chemical transformations analyzed for the synthesis of 128 drug molecules,^{8,70} chemical acylations are one of the most common transformations but are generally inefficient. Development of catalytic, low waste acylation methods would significantly improve the environmental performance of many syntheses. As for chemical *N*-alkylations, there is heavy reliance on the use of potentially toxic alkylating agents. An alternative construction of C–N bonds would be greatly beneficial. In addition, most chemical oxidation reactions involves metals or high energy oxidants giving rise to thermal hazards and a lack of chemoselectivity. The discovery of new regioselective and catalytic oxidations would greatly increase flexibility in synthetic design. Finally, amide bond formation is one of the most common and yet least efficient transformations, where a routine practice involves the hydrolysis of an ester to an acid, activation of the acid and conversion to an amide. As illustrated in the green and biocatalytic synthesis of pharmaceuticals, fine chemical and polymers in this review, biotransformations are uniquely suited to deliver high stereo- and regioselectivity in water at ambient temperature and atmosphere, and are able to catalyze reactions that are challenging for traditional chemistry. Biocatalysis is positioned to be a transformational technology for chemical production with improved synthetic efficiency. The key is to integrate synthetic chemistry, biological transformations and process development under the umbrella of green chemistry principles.⁷¹

Acknowledgements

The authors thank Dr Kim Albizati for helpful discussions in preparing the manuscript.

References

- The twelve principles are as follows: Prevention, Atom Economy, Less Hazardous Chemical Synthesis, Design Safer Chemicals, Safety Solvents, and Auxiliaries, Design for Energy Efficiency, Use Renewable Feedstocks, Reduce Derivatives, Catalysis, Design for Degradation, Real Time Analysis, Inherently Safer Chemistry, see P. T. Anastas, J. C. Warner, *Green Chemistry: Theory and Practice*, Oxford University Press, Oxford, 1998.
- (a) M. Poliakoff, J. M. Fitzpatrick, T. R. Farren and P. T. Anastas, Green chemistry: Science and politics change, *Science*, 2002, **297**, 807–810; (b) R. Noyori, Pursuing practical elegance in chemical synthesis, *Chem. Commun.*, 2005, 1807–1811; (c) V. Gewin, Special report: Chemistry's evolution, *Nature*, 2006, **440**, 378–379.
- (a) B. M. Trost, Atom economy—a challenge for organic synthesis: homogenous catalysis leads the way, *Angew. Chem., Int. Ed.*, 1995, **34**, 259–281; (b) T. Hudlicky, D. A. Frey, L. Koroniak, C. D. Claeboe and L. E. Brammer, Jr., Toward a 'reagent-free' synthesis, *Green Chem.*, 1999, **1**, 57–59.
- E-factor is a green chemistry performance matrix calculating the ratio of kg of wastes generated per kg of products: (a) R. A. Sheldon, Consider the environmental quotient, *Chem.-Tech.*, 1994, **24**, 38–47; (b) R. A. Sheldon, Catalysis and pollution prevention, *Chem. Ind.*, 1997, **1**, 12–15.
- D. J. C. Constable, A. D. Curzons and V. L. Cunningham, Metrics to 'green chemistry'—which are the best?, *Green Chem.*, 2002, **4**, 521–527.
- J. Andraos, Unification of reaction metrics for green chemistry II: Evaluation named organic reactions and application to reaction discovery, *Org. Process Res. Dev.*, 2005, **9**, 404–431 and references therein.
- (a) A. S. Matlack, *Introduction to Green Chemistry*, Marcel Dekker Inc., New York, 2001; (b) M. Lancaster, *Green Chemistry: An introductory Text*, The Royal Society of Chemistry, Cambridge, 2002; (c) J. H. Clark and D. Macquarrie, *Handbook of Green Chemistry & Technology*, Blackwell Science Ltd., Oxford, 2002.
- J. S. Carey, D. Laffan, C. Thomson and M. T. Williams, Analysis of the reactions used for the preparation of drug candidate molecules, *Org. Biomol. Chem.*, 2006, **4**, 2337–2347.
- J. Tao, L. Zhao and N. Ran, Recent advances in developing chemoenzymatic processes for active pharmaceutical ingredients, *Org. Process Res. Dev.*, 2007, **11**, 259–267.
- A. J. Straathof, S. Panke and A. Schmid, The production of fine chemicals by biotransformations, *Curr. Opin. Biotechnol.*, 2002, **13**, 548–556.
- (a) I. Ling, B. Podanyi, T. Hamori and S. Solyom, Asymmetric reduction of a carbon–nitrogen double bond: Enantioselective synthesis of 4,5-dihydro-3*H*-2,3-benzodiazepines, *J. Chem. Soc., Perkin Trans. 1*, 1995, **11**, 1423–1427 and references cited therein; (b) M. Zappala, S. Grasso, N. Micale, S. Polimeni and C. De Micheli, A simple and efficient synthesis of GYKI 52466 and GYKI 52895, *Syn. Commun.*, 2002, **32**, 527–533.
- (a) B. A. Anderson, M. M. Hansen, A. R. Harkness, C. L. Henry, J. T. Vicenzi and M. J. Zmijewski, Application of a practical biocatalytic reduction to an enantioselective synthesis of the 5*H*-2,3-benzodiazepine LY300164, *J. Am. Chem. Soc.*, 1995, **117**, 12358–12359; (b) B. A. Anderson, M. M. Hansen, J. T. Vicenzi, D. L. Varie, M. J. Zmijewski and A. R. Harkness, Physical form of dihydro-2,3-benzodiazepine derivative useful as an AMPA antagonist, *Eur. Pat. Appl. EP*, **699676**, 1996; (c) B. Erdelyi, A. Szabo, G. Seres, L. Birincsik, J. Ivanics, G. Szatzker and L. Poppe, Stereoselective production of (*S*)-1-alkyl- and 1-arylethanols by freshly harvested and lyophilized yeast cells, *Tetrahedron: Asymm.*, 2006, **17**, 268–274.
- <http://www.epa.gov/greenchemistry/pubs/docs>.
- M. S. Hoekstra, D. M. Sobieray, M. A. Schwindt, T. A. Mulhern, T. M. Grote, B. K. Huckabee, V. S. Hendrickson, L. C. Franklin, E. J. Granger and G. L. Karrick, Chemical development of CI-1008, an enantiomerically pure anticonvulsant, *Org. Process Res. Dev.*, 1997, **1**, 26–38.
- (a) S. Hu, C. Martinez, S. Tao, W. Tully, P. Kelleher and Y. Dumond, Preparation of pregabalin and related compounds, U. S. 20051222; (b) R. V. Noorden, Keep it Green, *Chem. World*, May 25, 2007, <http://www.rsc.org/chemistryworld/news/2007/may/25050701.asp>; (c) J. Tao, *et al.*, *Green Chemistry in the Redesign of Pregabalin Processes*, 2nd International Conference on Green and Sustainable Chemistry and 9th Annual Green Chemistry & Engineering Conference, Washington, D. C., June 20–24, 2005.
- C. Jiménez-González, A. D. Curzons, D. J. C. Constable and V. L. Cunningham, Cradle to gate life cycle inventory and assessment of pharmaceutical compounds, *Int. J. Life Cycle Assess.*, 2004, **9**, 115–121.
- (a) J. Tao, A. Pettman and A. Liese, "Biocatalytic Retrosynthesis, chapter in *Industrial Biotransformations*, ed. A. Liese, K. Seelbach and C. Wandrey, Wiley-VCH, 2nd edn, 2006, pp. 63–91; (b) J. Tao and M. Burkart, New enzymes for chemical synthesis: Exploring natural product biosynthesis, in *Catalysis Applications*, Chimica Oggi/Chemistry Today, 2007, **25**, 44–48.
- <http://www.epa.gov/greenchemistry/pubs/pgcc/winners/grca06.html>.
- (a) S. Desai, S. K. Prabhu, R. Melarkode, G. Sambasivam and S. Suryanarayan, Enzymatic stereoselective reduction of keto groups in 3-ketopropionic acid derivatives, WO2006131933, 2006; (b) I. Lee and S. Lee, New process for the preparation of optically active 2-[6-(substituted alkyl)-1,3-dioxan-4yl]acetic acid derivatives,

- WO2003053950, 2003; (c) A. Blacker, I. Houson and J. Wiffen, Process for the preparation of nitrile compounds by cyanation of optionally protected dihydroxy alkanesulfonates in the presence of phase transfer catalysts, and its application to the preparation of an atorvastatin intermediate, WO2003004459, 2003; (d) M. Mitsuda, M. Miyazaki and K. Inoue, Process for producing 6-cyanomethyl-1,3-dioxane-4-acetic acid derivatives, WO9957109, 1999; (e) P. L. Brower, D. E. Butler, C. F. Deering, T. V. Le, A. Millar, T. N. Nanninga and B. D. Roth, The synthesis of (4*R*-cis)-1,1-dimethylethyl 6-cyanomethyl-2,2-dimethyl-1,3-dioxane-4-acetate, a key intermediate for the preparation of CI-981, a high potent, tissue selective inhibitor of HMG-CoA reductase, *Tetrahedron Lett.*, 1992, **33**, 2279–2282.
- 20 (a) B. Hagemann, K. Junge, S. Enthaler, M. Michalik, T. Riermeier, A. Monsees and M. Beller, A general method for the enantioselective hydrogenation of β -keto esters using monodentate binaphthophosphine ligands, *Adv. Syn. Catal.*, 2005, **347**, 1978–1986 and references therein; (b) S. C. Davis, R. J. Fox, G. W. Huisman, V. Gavrilovic and L. M. Newman, Engineering of halohydrin dehalogenases for improved activity and resistance to ethyl-4-chloroacetate and other properties useful in commercial applications, *US Pat.*, 2005272064, 2005.
- 21 T. M. Poessl, B. Kosjek, U. Ellmer, C. C. Gruber, K. Edegger, K. Faber, P. Hildebrandt, U. T. Bornscheuer and W. Kroutil, Non-racemic halohydrins via biocatalytic hydrogen-transfer reduction of halo-ketones and one-pot cascade reaction to enantiopure epoxides, *Adv. Syn. Catal.*, 2005, **347**, 1827–1834.
- 22 (a) G. DeSantis, K. Wong, B. Farwell, K. Chatman, Z. Zhu, G. Tomlinson, H. Huang, X. Tan, L. Bibbs, P. Chen, K. Kretz and M. J. Burk, Creation of a productive, highly enantioselective nitrilase through gene site saturation mutagenesis (GSSM), *J. Am. Chem. Soc.*, 2003, **125**, 11476–11477; (b) S. Bergeron, D. Chaplin, J. H. Edwards, B. S. Ellis, C. L. Hill, K. Holt-Tiffin, J. R. Knight, T. Mahoney, A. P. Osborne and G. Rucroft, Nitrilase-catalyzed desymmetrization of 3-hydroxyglutaronitrile: preparation of a statin side-chain intermediate, *Org. Process Res. Dev.*, 2006, **10**, 661–665.
- 23 S. Hu, J. Tao and J. Xie, Process for producing atorvastatin, pharmaceutically acceptable salts thereof and intermediates thereof, WO 2006134482, 2006.
- 24 (a) T. D. Machajewski, C.-H. Wong and R. A. Lerner, The catalytic asymmetric aldol reaction, *Angew. Chem., Int. Ed.*, 2000, **39**, 1352–1374; (b) S. Jennewein, M. Schuermann, M. Wolberg, I. Hilker, R. Luiten, M. Wubbolts and D. Mink, Directed evolution of an industrial biocatalyst: 2-deoxy-D-ribose 5-phosphate aldolase, *Biotechnol. J.*, 2006, **1**, 537–548.
- 25 W. A. Greenberg, A. Varvak, S. R. Hanson, K. Wong, H. Huang, P. Chen and M. J. Burk, Development of an efficient, scalable, adolase-catalyzed process for enantioselective synthesis of statin intermediates, *Proc. Natl. Acad. Sci. USA*, 2004, **101**, 5788–5793.
- 26 J. Verweij and E. de Vroom, Industrial transformations of penicillins and cephalosporins, *Recl. Trav. Chim. Pays-Bas*, 1993, **112**, 66–81.
- 27 A. Bruggink, E. C. Roos and E. de Vroom, Penicillin acylase in the industrial production of β -lactam antibiotics, *Org. Process Res. Dev.*, 1998, **2**, 128–133.
- 28 M. C. Wani, H. L. Taylor, M. E. Wall, P. Coggon and A. T. McPhail, Plant antitumor agents. VI. Isolation and structural of taxol, a novel antileukemic and antitumor agent from *Taxus brevifolia*, *J. Am. Chem. Soc.*, 1971, **93**, 2325–2327.
- 29 M. Sufness and M. E. Wall, in *Taxol: Science and Applications*, ed. M. Sufness, CRC Press, Boca Raton, FL, 1995, pp. 3–25.
- 30 (a) R. A. Holton, Method for preparation of taxol using an oxazone, *US Pat.*, 5 015 744, 1991 and 5 136 060, 1992; (b) A. K. Singh, R. E. Weaver, G. L. Powers, V. W. Rosso, C. Wei, D. A. Lust, A. S. Kotnis, E. T. Comozoglu, M. Liu, K. S. Bembenek, B. D. Phan, D. J. Vanyo, M. L. Davies, R. J. Mathew, V. A. Palaniswamy, W.-S. Li, K. Gadamssetti, C. J. Spagnuolo and W. J. Winter, Trifluoroacetic acid-mediated cleavage of a Triethylsilyl protecting group: Application in the final step of the semisynthetic route to Paclitaxel (Taxol), *Org. Process Res. Dev.*, 2003, **7**, 25–27.
- 31 J. C. Walker, *Abstracts of Papers*, 37th Middle Atlantic Regional Meeting of the American Chemical Society, New Brunswick, NJ, 2005, GENE-616.
- 32 (a) R. N. Patel, Tour de paclitaxel: Biosynthesis for semisynthesis, *Annu. Rev. Microbiol.*, 1998, **98**, 361–395; (b) S. Jennewein and R. Croteau, Taxol: biosynthesis, molecular genetics, and biotechnological applications, *Appl. Microbiol. Biotechnol.*, 2001, **57**, 13–19.
- 33 (a) Y. Yukimune, H. Tabata, Y. Higashi and Y. Hara, Methyl jasmonate-induced overproduction of paclitaxel and baccatin III in *Taxus* cell suspension culture, *Nat. Biotechnol.*, 1996, **14**, 1129–1132; (b) M. Seki, C. Ohzora, M. Takeda and S. Furusaki, Taxol (Paclitaxel) production using free and immobilized cells of *Taxus cuspidata*, *Biotechnol. Bioeng.*, 1997, **53**, 214–219; (c) Review: J.-J. Zhong, Plant cell culture for production of Paclitaxel and other taxanes, *J. Biosci. Bioeng.*, 2002, **94**, 591–599.
- 34 http://www.epa.gov/greenchemistry/pubs/docs/award_recipients_1996_2004.pdf, pp. 6–7.
- 35 (a) M. Federspiel, R. Fischer, M. Hennig, H.-J. Mair, T. Oberhauser, G. Rimmler, T. Albiez, J. Bruhin, H. Estermann, C. Gandert, V. Göckel, S. Götzö, U. Hoffmann, G. Huber, G. Janatsch, S. Lauper, O. Röckel-Sätbler, R. Trussardi and A. G. Zwahlen, Industrial synthesis of the key precursor in the synthesis of the anti-influenza drug Oseltamivir phosphate (Ro 64-0796/002, GS-4104-02): Ethyl (3*R*,4*S*,5*S*)-4,5-epoxy-3-(1-ethyl-propoxyl)-1-cyclohexene-1-carboxylate, *Org. Process Res. Dev.*, 1999, **3**, 266–274; (b) S. Abrecht, P. Harrington, H. Iding, M. Karpf, R. Trussardi, B. Wirz and U. Zutter, The synthetic development of the anti-influenza neuraminidase inhibitor oseltamivir phosphate (Tamiflu): A challenge for synthesis & process research, *Chimia*, 2004, **58**, 621–629.
- 36 S. S. Chandran, J. Yi, K. M. Draths, R. von Daeniken, W. Weber and J. W. Frost, Phosphoenolpyruvate availability and the biosynthesis of shikimic acid, *Biotechnol. Prog.*, 2003, **19**, 808–814.
- 37 (a) K. M. Draths, D. R. Knop and J. W. Frost, Shikimic acid and quinic acid: Replacing isolation from plant sources with recombinant microbial biocatalysis, *J. Am. Chem. Soc.*, 1999, **121**, 1603–1604; (b) M. Krämer, J. Bongaerts, R. Bovenberger, S. Kremes, U. Müller, S. Orf, M. Wubbolts and L. Raeven, Metabolic engineering for microbial production of shikimic acid, *Metab. Eng.*, 2003, **5**, 277–283.
- 38 (a) M. Karpf and R. Trussardi, New, azide-free transformation of epoxides into 1,2-diamino compounds: Synthesis of the anti-influenza neuraminidase inhibitor Oseltamivir phosphate (Tamiflu), *J. Org. Chem.*, 2001, **66**, 2044–2051; (b) M. Karpf and R. Trussardi, Process for the preparation of 4,5-diamino shikimate acid derivatives, *US Pat. Appl.*, 20060047002, 2006; (c) J. Guo and J. W. Frost, Synthesis of aminoshikimic acid, *Org. Lett.*, 2004, **6**, 1585–1588; (d) J. W. Frost and J. Guo, Engineered pathway for biosynthesis of 3-aminoshikimic acid as a precursor oseltamivir carboxylate, *US Pat.*, 2007190621, 2007.
- 39 For other efforts: (a) P. J. Harrington, J. D. Brown, T. Foderaro and R. C. Hughes, Research and development of a second-generation process of oseltamivir phosphate, prodrug for a neuraminidase inhibitor, *Org. Process Res. Dev.*, 2004, **8**, 86–91; (b) Y.-Y. Yeung, S. Hongs and E. J. Corey, A short enantioselective pathway for the synthesis of the anti-influenza neuraminidase inhibitor oseltamivir from 1,3-butanediene and acrylic acid, *J. Am. Chem. Soc.*, 2006, **128**, 6310–6311; (c) Y. Fukuta, T. Mita, N. Fukuda, M. Kanai and M. Shibasaki, De novo synthesis of Tamiflu via a catalytic asymmetric ring-opening of meso-aziridine with TMSN₃, *J. Am. Chem. Soc.*, 2006, **128**, 6312–6313.
- 40 See A. Liese, K. Seelbach and C. Wandrey, *Industrial Biotransformations*, Wiley-VCH, 2006, pp. 481–484.
- 41 (a) H. Yamada and M. Kobayashi, Nitrile hydratase and its application to industrial production of acrylamide, *Biosci. Biotechnol. Biochem.*, 1996, **60**, 1391–1400; (b) D. Cowan, Q. Meyer, W. Stafford, S. Muiyanga, R. Cameron and P. Wittwer, Metagenomic gene discovery: past, present and future, *Trends Biotechnol.*, 2005, **23**, 321–329.
- 42 L. Mersinger, E. Hann, F. Cooling, J. Gavagan, A. Ben-Bassat, S. Wu, K. Petrillo, M. Payne and R. DiCosimo, Production of acrylamide using alginate-immobilized *E. coli* expressing *Comamonas testosteroni* 5-MGAM-4D nitrile hydratase, *Adv. Syn. Catal.*, 2005, **347**, 1125–1131.
- 43 A. Maksimov, Y. Maksimova, M. Kuznetsova, V. Olontsev and V. Demakov, Immobilization of *Rhodococcus ruber* strain gt1, possessing nitrile hydratase activity, on carbon supports, *Appl. Biochem. Microbiol.*, 2007, **43**, 173–177.
- 44 (a) W. Niu, K. M. Draths and J. W. Frost, Benzene-free synthesis of adipic acid, *Biotechnol. Prog.*, 2002, **18**, 201–211; (b) K. M. Draths and J. W. Frost, Environmentally compatible synthesis of adipic acid from D-glucose, *J. Am. Chem. Soc.*, 1994, **116**, 399–400; (c) K. M.

- Draths and J. W. Frost, Environmentally compatible synthesis of catechol from D-glucose, *J. Am. Chem. Soc.*, 1995, **117**, 2395–2400; (d) W. Li, D. Xie and J. W. Frost, Benzene-free synthesis of catechol: Interfacing microbial and chemical catalysis, *J. Am. Chem. Soc.*, 2005, **127**, 2874–2882.
- 45 D. D. Davis and D. R. Kemp, in *Kirk–Othmer Encyclopedia of Chemical Technology*, ed. J. I. Kroschwitz and M. Howe-Grant, Wiley, New York, 4th edn, 1997, vol. 1, pp. 466–493.
- 46 E. L. Neidle and L. N. Ornston, Cloning and expression of *Acinetobacter calcoaceticus* catechol 1,2-dioxygenase structural gene *catA* in *Escherichia coli*, *J. Bacteriol.*, 1986, **168**, 815–820.
- 47 L. Krumenacker, M. Costantini, P. Pontal and J. Sentenac, in *Kirk–Othmer Encyclopedia of Chemical Technology*, ed. J. I. Kroschwitz and M. Howe-Grant, Wiley, New York, 4th edn, 1995, vol. 13, p. 996.
- 48 http://www.epa.gov/greenchemistry/pubs/docs/award_recipients_1996_2004.pdf, pp. 64–65.
- 49 A-P. Zeng and H. Biebl, Bulk chemicals from biotechnology: The case of 1,3-propanediol production and new trends, *Adv. Biochem. Eng. Biotechnol.*, 2002, **74**, 239–259.
- 50 C. Brossmer and D. Arntz, Preparation of 1,3-propanediol and ion-exchanger catalysts for it, *US Pat.*, 6 140 543, 2000.
- 51 K. T. Lam, J. P. Powell and P. R. Wieder, Preparing 1,3-propanediol, WO 97/16250, 1997.
- 52 (a) L. A. Laffend, V. Nagarajan and C. E. Nakamura, Bioconversion of a fermentable carbon source to 1,3-propanediol by a single microorganism expressing a foreign glycerol or diol dehydratase gene, *US Pat.*, 5 686 276, 1997; (b) M. Emptage, S. Haynie, L. Laffend, J. Pucci and G. Whited, Genetically engineered *Escherichia coli* containing nonspecific dehydratase *yghD* and *dha* regulon for the biological production of 1,3-propanediol with high titer, *US Pat.*, 6 514 733, 2001.
- 53 C. E. Nakamura and G. M. Whited, Metabolic engineering for the microbial production of 1,3-propanediol, *Curr. Opin. Biotechnol.*, 2003, **14**, 454–459.
- 54 *Chem. Eng. News*, 2006, **84**, 31–32.
- 55 S. Kobayashi, H. Uyama and S. Kimura, Enzymatic polymerization, *Chem. Rev.*, 2001, **101**, 3793–3818.
- 56 (a) S. Matsumura, Y. Soeda and K. Toshima, Perspectives for synthesis and production of polyurethanes and related polymers by enzyme directed toward green and sustainable chemistry, *Appl. Microbiol. Biotechnol.*, 2006, **70**, 12–20; (b) R. A. Gross, B. Kalra and A. Kumar, Polyester and polycarbonate synthesis by in vitro enzyme catalysis, *Appl. Microbiol. Biotechnol.*, 2001, **55**, 655–660; (c) R. A. Gross, A. Kumar and B. Kalra, Polymer synthesis by in vitro enzyme catalysis, *Chem. Rev.*, 2001, **101**, 2097–2124.
- 57 A. Kumar, A. S. Kulshrestha, W. Gao and R. A. Gross, Versatile route to polyol polyester by lipase catalysis, *Macromolecules*, 2003, **36**, 8219–8221.
- 58 (a) K. S. Bisht, Y. Y. Svirkin, L. A. Henderson, R. A. Gross, D. L. Kaplan and G. Swift, Lipase-catalyzed ring-opening polymerization of trimethylene carbonate, *Macromolecules*, 1997, **30**, 7735–7742; (b) K. S. Bisht, L. A. Henderson, R. A. Gross, D. L. Kaplan and G. Swift, Enzyme-catalyzed ring-opening polymerization of ω -pentadecalactone, *Macromolecules*, 1997, **30**, 2705–2711.
- 59 K. S. Bisht, F. Deng, R. A. Gross, D. L. Kaplan and G. Swift, Ethyl glycoside as a multifunctional initiator for enzyme-catalyzed regioselective lactone ring-opening polymerization, *J. Am. Chem. Soc.*, 1998, **120**, 1363–1367.
- 60 A. Kumar and R. A. Gross, *Candida antarctica* lipase B-catalyzed transesterification: new synthetic routes to copolymers, *J. Am. Chem. Soc.*, 2000, **122**, 11767–11770.
- 61 For reviews see (a) L. L. Madison and G. W. Huisman, Metabolic engineering of poly(3-hydroxyalkanoates): from DNA to plastic, *Microbiol. Mol. Biol. Rev.*, 1999, **63**, 21–53; (b) T. M. Keenan, J. P. Nakas and S. W. Tanenbaum, Polyhydroxyalkanoate copolymers from forest biomass, *J. Ind. Microbiol. Biotechnol.*, 2006, **33**, 616–626; (c) L. S. Aldor and J. D. Keasling, Process design for microbial plastic factories: metabolic engineering of polyhydroxyalkanoates, *Curr. Opin. Biotechnol.*, 2003, **14**, 475–483.
- 62 For reviews see (a) R. Datta, S.-P. Tsai, P. Bonsignore, S.-H. Moon and J. R. Frank, Technological and economic potential of poly(lactic acid) and lactic acid derivatives, *FEMS Microbiol. Rev.*, 1995, **16**, 221–231; (b) D. Garlotta, A literature review of poly(lactic acid), *J. Polym. Environ.*, 2001, **9**, 63–84.
- 63 A. Steinbuechel and H. E. Valentin, Diversity of bacterial polyhydroxyalkanoic acids, *FEBS Microbiol. Lett.*, 1995, **128**, 219–228.
- 64 (a) J. Stubbe and J. Tian, Polyhydroxyalkanoate (PHA) homeostasis: the role of the PHA synthase, *Nat. Prod. Rep.*, 2003, **20**, 445–457; (b) J. Stubbe, J. Tian, A. He, A. J. Sinskey, A. G. Lawrence and P. Liu, Nontemplate-dependent polymerization processes: polyhydroxyalkanoate synthases as a paradigm, *Annu. Rev. Biochem.*, 2005, **74**, 433–480.
- 65 Y. Doi, Microbial synthesis, physical properties, and biodegradability of polyhydroxyalkanoates, *Macromol. Symp.*, 1995, **98**, 585–599.
- 66 E. R. Olivera, D. Carnicero, R. Jodra, B. Minambres, B. Garcia, G. A. Abraham, A. Gallardo, J. San Roman, J. L. Garcia, G. Naharro and J. M. Luengo, Genetically engineered *Pseudomonas*: a factory of new bioplastics with broad applications, *Environ. Microbiol.*, 2001, **3**, 612–618.
- 67 (a) K. D. Snell and O. P. Peoples, Polyhydroxyalkanoate polymers and their production in transgenic plants, *Metab. Eng.*, 2002, **4**, 29–40; (b) E. Rezzonico, L. Moire and Y. Poirier, Polymers of 3-hydroxyacids in plants, *Phytochem. Rev.*, 2002, **1**, 87–92; (c) L. Kourtz, O. P. Peoples and K. D. Snell, Chemical-inducible expression of biosynthetic pathway enzyme genes in plants, WO 2006101983, 2006.
- 68 J. Choi and S. Y. Lee, Factors affecting the economics of polyhydroxyalkanoate productions by bacterial fermentation, *Appl. Microbiol. Biotechnol.*, 1999, **51**, 13–21.
- 69 http://www.epa.gov/greenchemistry/pubs/docs/award_recipients_2005.pdf, pp. 3–4.
- 70 D. J. C. Constable, P. J. Dunn, J. D. Hayler, G. R. Humphrey, J. L. Leazer, Jr., R. J. Linderman, K. Lorenz, J. Manley, B. A. Pearlman, A. Wells, A. Zaks and T. Y. Zhang, Key green chemistry research areas—a perspective from pharmaceutical manufacturers, *Green Chem.*, 2007, **9**, 411–420.
- 71 J. Tucker, Green chemistry, a pharmaceutical perspective, *Org. Process Res. Dev.*, 2006, **10**, 315–319.

Sunflower and rapeseed oil transesterification to biodiesel over different nanocrystalline MgO catalysts†

Marian Verziu,^a Bogdan Cojocaru,^a Juncheng Hu,^b Ryan Richards,^{*b} Crinu Ciuculescu,^c Petru Filip^c and Vasile I. Parvulescu^{*a}

Received 7th August 2007, Accepted 14th November 2007

First published as an Advance Article on the web 12th December 2007

DOI: 10.1039/b712102d

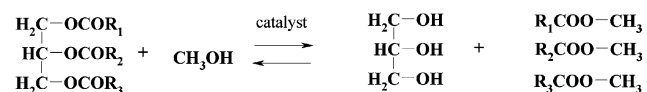
The catalytic activity for the production of biodiesel with three morphologically different nanocrystalline MgO materials prepared using simple, green and reproducible methods was investigated. The nanocrystalline samples studied were MgO(111) nanosheets (MgO (I)), conventionally prepared MgO (MgO (II)) and aerogel prepared MgO (MgO (III)). The methods to produce the catalysts included: (a) 4-methoxy-benzyl alcohol templated sol-gel process followed by supercritical drying and calcination in air at 773 K (MgO (I)), (b) from a commercial MgO that was boiled in water, followed by drying at 393 K, and dehydration under vacuum at 773 K (MgO (II)), and (c) *via* hydrolysis of Mg(OCH₃)₂ in a methanol–toluene mixture, followed by supercritical solvent removal with the formation of a Mg(OH)₂ aerogel that was dehydrated under vacuum at 773 K (MgO (III)). These catalysts were characterized by TEM, DRIFT, and DR-UV-Vis and tested in the transesterification of sunflower and rapeseed vegetable oils at low temperatures, under different experimental conditions: autoclave, microwave and ultrasound. Working with these materials under microwave conditions provided higher conversions and selectivities to methyl esters compared to autoclave or ultrasound conditions. Under ultrasound, a leaching of the magnesium has been evidenced as a direct consequence of a saponification reaction. These systems also allow working with much lower ratios of methanol to vegetable oil than reported in the literature for other heterogeneous systems. The activation temperature providing the most active catalysts was found to vary depending on the exposed facet: for MgO(111) structures (*i.e.* MgO (I)) this was 773 K, while for MgO (110) and (100) (*i.e.* MgO (II) and MgO (III)) this was 583 K.

Introduction

Biodiesel is the colloquial name for “fatty acid methyl ester” (FAME). In the present practice, this is produced *via* transesterification from vegetable oil and methanol in the presence of base catalysts. As vegetable oil, a very large family of resources can be used: palm oil, soybean oil, sunflower oil, rapeseed oil or recycled cooking oils. Biofuels from wood and other regenerative raw materials provide alternatives and will make a substantial contribution to long-term mobility in the future. Currently however, vegetable raw materials provide the most important, technically verified and readily viable option to substitute fossil energy sources, although the augmented demand for vegetable oils has increased production costs.

Alternative energy technologies are becoming increasingly important due to diminishing petroleum reserves and the environmental consequences of exhaust gases from petroleum-fueled engines. A number of studies have already shown that triglycerides hold promise as alternative diesel engine fuels.^{1–5}

The transesterification reaction with alcohol, represented by the general equation shown in Scheme 1, consists of a number of consecutive reversible reactions. The first step is the conversion of triglycerides to diglycerides, which is followed by the conversion of diglycerides to monoglycerides, and of monoglycerides to glycerol, yielding one methyl ester molecule at each step.



Scheme 1 Transesterification of triglycerides with methanol

This reaction can be catalyzed by both acid^{6,7} and alkali-catalysts.⁸ However, acid-catalyzed transesterification uses homogeneous non-green catalysts (sulfuric, phosphoric, hydrochloric, and organic sulfonic acids) and the reaction is much slower than that by alkali catalysis.^{5,9–10} This procedure seems to be more suitable when the oil component is a low grade material,

^aUniversity of Bucharest, Department of Chemical Technology and Catalysis, B-dul Regina Elisabeta 4-12, Bucharest 030016, Romania. E-mail: v_parvulescu@chem.unibuc.ro

^bColorado School of Mines, Department of Chemistry and Geochemistry, Golden, Colorado, USA. E-mail: rrichard@mines.edu

^cInstitute of Organic Chemistry, Bucharest, Romania

† This paper was published as part of the themed issue of contributions from the 3rd International Conference on Green and Sustainable Chemistry.

such as sulfur olive oil, has relatively high free fatty acid or water contents and also when ethyl esters of mono-unsaturated or short-chain fatty acids are to be obtained.⁵ Alkalis used for transesterification include NaOH, KOH, carbonates, and alkoxides, such as sodium methoxide, sodium ethoxide, sodium propoxide, and sodium butoxide. Alkali-catalyzed transesterification proceeds approximately 4000 times faster than acid-catalyzed,⁵ and therefore they are most often used commercially. Sodium methoxide has been found to be more effective than sodium hydroxide, presumably because a small amount of water is produced upon mixing NaOH and MeOH.¹¹ However, some alkali remains in the biodiesel produced and this fact has already generated concern from the automotive producers. Studies involving enzymes have been reported as well¹² but these procedures require large volumes and long reaction times. Other reported transesterification active catalysts are transition metal Mn(III) salen or vanadyl(IV) acetate complexes.¹³

A solution to the problems associated with the homogeneous catalysis might be the use of heterogeneous catalysts which can provide green, recyclable catalytic systems. The literature already contains many examples in this sense. MCM-41 prepared from gels containing 3-mercaptopropyl(methyl)-dimethoxysilane, leading to silicon atom bonded propylsulfonic moieties,^{14,15} have been reported as an alternative to the homogeneous acid catalysts. Ceria–yttria based Lewis acids were also indicated as catalysts for the transesterification of β -keto esters under environmentally safe heterogeneous reaction conditions.¹⁶ Unfortunately, the performances of these catalysts are still inferior compared with base catalysts. The preparation of monoglycerides by transesterification in the presence of heterogeneous basic catalysts, such as Sepiolite–Na–Cs, MCM-41–Cs, high surface area MgO, and hydrotalcites, was reported to be effective only for MgO and hydrotalcites and for temperatures higher than 500 K.^{17,18} Other metal oxides, such as CeO₂, La₂O₃ and ZnO, have also been used as solid base catalysts for the transesterification of glycerol, with methyl stearate in the absence of solvent.¹⁹ Other heterogeneous catalysts have also demonstrated some potential for activity in production of biodiesel from vegetable oils. Among these, zinc oxide modified with alkali earth metals,²⁰ a heterogeneous KF–ZnO catalyst²¹ and activated calcium oxide²² have shown some progress. However, all these heterogeneous systems require high methanol : oil ratios and are very sensitive to the activation temperature. Another environmentally benign process for the production of biodiesel from vegetable oils using a heterogeneous system involved a superbase Na–NaOH– γ -Al₂O₃ catalyst.²³ This catalyst showed similar activity under the optimized reaction conditions to the conventional homogeneous NaOH catalyst but is very sensitive to water.

The aim of the current paper is to compare the behavior of three different nanoscale-magnesium oxide catalysts in the transesterification of sunflower and rapeseed oils. There are numerous approaches to the preparation of nanoscale MgO that lead to different sizes and morphologies of the material, and ultimately the chemical reactivity. Examples of the ‘state of the art’ preparation methods include: hard templating leading to mesoporous,^{24,25} chemical vapor deposition leading to cubic nanoparticles,²⁶ or aerogel-supercritical drying—leading to interconnected network of cubic particles.^{27,28} However, although there are differences in the morphology of these systems, they

all possess the (100) facet as their primary surface, while the (111) surface is more interesting as it is composed of alternating monolayers of anions and cations and thus, a strong electrostatic field perpendicular to the (111) surface is created.²⁹ Generally, the catalytic performance of metal oxides can be finely tailored by their surface atomic arrangement and coordination, as the catalytic process occurs on solid surfaces and surface structure typically controls activity and selectivity kinetically. Fig. 1 shows the relation between the exposed face and the coordination of MgO.³⁰ Recently, we have discovered a simple method to prepare a sheet-like MgO with the highly ionic (111) facet as the major surface of the nano-sheet, and found that the polar (111) surface oriented MgO nano-sheets showed ultrahigh activity for the typically base-catalyzed Claisen–Schmidt condensation.³¹ Further, DRIFTS and TPRS studies of methanol indicate that MgO(111) nano-sheets are highly reactive towards the decomposition of methanol.³² The high activities of MgO nano-sheets are attributed to the novel crystalline structure with the high surface energy polar (111) surface as the main surface. It is anticipated that the MgO(111) nano-sheets may show increased activity in contrast to other nanocrystalline MgO for the transesterification of vegetable oil and methanol. Therefore, we decided to investigate the catalytic properties of these nanocrystalline MgO catalysts directly together with other highly active MgO nanoscale materials. The catalysts were tested in autoclave, microwave and ultrasound conditions. Previous reports indicated that microwave irradiation can provide a rapid and convenient method for transesterification of triglycerides, as well as phospholipids.³³

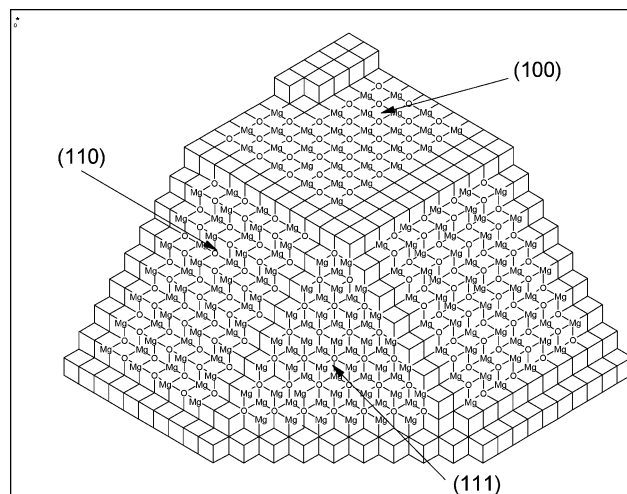


Fig. 1 The (100), (110) and (111) facets of MgO

Experimental

Catalyst preparation

All catalysts were synthesized using green procedures that have been reported elsewhere. Thus, MgO (I) was prepared starting from 4-methoxy-benzyl alcohol that was added to a 10 wt% Mg(OCH₃)₂ methanol solution, followed by addition of a water–methanol mixture to the system and subsequent supercritical treatment and calcination in air at 773 K.³¹ MgO (II) was

prepared starting from a commercial MgO (Aldrich) that was boiled for 5 h in water, followed by drying at 393 K for 15 h, and dehydration under vacuum at 773 K for 6 h.²⁸

MgO (III) was obtained *via* hydrolysis of Mg(OCH₃)₂ in a methanol–toluene mixture, followed by supercritical solvent removal with the formation of a Mg(OH)₂ aerogel, that was dehydrated under vacuum at 773 K.²⁸

Conventional MgO microcrystalline catalysts were prepared by a precipitation method from Mg(NO₃)₂ and NH₄OH.¹⁹ A solution of NH₄OH (30%, 100 mL) was added dropwise to a solution of Mg(NO₃)₂·6H₂O (50 g) in 80 mL of distilled water under stirring at 313 K. Magnesium hydroxide was precipitated and digested in the mother liquor at 323 K for 4 h. The precipitate was washed with distilled water, dried under vacuum at 373 K, and then calcinated at 773 K for 10 h in air.

Catalyst characterization

N₂ adsorption/desorption isotherms at 77 K were performed with a Quantachrome Autosorb 1-C, the data were analyzed by employing the Barrett–Joyner–Halenda (BJH) method; pore volume and pore size distribution curves were obtained from the desorption branch of the isotherm. The textural characteristics of these oxides are given in Table 1.

TEM characterization of the MgO samples was carried out on an FEI Tecnai F20 S-Twin operated at 200 kV. The samples were prepared by spreading an ultrasonicated suspension in ethanol on carbon-coated copper grids. TEM and high-resolution images of the nano-sheets were acquired with a Gatan 794 CCD camera. Electron diffraction simulation was performed using the software MS Modeling (MS Modeling V3.0 by Accelrys). Table 1 also compiles the crystallites size of these nanoscale metal oxides.

Temperature programmed desorption (TPD) of CO₂ measurements were performed using a Quantachrome Autosorb-1-C/MS. The sample (50 mg) was placed in the quartz reactor and pre-treated in Ar for 1 h at 500 °C, then cooled down to room temperature. CO₂ adsorption was performed by a stream of 100 mL CO₂ min⁻¹ at room temperature for 1 h. After the gas phase, physically adsorbed CO₂ was purged by an Ar flow at room temperature for 0.5 h. TPD was carried out in a stream of Ar (40 mL min⁻¹) with a heating rate of 10 °C min⁻¹ to 800 °C, and the effluent was detected by an on-line mass spectrometer.

For FTIR investigation of the catalyst, a Thermo 4700 spectrometer with a liquid nitrogen cooled detector and DRIFT accessory was used with the following parameters: 300 scans, 600–4000 cm⁻¹ scan range, 4 cm⁻¹ resolution. DR-UV-Vis spectra were collected with a Thermo Electron Specord 250 spectrometer in the range 200–800 nm using 15 scans.

Table 1 Textural characteristics of the investigated MgO catalysts

| Catalyst | BET surface area/m ² g ⁻¹ | Crystallite size/nm |
|-----------|---|-------------------------------------|
| MgO (I) | 198 | 50–200 nm diameter and 3–5 nm thick |
| MgO (II) | 80 | 8.8 |
| MgO (III) | 435 | 1–4.5 |

Catalytic tests

Typical experiments were carried out using 23 mL sunflower or rapeseed oil and 5 mL methanol (molar ratio oil : methanol of 1 : 4). To this system, 300 mg MgO were added and the reaction was carried out either in a stainless steel autoclave (2 h), under microwave (40 min) or ultrasound irradiation (2 h). Under autoclave and microwave conditions, the stirring rate was 1200 rpm. The temperature inside the vessel was controlled using either a thermocouple (autoclave and ultrasound) or fiber optic (microwave).

Analysis of the reaction products was made using a Varian ProStar 310 HPLC equipped with a C18 column with inner diameter of 4 mm and the length of 30 cm. The mobile phase was a mixture of methanol (pump A) and isopropanol : hexane in a volume ratio 5 : 4 (pump B), A : B of 85 : 15 with a flow of 0.8 mL min⁻¹. The analysis was made with a UV-Vis detector working at $\lambda = 205$ nm. The identification of the products was made using a GC-MS Carlo Erba Instruments QMD 1000 equipped with a Factor Four VF-5HT column with the following characteristics: 0.32 mm × 0.1 μ m × 15 m working with a temperature program at a pressure of 50.8 kPa, with He as the carrier gas. The samples were solubilized in CH₂Cl₂.

The experimental procedure to test the recyclability of the catalyst was as follows: the first run was carried out as described above. Before stopping the agitation, an aliquot was sampled and analysed following the method described above. Then the agitation was stopped and the mixture was rapidly centrifuged at 6000 rpm for 10 min. The solid was recovered and subjected to the reaction-sampling-analysis-centrifugation sequence for several successive runs without being subjected to any previous activation-outgassing step.

Leaching of magnesium was checked with an ICP-AES apparatus (Analyst 800 from Perkin-Elmer) working at $\lambda = 285.2$ nm (typical for Mg). The samples were prepared using a typical procedure for the analysis of oils by introducing 0.5 mL sample into the digestion vessel, then adding 10 mL of nitric acid 65 wt% and 2 mL hydrogen peroxide 30 wt%. The vessel was then closed and heated in the microwave oven at 483 K for 15 min.

Results and discussions

Catalyst characterization

As is observed from Table 1, all of the investigated nanoscale materials exhibit high surface areas. TEM images of the resultant catalysts showed that the syntheses perfectly reproduced the procedures described in the literature.^{28–31} For MgO (I) after calcination, highly isolated MgO nano-sheets were observed with the majority of the sheet-like nanoparticles oriented almost parallel to the support film, however, some of the sheets can be observed on their edge, as in Fig. 2. HRTEM analysis of isolated MgO nano-sheets shows that the main surface of the nano-sheets is the (111) lattice plane (Fig. 3). When imaging the nano-sheets edge on, the HRTEM images exhibit lattice fringes with a distance of 0.24–0.25 nm parallel to the main surface of the nano-sheet, in good agreement with the (111) lattice spacings of MgO. TEM characterization of MgO (II) corresponded to interconnected MgO domains about 2 nm with

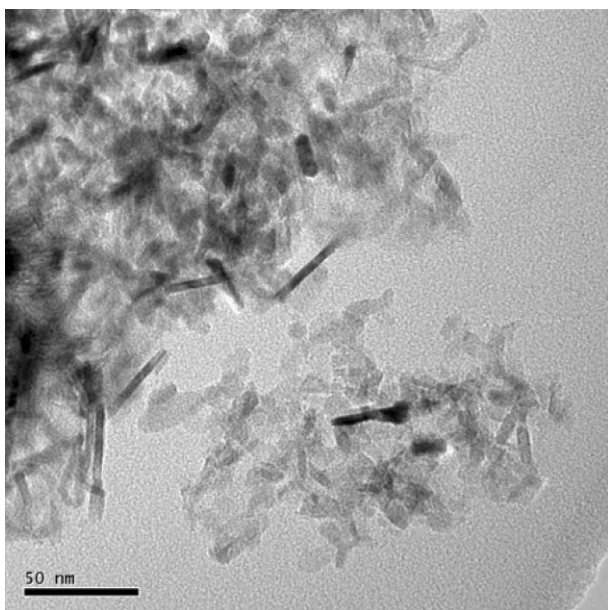


Fig. 2 TEM image of MgO (I).

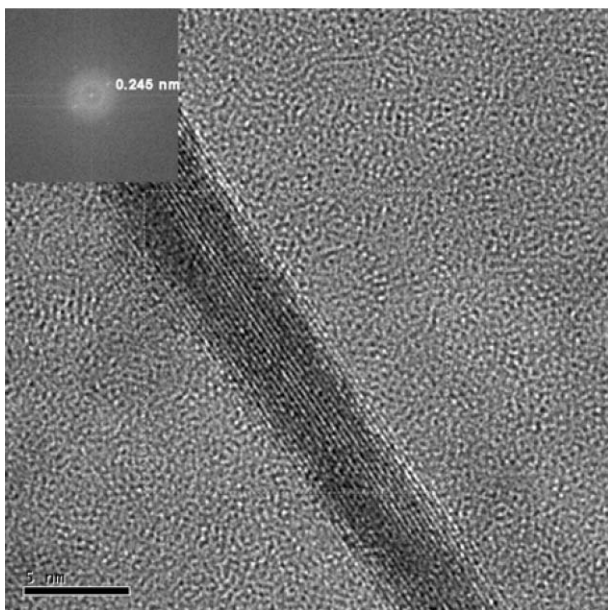


Fig. 3 HRTEM and FFT of an isolated MgO (I) nano-sheet.

parallel (110) planes with lattice spacing of 1.48 Å,²⁸ while for MgO (III) monocrystalline particles between 1 and 3 nm with lattice spacing of 2.1 Å corresponding to the (100) plane were determined.

CO₂-TPD was used to measure the surface basicity for each MgO system. From Fig. 4, it can be observed that the TPD profile of each MgO catalyst contains several CO₂ desorption peaks, indicating that a variety of basic sites with different strengths are present on each surface. The strength of basic sites increases as the temperature of the peaks appear in the TPD profile. The chemical nature of these basic sites determines the base strength order: low coordination oxygen anions > oxygen in Mg²⁺ and O²⁻ pairs > hydroxyl groups. To facilitate discussion, these desorption peaks have been divided into three groups exhibiting

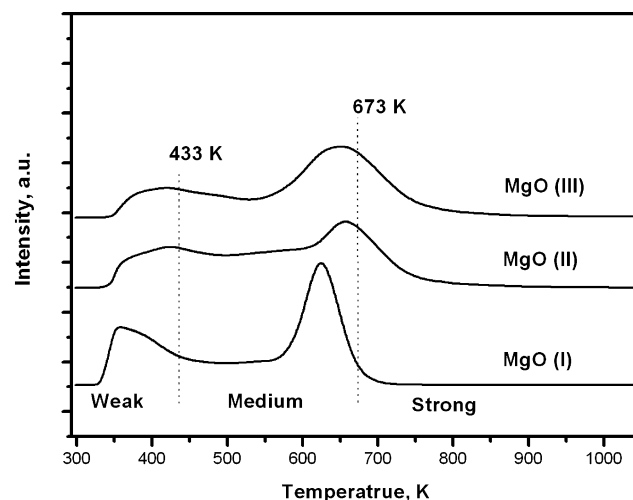


Fig. 4 TPD of CO₂ over different nanocrystalline MgO catalysts.

weak (CO₂ desorption between 293 K and 433 K), medium (CO₂ desorption between 433 K and 673 K) and strong basicity (CO₂ desorption higher than 673 K). The peaks between 293 K and 433 K can be attributed to the interaction of CO₂ with the weak basic sites that correspond to hydroxyl groups on the surface. The second group between 433 K and 673 K is most likely associated with oxygen in the Mg²⁺ and O²⁻ pairs. Finally, those higher than 673 K could be due to the presence of strong basic sites, probably corresponding to isolated O²⁻. For MgO (I), the large area peak between 433 K and 673 K centered at 623 K indicates the presence of a large number of medium basic sites, which most likely corresponds to the particular structure of MgO (111) with alternating ionic layers. Also, Fig. 4 shows the presence of smaller CO₂ desorption peaks in the strong basic site region for MgO (II) and MgO (III). Thus, among the three MgO materials, the MgO (I) catalyst with the (111) surface shows the greatest number of basic surface sites by comparison of the amount of CO₂ desorbed.

Catalytic behaviour

1. Transesterification of sunflower oil in autoclave conditions.

Testing the conventional microcrystalline MgO catalyst in transesterification of sunflower oil led to a conversion of 80% at 493 K, with a yield in methyl esters of 55%, while decreasing the temperature to 373 K corresponded to a decrease of the conversion to 25%, with a 32% yield of methyl esters. These results are in line with previous reports of Corma *et al.*¹⁷ and Barrault and coworkers³⁴ in other transesterification reactions. They attributed this behaviour to the greater lipophilicity of the fatty methyl esters compared to that of fatty acids.

Fig. 5 shows the conversion and yield in methyl esters on the investigated nano-MgO catalysts activated at different temperatures. In comparison with microcrystalline MgO, nanoscale MgO-catalysts exhibit higher activity and selectivity, even at 343 K. Also, MgO (I) with the (111) facet, is more active and selective than MgO (II) or (III), which is in accordance with the model depicted in Fig. 1. The temperature at which the nano-catalysts were activated before the catalytic tests is also important and is individual to each type of catalyst. While the

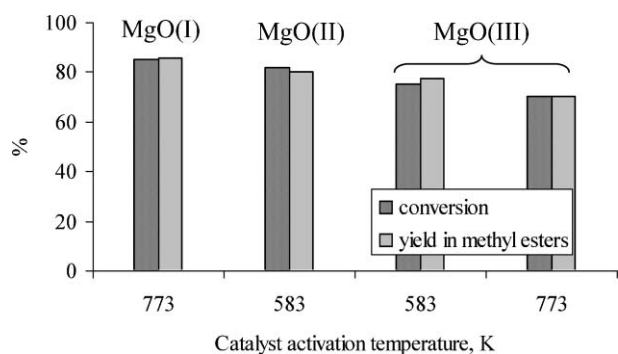


Fig. 5 Transesterification of sunflower oil on nanoscale MgO catalysts in autoclave conditions (23 mL sunflower oil, 5 mL methanol (molar ratio sunflower oil to methanol of 1 : 4), 300 mg MgO, 343 K, 2 h)

(111) structure (MgO (I)) requires an activation temperature of 773 K, for the MgO (II) and (III) catalysts with the (110) and (100) surfaces, the highest activity and selectivity was achieved after calcining at 583 K. These temperatures are much smaller than generally reported in the literature for MgO catalysts, which are typically over 973 K.¹⁷

Leaching of magnesium, as determined from ICP-AES measurements, showed that the magnesium content in the glycerol and biodiesel was less than 10 ppm, irrespective of the catalyst and the reaction conditions.

2. Transesterification of sunflower oil under microwave conditions. Transesterification under microwave conditions occurred with higher conversions for shorter reaction times as is typical using such conditions (Fig. 6–9). The differences between the conversion and yield are a consequence of the fact that the conversion was not always complete to methyl esters, and in several cases some di- and monoglycerides were not completely transformed to methyl esters. When calcined at 583 K, the catalyst is less active than that calcined at 773 K. However, recycling the catalysts without any additional treatment led, as a general tendency, to an increase of both the conversion and yield of methyl esters. After the fifth cycle, these reach a conversion of over 99%, with a yield of methyl ester over 98%. Practically no saponification of magnesium has been detected.

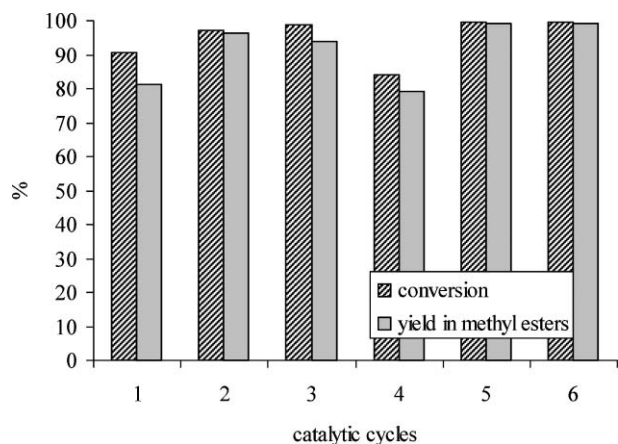


Fig. 6 Transesterification of sunflower oil under microwave conditions on nano-MgO (I) catalyst activated at 583 K (23 mL sunflower oil, 5 mL methanol (molar ratio sunflower oil to methanol of 1 : 4), 300 mg MgO, 343 K, 40 min).

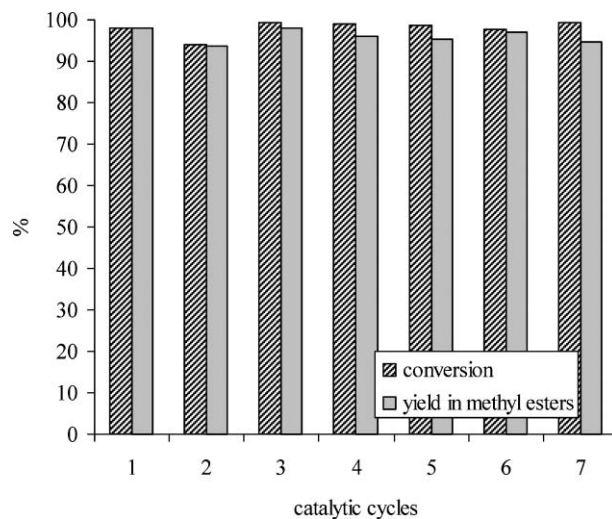


Fig. 7 Transesterification of sunflower oil under microwave conditions on nano-MgO (I) catalyst activated at 773 K (23 mL sunflower oil, 5 mL methanol (molar ratio sunflower oil to methanol of 1 : 4), 300 mg MgO, 343 K, 40 min).

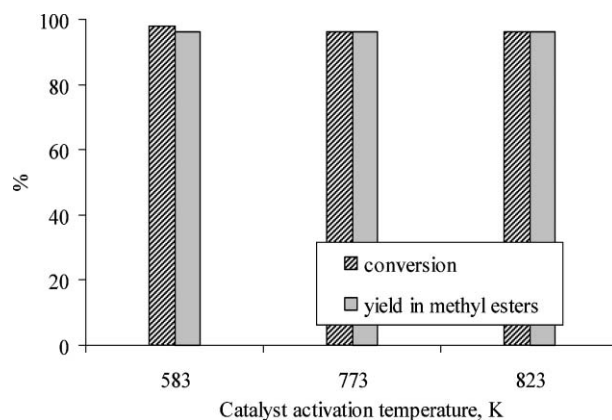


Fig. 8 Transesterification of sunflower oil under microwave conditions on nano-MgO (II) catalyst (23 mL sunflower oil, 5 mL methanol (molar ratio sunflower oil to methanol of 1 : 4), 300 mg MgO, 343 K, 40 min).

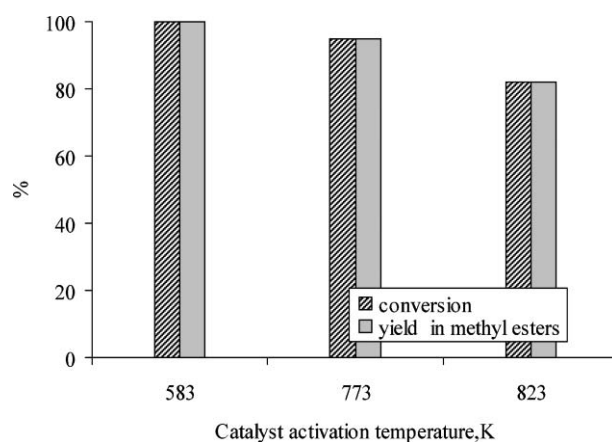


Fig. 9 Transesterification of sunflower oil under microwave conditions on nano-MgO (III) catalyst (23 mL sunflower oil, 5 mL methanol (molar ratio sunflower oil to methanol of 1 : 4), 300 mg MgO, 343 K, 40 min).

For the reactions carried out in autoclave conditions, ICP-AES analysis of both phases (glycerol and biodiesel) showed that the concentration of soluble magnesium species was less than 10 ppm. The modification of the catalyst activation temperature was not accompanied by any change in the leaching.

This quality allows the use of this biodiesel directly without any additional washing. However, passing the separated biodiesel over a column containing an ion-exchange resin can reduce this content further, to a level of less than 0.5 ppm.

Very high conversions and yields were also obtained for MgO (II) (Fig. 8) and MgO (III) (Fig. 9) and the data presented in these figures confirm the optimal activation temperature to be 583 K for these structures. Upon recycling of these catalysts, like MgO (I), no deterioration of performance was observed through a course of at least seven runs. Further, no saponification of magnesium has been detected over seven runs, while the soluble magnesium in biodiesel was less than 10 ppm.

3. Transesterification of sunflower oil under ultrasound conditions. Fig. 10 shows the performances of nano-MgO (II) and (III) catalysts in the transesterification of sunflower oil under ultrasound conditions. Very good conversions and yields were also obtained under these conditions. However, during the reaction, part of the magnesium is leached *via* saponification. This corresponds to contents between 1 and 3 percent per cycle and depends on the nature of the catalysts and the quality of the oil. Table 2 compiles these data. The leaching varied in the order Mg (111) > Mg (110) > MgO microcrystalline, that actually corresponds to the order of the exposed atoms in the network. The temperature at which the MgO has been activated exhibits

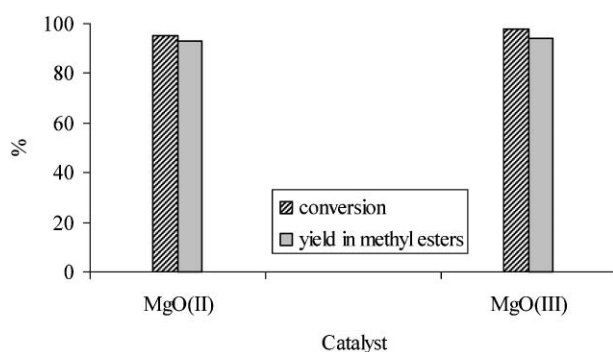


Fig. 10 Transesterification of sunflower oil under ultrasound conditions on nano-MgO (II) and (III) catalysts activated at 583 K (23 mL sunflower oil, 5 mL methanol (molar ratio sunflower oil to methanol of 1 : 4), 300 mg MgO, 343 K, 2 h).

no effect on leaching. However, the degree of affinage is a very important factor in this sense, with a more pure oil favouring an increased degree of leaching. After reusing the remaining amount of catalysts in the next catalytic cycles, the degree of leaching remained essentially the same.

Separate analysis of biodiesel indicates that the content in soluble magnesium species varied in the same order as for the saponification: MgO (I) (128 ppm) > MgO (II) (102 ppm) \approx MgO (III) 97 ppm. Approximately the same content was found in the glycerol.

The different behavior between the ultrasound and microwave conditions should be attributed to the fact that under ultrasound, the disruption of particles is favoured, thus allowing saponification and solving of nanoparticles in both glycerol and biodiesel.

4. Transesterification of rapeseed oil under microwave and ultrasound conditions. Fig. 11 and 12 present results in transesterification of rapeseed oil under microwave and ultrasound conditions. In both conditions, the conversions and yields were slightly lower than those obtained using sunflower oil as substrate. As in the case of transesterification of sunflower oil, recycling did not affect the performances of the catalysts. In ultrasound conditions, leaching of magnesium is still present, although the leached amount was always smaller than in the corresponding conditions using sunflower oil.

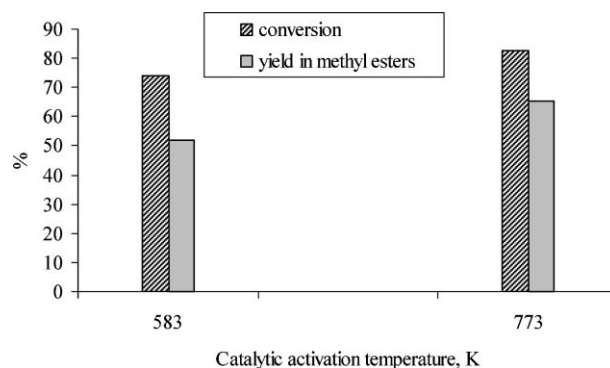


Fig. 11 Transesterification of rapeseed oil under microwave conditions on nano-MgO (II) catalyst (23 mL rapeseed oil, 5 mL methanol (molar ratio rapeseed oil to methanol of 1 : 4), 300 mg MgO, 343 K, 40 min).

Under microwave conditions the leaching was, as in the case of sunflower oil, on the order of a few ppm. However, working under ultrasound conditions, this was accelerated and as can

Table 2 Leaching of magnesium in saponificated salts under ultrasound conditions after the first cycle

| Catalyst | Activation temperature/K | Oil | Reaction conditions | Mg leached (%) |
|----------------------|--------------------------|---------------|---------------------|----------------|
| MgO microcrystalline | 773 | Sunflower oil | 343K | 0.54 |
| MgO microcrystalline | 773 | Rapeseed oil | 343K | 0.27 |
| MgO (I) | 583 | Sunflower oil | 343K | 2.90 |
| MgO (I) | 773 | Sunflower oil | 343K | 2.87 |
| MgO (I) | 583 | Rapeseed oil | 343K | 1.84 |
| MgO (I) | 773 | Rapeseed oil | 343K | 1.86 |
| MgO (I) | 773 | Sunflower oil | 343K | 2.34 |
| MgO (II) | 773 | Rapeseed oil | 343K | 1.18 |
| MgO (III) | 773 | Sunflower oil | 343K | 2.21 |
| MgO (III) | 773 | Rapeseed oil | 343K | 1.12 |

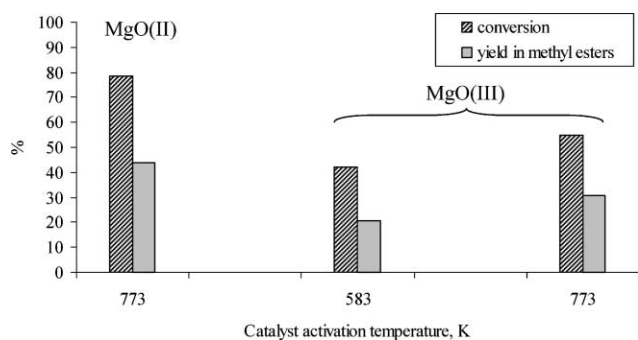


Fig. 12 Transesterification of rapeseed oil under ultrasound conditions on nano-MgO (II) and (III) catalysts activated at 583 K (23 mL rapeseed oil, 5 mL methanol (molar ratio rapeseed oil to methanol of 1 : 4), 300 mg MgO, 343 K, 2 h).

be seen from the Table 2, it was leaching in the direction of saponification. Comparing the leaching of the different MgO catalysts to saponificated salts in sunflower and rapeseed oils, leaching was consistently smaller in the rapeseed oil, indicating that the composition of the vegetable oil is playing an important role in this process. However, the analysis of the soluble magnesium in both the glycerol and biodiesel was higher in rapeseed oil than in the sunflower. Thus, it decreased in the following order: MgO (I) (289 ppm) > MgO (II) (251 ppm) \approx MgO (III) 242 ppm.

5. Effect of the molar ratio of vegetable oil to methanol. The molar ratio of vegetable oil to methanol is an important variable affecting the ester yield and the conversion. The stoichiometry of the transesterification reaction requires 3 moles of alcohol per mole of triglyceride to yield 3 moles of fatty esters and 1 mole of glycerol (see Scheme 1). Higher molar ratios result in greater ester conversion in a shorter time.^{35,36} These studies indicated that a molar ratio of vegetable oil to methanol of 1 : 6 is most effective using sodium methoxide as a catalyst, and as a consequence it is normally used in industrial processes to obtain methyl ester yields higher than 98% on a weight basis.

The patent literature provides the few examples of transesterification carried out at higher vegetable oil to methanol ratios, *i.e.* in the range of 1 : 4. These require rather severe conditions, such as one or two steps of esterification before the transesterification in homogeneous conditions with alkaline hydroxides,^{37,38} or under heterogeneous conditions: reaction in the presence of an ion-exchange resin in the OH form followed by the extraction of methyl esters under near-critical CO₂ or propane extraction,³⁹ or of a combination of zinc, titanium, bismuth and aluminum oxide at 170–270 °C and high pressure,⁴⁰ or accelerated esterification-transesterification *via* production of emulsions and then transesterification either with hydroxides or with ion-exchange resins in the OH form at a high speed to reach “high-shear” conditions.⁴¹

Typical heterogeneous catalysts reported as active in the last decade are active for much smaller ratios than 1 : 6.^{20–22} Therefore, it is indeed remarkable that these nano-MgO oxides are able to carry out the transesterification of vegetable oils with ratios (vegetable oil to methanol) as high as 1 : 4 under the investigated temperature and pressure conditions.

6. Activation temperature and active sites. The effect of the activation temperature and deactivation of the catalysts was also investigated by *in situ* DRIFTS experiments. Fig. 13 shows the effect of the thermal activation. For MgO (I) in the range 3800–3000 cm⁻¹, a large band due to the OH group vibrations of the bound H₂O on the surface of the sample and a weak band at 3764 cm⁻¹ assigned to basic OH groups is visible (Fig. 13a).⁴² The increase of the temperature caused a disappearance of the band assigned to adsorbed water and a shift of the basic OH into a very sharp and intense band associated with an OH frequency that does not form hydrogen bonds with the surface of the sample to 3733 cm⁻¹. A similar behavior was also found for MgO (II) and (III) (Fig. 13b). The maximum intensity of this band is achieved at 773 K for MgO (I) and 583 K for MgO (II) and (III), thus further explaining the catalytic results.

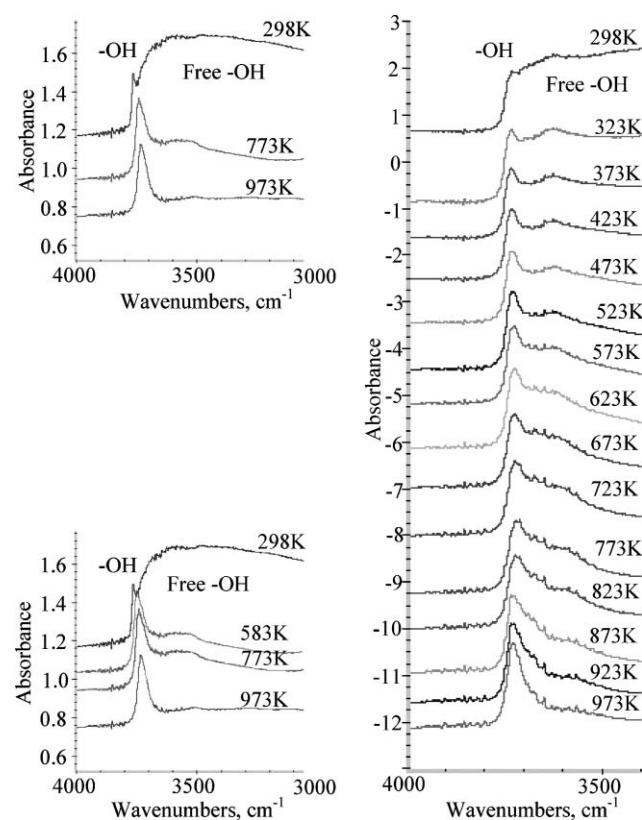


Fig. 13 FT-IR spectra of (a) fresh MgO (I), (b) fresh MgO (II) and (c) tested catalysts in the region 4000–3000 cm⁻¹

As previously mentioned, the catalysts were recycled without any reactivation. The used catalysts showed a weak shoulder at 3720 cm⁻¹ (Fig. 13c). Calcining these catalysts recovered the band at 3724 cm⁻¹, but at higher temperatures. These temperatures were required by the acidic species, which are more strongly chemisorbed than water.

A very interesting feature of these nano-MgO catalysts is the fact that they do not chemisorb CO₂. No band has been detected in the range 2400–2000 cm⁻¹. However, after reaction, the surface is covered with by-products and unreacted molecules (Fig. 14). Heating the samples results in the recovery of the surface. This fact demonstrates these species are not very strongly bound and explain the results in recycling the catalysts.

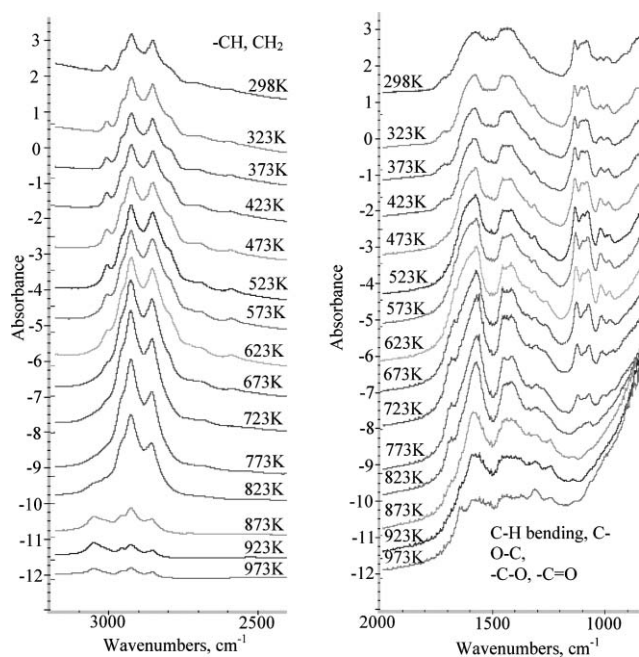


Fig. 14 FT-IR spectra of MgO (I) tested catalysts in the regions 3000–2500 and 2000–1000 cm^{-1}

After reaction, DRIFT spectra showed new peaks assigned to the C–H stretching, –CH deformation modes and C–CH₃ bond vibration, to C–O–C, –C–O, and –C=O vibrations as well (Fig. 14).⁴³ These peaks result from the contribution of both adsorbed glycerol and biodiesel molecules. However, both are soluble in the vegetable oil, and as we demonstrated, recycling can occur without any reactivation.

Fig. 15 gives the DR-UV-Vis spectra of the fresh and tested MgO (III) catalyst. The UV-Vis spectra of the initial sample exhibits two minima of reflectance (corresponding to a maximum of absorption) at 246 nm (I) and 380 nm (II), which correspond to exciton charge transfer transitions from a surface oxygen ($\text{O}^{2-}_{\text{sc}}$ and $\text{O}^{2-}_{\text{4c}}$) to its immediate surroundings.⁴⁴ After

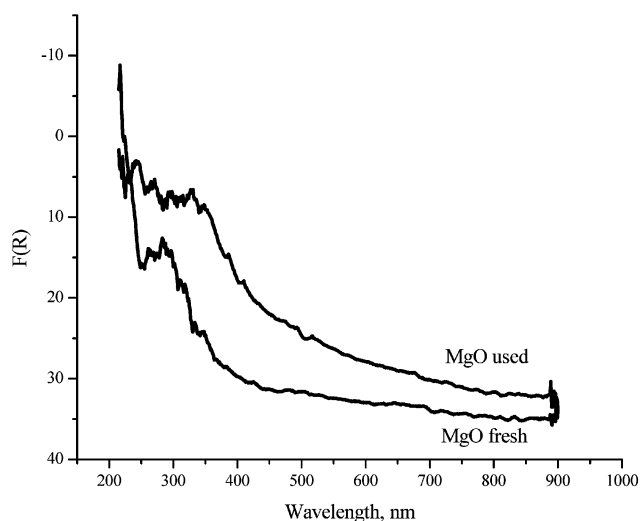


Fig. 15 The DR-UV-Vis spectra of fresh and tested MgO (III) catalyst

reaction, it was observed that these bands almost disappeared, indicating these species remain blocked by the substrates.

Conclusions

Nanostructures of MgO possessing the (111) (110) and (100) surfaces can be prepared in very simple and reproducible ways. In addition, these preparations are very green, involving non-toxic reagents and synthesis routes. These metal oxides are active, recyclable heterogeneous catalysts for transesterification of vegetable oils at low temperatures, as it has been demonstrated for sunflower and rapeseed oils. These systems allow working with much smaller methanol to vegetable oil ratios than reported in literature for other heterogeneous systems. The performances of these materials in transesterification was found to depend on the nature of the treated oil.

The activation temperature providing the most active catalysts was dependent on the exposed facet: for MgO (111) structures (*i.e.* MgO (I)) this was 773 K, while for MgO (110) and (100) (*i.e.* MgO (II) and MgO (III)) this was 583 K. The catalytic behaviour of these samples is mostly associated with the density of the basic sites and not necessarily with the basicity strength.

Working under microwave conditions with these systems led to higher conversions and selectivities to methyl esters, as compared to autoclave or ultrasound conditions. However, under ultrasound, a leaching of the magnesium has been evidenced as a direct consequence of a saponification reaction.

Thus, these investigations demonstrate that nanostructured MgO can be used effectively as a heterogeneous catalyst system for biodiesel transesterification and the facet of MgO exposed has an important influence regarding activity and selectivity.

References

- 1 D. Bartholomew, *J. Am. Oil Chem. Soc.*, 1981, **58**, 286A.
- 2 E. H. Pryde, *J. Am. Oil Chem. Soc.*, 1983, **60**, 1557.
- 3 C. Adams, J. F. Peters, M. C. Rand, B. J. Schroer and M. C. Ziemke, *J. Am. Oil Chem. Soc.*, 1983, **60**, 1574.
- 4 E. G. Shay, *Biomass Bioenerg.*, 1993, **4**, 227.
- 5 H. Fukuda, A. Kondo and H. Noda, *J. Biosci. Bioeng.*, 2001, **92**, 405.
- 6 E. J. Dufek, R. O. Butterfield and E. N. Frankel, *J. Am. Oil Chem. Soc.*, 1972, **49**, 302.
- 7 H. Nouredini and D. Zhu, *J. Am. Oil Chem. Soc.*, 1997, **74**, 1457.
- 8 B. Freedman, R. O. Butterfield and E. H. Pryde, *J. Am. Oil Chem. Soc.*, 1986, **63**, 1375.
- 9 F. Ma and M. A. Hanna, *Bioresour. Technol.*, 1999, **70**, 1.
- 10 A. Srivastava and R. Prasad, *Renew. Sust. Energ. Rev.*, 2000, **4**, 111.
- 11 R. Alcantara, J. Amores, L. Canoira, E. Fidalgo, M. J. France and A. Navarro, *Biomass Bioenerg.*, 2000, **18**, 515.
- 12 M. Kaieda, T. Samukawa, T. Matsumoto, K. Ban, A. Koudo, Y. Shimada, H. Noda, F. Nomoto, K. Ohtsuka, E. Izumoto and H. Fukuda, *J. Biosci. Bioeng.*, 1999, 627.
- 13 M. Lakshmi Kantam, V. Neeraja, B. Bharathi and Ch. Venkat Reddy, *Catal. Lett.*, 1999, **62**, 67.
- 14 I. Draz, F. Mohino, J. Perez-Pariente and E. Sastre, *Appl. Catal., A*, 2003, **242**, 161.
- 15 C. Marquez-Alvarez, E. Sastre and J. Perez-Pariente, *Top. Catal.*, 2004, **27**, 105.
- 16 R. Kumar Pandey and P. Kumar, *Catal. Commun.*, 2007, **8**, 1122.
- 17 A. Corma, S. Iborra, S. Miquel and J. Primo, *J. Catal.*, 1998, **173**, 315.
- 18 B. M. Choudary, M. Lakshmi Kantam, Ch. Venkat Reddy, S. Aranganathan, P. Lakshmi Santhi and F. Figueras, *J. Mol. Catal. A: Chem.*, 2000, **159**, 411.
- 19 S. Bancquart, C. Vanhove, Y. Pouilloux and J. Barrault, *Appl. Catal., A*, 2001, **218**, 1.

- 20 Z. Yang and W. Xie, *Fuel Process. Technol.*, 2007, **88**, 631.
- 21 W. Xie and X. Huang, *Catal. Lett.*, 2006, **107**, 53.
- 22 M. Lopez Granados, M. D. Zafra Poves, D. Martın Alonso, R. Mariscal, F. Cabello Galisteo, R. Moreno-Tost, J. Santamarıa and J. L. G. Fierro, *Appl. Catal., B*, 2007, **73**, 317.
- 23 H.-J. Kim, B.-S. Kang, M.-J. Kim, Y. M. Park, D.-K. Kim, J.-S. Lee and K.-Y. Lee, *Catal. Today*, 2004, **93–95**, 315.
- 24 W. C. Li, A. H. Lu, C. Weidenthaler and F. Schüth, *Chem. Mater.*, 2004, **16**, 5676.
- 25 J. Roggenbuck and M. Tiemann, *J. Am. Chem. Soc.*, 2005, **127**, 1096.
- 26 S. Stankic, M. Mueller, O. Dewald, M. Sterrer, E. Knözinger and J. Bernardi, *Angew. Chem.*, 2005, **117**, 4996; *Angew. Chem., Int. Ed.*, 2005, **44**, 4917.
- 27 S. Utamapanya, K. J. Klabunde and J. R. Schlup, *Chem. Mater.*, 1991, **3**, 175.
- 28 R. Richards, W. Li, S. Decker, C. Davidson, O. Koper, V. Zaikovski, A. Volodin, T. Rieker and K. J. Klabunde, *J. Am. Chem. Soc.*, 2000, **122**, 4921.
- 29 P. W. Tasker, *J. Phys. C: Solid State Phys.*, 1979, **12**, 4977.
- 30 K. J. Klabunde, *Nanoscale Materials in Chemistry*, ed. K. J. Klabunde, Wiley Interscience, New York, New York, 2001, pp. 223–261.
- 31 K. Zhu, J. Hu, C. Kuebel and R. Richards, *Angew. Chem., Int. Ed.*, 2006, **45**, 7277.
- 32 J. Hu, K. Zhu, L. Chen, C. Kübel and R. Richards, *J. Phys. Chem. C*, 2007, **111**, 12038.
- 33 A. Dasgupta, P. Banerjee and S. Malik, *Chem. Phys. Lipids*, 1992, **62**, 281.
- 34 G. Kharchafi, F. Jérôme, I. Adam, Y. Pouilloux and J. Barrault, *New J. Chem.*, 2005, **29**, 928.
- 35 K. Krisnangkura and R. Simamaharnnop, *J. Am. Oil Chem. Soc.*, 1992, **69**, 166.
- 36 R. Fillieres, B. Benjelloun-Mlayah and M. Delmas, *J. Am. Oil Chem. Soc.*, 1995, **72**, 427.
- 37 H. Lepper and L. Friesenhagen, *US Pat.*, 4652406A1, 1987.
- 38 M. Gross and G. Tschampel, *DE Pat.*, 4301686C1, 1994.
- 39 S. Peter, R. Ganswindt and E. Weidner, *US Pat.*, 6211390B1, 2001.
- 40 B. Delfort, G. Hillion, D. Le Pennec and C. Lendresse, *US Pat.*, 2005261509A1, 2005.
- 41 M. A. Portnoff, D. A. Purta, M. A. Nasta, J. Zhang and F. Pourarian, *US Pat.*, 2005274065A1, 2005.
- 42 J. A. Wang, O. Novaro, X. Bokhimi, T. Lopez, R. Gomez, J. Navarrete, M. E. Llanos and E. Lopez-Salinas, *Mater. Lett.*, 1998, **35**, 317.
- 43 Spectral Database for Organic Compounds, www.aist.go.jp.
- 44 G. Spoto, E. N. Gribov, G. Ricchiardi, A. Damin, D. Scarano, S. Bordiga, C. Lamberti and A. Zecchina, *Prog. Surf. Sci.*, 2004, **76**, 71.

Palladium nanoparticles on polysaccharide-derived mesoporous materials and their catalytic performance in C–C coupling reactions†

Vitaly L. Budarin, James H. Clark,* Rafael Luque, Duncan J. Macquarrie and Robin J. White

Received 9th October 2007, Accepted 5th November 2007

First published as an Advance Article on the web 26th November 2007

DOI: 10.1039/b715508e

Palladium nanoparticles were successfully prepared using porous materials derived from starch as support media. The nanoparticle size distribution was controllable by selection of the preparation solvent. Materials were characterised and catalytically tested in various C–C coupling reactions, exhibiting excellent catalytic activities in the microwave-assisted Heck, Suzuki and Sonogashira reactions. The palladium-supported materials were also reusable, preserving their catalytic activities after four reuses.

Introduction

Metal nanoparticles have attracted much attention over the last decade due to their potential tuneability in terms of size, shape and activity. This makes them particularly interesting in a variety of applications including sensors, non-linear optics, medical dressings and catalysis.¹ The support material on which these nanoparticles are synthesized has also received significant attention in the literature. Many different materials have been employed to support nanoparticles, including mesoporous silicas,² activated carbons,³ (bio)polymers⁴ and even biomass.⁵ However, control of nanoparticle properties, with particular respect to shape, size, and dispersity, is imperative as this will determine activity in the desired application. The selection of the support in the design of heterogeneous catalysts can help control their properties and enhance activity.

We have recently developed a wide range of Pd-supported materials and complexes with multiple uses as catalysts.⁶ With particular regard to catalytic applications, palladium catalysts have several interesting features for organic synthesis, especially for C–C bond formation, due to their versatility among many transition metals employed in these reactions.⁷ Herein, we highlight the use of mesoporous starch⁸ as a promising support for nanoparticle catalyst preparation, rendering materials active in a wide range of C–C coupling reactions. The catalytic performance of such materials is dependent on the nature and stability of the metal–support interaction.

The preparation of porous materials from renewable polysaccharides such as starch is a relatively new area but new applications are developing, mainly as a consequence of a demand for biodegradable and naturally-derived products. The textural properties of such porous starches presents a unique

textural and chemical environment in which nanoparticles may be synthesized. Starch has been widely employed as a stabilising agent (capping agent) in the preparation of metal nanoparticles.⁴

Conventionally, the preparation of metal nanoparticles requires the use of a reducing agent such as NaBH₄, hydrazine, or molecular hydrogen. However, in most examples, the kinetics of the reduction process are not easily controllable. Nor are the procedures employed particularly ‘green’ or simple. The product also needs to be thoroughly washed and conditioned in order to remove excess reducing agent. Recently, Raveendran *et al.* have employed glucose as an environmentally benign reducing agent to prepare well-dispersed Au and Ag nanoparticles.^{4b} Herein, we report the preparation of well-defined Pd nanoparticles on mesoporous starch, an inexpensive and non-toxic support media, without the need for additional reductant. Here we report and discuss the influence of the preparation route on the catalytic performance in the Suzuki, Heck and Sonogashira C–C coupling reactions. Interestingly, the characteristics of the nanoparticles are reflective of the pore structure present in the starch support.

Experimental

Material preparation

100 g of starch (*e.g.* high amylose corn starch) and 2 L of deionised water were stirred at 700 rpm for 10 min in a modified household pressure cooker prior to heating (volume = 3 L; operating conditions 120 °C/80 kPa). The lid component of the device was modified with an aluminium enclosure facilitating the insertion of a thermocouple. The system was heated to 120 °C (30 min) and held at this temperature for a further 45 min. Upon returning to atmospheric pressure, the lid was detached, and the resulting solution decanted into powder drying jars. The vessels were then sealed and the gels retrograded at 5 °C overnight. Predominantly mesoporous starch was obtained after solvent exchanging the starch–water gel with ethanol and drying.

The palladium nanoparticles on starch were subsequently prepared as follows: 10 g mesoporous starch and the desired

Green Chemistry Centre of Excellence, Department of Chemistry, The University of York, York, UK. E-mail: jhc1@york.ac.uk; Fax: +44 1904 432705; Tel: +44 1904 432559

† This paper was published as part of the themed issue of contributions from the 3rd International Conference on Green and Sustainable Chemistry.

Table 1 Textural properties of Pd–starch materials

| Entry | Material | Pd loading (wt%) | Solvent | Surface area/m ² g ⁻¹ | Pore diameter ^a /nm |
|-------|-------------|------------------|---------|---|--------------------------------|
| 1 | Pd–starch-1 | 0.5 | EtOH | 102 | 6.6 |
| 2 | Pd–starch-2 | 2.5 | EtOH | 119 | 6.3 |
| 3 | Pd–starch-3 | 5.0 | EtOH | 12 | 13.0 |
| 4 | Pd–starch-4 | 0.5 | Acetone | 158 | 7.3 |
| 5 | Pd–starch-5 | 2.5 | Acetone | 177 | 7.1 |
| 6 | Pd–starch-6 | 5.0 | Acetone | 13 | 10.5 |

^a Maximum in the mesopore region (2–50 nm).

palladium quantity (using Pd acetate as precursor, previously dissolved in acetone) were dispersed in ethanol and stirred overnight at room temperature. The solution was then filtered and thoroughly washed with acetone. Three different palladium-supported materials were prepared with palladium contents of 0.5, 2.5 and 5 wt% Pd (Pd–starch-1, -2 and -3), respectively. To investigate the effect of solvent on the preparation of palladium nanoparticles, three additional palladium-supported materials were prepared, following an identical procedure using acetone (Pd–starch-4, -5 and -6) instead of ethanol. The equivalent materials were also prepared on non-processed native starch.

Characterisation

Powder X-ray diffraction patterns (XRD) were recorded on a Bruker AXS diffractometer with CuK α ($\lambda = 1.5418 \text{ \AA}$), over a 2θ range from 5 to 85°, using a step size of 0.1° and a counting time per step of 4 s.

Nitrogen physisorption measurements were conducted on a Micromeritics ASAP 2010 instrument at 77 K. Samples were outgassed at 120 °C for 4 h under vacuum ($p < 10^{-2}$ Pa) and subsequently analysed. The linear part of the BET equation (relative pressure between 0.05 and 0.22) was used for the determination of the specific surface area. The pore size distribution was calculated from the adsorption branch of the N₂ physisorption isotherms and the Barret–Joyner–Halenda (BJH) formula.⁹ The cumulative mesopore volume V_{BJH} was obtained from the PSD curve.

Transmission Electron Micrographs (TEM) were recorded in a JEOL JSM-6490LV. Samples were Au/Pd coated on a high resolution sputter SC7640 at a sputtering rate of 1500 V min⁻¹, up to 7 nm thickness.

Catalyst testing

Microwave experiments were carried out in a CEM-DISCOVER model with PC control and monitored by sampling aliquots of reaction mixture that were subsequently analysed by GC/GC–MS using an Agilent 6890N GC model equipped with a 7683B series autosampler fitted with a capillary column and an FID detector.

Results and discussion

The starch-derived support exhibited the typical characteristics of a mesoporous solid (*i.e.* a Type IV isotherm) The BET surface area of the parent material prior to palladium addition was

measured as 190 m² g⁻¹ with an average pore size of 8.2 nm. Table 1 summarises the textural properties and the palladium content of a series of mesoporous starch-supported materials. The surface area and the mesoporous structure of the material were preserved at lower Pd content. An increase of Pd content from 2.5 to 5 wt% resulted in a significant decrease in the surface area of the materials (Table 1, entries 3 and 6), as expected due to Pd deposition within the pores and/or on the surface that may lead to pore blocking. This is in good agreement with porosimetry results, in which a reduction of the average pore diameter was initially observed, followed by an increase as the smaller mesopores became filled at higher Pd loadings (Fig. 1).

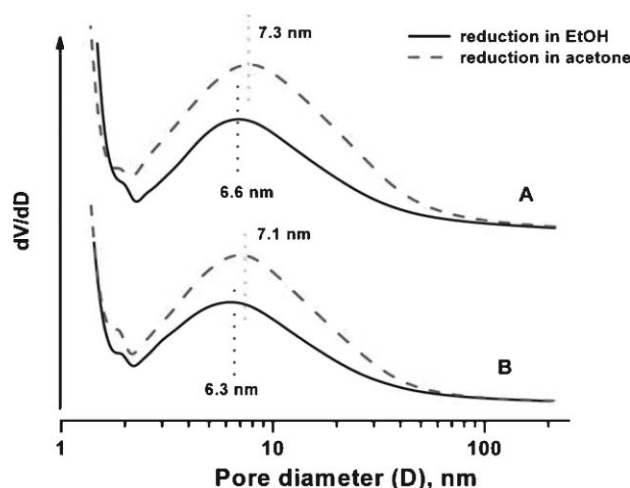


Fig. 1 Pore size distribution of A) Pd–starch-1 and Pd–starch-4 materials (0.5 wt% Pd) and B) Pd–starch-2 and -5 materials (2.5 wt% Pd).

Upon incorporation of the Pd into the mesoporous starch, the pore size was reduced to *ca.* 7 nm for the materials prepared under reduction in acetone and to *ca.* 6 nm for the catalysts reduced in EtOH.

Powder XRD diffraction patterns (Fig. 2) obtained for the Pd–starch materials exhibited a broad reflection corresponding to the amorphous starch support. Four additional reflections were found in the XRD pattern that could be attributed to elemental palladium, in good agreement with JCPDS file: 46-1043.¹⁰ All materials prepared exhibited a similar XRD pattern. Of note was the absence of any reflections in the diffractogram due to the presence of significant quantities of the Pd precursor on the support.

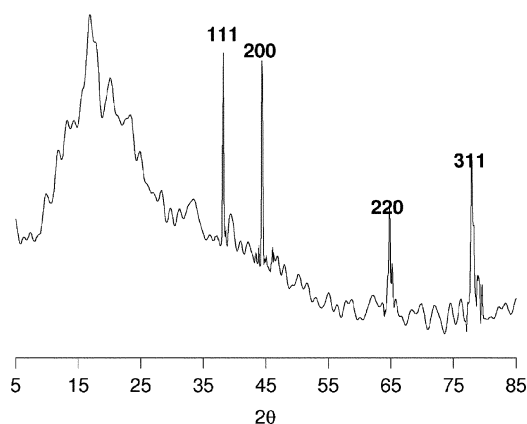


Fig. 2 XRD diffraction patterns of the Pd-starch-3 material (5 wt% Pd).

The resulting Pd loaded materials were also investigated using Transmission Electron Microscopy (TEM). The TEM micrographs (Fig. 3) showed well-dispersed Pd nanoparticles homogeneously distributed with a reasonably narrow distribution of nanoparticle diameters (*ca.* 5 nm), in good agreement with the results obtained for the XRD measurements.

The nanoparticle morphology was spherical with the average particle diameter being 4.0 and 2.5 nm, respectively, for the materials prepared using ethanol and acetone as solvents. Importantly, no significant Pd cluster formation was observed in the materials, even at high Pd content (*i.e.* 5 wt%) (Fig. 3).

The average nanoparticle size distribution was further investigated from the TEM micrographs. There was a significant difference in particle size and nanoparticle size distribution, as shown on Fig. 3, for the two different solvents (ethanol and acetone) employed in the synthesis procedure. Both materials, irrespective of the palladium loading, exhibited two major peaks in the nanoparticle size distribution at *ca.* 1.5–2.0 and 3.5–4.5 nm. The smaller nanoparticles are believed to be formed within the starch micropores whereas the bigger palladium clusters grow within the starch mesopores.

The nanoparticle size distribution resembles the pore size distribution of the parent mesoporous starch. This difference in nanoparticle size can be related to the way the palladium nanoparticles are either reduced mainly by the solvent (ethanol) or by the functionalities present on the starch surface (acetone). The differences in nanoparticle sizes can be expected to have a notable effect on the catalytic activity of the materials.

Catalytic activity

A Pd content of between 2.5 and 3 wt% was found to be the optimum for the materials prepared in terms of a balance between desirable textural properties and catalytic activity.

Heck reaction

Tables 2–4 summarise the main results of the Heck reaction (Scheme 1) using iodobenzene as the aryl substrate and methyl

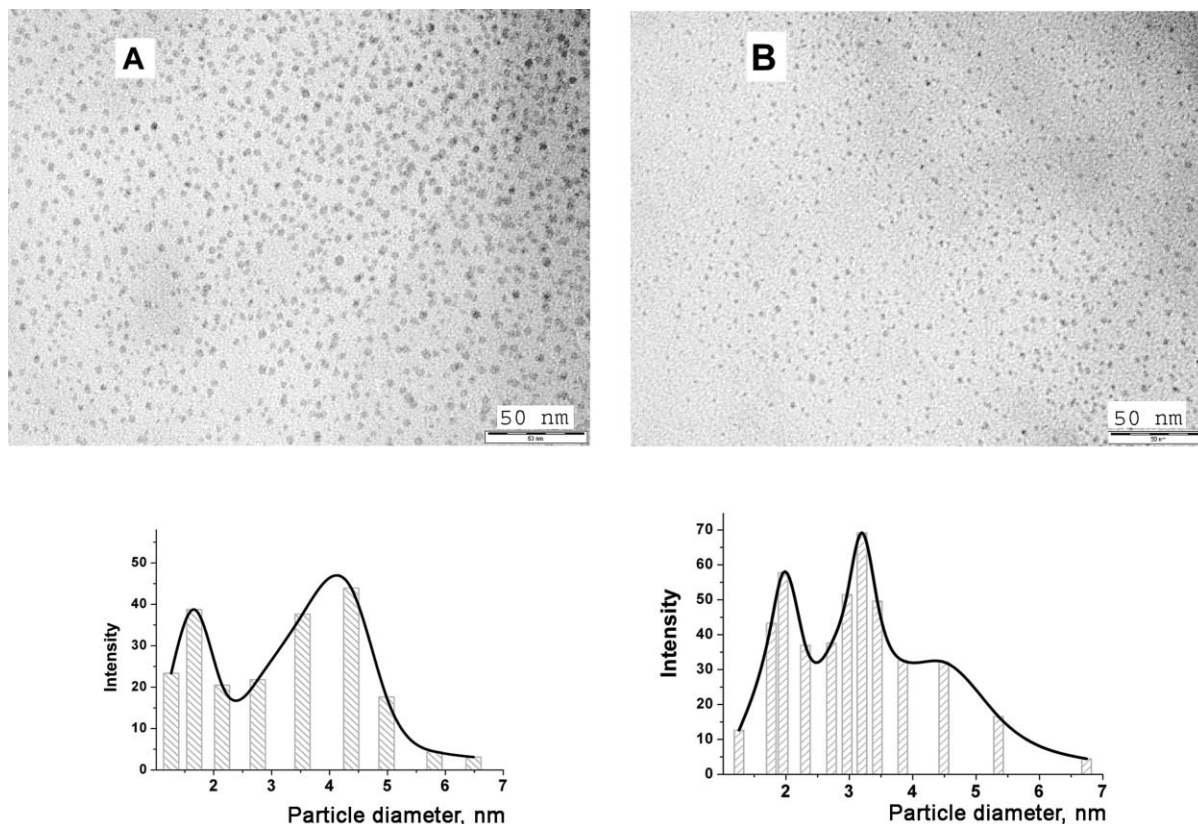
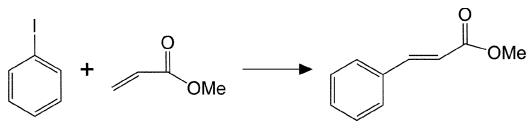


Fig. 3 TEM micrographs and nanoparticle size distribution (calculated from TEM) of Pd-starch materials (5 wt% Pd) prepared in (A) acetone and (B) ethanol.

acrylate (Tables 2 and 3) and styrene (Table 4) as alkenes for the different catalysts synthesized.



Scheme 1 Heck coupling of iodobenzene and methyl acrylate.

The catalytic activity increased, as expected, with an increase in the Pd content in the materials. However, the Pd–starch-2 sample (2.5 wt% Pd) provided the best conversion : selectivity ratios for the two substrates investigated.

A further increase in the Pd content (from 2.5 to 5 wt%) did not significantly improve the conversion in the systems and the selectivity to the main product (*E*-methyl cinnamate and *trans*-stilbene) was significantly reduced (entries 3 and 6, Tables 2–4).

Table 2 Heck reaction of iodobenzene and methyl acrylate using Pd–starch-supported materials^a

| Entry | Reaction conditions | X_T (mol%) | $S_{\text{methyl cinnamate}}$ (mol%) |
|-------------|---------------------|--------------|--------------------------------------|
| Pd–starch-1 | Microwave | <20 | >99 |
| Pd–starch-2 | 300 W | 40 | >99 |
| Pd–starch-3 | 90 °C 1 min | 68 | 90 |
| Pd–starch-4 | | 35 | >99 |
| Pd–starch-5 | | 75 | >95 |
| Pd–starch-6 | | 83 | 90 |

^a Reaction conditions: 8 mmol iodobenzene, 8 mmol methyl acrylate, 5 mmol triethylamine, 0.1 g catalyst, 300 W, 90 °C, 1 min.

Table 3 Heck reaction of iodobenzene and methyl acrylate using Pd–starch-supported materials^a

| Entry | Reaction conditions | X_T (mol%) | $S_{\text{methyl cinnamate}}$ (mol%) |
|-------------|---------------------|--------------|--------------------------------------|
| Pd–starch-1 | Microwave | 50 | >99 |
| Pd–starch-2 | 300 W | >90 | >90 |
| Pd–starch-3 | 90 °C 5 min | >99 | 85 |
| Pd–starch-4 | | 70 | >99 |
| Pd–starch-5 | | >95 | >95 |
| Pd–starch-6 | | >95 | 85 |

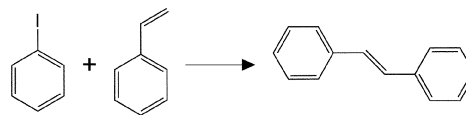
^a Reaction conditions: 8 mmol iodobenzene, 8 mmol methyl acrylate, 5 mmol triethylamine, 0.1 g catalyst, 300 W, 90 °C, 5 min.

Table 4 Heck reaction of iodobenzene and styrene using Pd–starch-supported materials^a

| Entry | Reaction conditions | X_T (mol%) | S_{stilbene} (mol%) |
|-------------|---------------------|--------------|------------------------------|
| Pd–starch-1 | Microwave | 35 | >95 |
| Pd–starch-2 | 300 W | 70 | >90 |
| Pd–starch-3 | 90 °C 5 min | 75 | 85 |
| Pd–starch-4 | | 55 | >95 |
| Pd–starch-5 | | 80 | >90 |
| Pd–starch-6 | | 85 | 80 |

^a Reaction conditions: 8 mmol iodobenzene, 12 mmol styrene, 5 mmol triethylamine, 0.1 g catalyst, 300 W, 90 °C, 10 min.

The less reactive styrene (Scheme 2, Table 4) was also coupled in moderate to excellent yields with an extremely good selectivity to the *trans* isomer.



Scheme 2 Heck coupling of iodobenzene and styrene.

In both cases, the materials prepared using acetone were more active than the ethanol-prepared materials, in good agreement with the predictions made from the porosimetry and pore size distribution experiments. Starch has been reported as a heavy metal reducing agent,¹¹ while EtOH has been reported as a reducing agent for silver ions. We believe the nanoparticle growth takes place through a competitive reduction of the Pd²⁺ between the EtOH (when present) and the starch surface functionalities. In the presence of EtOH as solvent, both the starch surface and the EtOH compete in the reduction of the metal ions. The kinetics of the reduction process seem to be quicker for EtOH compared to the starch surface, therefore leading to a less well dispersed and heterogeneous particle distribution. In the absence of EtOH (acetone as solvent), the starch surface functionalities slowly reduces the Pd²⁺ to Pd⁰, generating a more evenly dispersed and smaller nanoparticle system (*ca.* 3.2 nm) which agrees well with the particle dispersity observed by TEM.

This higher palladium dispersion may be the reason for the substantial differences in catalytic activity for the low Pd loaded materials. Nevertheless, no significant differences in the catalytic activity of EtOH- and acetone-reduced materials were found with an increase in the Pd loading from 0.5 to 2.5 wt%.

Suzuki reaction

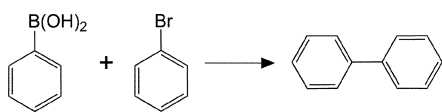
Our materials were then tested in the Suzuki reaction. Table 5 summarises the main results obtained for the Pd–starch samples in the synthesis of biphenyl from benzeneboronic acid and bromobenzene (Scheme 3).

The results obtained in the Suzuki reaction were similar for all the materials screened. Quantitative conversion values (>95%) and selectivities to biphenyl (>99%) were found for all Pd–starch catalysts except Pd–starch-1 (75% conversion, >99% selectivity) and Pd–starch-4 (85% conversion, >99% selectivity). Conversion values increased with an increase in the

Table 5 Suzuki reaction of bromobenzene and benzeneboronic acid using Pd–starch-supported materials^a

| Entry | Reaction conditions | X_T (mol%) | S_{biphenyl} (mol%) |
|-------------|---------------------|--------------|------------------------------|
| Pd–starch-1 | Microwave | 75 | >99 |
| Pd–starch-2 | 300 W | >95 | >99 |
| Pd–starch-3 | 130 °C 2 min | >95 | >99 |
| Pd–starch-4 | | 85 | >99 |
| Pd–starch-5 | | >95 | >99 |
| Pd–starch-6 | | >95 | >99 |

^a Reaction conditions: 1 mmol bromobenzene, 1.1 mmol benzeneboronic acid, 7 mmol K₂CO₃, 0.1 g catalyst, 300 W, 130 °C, 2 min.

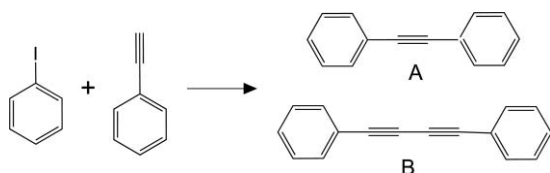


Scheme 3 Suzuki coupling of bromobenzene and benzenboronic acid.

Pd content (from 0.5 to 2.5 wt%) but a further increase did not have any effect on conversions and selectivities. Interestingly, selectivities remained almost unchanged in the materials despite the synthesis procedure and the loading of Pd in the catalysts. No significant quantities of the homocoupling product were found in the reaction. These mesoporous starch-based catalysts showed good activity as compared to our previously report Schiff base palladium-supported catalysts (Table 6).

Sonogashira reaction

The Sonogashira coupling reaction (Scheme 4) allows the production of a wide range of products with important uses as pharmaceuticals, agrochemicals and materials science.¹²



Scheme 4 Sonogashira coupling of iodobenzene and phenylacetylene.

We recently reported a copper, phosphine and solvent-free route to aryl alkynes and derivatives employing various heterogeneous catalysts.⁶ Following this protocol, we investigated the catalytic activity of our Pd–starch materials in the reaction. Data are summarised in Table 6. Excellent conversions of the starting materials were found for all the catalysts screened in this coupling reaction and the catalysts performed well utilising a rapid and simple microwave route.

However, an increase in the production of the homocoupling product (B in Scheme 4) was observed, as compared to our previously reported results which gave almost complete selectivity to the cross-coupling product (A in Scheme 4). Interestingly, the selectivity to the main cross-coupled product was not significantly altered with an increase in the Pd content in the materials (Table 6).

Comparison with reported systems

Table 7 provides a comparison of the results obtained for our best systems (Pd–starch-2 and Pd–starch-5) with those reported previously. Our Pd–starch materials exhibited improved conversions and selectivities compared to the Starcat material and to other reported systems. Reaction rates were much quicker compared to Pd–C and Pd–silica materials in both the Heck, Suzuki and Sonogashira reactions.

Of note was also the materials' reusability. The strong interaction between the Pd nanoparticles and the starch surface prevented metal leaching during/after the reactions, rendering materials highly active, selective and reusable after four reuses in each one of the reactions screened.

Finally, the solids were filtered after the reaction and the liquid filtrate was tested in another reaction cycle. No conversion was detected in the filtrate when returned to reaction conditions, confirming the truly heterogeneous nature of the palladium-supported catalysts.

The advantage of our nanoparticles compared to previously reported systems is the use of non-toxic, natural support media, with easily tuneable properties, and a simple nanoparticle preparation route, eliminating the use of a reducing agents such as those mentioned earlier. Noble metal nanoparticles (e.g. Pd, Au and Ag; or combinations thereof) may be synthesized at the surface of the porous polysaccharide-derived material, generating interesting materials in which the metal particle size can be easily tuned and optimised for a particular application.

Conclusions

Well-dispersed palladium nanoparticles have been prepared on a mesoporous starch heterogeneous support and have been successfully employed and tested in the Heck, Suzuki and Sonogashira C–C coupling reactions. The properties of the metal nanoparticles are reflective of the unique porous environment that these novel polysaccharide-derived porous materials provide, allowing access to a wide range of surface chemistries thus facilitating the preparation of metal nanoparticles of a controllable size and nature. Interesting differences in catalytic activity between materials in which the Pd was reduced with EtOH and/or the starch surface were found. Materials were found to be highly stable, active and reusable under the various reaction conditions screened.

Table 6 Sonogashira reaction of iodobenzene and phenylacetylene using Pd–starch-supported materials^a

| Entry | Reaction conditions | X_T (mol%) | S_{Sono} (mol%) | $S_{\text{homocoupling}}$ (mol%) |
|-------------|---------------------|--------------|--------------------------|----------------------------------|
| Pd–starch-1 | Microwave | >90 | 65 | 35 |
| Pd–starch-2 | 300 W | >95 | 60 | 40 |
| Pd–starch-3 | 130 °C 2 min | >99 | 55 | 45 |
| Pd–starch-4 | | >95 | 62 | 38 |
| Pd–starch-5 | | >95 | 73 | 27 |
| Pd–starch-6 | | >99 | 66 | 34 |

^a Reaction conditions: 2 mmol iodobenzene, 2 mmol phenylacetylene, 2 mmol DABCO, 0.025 g catalyst, 300 W, 130 °C, 2 min.

Table 7 Comparison of the catalytic activity of our Pd–starch materials with other related reported systems

| Entry | Reaction conditions | Reaction | X_T (mol%) | $S_{\text{main product}}$ (mol%) | $S_{\text{homocoupling}}$ (mol%) |
|--|--|--------------------------------------|--------------|----------------------------------|----------------------------------|
| Pd–starch-2 | Microwave 300 W, 130 °C 2 min, 0.1 g catalyst | Heck | >90 | >90 | — |
| Pd–starch-5 | | (iodobenzene + methyl acrylate) | >99 | >95 | — |
| Starcat ^{6b} | Heating 140 °C, 8 h, 0.1 g catalyst | | 77 | >99 | — |
| Pd-PDMP ¹³ | Heating 75 °C, 4 h | | >95 | >99 | — |
| Pd–starch-2 | Microwave 300 W, 130 °C 2 min, 0.1 g catalyst | Suzuki | >95 | >99 | — |
| Pd–starch-5 | | (benzeneboronic acid + bromobenzene) | >99 | >99 | — |
| Starcat ^{6b} | Heating 140 °C, 7 h, 0.1 g catalyst | | >99 | >99 | — |
| SiO ₂ -TEG–Pd ¹⁴ | Heating 110 °C, 12 h, 0.1 g catalyst | | 86 | >99 | — |
| Pd–starch-2 | Microwave 300 W, 130 °C 2 min, 0.025 g catalyst | Sonogashira | >90 | 65 | 35 |
| Pd–starch-5 | | (iodobenzene + phenylacetylene) | >95 | 60 | 40 |
| Starcat ^{6b} | Heating 100 °C, 0.5 h, 0.1 g catalyst | | >90 | >99 | — |
| | Microwave 300 W, 150 °C 5 min, 0.1 g catalyst | | >90 | 80 | 20 |
| Pd–silica ^{6a} | Heating 70 °C, 12 h, 0.03 g catalyst | | 87 | 91 | 9 |

References

- (a) X. L. Luo, A. Morrin, A. J. Killard and M. R. Smyth, *Electroanalysis*, 2006, **18**, 319; (b) K. H. Hong, J. L. Park, I. H. Sul, J. H. Youk and T. J. Kang, *J. Pol. Sci.*, 2006, **44**, 2468; (c) Y. C. Chen, Z. M. Tang, M. Z. Gui, J. Q. Cheng, X. Wang and Z. H. Lu, *Chem. Lett.*, 2000, 1140; (d) M. J. Gronnow, R. J. White, J. H. Clark and D. J. Macquarrie, *Org. Process Res. Dev.*, 2005, **9**, 516; (e) M. Harada, K. Asakura and N. Toshima, *J. Phys. Chem.*, 1993, **97**, 5103.
- A. Barau, R. Luque, V. Budarin, A. Preme, V. S. Teodorescu, A. Caragheorghopol, D. J. Macquarrie and M. Zaharescu, 14th International Sol–Gel Conference, Montpellier (France), Book of Abstracts, 2007, p. 604.
- (a) A. Safavi, M. Afsaneh, N. Maleki, F. Tajabadi and E. Farjami, *Electrochem. Commun.*, 2007, **9**, 1963; (b) W. C. Ketchie, M. Murayama and R. J. Davis, *J. Catal.*, 2007, **250**, 264.
- (a) P. Raveendran, J. Fu and S. L. Wallen, *J. Am. Chem. Soc.*, 2003, **125**, 13940; (b) P. Raveendran, J. Fu and S. L. Wallen, *Green Chem.*, 2006, **8**, 34; (c) F. He and D. Zhao, *Environ. Sci. Technol.*, 2005, **39**, 3314.
- (a) M. F. Lengke, M. E. Fleet and G. Southam, *Langmuir*, 2007, **23**, 8982; (b) K. Pollmann, M. Merroun, J. Raff, C. Hennig and S. Selenska-Pobell, *Lett. Appl. Microbiol.*, 2006, **43**, 39.
- (a) M. Bandini, R. Luque, V. Budarin and D. J. Macquarrie, *Tetrahedron*, 2005, **61**, 9860; (b) M. J. Gronnow, R. Luque, D. J. Macquarrie and J. H. Clark, *Green Chem.*, 2005, **7**, 552; (c) D. J. Macquarrie, J. J. E. Hardy, S. Hubert, A. J. Deveaux, M. Bandini, R. Luque-Alvarez and M. Chabrel, in *Feedstocks for the Future: Renewables for the Production of Chemicals and Materials*, ed. J. J. Bozell and M. K. Patel, ACS Symposium Series 921, American Chemical Society, New York, 2006, p. 170.
- J. Tsuji, *Palladium Reagents and Catalysts*, Wiley, Chichester, 2004.
- V. Budarin, J. H. Clark, F. E. I. Deswarte, J. J. E. Hardy, A. J. Hunt and F. M. Kerton, *Chem. Commun.*, 2005, 2903.
- E. P. Barret, L. G. Joyner and P. P. Halenda, *J. Am. Chem. Soc.*, 1951, **73**, 373.
- Palladium, JCPDS 46-1043, 1969.
- D. J. Gallant, B. Bouchet and P. M. Baldwin, *Carbohydr. Polym.*, 1997, **32**, 177.
- (a) K. Sonogashira, in *Metal Catalysed Cross-Coupling Reactions*, ed. F. Diederich and P. J. Stang, Wiley-VCH, New York, 1998, pp. 203–229; (b) K. Sonogashira, in *Handbook of Organopalladium Chemistry for Organic Synthesis*, ed. E. Negishi, Wiley-VCH, New York, 2002, pp. 493–530.
- N. Panziera, P. Pertici, L. Barazzone, A. M. Caporusso, G. Vitulli, P. Salvadori, S. Borsacchi, M. Geppi, C. A. Veracini, G. Martra and L. Bertinetti, *J. Catal.*, 2007, **246**, 351.
- N. Kim, M. S. Kwon, C. M. Park and J. Park, *Tetrahedron Lett.*, 2004, **45**, 7057.

Au–Pd supported nanocrystals as catalysts for the direct synthesis of hydrogen peroxide from H₂ and O₂†

Jennifer K. Edwards,^a Adrian Thomas,^a Albert F. Carley,^a Andrew A. Herzing,^b Christopher J. Kiely^b and Graham J. Hutchings^{*a}

Received 20th September 2007, Accepted 5th November 2007

First published as an Advance Article on the web 20th November 2007

DOI: 10.1039/b714553p

The direct synthesis of hydrogen peroxide with Au–Pd catalysts is described and discussed: in particular, the roles of the support and promoters. Catalysts prepared by co-impregnation on various supports with calcination at 400 °C were stable and could be re-used several times without loss of metal. Catalysts calcined at lower temperatures were found to be unstable and could not be successfully re-used. Au–Pd/carbon and Au–Pd/silica catalysts gave the highest rate of H₂O₂ production, and the order of reactivity observed for the support materials investigated is: carbon ~ silica > TiO₂ > Al₂O₃. Bimetallic Au–Pd particles on TiO₂ and Al₂O₃ were found to exhibit a core–shell structure, Pd being concentrated on the surface. It is considered that the Au–Pd/silica catalysts have a similar core–shell morphology based on X-ray photoelectron spectroscopy studies, whereas, in contrast, the calcined Au–Pd/carbon catalysts are observed to be homogeneous alloys. TEM studies showed that the silica contains impurities of carbon and that the Au–Pd alloys all preferentially interact with these carbonaceous impurities, hence resulting in a rather similar catalytic performance to that of the carbon supported Au–Pd catalysts. The origin of the enhanced activity for the silica and carbon supported catalysts is a result of higher H₂ selectivity for the formation of hydrogen peroxide, which is due to the surface composition and size distribution of the nanoparticles. The effect of promoters is investigated, and it is shown that addition of Br[−] and PO₄^{3−} is deleterious under our conditions, which contrasts markedly with Pd catalysts for which such species are essential. Furthermore, we show the acid solution formed by CO₂ in water increases the rate of H₂O₂ synthesis, and thereby the CO₂ diluent in our experiments acts as green *in situ* acid promoter.

Introduction

The direct oxidation of H₂ and O₂ to give hydrogen peroxide remains one of the grand challenges in catalytic chemistry, since the direct reaction could be preferable to the current indirect process.^{1,2} It is a reaction that has both fascinated and intrigued catalytic chemists for almost a century.³ There is a recent report¹ that a direct process using a Pd based catalyst is being commercialised and this would be a major step forward in the manufacture of this important material, which is produced on a major scale, *ca.* 2 M tons per annum, and is used mainly as a bleach and disinfectant. Hydrogen peroxide is produced currently by the sequential hydrogenation and oxidation of an alkyl anthraquinone, which avoids explosive mixtures of hydrogen and oxygen.² This process has, in the main, replaced all its competitors and has remained largely unchanged for decades. Despite its widespread use this indirect

process has many non-green features and disadvantages. It requires many energy intensive unit processes and distillation steps to purify and concentrate the product. The anthraquinone can be over-hydrogenated or form by-products which makes it necessary to regularly ‘top-up’ the anthraquinone level. In addition, the process is only economically viable on a relatively large scale and this necessitates the transportation and storage of concentrated solutions of hydrogen peroxide, which can be hazardous. However, most hydrogen peroxide is used on a much smaller scale and at much more dilute concentrations (typically *ca.* 3–5 vol%) for cleaning or in the paper and textile industries. There is, therefore, a very significant mismatch between the concentration at which H₂O₂ is manufactured and that at which it is used. Hence, a direct process producing a less hazardous dilute solution of hydrogen peroxide would permit on-site manufacture on a scale and concentration at which it is needed. This would be preferable to the currently used indirect process and would be intrinsically greener in nature.

The direct reaction between hydrogen and oxygen has been a research target for many years, with the first reported study in 1914³ using a Pd catalyst. Since then, there have been a number of investigations and virtually all of these have been pioneered in industrial laboratories.^{3–16} Early studies used H₂–O₂ mixtures in the explosive region but, more recently, studies have concentrated on carrying out the reaction with dilute

^aSchool of Chemistry, Cardiff University, Main Building, Park Place, Cardiff, UK CF10 3AT. E-mail: hutch@cardiff.ac.uk; Fax: +44 29 2087 4030; Tel: +44 29 2087 4805

^bCenter for Advanced Materials and Nanotechnology, Lehigh University, 5 East Packer Avenue, Bethlehem, PA 18015-3195, USA

† This paper was published as part of the themed issue of contributions from the 3rd International Conference on Green and Sustainable Chemistry.

H₂–O₂ mixtures well away from the explosive regime.^{12,15} It is reported that the hydrogen peroxide yield is improved by the addition of acid and bromide,^{8,9} and solutions of over 35 wt.% hydrogen peroxide have been made by reacting H₂–O₂ over Pd catalysts at elevated pressures.⁸ Hence, previous work on direct hydrogen peroxide synthesis has focused on the use of Pd as a catalyst.

The recent discovery of the catalytic efficacy of gold for oxidation and reduction reactions has given a vital impetus in the search for selective redox catalysts,^{17–23} and new discoveries are being made on a regular basis. Supported gold catalysts have been shown to be effective for low temperature oxidation of CO,²⁴ especially in the presence of H₂, H₂O and CO₂, and this reaction is finding some potential application in fuel cells.^{25,26} Gold has also been found effective for the selective oxidation of alkenes^{27,28} and alcohols,²⁹ and for the selective hydrogenation of unsaturated carbonyl compounds and nitro groups.³⁰ In all these applications it is the selectivity coupled with high activity that is viewed as important. Recently, we have shown that supported gold–palladium alloys are very active and selective for the oxidation of alcohols,³¹ being 25 times more active than the corresponding gold or palladium monometallic catalysts. Furthermore, we have shown that the addition of Au to Pd increases the catalytic efficiency for the direct formation of hydrogen peroxide.^{32–37} The increase in activity is significant, and in this paper we contrast the use of different supports on the structure and activity of Au–Pd alloy catalysts and investigate the role of catalyst promoters in these systems.

Experimental

Catalyst preparation

5 wt% Pd-only, 5 wt% Au-only and a range of Au–Pd bimetallic catalysts were prepared by impregnation of four supports (silica (Grace), carbon (Darco G60, Aldrich), TiO₂ (Degussa P25, mainly anatase), Al₂O₃ (Aldrich)) *via* an incipient wetness method using aqueous solutions of PdCl₂ (Johnson Matthey) and/or HAuCl₄·3H₂O (Johnson Matthey). For the 2.5% Au–2.5% Pd/TiO₂ catalyst, the detailed preparation procedure employed is described below. An aqueous solution of HAuCl₄·3H₂O (10 ml, 5 g dissolved in water (250 ml)) and an aqueous solution of PdCl₂ (4.15 ml, 1 g in water (25 ml)) were simultaneously added to TiO₂ (3.8 g). The paste formed was ground and dried at 80 °C for 16 h and calcined in static air, typically at 400 °C for 3 h, although other heat treatment conditions have been investigated. Other Au–Pd ratios were prepared by varying the amounts of starting reagents accordingly. Catalysts on other supports were prepared in a similar manner.

Hydrogen peroxide synthesis

Catalyst testing was performed using a stainless steel autoclave (Parr Instruments) with a nominal volume of 50 ml and a maximum working pressure of 14 MPa. The autoclave was equipped with an overhead stirrer (0–2000 rpm) and provision for measurement of temperature and pressure. Typically, the autoclave was charged with the catalyst (0.01 g unless otherwise stated), solvent (5.6 g MeOH and 2.9 g H₂O), purged three times with 5% H₂–CO₂ (3 MPa) and then filled with 5% H₂–CO₂ and 25% O₂–CO₂ to give a hydrogen to oxygen ratio of 1:2

at a total pressure of 3.7 MPa. Stirring (1200 rpm unless otherwise stated) was commenced on reaching the desired temperature (2 °C), and experiments were carried out for 30 min unless otherwise stated. Gas analysis for H₂ and O₂ was performed by gas chromatography using a thermal conductivity detector and a CP-Carboplot P7 column (25 m, 0.53 mm id). Conversion of H₂ was calculated by gas analysis before and after reaction. The H₂O₂ yield was determined by titration of aliquots of the final filtered solution with acidified Ce(SO₄)₂ (7 × 10^{−3} mol l^{−1}). Ce(SO₄)₂ solutions were standardised against (NH₄)₂Fe(SO₄)₂·6H₂O using ferroin as indicator.

Catalyst characterisation

Atomic absorption spectroscopy (AAS) was performed with a PerkinElmer 2100 atomic absorption spectrometer using an air–acetylene flame. Gold–palladium samples were recorded at wavelengths of 242.8 nm (Au) and 247.6 nm (Pd). Samples for AAS analysis were prepared by dissolving 0.1 g of the dried catalyst in an aqua regia solution, followed by the addition of 250 ml of de-ionised water to dilute the sample. AAS was used to determine the weight% of the metal incorporated into the support after impregnation and also the concentration (ppm) of leached Au or Pd in solution during reaction, by determining the Au and Pd content of the used catalyst and comparing it with that of the fresh catalyst.

Samples for examination by transmission electron microscopy (TEM) were prepared by dispersing the catalyst powder in high purity ethanol, then allowing a drop of the suspension to evaporate on a holey carbon film supported by a 300 mesh copper TEM grid. Samples were then subjected to chemical microanalysis and annular dark-field imaging in a VG Systems HB603 scanning transmission electron microscope (STEM) operating at 300 kV, equipped with a Nion C_s corrector. The instrument was also fitted with an Oxford Instruments INCA TEM 300 system for energy dispersive X-ray (XEDS) analysis. Bright field imaging experiments were carried out on a JEOL 2000FX TEM operating at 200 kV.

X-ray photoelectron spectra were recorded on one of two different instruments: (i) a VG EscaLab 220i spectrometer, using a standard Al K_α X-ray source (300 W) and an analyser pass energy of 100 eV (survey scans) or 20 eV (detailed scans); (ii) a Kratos Axis Ultra DLD spectrometer employing a monochromatic Al K_α X-ray source (75–150 W) and analyser pass energies of 160 eV (for survey scans) or 40 eV (for detailed scans). Samples were mounted using double-sided adhesive tape and binding energies referenced to the C (1 s) binding energy of adventitious carbon contamination, which was taken to be 284.7 eV.

Results and discussion

Evaluation of calcined pure Au, pure Pd and Au–Pd supported catalysts

In our previous studies^{32–37} we have examined four support materials in detail for Au–Pd nanoparticles, namely carbon, TiO₂, Al₂O₃ and Fe₂O₃. We have now additionally evaluated silica as a potential support for Au and Au–Pd nanocrystals. Previously, Haruta and co-workers³⁸ have shown that silica is an effective

Table 1 Formation of hydrogen peroxide using Au, Pd and Au–Pd supported catalysts^a

| Catalyst | Hydrogen peroxide formation (mol H ₂ O ₂ /kg _{cat} -h) | Hydrogen selectivity (%) |
|--|---|--------------------------|
| 5% Au/silica | 1 | nd |
| 2.5% Au–2.5% Pd/silica | 108 | 80 |
| 5% Pd/silica | 80 | 80 |
| 5% Au/carbon | 1 | nd |
| 2.5% Au–2.5% Pd/carbon | 110 | 80 |
| 5% Pd/carbon | 55 | 34 |
| 5% Au/Al ₂ O ₃ | 2.6 | nd |
| 2.5% Au–2.5% Pd/Al ₂ O ₃ | 15 | 14 |
| 5% Pd/Al ₂ O ₃ | 9 | nd |
| 5% Au/TiO ₂ | 7 | nd |
| 2.5% Au–2.5% Pd/TiO ₂ | 64 | 70 |
| 5% Pd/TiO ₂ | 30 | 21 |

^a Standard reaction conditions, nd = not determined as the yield is too low for reliable measurement.

support for Au nanocrystals for the direct reaction, and we now evaluate Au/SiO₂ and Au–Pd/SiO₂ catalysts under our reaction conditions and compare these directly with previously published data.^{32–37} A series of catalysts, prepared either by impregnation or co-impregnation using incipient wetness with silica, carbon, TiO₂ and Al₂O₃ as supports, were investigated for the direct synthesis of hydrogen peroxide and the results for reaction at 2 °C are shown in Table 1. Prior to testing, all the catalysts were calcined at 400 °C. In all cases, the pure Au catalysts generate H₂O₂ but at very low rates, and at an insufficient level to enable the hydrogen selectivity to be determined with any reasonable accuracy. It is apparent that for the Au monometallic catalysts TiO₂ is far more effective a support when compared with silica and carbon. This contrasts with the earlier findings of Haruta and co-workers³⁸ where silica was found to be an optimal support for Au for this reaction: however, the reaction conditions were different and this may merely highlight the sensitivity of this reaction to many factors, which we will discuss further later in the paper. For the Pd monometallic catalysts, silica was found to be the best support with the order of activity being SiO₂ > C > TiO₂ > Al₂O₃. The addition of Pd to Au, to give catalysts comprising 2.5 wt% Au–2.5 wt% Pd, dramatically enhances the catalytic performance for the synthesis of H₂O₂ for all the catalysts, irrespective of the support as we have previously noted.^{32–37} The highest rates of hydrogen peroxide formation and hydrogen selectivities are observed for the Au–Pd/carbon catalyst and the Au–Pd/silica catalysts, both materials yielding very similar performances in terms of activities and H₂ selectivities.

Effect of calcination temperature on catalyst performance

It is an important consideration that heterogeneous catalysts that are evaluated in batch reactors should be capable of being successfully re-used. It is possible that during use the metals can leach from the catalysts and these could play a key role in the activity that is observed, since their leaching into solution could, in principle, lead to the formation of an active *homogeneous* catalyst.³⁹ In addition, reaction products and by-products could be deposited on the catalyst resulting in catalyst deactivation. Since the ability to re-use a catalyst successfully is at the heart of

green chemistry we have examined this for the 2.5% Au–2.5% Pd catalysts supported on SiO₂, TiO₂ and Al₂O₃. Furthermore, we have considered this aspect as a function of calcination temperature (Fig. 1). Catalysts that are calcined at temperatures < 400 °C are much more active than their counterpart catalysts calcined at 400 °C when used for the first time. The TiO₂-supported material dried at room temperature was by far the most active catalyst evaluated, and the order of activity for the dried samples in terms of their support material was: TiO₂ > SiO₂ > Al₂O₃. For TiO₂- and Al₂O₃-supported Au–Pd catalysts the activity decreased steadily with increasing calcination temperature, whereas the SiO₂-supported sample showed a steady increase in activity with calcination temperature up to 300 °C, which could be associated with enhanced alloying of the nanoparticles: however, the activity of AuPd/SiO₂ decreased significantly at 400 °C, which is probably due to sintering of the particles at the elevated temperature. However, on subsequent re-use catalysts calcined at temperatures lower than 400 °C are much less active. We have previously shown^{36,37} that the catalysts calcined at low temperatures readily lose Pd and Au on use. In contrast, catalysts that are pre-calcined at 400 °C before use are very stable and do not leach any detectable Au or Pd into solution. We find that catalysts treated and stabilized in this way can be re-used many times. Hence, the final heat treatment used to activate the catalyst is a very important factor in controlling activity. Use of calcination temperatures lower than 400 °C, even for a longer time period, leads to catalysts that leach Au and Pd upon use. This heat treatment is considered to be important in promoting the alloying of Pd with Au and ensuring that very small particles (< 1 nm) are sintered into larger alloy nanocrystals.

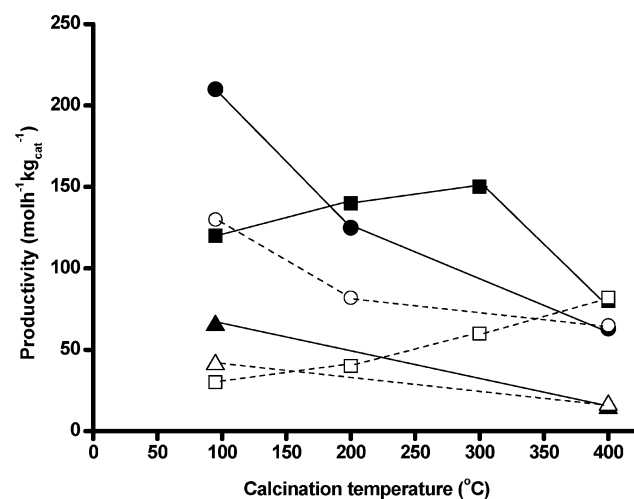


Fig. 1 Effect of calcination temperature on the formation of hydrogen peroxide using standard reaction conditions. Key: ▲ 2.5 wt% Au–2.5 wt% Pd/Al₂O₃; ■ 2.5 wt% Au–2.5 wt% Pd/SiO₂; ● 2.5 wt% Au–2.5 wt% Pd/TiO₂; closed and open symbols represent first and second use, respectively.

Catalyst characterisation

To determine the nature of the supported Au–Pd catalysts, a detailed structural and chemical characterization study was carried out using a combination of transmission electron microscopy (TEM) and X-ray photoelectron spectroscopy (XPS).

Electron microscopy characterisation

Transmission electron microscopy (TEM) was used to evaluate the degree of dispersion of the metals on the support surface. Fig. 2 shows the wide distribution of particles that are observed for the 2.5% Au–2.5% Pd/C and the 2.5% Au–2.5% Pd/SiO₂ catalyst following calcination at 400 °C. With the carbon

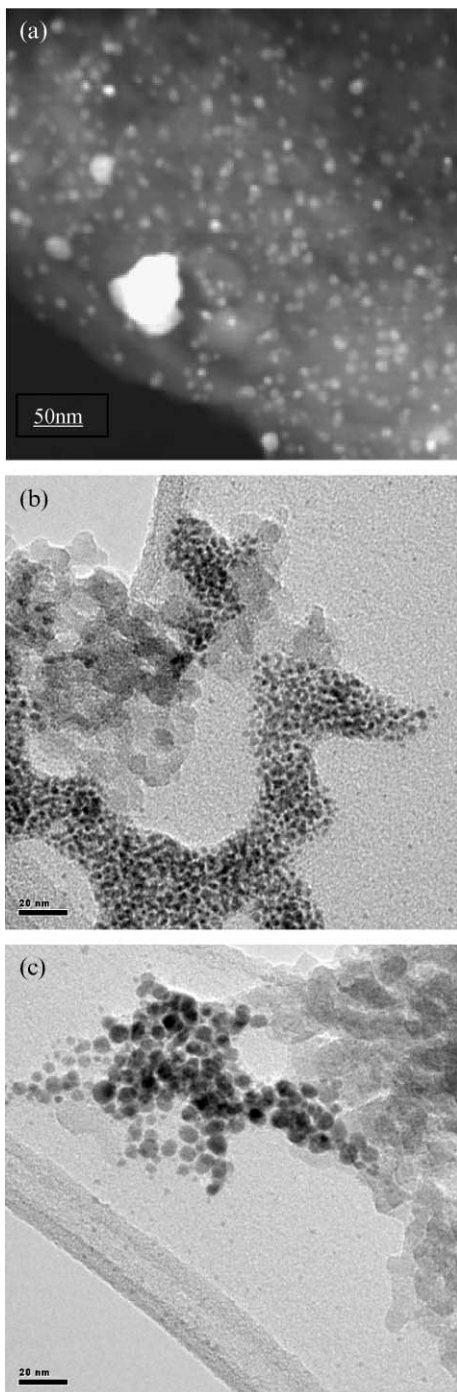


Fig. 2 (a) ADF STEM image of 2.5 wt% Au–2.5 wt% Pd/carbon,³⁷ showing that the nanocrystals are well dispersed over the support surface and there is a broad range of particle sizes; (b) and (c) BF micrographs of a 2.5 wt% Au–2.5 wt% Pd/SiO₂ catalyst, showing that the nanocrystals are not well dispersed and have a very strong tendency to cluster together on carbonaceous patches contained within the SiO₂.

supported catalyst (Fig. 2(a)) annular dark field (ADF) imaging showed the particles to be well dispersed, with a very broad particle size distribution. Very recently, we have shown⁴⁰ that the particles all contain Au and Pd and that they are homogeneous alloys: however, the composition is highly dependent on the particle size, with the fraction of gold contained in the bimetallic nanocrystal increasing as the particle diameter increases. The observation of homogeneous alloy particles contrasted with our previous observations for the TiO₂, Fe₂O₃ and Al₂O₃ supported Au–Pd catalysts as these were observed to be core shell structures with Pd-rich shells.^{34–37,40} In stark contrast to the observations with the carbon-supported catalyst, we often observed many Pd-rich nanocrystals clustering together in the silica supported material (Figs. 2 (b) and (c))

We therefore carried out X-ray energy dispersive spectroscopy (XEDS) of the Au–Pd 2.5 wt% Au–2.5 wt% Pd catalyst supported on silica calcined at 400 °C and some typical results are presented in Fig. 3. STEM-XEDS maps of a support particle show that occasional fairly large Au–Pd bimetallic particles are present as well as many dense agglomerates of very small Pd-rich alloy particles. Unfortunately, we have not yet been able to discern whether the bimetallic particles on SiO₂ are core-shell or homogeneous alloy structures. Most of the Pd was distributed very inhomogeneously around the sample and this was always clustered in or on particles of amorphous carbon (Fig. 2 (b) and (c)). The amorphous carbon was an impurity in the silica support and in this particular region the carbon K_α map (Fig. 3) shows this to be fairly well dispersed within the silica. It is therefore possible that the silica supported material may involve aspects of being a partially carbon-supported material, and the similarity in the catalytic results we have observed seems to confirm this.

XPS characterisation

The combined Au(4d) and Pd(3d) XPS spectra for representative Au–Pd catalysts supported on SiO₂, carbon, TiO₂ and Al₂O₃ following (i) drying and (ii) calcination at 400 °C are shown in Figs. 4 and 5, respectively. For the dried samples, which all exhibit higher rates of H₂O₂ production when compared with the calcined catalysts, there are clear spectral contributions from both Au and Pd, leading to severe overlap of peaks (Fig. 4). For the dried SiO₂ and TiO₂ supported catalysts, the Pd:Au surface ratio (by weight) is significantly different from the bulk value of 1:1 (Table 2), whereas the Pd:Au surface ratio for the Al₂O₃ and carbon supported catalysts is similar to that of the corresponding nominal bulk composition. After calcination at 400 °C, for the SiO₂-, TiO₂- and Al₂O₃-supported catalysts there is a decrease in the intensity of the Au (4d) peaks (Fig. 5). Hence, for these materials the metal surface has become enhanced in Pd on calcination at 400 °C (Table 2). This is consistent with the formation of core-shell structures for the Au–Pd nanoparticles, and we have previously shown calcination using STEM-XEDS mapping of individual particles.^{34–36,40} Also, alloy nanoparticles with Pd-rich shells and Au-rich cores are generated during calcination in air. Based on the XPS analysis we consider that the Au–Pd nanoparticles supported on SiO₂ are most probably core shell structures, but we need additional STEM-XEDS mapping to confirm this. As was noted earlier³⁷ the carbon supported catalyst which demonstrates no differences, either in the

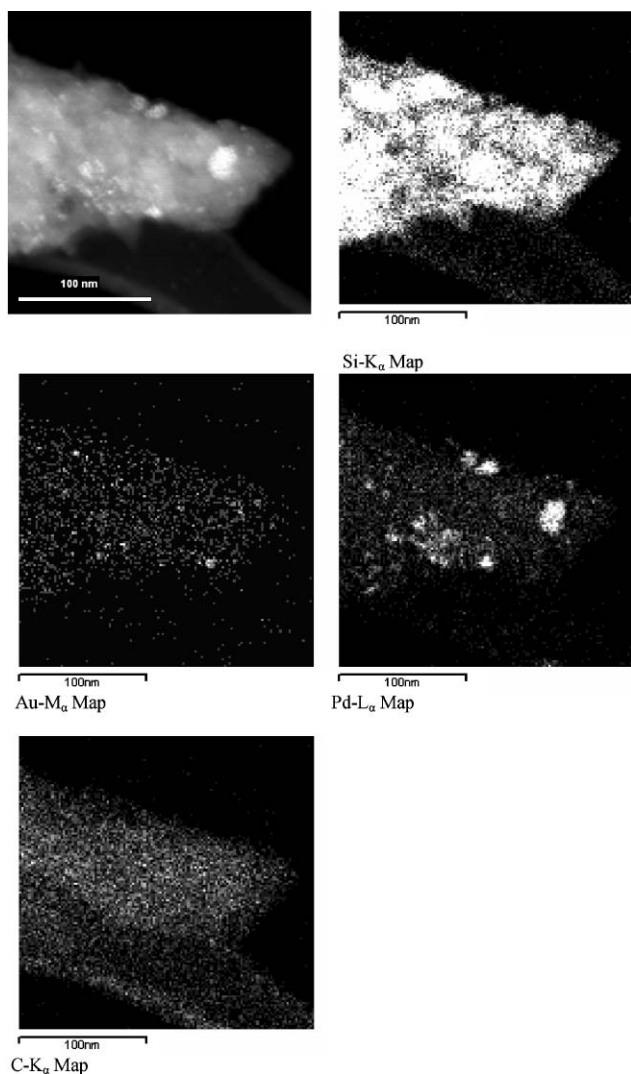


Fig. 3 ADF STEM image and Au M_{α} , Pd L_{α} , Si K_{α} and C K_{α} STEM XEDS maps showing the spatial and chemical distribution of alloy particles in the calcined 2.5 wt% Au–2.5 wt% Pd/SiO₂ sample, and the widespread distribution of the carbon impurities.

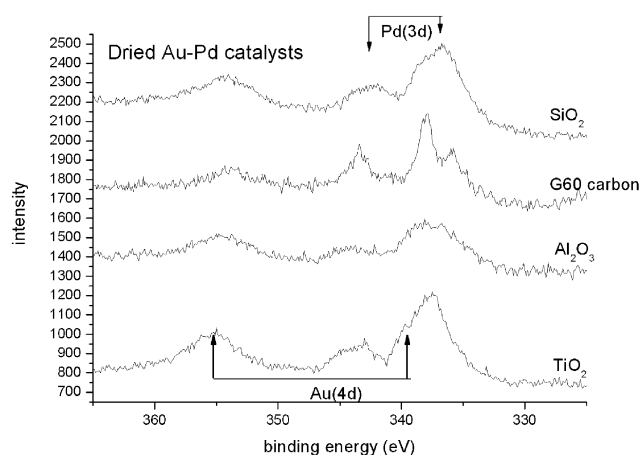


Fig. 4 Au (4d) and Pd (3d) spectra for uncalcined 2.5 wt% Au–2.5 wt% Pd catalysts.

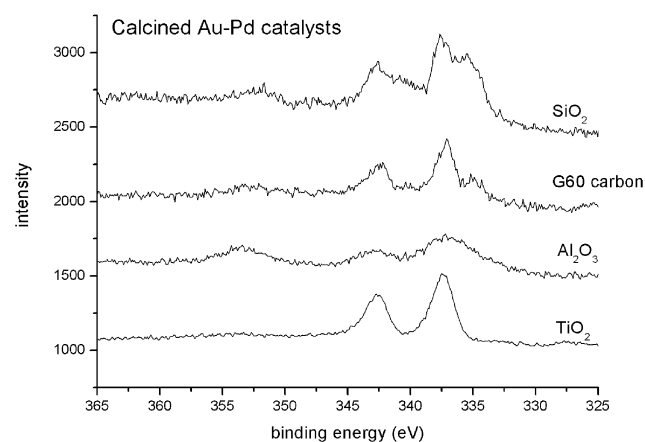


Fig. 5 Au (4d) and Pd (3d) spectra for 2.5 wt% Au–2.5 wt% Pd catalysts calcined at 400 °C in air.

Table 2 Pd:Au ratios measured by XPS for silica, titania, alumina and carbon supported Au–Pd catalysts

| Catalyst | Measured Pd:Au by weight | |
|---|--------------------------|----------|
| | Dried | Calcined |
| 2.5 wt% Pd–2.5 wt% Au/SiO ₂ | 0.2 | 1.8 |
| 2.5 wt% Pd–2.5 wt% Au/TiO ₂ | 0.3 | 5.1 |
| 0.8 wt% Pd–4.2 wt% Au/Al ₂ O ₃ ^a | 0.2 | 0.5 |
| 2.5 wt% Pd–2.5 wt% Au/G60 C | 1.0 | 1.1 |

^a This ratio has been found optimal for the alumina support.³⁵

dried or calcined states, between the surface Pd:Au ratio and the bulk value of 1:1 by weight (Table 2) are homogeneous alloys and, therefore, have a different morphology from the oxide-supported catalysts. However, given the similarity between the activity and selectivity of the silica- and the carbon-supported Au–Pd catalysts we conclude that the presence or ‘lack-of’ core-shell morphology of the Au–Pd nanocrystals is not a crucial factor that controls reactivity.

The effect of promoters and the CO₂ diluent

The key problem that dominates the catalytic direct formation of hydrogen peroxide is the selectivity of H₂ utilisation. The primary reaction is the hydrogenation of di-oxygen, and hence the H₂ has to be activated. Consequently any catalyst that is active for the initial hydrogenation reaction will almost certainly be active for the secondary hydrogenation of hydrogen peroxide to water. In addition, there are two other pathways by which non-selective chemistry can occur, and the full range of reactions is shown below:

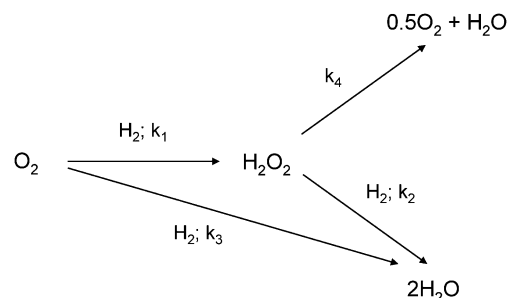


Table 3 Effect of Br⁻ and H₃PO₄ on hydrogen peroxide synthesis

| Catalyst | Pre-treatment | Productivity ^a |
|---|----------------|---------------------------|
| 2.5 wt% Au–2.5 wt% Pd/TiO ₂ | Air 400 °C 3 h | 64 |
| 2.5 wt% Au–2.5 wt% Pd/TiO ₂ | Air 400 °C 3 h | 53 ^b |
| 2.5 wt% Au–2.5 wt% Pd/TiO ₂ | Air 400 °C 3 h | 4 ^c |
| 2.5 wt% Au–2.5 wt% Pd/carbon | Air 400 °C 3 h | 110 |
| 2.5 wt% Au–2.5 wt% Pd/carbon | Air 400 °C 3 h | 20 ^c |
| 5% Pd/TiO ₂ | Air 400 °C 3 h | 31 |
| 5% Pd/TiO ₂ | Air 400 °C 3 h | 25 ^b |
| 5 wt% Pd/BaSO ₄ ^d | None | 21 |
| 5 wt% Pd/BaSO ₄ ^d | None | 80 ^c |
| 5 wt% Pd/carbon ^e | None | 15 |
| 5 wt% Pd/carbon ^e | None | 110 ^c |

^a Standard conditions with CO₂ as diluent: 420 psi 5% H₂–CO₂ + 150 psi 25% O₂–CO₂, 4 vol% H₂, 2 °C, solvent (5.6 g MeOH and 2.9 g H₂O), H₂:O₂ molar ratio = 1:2, 3.7 MPa, stirring 1200 rpm, catalyst 10 mg.

^b Standard reaction conditions with H₃PO₄ (1.6 M), 0.0006 M NaBr.

^c Reaction carried out according to Van Weynbergh *et al.*¹²: H₃PO₄ (30 ml, 1.6 M), NaBr (0.0006 M), catalyst 30 mg, 25 °C, 420 psi 5% H₂–CO₂ + 150 psi 25% O₂–CO₂, stirring 1200 rpm. ^d Aldrich. ^e Johnson Matthey.

To overcome these non-selective and parallel reactions promoters such as halides (Br⁻) and phosphoric acid are added to stabilise the hydrogen peroxide, by ensuring that the rate constants for hydrogen peroxide consumption (k_2 and k_4) are decreased relative to the rate constant for synthesis (k_1).^{41–43} These promoters are essential when using supported Pd catalysts, and some of the highest productivity data has been disclosed by researchers from Solvay Interlox, notably Van Weynbergh *et al.*,¹² using supported Pd catalysts with N₂ as diluent. We have now investigated the addition of promoters and have utilised similar concentrations of NaBr and H₃PO₄ to those used by Van Weynbergh *et al.*¹² but instead using our standard reaction conditions with CO₂ as diluent and with the Au–Pd catalyst supported on TiO₂ (Table 3). It is clear that the addition of Br⁻ and H₃PO₄ with the Au–Pd catalyst is deleterious, as is the use of the reaction conditions disclosed by Van Weynbergh *et al.*¹² using N₂ as diluent. Indeed, these conditions lead to an almost complete loss of catalyst activity for the TiO₂-supported Au–Pd catalyst, and also result in a significant loss of activity for the carbon-supported catalyst (Table 3). Interestingly, the effect was not so marked for the monometallic Pd/TiO₂ catalyst (Table 3). Furthermore, Pd/carbon and Pd/BaSO₄ catalysts gave improved performance using the reaction conditions of Van Weynbergh *et al.*⁴³ with N₂ as diluent, when compared with the same catalysts used with CO₂ as diluent (Table 3). These results lead to two interesting and important conclusions. First, the monometallic supported Pd catalysts generally perform better with the reaction conditions of Van Weynbergh *et al.*¹² which have NaBr and phosphoric acid present. By way of contrast, the addition of these materials with the Au–Pd catalysts, when using our standard reaction conditions, leads to a significant loss of activity. As the catalysts are stable under these conditions and do not leach gold or palladium into solution, we consider that the loss in activity could be due to the anions blocking sites on the catalyst surface that are active for the synthesis of hydrogen peroxide. Indeed, using our reaction conditions the supported Au–Pd catalysts do not require the addition of these promoters and readily produce hydrogen peroxide

Table 4 Effect of CO₂ diluent on the synthesis of hydrogen peroxide

| Catalyst | Pre-treatment | Productivity |
|--|----------------|------------------|
| 2.5 wt% Au–2.5 wt% Pd/TiO ₂ | Air 400 °C 3 h | 64 ^a |
| 2.5 wt% Au–2.5 wt% Pd/TiO ₂ | Air 400 °C 3 h | 29 ^b |
| 2.5 wt% Au–2.5 wt% Pd/G60 | Air 400 °C 3 h | 110 ^a |
| 2.5 wt% Au–2.5 wt% Pd/G60 | Air 400 °C 3 h | 10 ^b |

^a Standard conditions with CO₂ as diluent: 420 psi 5% H₂–CO₂ + 150 psi 25% O₂–CO₂, 4 vol% H₂, 2 °C, solvent (5.6 g MeOH and 2.9 g H₂O), H₂:O₂ molar ratio = 1:2, 3.7 MPa, stirring 1200 rpm. ^b N₂ used as diluent: 5% H₂–Ar (290 psig) + 10% O₂–He (290 psig), 4 vol% H₂, 2 °C, solvent (5.6 g MeOH and 2.9 g H₂O), H₂:O₂ molar ratio = 1:2, 3.7 MPa, stirring 1200 rpm.

yields that are comparable to, or even higher than, those of the Pd catalysts under the optimal conditions using the added promoters. Furthermore, we have previously shown⁴⁴ that water alone can act as a suitable solvent for the generation of hydrogen peroxide in the absence of added promoters, and hence our methodology represents an intrinsically greener approach to the direct synthesis of hydrogen peroxide. Secondly, CO₂ appears to play a significant role in the reaction. We therefore investigated the role of CO₂ as a diluent under our reaction conditions and contrasted it with the results obtained by using N₂ as a diluent (Table 4). It is apparent that in the absence of CO₂ much lower yields of hydrogen peroxide are obtained. CO₂ is soluble in the solvent and the degree of solubility is favoured by the low reaction temperature (2 °C) and high partial pressure of CO₂ (3.1 MPa). The carbonic acid that is formed acts as an *in situ* acidic promoter stabilising the hydrogen peroxide that is formed. We calculate that the pH of the solvent during the reaction using CO₂ as diluent will be ca. 4. When using N₂ as diluent, in place of CO₂, with a solvent acidified with HNO₃ to pH 4, we obtain an enhancement in the yield of hydrogen peroxide that is directly comparable to that observed when CO₂ is present. However, CO₂ has the advantage that the effect is reversible, since upon depressurisation the CO₂ is de-gassed from the hydrogen peroxide solution and hence it operates as a reversible *in situ* promoter. This effect of *in situ* acid generation using CO₂ in the direct hydrogen peroxide synthesis has also been observed in previous studies by Hâncu and Beckman,⁴⁵ and we consider that the use of CO₂ could be highly beneficial in the direct hydrogen peroxide synthesis reaction.

Conclusions

In the direct synthesis of hydrogen peroxide from the reaction of H₂ and O₂, the addition of Au (which is relatively inert for this reaction) to Pd produces Au–Pd nanoalloy particles and results in catalysts which have significant activity. The highest yields of hydrogen peroxide are achieved using Au–Pd catalysts supported on carbon and silica. On TiO₂, Al₂O₃ and, possibly, SiO₂ supports, the bimetallic nanoparticles exhibit core–shell structures, with Pd-rich surfaces, which form spontaneously upon calcination. However, these core–shell morphologies clearly are not essential for the observation of high reaction rates and selectivities because the calcined carbon supported Au–Pd nanoparticles invariably exhibit homogeneous Au–Pd alloy particles, which give activities that are comparable to those

found in the silica-supported catalysts. The calcined catalysts are stable and re-usable, and no loss of Au or Pd is observed as long as care is taken during the calcination of the catalysts. Furthermore, no NaBr and H₃PO₄ promoters are required when using supported catalysts in order to observe high reaction rates; indeed, these additives are deleterious to their catalytic performance. NaBr and H₃PO₄ promoters can be effective with monometallic supported Pd catalysts, clearly demonstrating that the addition of Au to Pd is significantly changing the nature of the active sites for the direct reaction. In addition, CO₂, when used as a diluent, dissolves in the solvent under the reaction conditions and this leads to the formation of carbonic acid, which enhances the stability of hydrogen peroxide in the direct synthesis reaction. Furthermore, since the acidification is reversible on depressurisation, it is apparent that CO₂ represents a green promoter for the direct synthesis of hydrogen peroxide.

Acknowledgements

This work formed part of the EU AURICAT project (Contract HPRN-CT-2002-00174) and the EPSRC/Johnson Matthey funded ATHENA project and we thank them for funding this research. We also thank the World Gold Council (through the GROW scheme), and Cardiff University (AA Reed studentship) for providing support for JKE. CJK and AH would also like to acknowledge the generous support of NSF Materials Research Science and Engineering Center (NSF DMR-0079996).

References

- 1 'Degussa Headwaters builds peroxide demonstrator', *Chem. Eng. (Rugby, Engl.)*, 2005, 766, 16.
- 2 H. T. Hess, in *Kirk-Othmer Encyclopaedia of Chemical Engineering*, ed. I. Kroschwitz and M. Howe-Grant, Wiley, New York, 1995, vol. 13, p. 961.
- 3 H. Henkel and W. Weber, US Pat. 1108752, 1914.
- 4 G. A. Cook, US Pat. 2368640, 1945.
- 5 Y. Izumi, H. Miyazaki and S. Kawahara, US Pat. 4009252, 1977.
- 6 Y. Izumi, H. Miyazaki and S. Kawahara, US Pat. 4279883, 1981.
- 7 H. Sun, J. J. Leonard and H. Shalit, US Pat. 4393038, 1981.
- 8 L. W. Gosser and J.-A. T. Schwartz, US Pat. 4772458, 1988.
- 9 L. W. Gosser, US Pat. 4889705, 1989.
- 10 C. Pralins and J.-P. Schirmann, US Pat. 4996039, 1991.
- 11 T. Kanada, K. Nagai and T. Nawata, US Pat. 5104635, 1992.
- 12 J. Van Weynbergh, J.-P. Schoebrechts and J.-C. Colery, US Pat. 5447706, 1995.
- 13 S.-E. Park, J. W. Yoo, W. J. Lee, J.-S. Chang, U. K. Park and C. W. Lee, US Pat. 5972305, 1999.
- 14 G. Paparatto, R. d'Aloisio, G. De Alberti, P. Furlan, V. Arca, R. Buzzoni and L. Meda, EP Pat. 0978316A1, 1999.
- 15 B. Zhou and L.-K. Lee, US Pat. 6168775, 2001.
- 16 M. Nystrom, J. Wangard and W. Herrmann, US Pat. 6210651, 2001.
- 17 G. C. Bond and D. T. Thompson, *Catal. Rev.–Sci. Eng.*, 1999, **41**, 319.
- 18 G. C. Bond and D. T. Thompson, *Gold Bull.*, 2000, **33**, 41.
- 19 M. Haruta, *Gold Bull.*, 2004, **37**, 27.
- 20 A. S. K. Hashmi, *Gold Bull.*, 2004, **37**, 51.
- 21 R. Meyer, C. Lemaire, Sh. K. Shaikutdinov and H.-J. Freund, *Gold Bull.*, 2004, **37**, 72.
- 22 G. J. Hutchings, *Gold Bull.*, 2004, **37**, 37.
- 23 A. S. K. Hashmi and G. J. Hutchings, *Angew. Chem., Int. Ed. Engl.*, 2006, **45**, 7896.
- 24 M. Haruta, T. Kobayashi, H. Sano and N. Yamada, *Chem. Lett.*, 1987, **16**, 405.
- 25 P. Landon, J. Ferguson, B. E. Solsona, T. Garcia, A. F. Carley, A. A. Herzing, C. J. Kiely, S. E. Golunski and G. J. Hutchings, *Chem. Commun.*, 2005, 3385.
- 26 P. Landon, J. Ferguson, B. E. Solsona, T. Garcia, S. Al-Sayari, A. F. Carley, A. Herzing, C. J. Kiely, M. Makkee, J. A. Moulijn, A. Overweg, S. E. Golunski and G. J. Hutchings, *J. Mater. Chem.*, 2006, **16**, 199.
- 27 A. K. Sinha, S. Seelan, S. Tsubota and M. Haruta, *Angew. Chem., Int. Ed. Engl.*, 2004, **43**, 1546.
- 28 M. D. Hughes, Y.-J. Xu, P. Jenkins, P. McMorn, P. Landon, D. I. Enache, A. F. Carley, G. A. Attard, G. J. Hutchings, F. King, E. H. Stitt, P. Johnston, K. Griffin and C. J. Kiely, *Nature*, 2005, **437**, 1132.
- 29 A. Abad, P. Conception, A. Corma and H. Garcia, *Angew. Chem., Int. Ed. Engl.*, 2005, **44**, 4066.
- 30 A. Corma and P. Serna, *Science*, 2006, **313**, 332.
- 31 D. I. Enache, J. K. Edwards, P. Landon, B. Solsona-Espriu, A. F. Carley, A. A. Herzing, M. Watanabe, C. J. Kiely, D. W. Knight and G. J. Hutchings, *Science*, 2006, **311**, 362.
- 32 P. Landon, P. J. Collier, A. J. Papworth, C. J. Kiely and G. J. Hutchings, *Chem. Commun.*, 2002, 2058.
- 33 P. Landon, P. J. Collier, A. F. Carley, D. Chadwick, A. J. Papworth, A. Burrows, C. J. Kiely and G. J. Hutchings, *Phys. Chem. Chem. Phys.*, 2003, **5**, 1917.
- 34 B. E. Solsona, J. K. Edwards, P. Landon, A. F. Carley, A. Herzing, C. J. Kiely and G. J. Hutchings, *Chem. Mater.*, 2006, **18**, 2689.
- 35 J. K. Edwards, B. Solsona, P. Landon, A. F. Carley, A. Herzing, M. Watanabe, C. J. Kiely and G. J. Hutchings, *J. Mater. Chem.*, 2005, **15**, 4595.
- 36 J. K. Edwards, B. E. Solsona, P. Landon, A. F. Carley, A. Herzing, C. J. Kiely and G. J. Hutchings, *J. Catal.*, 2005, **236**, 69.
- 37 J. K. Edwards, A. F. Carley, A. A. Herzing, C. J. Kiely and G. J. Hutchings, *Faraday Discuss. R. Soc. Chem.*, 2008, in the press.
- 38 Y. Okumura, K. Kitagawa, T. Yamaguchi, S. Akita, M. Tsubota and M. Haruta, *Chem. Lett.*, 2003, 822.
- 39 R. A. Sheldon, I. Arends, G.-J. ten Brink and A. Dijkman, *Acc. Chem. Res.*, 2002, **35**, 774.
- 40 A. A. Herzing, J. E. Edwards, Z.-R. Tang, M. Conte, G. J. Hutchings and C. J. Kiely, *Faraday Discuss. R. Soc. Chem.*, 2007, in the press.
- 41 V. R. Choudhary and C. Samanta, *J. Catal.*, 2006, **238**, 28.
- 42 C. Samanta and V. R. Choudhary, *Catal. Commun.*, 2006, **8**, 73.
- 43 V. R. Choudhary, C. Samanta and P. Jana, *Appl. Catal., A*, 2007, **317**, 234.
- 44 J. K. Edwards, B. E. Solsona, P. Landon, A. F. Carley and G. J. Hutchings, *Catal. Today*, 2007, **122**, 397.
- 45 D. Hâncu and E. J. Beckman, *Green Chem.*, 2001, **3**, 80.

Nitrile hydratase CLEAs: The immobilization and stabilization of an industrially important enzyme†

Sander van Pelt,^a Sandrine Quignard,^a David Kubáč,^c Dimitry Y. Sorokin,^{b,d} Fred van Rantwijk^a and Roger A. Sheldon^{*a}

Received 14th September 2007, Accepted 29th November 2007

First published as an Advance Article on the web 17th December 2007

DOI: 10.1039/b714258g

The successful immobilization and stabilization of a nitrile hydratase in the form of a cross-linked enzyme aggregate (CLEA[®]) is described. CLEAs were prepared by using ammonium sulfate as an aggregation agent followed by cross-linking with glutaraldehyde. The effect of different glutaraldehyde concentrations on the recovery of enzyme activity in the CLEA and enzyme leakage from the CLEA matrix was investigated. Although activity recovery was low (21%) the CLEA facilitates easy separation and recycling of the nitrile hydratase. It was also found that the nitrile hydratase CLEA had substantially increased storage stability as well as increased operational stability during exposure to high concentrations of acrylamide and acrylonitrile compared to that of the nitrile hydratase in the crude cell-free extract and whole cell formulation.

Introduction

Nitrile hydratase (NHase, EC 4.2.1.84) is an enzyme class that catalyzes the hydration of a very broad scope of nitrile compounds into the higher value amides.^{1,2} NHases are industrially important enzymes. The best known process in which a NHase is used is the production of acrylamide. Mitsubishi Rayon uses the enzyme from the genetically modified *Rhodococcus* J1 for the production of >100 000 ton year⁻¹ of acrylamide.³⁻⁶ SNF Floerger licenced the Mitsubishi Rayon process and announced the production of 100 000 ton year⁻¹ of acrylamide in Europe.⁷ Another process is the NHase catalyzed hydration of 3-cyanopyridine into nicotinamide, which is carried out by Lonza at >3500 ton year⁻¹ using the same organism.⁸

The enzymatic process for the hydration of acrylonitrile replaced one which employed a heterogeneous copper catalyst and was performed at 120 °C. The latter process afforded a product that is contaminated with traces of copper and significant amounts of acrylic acid byproduct which complicates downstream processing. NHases, in contrast, catalyse the hydration reaction at ambient temperature and pH in high selectivity and high yield. This affords a process that is highly energy efficient, environmentally friendly, and safe and a product of high quality

such that no further purification is necessary.^{5,8,9} Consequently, the pioneering efforts of Mitsubishi Rayon and Lonza are leading to the widespread replacement of abiological hydration of nitriles by greener enzymatic nitrile hydration using NHases.

However, one of the drawbacks of using NHases is that they are remarkably unstable under reaction conditions, especially when the enzyme is used in a cell-free formulation.^{10,11} This explains why most enzymatic hydrations are carried out using whole cells or immobilized whole cell formulations¹²⁻¹⁴ and not the free (purified) enzyme.²

Because of the possible utilization of products by cells, and because of the presence of other enzymes such as amidases or proteases, the use of (partially) purified cell-free NHases would be preferred above whole cell catalysis. An efficient immobilization method for cell-free NHase will make the application of green enzymatic hydration processes even more attractive.

In this study, the immobilization and stabilization of a cell-free NHase from a haloalkaliphilic actinobacterium strain in the form of a cross-linked enzyme aggregate (CLEA) is described. This latter method comprises the aggregation of the free enzyme from an aqueous solution using a precipitation agent, followed by cross-linking of the formed aggregates using a bifunctional cross-linker.¹⁵⁻¹⁷

Parameters of catalyst performance, such as activity retention and storage, recyclability, pH and temperature stability will be assessed. Since the production of acrylamide is now the major application for NHases in industry, the performance of the NHase CLEA in the hydration of acrylonitrile is compared to that of the NHase in whole-cell and cell-free formulation.

Results and discussion

CLEA preparation

The preparation of a CLEA involves the semi-purification and precipitation of the enzyme using an aggregation agent, followed

^a*Biocatalysis and Organic Chemistry, Department of Biotechnology, Delft University of Technology, 2628 BL, Delft, The Netherlands. E-mail: R.A.Sheldon@tudelft.nl; Fax: +31 152781415; Tel: +31 152782683*

^b*Environmental Biotechnology, Department of Biotechnology, Delft University of Technology, 2628 BC, Delft, The Netherlands*

^c*Institute of Microbiology, Academy of Sciences of the Czech Republic, 142 20, Prague 4, Czech Republic*

^d*Winogradsky Institute of Microbiology, Russian Academy of Sciences, 117811, Moscow, Russia*

† This paper was published as part of the themed issue of contributions from the 3rd International Conference on Green and Sustainable Chemistry.

by cross-linking using a compound with two or more aldehyde groups. Because CLEAs are prepared using the cell-free enzyme, breaking the cell walls of the enzyme host is a necessary first step.

Cell disruption by rapid decompression was effective, leading to a NHase deactivation of only 8.5% by volume.‡ The crude extract was semi-purified *via* an ammonium sulfate cut. All proteins that precipitated at an ammonium sulfate saturation of 41% (v/v) were discarded. Of the total NHase activity 3% was lost in the precipitate but 40 wt% of non-catalytic protein was removed in the process.

Ammonium sulfate (67% v/v, total saturation) was chosen as the aggregation agent for CLEA preparation. Approximately 80% of NHase activity was recovered after precipitation of all soluble proteins and redissolution of the precipitate in a buffer.§ Because of the good results obtained with ammonium sulfate it was decided not to investigate other possible precipitation agents.¹⁸

Subsequently, CLEAs were prepared from the precipitate with different concentrations of glutaraldehyde (Table 1). Leakage of enzyme from the CLEA matrix in the first 3 washing steps decreased substantially when the glutaraldehyde concentration during the cross-linking process was higher. This decrease in leakage is ascribed to more intensive cross-linking. The effect of a higher degree of cross-linking was also visually observed after centrifugation of the CLEAs. The CLEA became more solid, and more difficult to resuspend after the first washing and centrifugation steps, as the glutaraldehyde concentration was increased. For the two highest glutaraldehyde concentrations (3.3 and 4.2 wt%) it was even necessary to cut the precipitated CLEA in smaller pieces, since resuspension was impossible. The remaining activity in the CLEA first increased with increasing glutaraldehyde concentration, presumably due to a decrease in initial enzyme leakage. At a glutaraldehyde concentration > 0.6 wt% the remaining activity declined again. This decrease in activity is ascribed to deformation of the enzyme quaternary structure because of more intensive cross-linking.

For further tests CLEAs were prepared using 1.2 wt% of glutaraldehyde since this was the CLEA preparation with the highest activity of the preparations where no leakage was detected after the third washing step. Recovery of activity in this CLEA was 21%. Loss of NHase activity during the CLEA

preparation, besides initial enzyme leakage and deactivation because of precipitation, can be ascribed to either deformation of the enzyme quaternary structure caused by the fixation during cross-linking or by mass transfer limitation in the CLEA matrix.

Dextranpolyaldehyde with a M_w of 100–200 kDa was tried as an alternative cross-linking agent in an attempt to increase CLEA residual activity.¹⁹ Although the residual activity increased to 40–45%, the storage stability and stability during exposure to high concentrations of nitrile and amide were substantially lower (data not shown). The main problem of the CLEA in this form is the difficulty in handling the immobilized enzyme. The CLEA is very amorphous in suspension and has a low density. Obtaining a good dispersion of the CLEA in the reaction mixture is almost impossible and recycling the CLEA is difficult, since it is hard to separate the CLEA by means of centrifugation.

Storage stability

Fig. 1 compares storage stabilities of the NHase in crude cell-free extract, whole cell and CLEA formulation at 21 °C in buffer. The NHase activity in the cell-free extract disappeared completely after 17 days. Cells still have 20% residual activity at this point in time, while the CLEA did not lose any activity. Even after 4 months of storage the CLEA was still fully active. Apparently, cross-linking the NHase leads to drastic stabilization of the enzyme under these storage conditions.

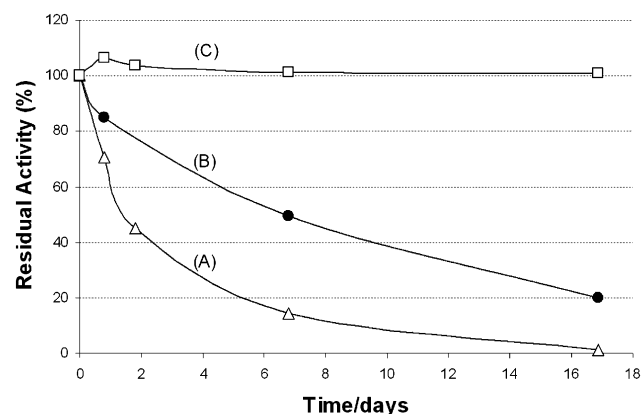


Fig. 1 Comparison of storage stabilities at 21 °C of crude cell-free extract (A), whole cells (B) and CLEA (C) in 0.01 M Tris-HCl buffer of pH 8.

‡ Volumetric activity of cell suspension *vs.* volumetric activity of extract after disruption.

§ Unless stated otherwise buffer used is 0.01 M Tris-HCl buffer of pH 8.

Table 1 Preparation of CLEAs using different concentrations of glutaraldehyde

| Glutaraldehyde concentration (wt%) | Protein concentration/mg mL ⁻¹ | Activity in supernatant after 1st wash (%) ^a | Activity in supernatant after 3rd wash (%) ^a | Remaining activity in CLEA (%) ^{b,c} |
|------------------------------------|---|---|---|---|
| 0.3 | 3.8 | 4.5 | 0.7 | 15 |
| 0.6 | 3.8 | 2 | 0.3 | 23 |
| 1.2 | 3.7 | 0.02 | 0 | 21 |
| 2.3 | 3.5 | 0.02 | 0 | 16 |
| 3.3 | 3.4 | 0 | 0 | 10 |
| 4.2 | 3.2 | 0 | 0 | 4 |

^a % of total CLEA activity. ^b Activity of CLEA is tested after 3 washing and centrifugation steps. ^c Remaining activity is determined by comparison with the total amount of units in 500 µL crude extract.

Freeze drying of the CLEA in most cases caused high activity loss (70–80% of total activity). Since the stability of the CLEA stored in buffer was excellent, optimization of the freeze drying process was not pursued any further.

Temperature stability and pH profile

Fig. 2 shows the residual activities of the NHase in whole cell, cell-free extract and CLEA formulation after 20 min incubation at different temperatures. Although there seems to be a trend in stability at elevated temperatures of CLEA > whole cell > crude extract, the differences are small. It is well-known that NHases are not stable for a long time at temperatures > 30 °C, except for the NHases that were isolated from thermophilic organisms.^{20–23} The low temperature stability of the NHase enzyme is one of the reasons why the production of acrylamide is usually carried out at $T < 10$ °C. Cross-linking the enzyme clearly does not have a significant effect on the stability of the NHase at elevated temperatures.

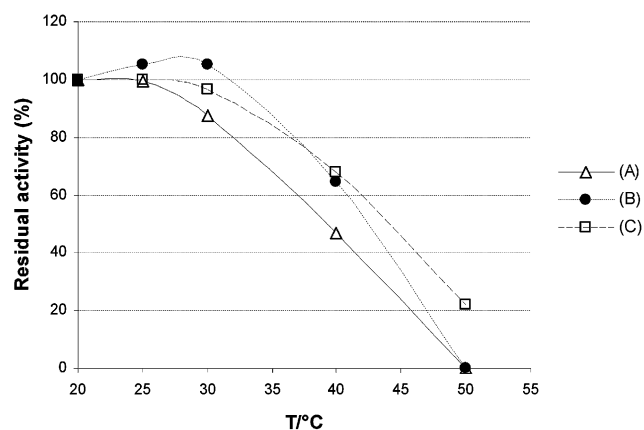


Fig. 2 Comparison of temperature stability of NHase in crude cell-free extract (A), whole cell (B) and CLEA (C) preparation.

The pH profiles (Fig. 3) of the NHase in whole cell, crude extract and CLEA formulation are largely similar. The NHase in whole cell formulation is less susceptible to pH change than the NHase in the crude extract. This can be caused by the pH regulating capacity of the cells. This effect is most noticeable at

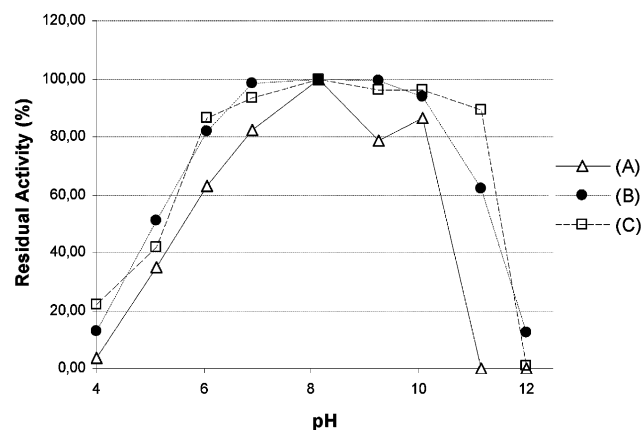


Fig. 3 Comparison of pH profiles of NHase in crude cell-free extract (A), whole cell (B) and CLEA (C) preparation.

pH 11 and 12 where no activity was found for the free enzyme. The CLEA seems to be the least susceptible to pH change. Between pH values of 6–11 the activity differences stay within 20%. The activity range of the CLEA is large, between pH 4 and pH 11. The better stability of the CLEA during the 20 min incubation is the main reason for this behaviour.

Operational stability in acrylamide production

In the production of acrylamide (Fig. 4), whether it is performed in batch or fed-batch fashion, the NHase is by far most stable in CLEA formulation (Fig. 5, 6 and Table 2), especially during exposure to high nitrile and/or amide concentrations. The NHase in cell-free crude extract clearly has the lowest stability. Apparently free NHase is much more sensitive to high acrylamide and acrylonitrile concentrations than NHase contained in cells or cross-linked as a CLEA.

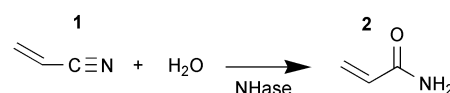


Fig. 4 Acrylonitrile (1) hydration to acrylamide (2) using a NHase.

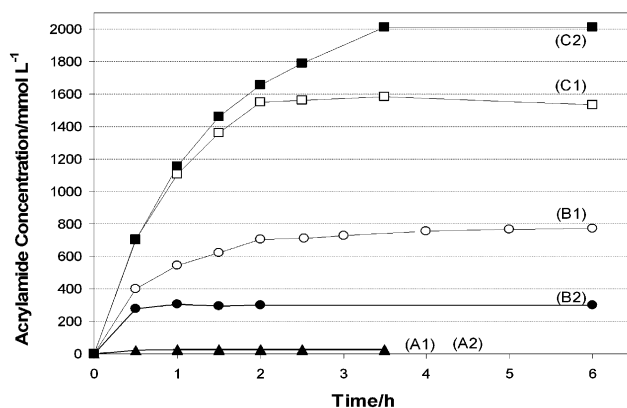


Fig. 5 Comparison of the stabilities of NHase in crude cell-free extract (A), whole cell (B) and CLEA (C) preparation in batch reactions using acrylonitrile concentrations of 1630 (1) and 1980 (2) mmol L⁻¹.

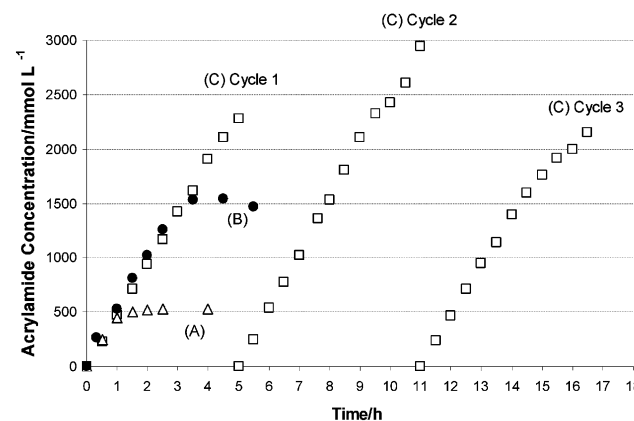


Fig. 6 Comparison of the stabilities of NHase in crude cell-free extract (A), whole cell (B) and CLEA (C) in the fed-batch production of acrylamide.

Table 2 Effect of starting acrylonitrile concentration on the reaction stability of NHase in different formulations. Residual activities of the CLEA after the batch experiments and during the fed-batch reactions are included

| NHase formulation | Acrylonitrile concentration (% v/v) | Acrylonitrile concentration/mmol L ⁻¹ | Final conversion (%) | Residual activity (%) |
|-------------------|-------------------------------------|--|----------------------|-----------------------|
| Crude extract | 2.9 | 440 | >98 | n.d. ^a |
| | 5.7 | 860 | 75 | |
| | 8.3 | 1250 | 8 | |
| | 10.7 | 1630 | 2 ^b | |
| | 13 | 1980 | 1 ^b | |
| Whole cell | 2.9 | 440 | >98 | n.d. ^a |
| | 5.7 | 860 | >98 | |
| | 8.3 | 1250 | >98 | |
| | 10.7 | 1630 | 49 ^b | |
| | 13 | 1980 | 15 ^b | |
| CLEA | 8.3 | 1250 | >98 | 77 |
| | 10.7 | 1630 | >98 ^b | 65 |
| | 13 | 1980 | >98 ^b | 72 |
| CLEA | Fed-batch cycle #1 ^c | | | 68 |
| | Fed-batch cycle #2 ^c | | | 53 |
| | Fed-batch cycle #3 ^c | | | 27 |

^a n.d. = not determined. ^b See also Fig. 4. ^c See also Fig. 5.

One explanation for the increased stability of the CLEA could be that the NHase in this formulation is quite rigidly bound to its neighbours, preventing dissociation of subunits. Dissociation of subunits can lead to lower stability since subunits are usually more susceptible to deactivation factors such as temperature, pH and high concentrations of organic compounds.²⁴ This effect can also explain the higher stability of the NHase in a whole cell formulation, since the cells are able to maintain a local high concentration of enzyme which is favourable for the dissociation equilibrium. However, cells have the tendency to lyse during exposure to high concentrations of organics after which the enzyme loses this natural barrier to the environment.

Another reason for the higher stability of the CLEA could be the existence of concentration gradients inside the CLEA particles. If this is the case, only the outside layer of enzyme in the particle is subjected to high concentrations of amide and nitrile. The outside layer of enzyme can deactivate but will in this way still protect the enzyme that is situated in the inner part of the CLEA particle.

Another important operational parameter is the recycling stability of the CLEA. Centrifugation and washing of the CLEA after short reactions had practically no effect on the activity[¶] (35 cycles were performed) as long as decantation of reaction and washing liquids is performed with care. The particle size distribution of the CLEA is broad and approximately 30–40% of the CLEA is present in fine powder form. The CLEA powder easily resuspends and can be discarded if decantation does not take place carefully.

Experimental

Haloalkaliphilic actinobacterium strain ANL-iso2, enriched from soda lake sediments, was grown as described previously with isobutyronitrile as the only carbon, energy and nitrogen source.²⁵ Freshly grown cells were washed in 0.3 M sodium

carbonate/bicarbonate buffer, pH 9 and stored at –80 °C as a dense suspension until further use. Protein concentration was measured by using the Lowry method. Hexanenitrile (98%), hexanamide (98%) and hexanoic acid (99.5+%) were purchased from Aldrich. Acrylonitrile (>99.5%), acrylamide puriss. p.a. standard for GC (>99.8%) and anhydrous acrylic acid (>99%) were purchased from Fluka. A 25 wt% solution of glutaraldehyde in water was purchased from Acros. Deoxyribonuclease 1 and ribonuclease A, both from bovine pancreas, were purchased from Sigma. In all experiments the buffer that was used is 0.01 M Tris-HCl buffer of pH 8 unless stated otherwise.

Cell disruption

Frozen dense cell suspension (protein concentration: 60 mg mL⁻¹) was allowed to melt slowly on ice. To 2 mL of this dense cell suspension 3 mL buffer was added and the resulting mixture was vortexed until a homogenous suspension was obtained. Before cell disruption a small amount of RNase, DNase and magnesium chloride were added to the suspension to prevent the formation of a dense and viscous cell-free extract (due to DNA release from the lysed cells). Disruption at a pressure of 2 kbar (IKS Lab Equipment Constant Cell Disruption System) gave a liquid non-viscous cell free extract. Cell debris and remaining whole cells were spun down using a Sorvall RC-5B refrigerated superspeed centrifuge (18 000 rpm, 4 °C, 30 min). Cell-free extract was stored on ice without additions until further use.

CLEA preparation

An amount of 500 µL of cell free extract (protein concentration: 16.2 mg mL⁻¹) was shaken in an Eppendorf tube (500 rpm, 4 °C, ThermoTWISTER comfort, QUANTIFOIL Instruments). Total amount of units in 500 µL of extract was approximately 100. To the extract, 350 µL of saturated ammonium sulfate (pH adjusted to 8 using NaOH) was slowly added (41% v/v total saturation). The resulting mixture was shaken again (500 rpm, 4 °C, 30 min), after which the precipitated protein was centrifuged off with a Sigma 1–13 centrifuge (13 000 rpm, 5 min,

[¶] No activity loss was observed after the 3 initial washing and centrifugation steps.

RT). The supernatant was decanted and another 650 μL of the saturated ammonium sulfate was added to the supernatant (67% v/v total saturation) after which the mixture was again shaken gently (500 rpm, 30 min, 4 °C). After 30 min 1 mL of this mixture was transferred to another Eppendorf tube and 12.5–200 μL of 25 wt% glutaraldehyde were added. After shaking (500 rpm, 4 °C, 3 h) the suspended CLEA was centrifuged (13 000 rpm, 10 min) and washed 3 times with 1 mL buffer to remove all remaining glutaraldehyde and non-cross-linked protein. The CLEA was stored on ice in buffer until further use. To 500 μL of each of the three washing supernatants 500 μL of buffer were added. The resulting mixture was assayed for activity using hexanenitrile to determine enzyme leakage.

HPLC analysis

Hexanenitrile, hexanamide and hexanoic acid concentration in the reaction were analysed by HPLC using a 4.6×50 Merck Chromolith SpeedROD RP-18e, eluent H_2O –ACN, 90 : 10 (v/v) containing acetic acid (0.1%, v/v) at 1 mL min^{-1} and a column temperature of 21 °C. Hexanoic amide and hexanoic acid were detected using a Shimadzu SPD-10A VP UV-VIS detector at a wavelength of 210 nm. Hexanenitrile was detected using a Shimadzu RID 10A refractive index detector.

Acrylonitrile, acrylamide and acrylic acid concentration in the reaction were analysed by HPLC using a 4.6×50 Merck Chromolith SpeedROD RP-18e, eluent H_2O –ACN, 99 : 1 (v/v) containing acetic acid (0.1%, v/v) at 1 mL min^{-1} and a column temperature of 21 °C. Acrylamide and acrylic acid were detected using a Shimadzu SPD-10A VP UV-VIS detector at a wavelength of 230 nm. Acrylonitrile was detected using a Shimadzu RID 10A refractive index detector.

Activity assay

Cell suspension and cell-free extract. To 1500 μL buffer 10 μL of cell-suspension or cell-free extract with a known protein concentration were added together with 10 μL of pure hexanenitrile (~ 54 mmol L^{-1}) in an Eppendorf tube. The tubes were shaken (700 rpm, 21 °C) for 5 min. After 5 min a 200 μL sample was withdrawn and mixed with the same amount of 1 M HCl to quench the reaction. The sample was centrifuged (13 000 rpm, RT, 15 min) and the supernatant was injected directly on HPLC.

CLEA. To a certain amount (mg) of CLEA in an Eppendorf tube, 1000 μL of buffer and 15 μL of hexanenitrile were added (~ 120 mmol L^{-1}). The reaction was allowed to proceed for 5 min after which the CLEA was centrifuged off in 10–20 s. A 200 μL sample was withdrawn and mixed with the same amount of 1 M HCl to make sure that any accidentally transferred CLEA was deactivated. After centrifugation the supernatant was directly injected on HPLC.

Activity: one unit (U) of NHase will form one μmol of hexanoic amide per min.

Storage stability

Cell suspension, cell-free extract and CLEA were stored at 21 °C in buffer in the following concentrations: cell suspension (24 mg mL^{-1} protein), cell-free extract (16 mg mL^{-1} protein)

and CLEA (3.7 mg mL^{-1} protein). The residual activities (%) were determined by following the activities of the different formulations during time using the activity assay and comparing these activities to the initial activities.

Recycling stability

Recycling stability was determined by carrying out a standard CLEA activity test. After the reaction the CLEA was washed three times using buffer to make sure all hexanoic amide was removed. After washing another activity assay was carried out and residual activity was determined.

Temperature stability

In 1000 μL of buffer, 20 μL of cells or cell-free extract and around 3.7 mg of CLEA were incubated at 20–50 °C for 20 min. After incubation the solution was cooled until it reached 21 °C and residual activity of the different NHase formulations were determined in a standard activity test.

pH Profile

In 1000 μL of buffer, 20 μL of cells or cell-free extract and around 3.7 mg of CLEA were incubated at different pH values (pH 4–6: 0.01 M citrate buffer, pH 7–9: 0.01 M Tris-HCl buffer, pH 10–12: 0.01 M phosphate buffer) at 21 °C for 20 min. After incubation activity was determined.

Starting concentration experiment

Whole cells, cell-free extract or CLEA of different amounts (necessary to assure the use of a total of 18 units in each reaction) were mixed with buffer to a volume of 1000 μL , after which 30–150 μL of acrylonitrile (2.9–13%, v/v, 440–1980 mmol L^{-1}) were added. This solution was shaken at 21 °C at 700 rpm for cell-free extract and whole cells and 900 rpm for the CLEA. Every 30 min, a 10 μL sample was withdrawn. The withdrawn sample was quenched with 1 M HCl. After centrifugation and, when necessary, dilution with Milli-Q water the sample was analyzed by HPLC. The reaction was monitored in this fashion until increase in amide concentration was no longer detected. In the case of CLEA, the catalyst was washed several times with buffer after the reaction was completed to remove all acrylamide. Subsequently residual activity of the catalyst was determined using the activity test.

Fed-batch experiment

Whole cells, cell-free extract or CLEA of different amounts (necessary to assure the use of a total of 18 units in each reaction) were mixed with buffer to a volume of 1000 μL , after which 20 μL of acrylonitrile (~ 300 mmol L^{-1}) were added. This solution was shaken at 21 °C at 700 rpm for cell-free extract and whole cells and 900 rpm for the CLEA. Every 30 min, a 10 μL sample was withdrawn and 20 μL of acrylonitrile was added. The withdrawn sample was quenched with 1 M HCl. After centrifugation and, when necessary, dilution with Milli-Q water, the sample was analyzed by HPLC. The reaction was monitored in this fashion until increase in amide concentration was no longer detected.

In the case of the CLEA, the reaction was continued to a concentration of 2–3 mol L⁻¹ of acrylamide, after which the CLEA was washed with buffer until acrylamide was no longer detected in the washing supernatant. After washing the CLEA residual activity was determined using the activity assay. The CLEA was stored on ice until the next fed-batch cycle was started.

Conclusion

Although there is room for improvement, the CLEA immobilization technique can be used to successfully immobilize and stabilize crude cell-free NHase. This is the first time that successful immobilization of free NHase is reported in the literature. Preparation of the CLEAs starting from the whole cell suspension is simple and straightforward, which makes it a very accessible method of immobilization. Continuously improving the methods of NHase immobilization will contribute to more applications of this enzyme as a green nitrile hydration catalyst in industry and therefore will contribute to green chemistry in general.

Acknowledgements

The authors wish to thank Dr Menno Sorgedraeger of CLEA Technologies for helpful discussions and the Delft Research Center of Life Sciences and Technology (DRC-LST) for financial support. D. Y. Sorokin was supported by RFBR grant 07-04-00153. Support by COST D25/0002/02 is also gratefully acknowledged.

References

- 1 A. Banerjee, R. Sharma and U. C. Banerjee, *Appl. Microbiol. Biotechnol.*, 2002, **60**, 33–44.
- 2 L. Martinkova and V. Mylerova, *Curr. Org. Chem.*, 2003, **7**, 1279–1295.
- 3 M. Kobayashi, T. Nagasawa and H. Yamada, *Trends Biotechnol.*, 1992, **10**, 402–408.
- 4 T. Nagasawa, H. Shimizu and H. Yamada, *Appl. Microbiol. Biotechnol.*, 1993, **40**, 189–195.
- 5 T. Nagasawa and H. Yamada, *Pure Appl. Chem.*, 1995, **67**, 1241–1256.
- 6 H. Yamada and M. Kobayashi, *Biosci., Biotechnol., Biochem.*, 1996, **60**, 1391–1400.
- 7 S. M. Thomas, R. DiCosimo and A. Nagarajan, *Trends Biotechnol.*, 2002, **20**, 238–242.
- 8 N. M. Shaw, K. T. Robins and A. Kiener, *Adv. Synth. Catal.*, 2003, **345**, 425–435.
- 9 J. Raj, A. Seth, S. Prasad and T. C. Bhalla, *Appl. Microbiol. Biotechnol.*, 2007, **74**, 535–539.
- 10 Y. J. Wang, Y. G. Zheng, R. C. Zheng and Y. C. Shen, *Appl. Biochem. Microbiol.*, 2006, **42**, 384–387.
- 11 L. Song, M. Wang, X. Yang and S. Qian, *Biotechnol. J.*, 2007, **2**, 717–724.
- 12 L. J. Mersinger, E. C. Hann, F. B. Cooling, J. E. Gavagan, A. Ben Bassat, S. J. Wu, K. L. Petrillo, M. S. Payne and R. DiCosimo, *Adv. Synth. Catal.*, 2005, **347**, 1125–1131.
- 13 X. L. Guo, G. Deng, J. Xu and M. X. Wang, *Enzyme Microb. Technol.*, 2006, **39**, 1–5.
- 14 D. Kubac, A. Cejkova, J. Masak, V. Jirku, M. Lemaire, E. Gallienne, J. Bolte, R. Stloukal and L. Martinkova, *J. Mol. Catal. B: Enzym.*, 2006, **39**, 59–61.
- 15 L. Q. Cao, F. van Rantwijk and R. A. Sheldon, *Org. Lett.*, 2000, **2**, 1361–1364.
- 16 R. A. Sheldon, R. Schoevaart and L. M. van Langen, *Biocatal. Biotransform.*, 2005, **23**, 141–147.
- 17 R. A. Sheldon, *Adv. Synth. Catal.*, 2007, **349**, 1289–1307.
- 18 R. Schoevaart, M. W. Wolbers, M. Golubovic, M. Ottens, A. P. G. Kieboom, F. van Rantwijk, L. A. M. van der Wielen and R. A. Sheldon, *Biotechnol. Bioeng.*, 2004, **87**, 754–762.
- 19 C. Mateo, J. M. Palomo, L. M. van Langen, F. van Rantwijk and R. A. Sheldon, *Biotechnol. Bioeng.*, 2004, **86**, 273–276.
- 20 T. Yamaki, T. Oikawa, K. Ito and T. Nakamura, *J. Ferment. Bioeng.*, 1997, **83**, 474–477.
- 21 R. A. Pereira, D. Graham, F. A. Rainey and D. A. Cowan, *Extremophiles*, 1998, **2**, 347–357.
- 22 Y. Takashima, Y. Yamaga and S. Mitsuda, *J. Ind. Microbiol. Biotechnol.*, 1998, **20**, 220–226.
- 23 R. Padmakumar and P. Oriel, *Appl. Biochem. Biotechnol.*, 1999, **77–79**, 671–679.
- 24 L. Wilson, L. Betancor, G. Fernandez-Lorente, M. Fuentes, A. Hidalgo, J. M. Guisan, B. C. C. Pessela and R. Fernandez-Lafuente, *Biomacromolecules*, 2004, **5**, 814–817.
- 25 D. Y. Sorokin, S. van Pelt, T. P. Tourova and G. Muyzer, *Appl. Environ. Microbiol.*, 2007, **73**, 5574–5579.

Base supported ionic liquid-like phases as catalysts for the batch and continuous-flow Henry reaction†

M. Isabel Burguete, Hanno Erythropel, Eduardo Garcia-Verdugo,* Santiago V. Luis* and Victor Sans

Received 28th September 2007, Accepted 10th December 2007

First published as an Advance Article on the web 17th January 2008

DOI: 10.1039/b714977h

New solid basic catalysts immobilised onto supported ionic liquid-like phases have been prepared, having suitable mechanical stability for their use for the continuous-flow Henry reaction.

Introduction

The need to reduce the amount of toxic waste and by-products arising from chemical processes requires an increasing emphasis on the use of less toxic and environmentally compatible materials and the design of new synthetic methods.¹ Base catalysed reactions are widely employed in the bulk and fine chemical industries. Examples include the aldol,² Knoevenagel,³ Henry⁴ and Michael⁵ reactions. Under the former perspective, this requires achieving selective processes yielding the desired product and reducing the salts formed as a result of neutralisation of soluble bases. Within this context, the design and development of environmentally friendly basic catalysts for C–C bond formation in organic transformations is highly important.

To catalyse these processes organic amines, alkali alkoxides, and alkali hydroxides are commonly used in a homogeneous phase with the reagents. Although the approach is effective, these reagents are difficult to separate and, in many cases, are not recycled. Moreover, the presence of acids in the work up may catalyze side reactions, like dehydration, leading to lower selectivities. To alleviate these problems, solid basic catalysts have been developed utilizing either inorganic solid materials, such as basic metal oxides and carbonates, or by supporting organic bases, for example amines, on inorganic or polymeric supports. This approach has attracted intense interest. Effective heterogeneous basic catalysts have been found for aldol, Knoevenagel, Henry and Michael reactions and, in many cases, the solid base is recyclable.⁶

Recently, ionic liquid technology has been utilized to enable base catalysed reactions to occur, allowing the base to be recycled and, in some cases, showing higher selectivities compared with molecular solvents.⁷

Although ILs have become commercially available, they are still relatively expensive compared to traditional solvents. Besides, some of them show evidence of low biodegradability and (eco)toxicological properties.⁸ Hence, the immobilisation of ILs onto a support is a highly attractive strategy to minimize

the amount of ILs used, maintaining their catalytic properties. Additionally, supported ILs have the advantage of an easy separation and recyclability as well as the potential for the development of continuous processes.⁹

We have recently reported the preparation of supported ionic liquid-like phases (SILLPs) by the modification of either macroporous or gel type polystyrene-divinylbenzene (PS-DVB) resins.¹⁰ As these materials are not able to adsorb ILs as films onto the surface, as occurs in the case of silica gel,¹¹ our approach was based on the immobilisation by covalent binding of IL-like units (alkyl-imidazolium cations). In our approach, ILs properties are transferred to the solid phase leading to either monolithic supported ionic liquid-like phases (M-SILLPs) or gel supported ionic liquid-like phases (G-SILLPs), with similar characteristics than the homogeneous analogues.¹² Furthermore, their controlled solid nature enable them to be used to develop mini-flow reactors for continuous processes.¹³

In this paper, we report the preparation of new solid base catalysts with suitable mechanical stability for their application for continuous-flow processes. The catalytic systems are based on basic anions immobilised by metathesis onto SILLPs, and were applied for batch and continuous nitroaldol reactions. This approach synergically combines the advantages of supported ionic liquids as a “supported liquid solvent”, those of an immobilised base as a “green” catalyst and those of solventless reactions with the advantages of a continuous flow process, easy product separation and catalyst reuse.

Experimental

General considerations

All the reagents were used as received, without any further purification. Raman spectroscopy was done by means of a JASCO NRS-3100 dispersive spectrometer. Conditions: 785 nm laser with a single monochromator, grating 600 mm⁻¹, slit 0.2 mm, resolution 12.75 cm⁻¹; with a center wavenumber of 1200 cm⁻¹, a laser power of 90.1 mW and 10 accumulations of 5 s. The IR spectra were recorded on a Perkin-Elmer 2000. NMR spectroscopy was done by means of a Varian Mercury 500 MHz with chemical shifts expressed in ppm. Mass spectra were recorded on a Quattro LC (quadrupole–hexapole–quadrupole) mass spectrometer with an orthogonal Z-spray electrospray

Dtp. Química Inorgánica y Orgánica, Universidad Jaime I, Avda. Sos Baynat s/n, 12071, Castellón, Spain.

E-mail: eduardo.garcia-verdugo@qio.uji.es, luiss@qio.uji.es; Fax: +34 964728214; Tel: +34 964728239

† This paper was published as part of the themed issue of contributions from the 3rd International Conference on Green and Sustainable Chemistry.

interface. Elemental analysis were performed on an Elemental Carlo Erba 1108 apparatus.

General procedure for the synthesis of G-SILLPs

A Merrifield resin (2 g, 1.1 mmol g⁻¹, 1% DVB) was suspended in 25 mL of a 1 M solution of 1,2-dimethylimidazole in DMF. The system was heated at 80 °C and periodically, samples of ca. 20 mg of polymer were extracted, washed with MeOH and dried under vacuum for Raman analysis. After 3 h, the polymer was filtered, washed with DMF (3 × 20 mL), MeOH (3 × 20 mL), CH₂Cl₂ (3 × 20 mL) and dried under vacuum at 60 °C.

General procedure for the synthesis of M-SILLP 3

Monolithic materials were prepared by copolymerization of the corresponding monomeric mixture inside a HPLC column (stainless column, 15 cm–1/4 inch id) as has been described elsewhere.^{10a} Monomeric mixture 40 : 60 CIVB : DVB mass%; porogenic mixture toluene : dodecanol 10 : 50 mass%; monomers: porogens ratio 40 : 60 mass%. 1% AIBN, 24 h, 70 °C.

G-SILLP 4a

IR (cm⁻¹) KBr. 3053, 3023, 2920, 1602, 1587, 1535, 1512, 1451, 1421, 1269, 1239, 1162, 1112, 1081, 1019, 855,823, 762, 695, 665, 607, 545, 471. Raman (cm⁻¹): 1595, 1575, 1506, 1442, 1323, 1192, 1177, 1148, 1064, 1024, 995, 900, 825, 788, 755, 720, 663, 637, 616, 540, 401, 310. Elemental analysis observed: %N 2.5. Calculated for (C₁₀H₁₀)_{0.02}(C₈H₈)_{0.87}(C₁₄H₁₇ClN₂)_{0.11} %N 2.6. Loading: 0.91 mmol functional group g⁻¹ resin.

G-SILLP 4b

Elemental analysis observed. %N 4.3. Calculated for (C₁₀H₁₀)_{0.02}(C₈H₈)_{0.74}(C₁₄H₁₇ClN₂)_{0.24} %N 4.8. Loading: 1.78 mmol functional group g⁻¹ of resin.

G-SILLP 4c

Elemental analysis observed. %N 8.05. Calculated for (C₁₀H₁₀)_{0.02}(C₈H₈)_{0.46}(C₁₄H₁₇ClN₂)_{0.52} %N 8.10. Loading: 2.89 mmol functional group g⁻¹ of resin.

SILLP 5

Elemental analysis observed. %N 2.35. DVB content estimated by Raman spectroscopy.¹⁴ Calculated for (C₁₀H₁₀)_{0.55}(C₈H₈)_{0.26}(C₁₄H₁₇ClN₂)_{0.14} %N 2.83. Loading: 1.07 mmol of functional group g⁻¹ of resin.

M-SILLP 6

A 1 M solution of 1,2-dimethylimidazole in DMF was pumped into a monolithic column by means of a HPLC pump. After filling the column, the system was closed and heated at 70 °C for 24 h in an oven. Afterwards, the system was washed with DMF and MeOH. IR (cm⁻¹) KBr: 3053, 3023, 2920, 1602, 1587, 1535, 1512, 1451, 1421, 1269, 1239, 1162, 1112, 1081, 1019, 855,823, 762, 695, 665, 607, 545, 471. Raman (cm⁻¹): 1595, 1575, 1506, 1442, 1323, 1192, 1177, 1148, 1064, 1024, 995, 900, 825, 788, 755, 720, 663, 637, 616, 540, 401, 310. Elemental analysis

observed: %N 4.68. Calculated for (C₁₀H₁₀)_{0.64}(C₁₄H₁₇ClN₂)_{0.36} %N 6.0. Loading: 2.14 mmol functional group g⁻¹ of resin.

General procedure for anion metathesis

The resin (1 g) was suspended in 15 mL of a 1 M solution of the corresponding salt in MeOH or MeOH : H₂O. For the introduction of hydroxyl groups in the resin, it was suspended in 10 mL of an aqueous solution of NH₃. The system was stirred for 24 h at room temperature. Afterwards the polymer was filtered and washed with MeOH, MeOH : H₂O (1 : 1), H₂O and MeOH.

G-SILLP 7a (X = OH)

IR (cm⁻¹) KBr. 3023, 2921, 2849, 1707, 1670, 1587, 1534, 1513, 1452, 1420, 1269, 1239, 1160, 1112, 1018, 965, 823, 762, 695, 665, 543. Raman (cm⁻¹): 1595, 1575, 1506, 1442, 1323, 1192, 1177, 1148, 1064, 1024, 995, 900, 825, 788, 755, 720, 663, 637, 616, 540, 401, 310. E. analysis calc: %N 2.4. Calculated for (C₁₀H₁₀)_{0.02}(C₈H₈)_{0.86}(C₁₆H₂₀N₂O₂)_{0.11} %N 2.6. Loading: 1.04 mmol functional group g⁻¹ of resin.

G-SILLP 7b (X = OH)

Elemental analysis observed. %N 4.2. Calculated for (C₁₀H₁₀)_{0.02}(C₈H₈)_{0.74}(C₁₄H₁₈N₂O)_{0.24} %N 4.9. Loading: 1.78 mmol functional group g⁻¹ resin.

G-SILLP 7c (X = OH)

Elemental analysis observed. %N 7.56. Calculated for (C₁₀H₁₀)_{0.02}(C₈H₈)_{0.46}(C₁₄H₁₈N₂O)_{0.52} %N 7.66. Loading: 2.71 mmol functional group g⁻¹ resin.

G-SILLP 7d (X = proline)

Elemental analysis observed. %N 2.6. Calculated for (C₁₀H₁₀)_{0.02}(C₈H₈)_{0.86}(C₁₉H₂₅N₃O₂)_{0.11} %N 3.6. Loading: 0.86 mmol functional group g⁻¹ of resin.

Characterization of 8 (X = OH)

IR (cm⁻¹) KBr. 3053, 3023, 2920, 1602, 1587, 1535, 1512, 1451, 1421, 1269, 1239, 1162, 1112, 1081, 1019, 855,823, 762, 695, 665, 607, 545, 471. Raman (cm⁻¹): 1595, 1575, 1506, 1442, 1323, 1192, 1177, 1148, 1064, 1024, 995, 900, 825, 788, 755, 720, 663, 637, 616, 540, 401, 310. Elemental analysis observed: %N 2.38. Calculated for (C₁₀H₁₀)_{0.55}(C₈H₈)_{0.26}(C₁₄H₁₈N₂O)_{0.14} %N 2.88. Loading: 1.05 mmol functional group g⁻¹ of resin.

Characterization of 9 (X = OAc)

IR (cm⁻¹) KBr. 3053, 3023, 2920, 1602, 1587, 1535, 1512, 1451, 1421, 1269, 1239, 1162, 1112, 1081, 1019, 855,823, 762, 695, 665, 607, 545, 471. Raman (cm⁻¹): 1595, 1575, 1506, 1442, 1323, 1192, 1177, 1148, 1064, 1024, 995, 900, 825, 788, 755, 720, 663, 637, 616, 540, 401, 310. Elemental analysis observed: %N 4.68. Calculated for (C₁₀H₁₀)_{0.64}(C₁₆H₂₀N₂O₂)_{0.36} %N 5.56. Loading: 1.99 mmol functional group g⁻¹ of resin.

Synthesis of 1-benzyl-2,3-dmim[Cl]

1,2-dimethylimidazole (1.5 g, 15.6 mmol) was dissolved in 20 mL of EtOH in a 50 mL flask. Then, benzyl chloride (2.4 mL, 20 mmol) was added. The solution was heated at 80 °C for 5 h. The product was washed with CH₂Cl₂/H₂O and later the organic phase was evaporated under vacuum. The product was recrystallized in CH₂Cl₂ to obtain 1.57 g of solid (7.07 mmol, 45% yield). ¹H (CD₃OD, δ): 2.66 (s, 3H), 3.86 (s, 3H), 5.44 (s, 2H), 7.36–7.44(m, 5 H), 7.55(s, 2H). ¹³C (CD₃OD, δ): 9.11, 34.67, 51.68, 121.44, 122.75, 127.95, 128.85, 129.24, 134.08, 145.15. IR (cm⁻¹) KBr: 3067, 2851, 1572, 1497, 1456, 1364, 1334, 1162, 1082, 1030, 873, 823, 723, 699, 663, 624, 470, 449, 433. Raman (cm⁻¹): 1597, 1578, 1505, 1444, 1375, 1328, 1265, 1198, 1150, 1084, 1042, 1024, 994, 874, 811, 715, 668, 612, 562, 425, 308. MS (*m/z*): 187. MP 125–130 °C. Elemental analysis calculated for (C₁₂H₁₅ClN₂): %C 64.71 %H 6.79 %N 12.58 observed %C 64.57 %H 6.91 %N 12.47.

General procedure for the Henry reaction in batch

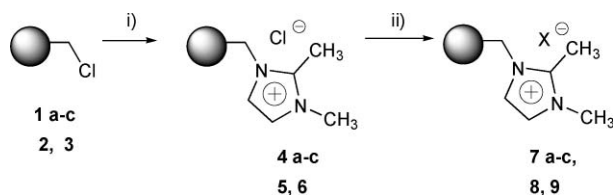
p-Nitrobenzaldehyde (0.25 g, 1.66 mmol) was dissolved in 2.25 g of nitromethane (25 equiv.). Later 0.5 mmol of the supported base were added to the solution, and the system was stirred at room temperature. Periodically, liquid samples were taken and analyzed by Raman spectroscopy. At the end of the reaction, the polymer was filtered, the excess of aldehyde evaporated and the product was characterized by ¹H NMR.

General procedure of the Henry reaction in continuous flow mode

A Gilson HPLC pump was used to carry out the Henry reaction in continuous flow mode. The column was connected and the solution of aldehyde into nitromethane was pumped through the column at room temperature. The samples were later analyzed by Raman spectroscopy and also by ¹H NMR. Once the reaction was finished, the system was washed with MeOH pumped through the column.

Synthesis of base-SILLPs

The SILLPs were prepared by modification of a series of Merrifield resins with microporous nature (2% of crosslinking) and different functionalisation degrees (1.2, 2.1 and 4.3 mequiv. Cl g⁻¹) (Scheme 1). Besides, macroporous polymers were also used in either beads or monolithic form. The synthesis of base-SILLPs were carried out by reaction of 1,2-dimethylimidazole (1,2-DMIM) with the different chloromethylated resins at a constant concentration of 1 M of 1,2-DMIM in DMF. The



Scheme 1 Synthesis of base-SILLPs. **1a–c** gel type polymer, **1a** (1.1 mequiv. Cl g⁻¹), **1b** (2.1 mequiv. Cl g⁻¹), **1c** (4.3 mequiv. Cl g⁻¹); **2** macroporous, beads (1.2 mequiv. Cl g⁻¹); **3** macroporous monolith (2.1 mequiv. Cl g⁻¹). (i) 1,2 dimethylimidazole, 90 °C. (ii) NaX or HX, H₂O.

reaction was followed by Raman spectroscopy. Monitoring reactions by means of spectroscopic techniques provide us a structural information of reagents and products, as well as information about reaction mechanisms.¹⁴

Fig. 1 shows the variation of four different peaks with the reaction time. The band at 647 cm⁻¹ (C–Cl stretching band) and at 1265 cm⁻¹ (down arrows) (wagging bands of CH₂–Cl) disappearing with time and being substituted by IL-like moieties. The peaks at 1506 cm⁻¹ and 720 cm⁻¹ (up arrows) correspond to symmetric and antisymmetric stretching of methyl group in the C₂ position of 1,2-DMIM increasing with time. The grafting of the imidazole moieties onto the polymer can be monitored through such variations. The kinetics plots (conversion vs. time, Fig. 2d) were calculated by following the evolution with time of the area of each characteristic peak.

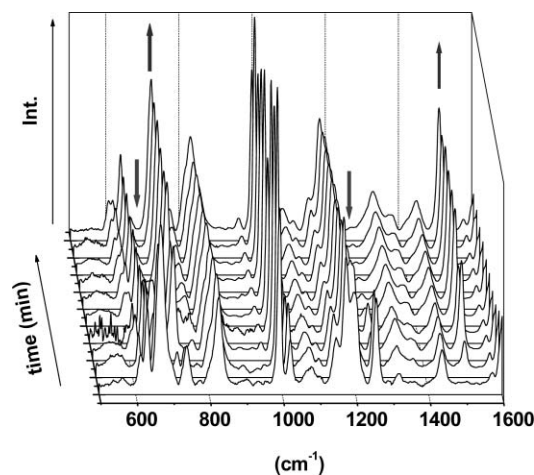


Fig. 1 Raman spectra vs. time for the alkylation of **1c** (4.3 mequiv. Cl g⁻¹) with 1,2-DMIM to yield to **4c**.

First, the effect of the amount of alkylating agent used for the synthesis of SILLPs was investigated. The reaction was followed by the disappearance and appearance of the above mentioned bands. When the synthesis of SILLPs was carried out with a Merrifield resin (1.19 mmol g⁻¹) using a 3 or 6 fold excess of 1,2-DMIM at 90 °C in DMF, no differences in the reaction kinetics were found. In 2.5 h the quantitative grafting of the IL-like groups was achieved. By contrast, less than 10 min were needed if the reaction was performed using melt 1,2-DMIM as solvent and reagent. However, the solidification of 1,2-DMIM in excess makes the thorough washing of the final resin difficult.

The loading and structure (macroporous/gel type) of the polymer may have an effect on kinetics for the grafting of the IL-like moieties.¹⁵ Hence, the synthesis of four different (**4a–c**, **5** and **6**) supported ionic liquid-like phases were studied. Besides, the synthesis of the analogous ionic liquid in solution was also performed in order to compare the reaction kinetics, the future applications, and the behaviour of the homogeneous vs. supported ionic liquid. The reactions were followed by Raman spectroscopy, as in the previous cases.

Some of the results are displayed in Fig. 2 showing the disappearance of the CH₂–Cl band (1265 cm⁻¹) for the polymers in each studied case. Surprisingly, under similar conditions, the homogeneous reaction was slower than the heterogeneous ones (Fig. 3). It is likely that as the grafting of the IL-like moieties

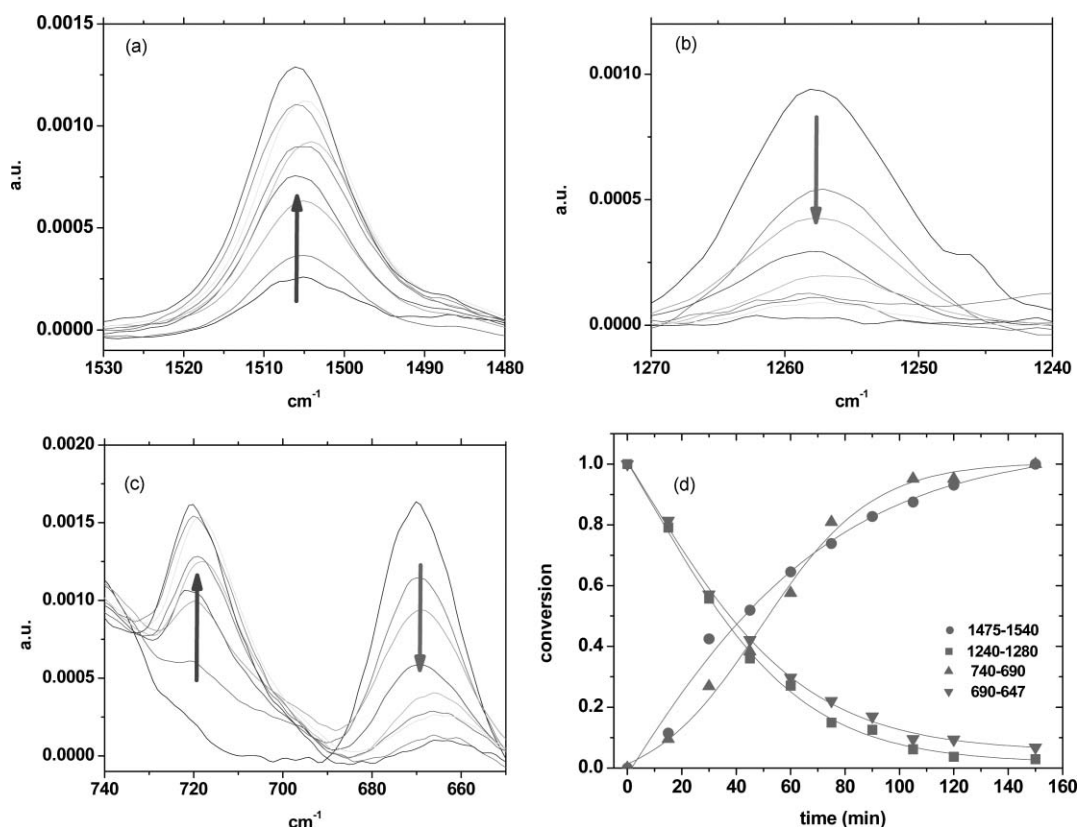


Fig. 2 (a) Raman onset for the 1530–1480 cm^{-1} region. (b) Raman onset for the 1270–1240 cm^{-1} region. (c) Raman onset for the 740–640 cm^{-1} region. (d) Kinetics plot conversion vs. time for the different peaks for the synthesis of **4c**.

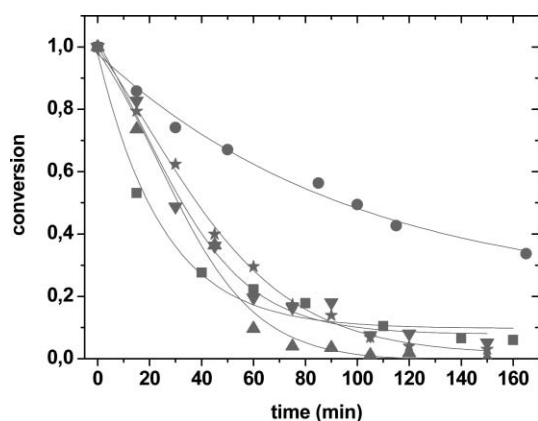


Fig. 3 Conversion vs. time plot for the synthesis of SILLPs in DMF. (●) Homogeneous alkylation of 1,2-DMIM with chloromethylbenzene. (★) Alkylation of 1,2-DMIM with **1a** (gel type 2.1 mequiv. Cl g^{-1}). (▼) Alkylation of 1,2-DMIM with **1b** (gel type 1.2 mequiv. Cl g^{-1}). (▲) Alkylation of 1,2-DMIM with **1c** (gel type 4.3 mequiv. Cl g^{-1}). (■) Alkylation of 1,2-DMIM with **2** (macroporous 1.2 mequiv. Cl g^{-1}).

progressed the polarity of the support was also modified. Thus, the un-reacted $\text{CH}_2\text{-Cl}$ groups were surrounded by a more polar environment favouring the substitution reaction. Such effects are less efficient in the homogeneous system. Kinetics for the different supports did not show important differences due to either loading or nature of the backbone matrix. The reaction was slightly faster at the beginning in the case of the macroporous polymer. This polymer has a rigid structure with

some functional groups placed in the outer surface, and therefore more accessible to the alkylating agents. Other groups, however, are located in the non-swollable crosslinked region being thus less accessible. This fact explains why the reaction is faster in the beginning, but slower afterwards, showing an almost complete functionalization in approximately 150 min. In the microporous resins, this phenomenon is not of importance, the appropriate swelling of the polymer controlling the accessibility of the reactive sites.¹⁵ This is in fact reflected by the results obtained using different solvents with differing swelling properties as can be seen in Fig. 4.

Henry reaction catalysed by base-SILLPs

The classical nitroaldol reaction is usually performed in the presence of a base (Scheme 2) in an organic solvent. Since basic reagents are also catalysts for the aldol condensation and for the Cannizzaro reaction when aldehydes are used as carbonyl sources, it is necessary to adopt appropriate experimental conditions to suppress these competitive reactions.¹⁶ To obtain better yields of 2-nitro alcohols a careful control of the basicity of the reaction medium is necessary, and long reaction times are demanded. Furthermore, the α -nitroalkanol formed may undergo base-catalyzed elimination¹⁷ of water to give nitroalkenes that readily polymerise. This elimination is difficult to avoid when aryl aldehydes are employed.

We decided to investigate the Henry reaction between *p*-nitrobenzaldehyde and nitromethane under solventless conditions using the supported ionic liquid-like phases as basic

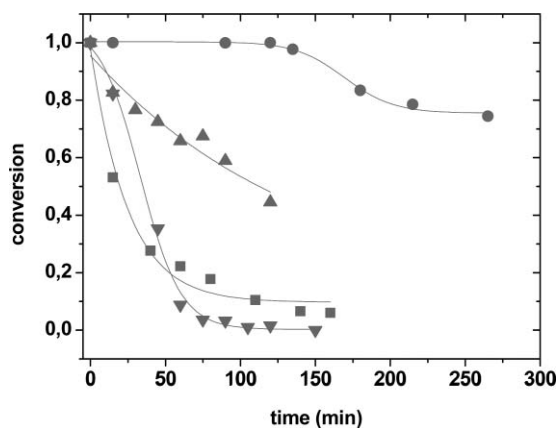
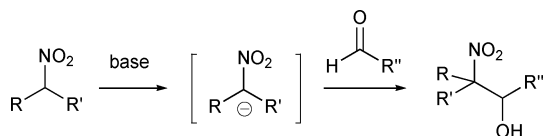


Fig. 4 Conversion vs. time plot for the synthesis of SILLPs. (●) Alkylation of 1,2-DMIM with **2** (macroporous 1.2 mequiv. Cl g⁻¹) in water. (▲) Alkylation of 1,2-DMIM with **2** (macroporous 1.2 mequiv. Cl g⁻¹) in DMF. (■) Alkylation of 1,2-DMIM with **1a** (gel type 1.2 mequiv. Cl g⁻¹) in water. (▼) Alkylation of 1,2-DMIM with **1a** (gel type 1.2 mequiv. Cl g⁻¹) in DMF.



Scheme 2 Henry reaction.

catalysts. The corresponding bases were prepared by methathesis of Cl⁻ by different basic anions (Table 1). The SILLPs based on 1,2-dimethylimidazole groups were chosen to avoid the C-2 basic protons in the imidazole group. Indeed, when the reaction was performed with base-SILLPs derived from 1-methylimidazole, products derived from both Cannizzaro and elimination reactions were observed. Table 1 summarised some of our results for the batch Henry reaction for different basic anions. No side products were observed for any of the basic anions assayed. Acetate and

hydroxy anions were the most efficient catalyst in terms of yield and reaction rate. The catalyst can be reused without losing activity. No chiral induction was observed when L-proline was used.

We also studied the influence of the base loading onto the SILLPs. Thus, supported bases with different amount of IL-like moieties were used (**7a–c**, X = OH⁻). All the reactions were performed for 30% catalysts/aldehyde molar ratio. As it can be seen in Fig 5 no significant differences on reaction rate were found. However, both yield and rate were reduced by decreasing the amount of base from a 30% to a 16%.

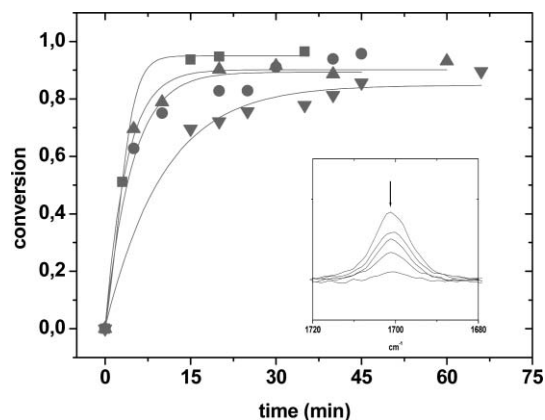


Fig. 5 Conversion vs. time for the batch Henry reaction catalysed by different SILLPs. (●) 30% cat, **7a** 1.04 mequiv. cat g⁻¹. (▲) 30% cat, **7b** 1.78 mequiv. cat g⁻¹. (▼) 16% cat, **7b** 1.78 mequiv. cat g⁻¹. (■) 30% cat, **7c** 3.02 mequiv. cat g⁻¹. Conversion followed by the disappearing of the carbonyl band in Raman spectroscopy.

Therefore, once the efficiency of base-SILLPs was proved under batch solventless conditions, we decided to evaluate their behaviour under continuous-flow conditions.¹⁸ An experimental set-up as shown in Fig. 6 would allow the easy recovery of the excess of nitromethane as well as the easy separation

Table 1 Henry reaction catalysed by basic-SILLPs^a

| Entry | X ⁻ | Loading/mequiv. g ⁻¹ | Time/min | Yield ^c (%) | TON/g g-cat ⁻¹ | TOF/g g-cat ⁻¹ h ⁻¹ |
|-------|------------------|---------------------------------|----------|------------------------|---------------------------|---|
| 1 | Cl | 1.05 | 405 | 26 | 0.6 | 0.09 |
| 2 | AcO | 1.04 | 30 | 97 | 2.2 | 4.4 |
| 3 | AcO ^b | 1.04 | 30 | 98 | 2.2 | 4.4 |
| 4 | OH | 1.09 | 30 | 99 | 2.2 | 4.4 |
| 5 | L-Proline | 0.98 | 420 | 75 | 1.7 | 0.2 |
| 6 | Merrifield | — | 420 | 0 | — | — |
| 7 | Cl im | 0.99 | 420 | 2 | — | — |

^a All reactions were performed using 250 mg *p*-nitrobenzaldehyde, 150 mg of base-SILLP and 1 mL of nitromethane. ^b 2nd use. ^c Yield determined by NMR.

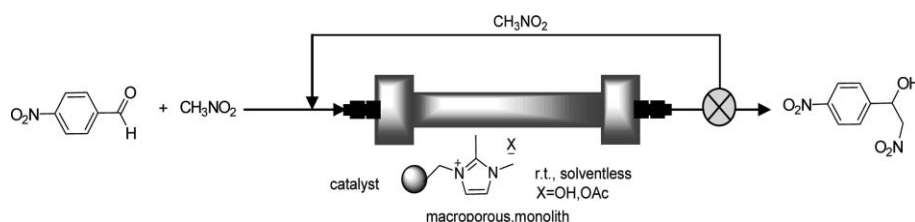


Fig. 6 Continuous-flow solventless Henry reaction catalysed by basic-SILLPs.

and isolation of the product from the catalysts. The recycling of nitromethane was done by evaporating under vacuum the product phase.

Although the initial screenings under batch condition were performed using gel type SILLPs, the flow experiments were run using a macroporous polymer. When gel type polymers were packed in a column and reactants were pumped, the high swelling of the materials led to high back pressures. However, basic-SILLPs based on either a macroporous beads polymer or a monolith did not show this technical inconvenient. Therefore fixed-bed mini-flow reactors with different amounts of catalyst and volumes can be easily prepared. Table 2 summarises some of the results achieved for the continuous-flow Henry reaction using such reactors.

The fixed-bed mini-flow reactor based on a monolithic material (Entry 1, Table 2) was attached to a high pressure pump. Then, a solution of *p*-nitrobenzaldehyde in nitromethane was pumped through the reactor at a constant flow rate (100 $\mu\text{L min}^{-1}$) over *ca.* 7 h. Aliquots were analyzed for the product content at regular time intervals by both NMR and Raman spectroscopy. Fig. 7 displays the observed behaviour during this period of time. Thus, the reaction proceeded continuously with 95% yield at room temperature with no noticeable changes on both product yield and selectivity after 342 min (*ca.* 47 bed-volumes) of continuous use under the same conditions. However, after this time some decay on activity was observed. At that time, the reactor was washed and regenerated by pumping a solution of NaOAc in water. Once the reactor was washed, a new reaction cycle was performed under the same conditions. The catalyst showed the same performance than before washing (Fig. 6 and Entry 2 Table 2). Accordingly, deactivation of the catalyst could be due to the slow exchange of the catalytic anion (AcO^-) by other less active anions such as $^- \text{CH}_2\text{NO}_2$.

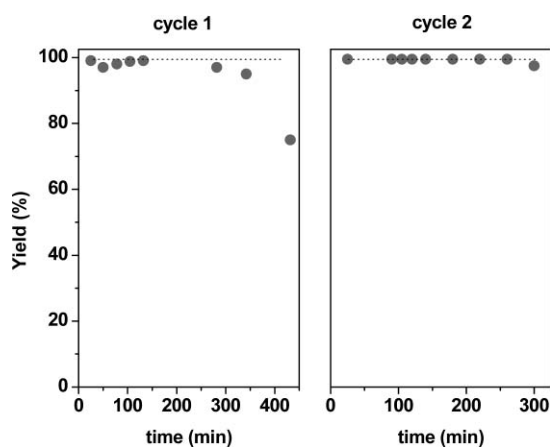


Fig. 7 Solventless continuous-flow Henry reaction.

Different flow rates, reactants, concentrations, type of materials (monolith *vs.* beads) and basic anions were tested (Table 2). All the conditions assayed led to full conversion of the aldehyde into the product. However, changes in the conditions were reflected in the presence of different deactivation patterns of the catalyst. Best results were achieved when using OH^- as anion (Entry 6). The use of hydroxyl as anion is advantageous since

Table 2 Continuous-flow Henry reaction catalysed by basic-SILLPs

| Entry | X ⁻ | G cat. | Type | Loading cat/ mmol g ⁻¹ | [RCHO]/M | Flow/ mL min ⁻¹ | Vol./mL | LHSV/ g g-cat ⁻¹ h ⁻¹ | Residence time ^e /min | TON cycle/ g g-cat ⁻¹ | Cycles ^c | Productivity/ g g-cat ⁻¹ | Final product/g |
|-------|----------------|--------|--------------------|--------------------------------------|----------|-------------------------------|---------|--|-------------------------------------|-------------------------------------|---------------------|--|--------------------|
| 1 | AcO | 0.48 | Monolith | 1.99 | 0.33 | 0.10 | 0.72 | 0.87 | 7.2 | 0.10 | 47.22 | 4.81 | 2.4 |
| 2 | AcO | 0.48 | Monolith | 1.99 | 0.33 | 0.10 | 0.72 | 0.87 | 7.2 | 0.10 | 41.67 | 4.28 | 2.1 |
| 3 | AcO | 0.23 | Monolith | 1.99 | 0.20 | 0.50 | 0.35 | 5.43 | 0.7 | 0.06 | 86.21 | 4.88 | 1.3 |
| 4 | AcO | 0.31 | Beads | 1.05 | 0.72 | 0.10 | 0.48 | 2.95 | 4.8 | 0.24 | 24.84 | 5.85 | 1.8 |
| 5 | AcO | 0.31 | Beads ^a | 1.05 | 0.72 | 0.25 | 0.48 | 7.39 | 1.9 | 0.21 | 7.76 | 1.66 | 0.6 |
| 6 | OH | 0.47 | Beads | 1.10 | 0.72 | 0.50 | 0.81 | 9.64 | 1.6 | 0.26 | 31.06 | 7.95 | 3.8 |
| 7 | AcO | 0.48 | Monolith | 1.99 | 0.73 | 0.10 | 0.58 | 1.95 | 5.8 | 0.17 | 17.24 | 2.92 | 1.6 |

^a Recycle of entry 4. ^b Calculated according to standard literature.¹⁹ ^c Number of bed volumes per cycle with a yield higher than 90%.

the recycling is facilitated by just using an aqueous solution of ammonia.

Conclusion

The use of SILLPs allowed us to prepare efficient basic catalysts using a basic anion. The reaction can be carried out either in a batch or continuous flow system. The latter one proved to be more suitable for the easy separation and isolation of the final product. In flow systems, a small amount of the substrate is actually forced into intimate contact with an "excess" of the catalyst. Thus, a total conversion of product can be achieved with residence times as short as 1–3 min, using a monolithic mini-reactor with a free-volume of ca. 500–800 μL . Indeed, if the TON for batch and continuous flow process are compared, higher values are obtained for the flow systems. The base-supported systems present a high throughput and are advantageous to the upscale of the process. Although the activity of catalysts decays with time, the continuous flow set-up allows an easy and efficient washing and recycling of the catalytic system. Indeed, a set-up with parallel reactors would allow the continuous production for long periods of time, by switching from one to other when the catalytic activity decreased.

Acknowledgements

Financial support has been provided by MCYT and Fundació Bancaixa-UJI (CTQ2005-08016-003, P11B2004-13). E. Garcia-Verdugo thanks MECyT for a personal grant (Ramon y Cajal program).

Notes and references

- (a) P. T. Anastas, M. M. Kirchhoff and T. C. Williamson, *Appl. Catal., A*, 2001, **221**, 3; (b) P. T. Anastas, J. C. Warner, *Green Chemistry: Theory and Practice*, Oxford University Press, 2000.
- (a) M. Mase, Y. Nakai, N. Ohara, H. Yoda, K. Takabe, F. Tanaka and C. F. Barbas, *J. Am. Chem. Soc.*, 2006, **3**, 734–735; (b) P. I. Dalko and L. Moisan, *Angew. Chem., Int. Ed.*, 2004, **43**, 5138–5175.
- (a) L. Martins, T. J. Bonagamba, E. R. de Azevedo, P. Bargiela and D. Cardoso, *Appl. Catal., A*, 2006, **312**, 77–85; (b) J. S. Yadav, B. V. S. Reddy, A. K. Basak, B. Visali, A. V. Narsaiah and K. Nagaiah, *Eur. J. Org. Chem.*, 2004, **3**, 546–551; (c) S. Chalais, P. Laszlo and A. Mathy, *Tetrahedron Lett.*, 1984, **26**, 4453–4454.
- (a) G. Rosini, *Comprehensive Organic Synthesis*, ed. B. M. Trost and C. H. Heathcock, Pergamon, Oxford, 1991, vol. 2, p. 321; (b) F. A. Luzzio, *Tetrahedron*, 2001, **57**, 915; (c) N. Ono, *The Nitro Group in Organic Synthesis*, Wiley-VCH, New York, 2001, ch. 3, p. 30.
- (a) J. Comelles, M. Moreno-Mañas, A. Vallribera, ARKIVOC, Part 9, 2005, pp. 207–238; (b) T. Hara, S. Kanai, K. Mori, T. Mizugaki, K. Ebitani, K. Jitsukawa and K. Kaneda, *J. Org. Chem.*, 2006, **71**, 7455–7462.
- H. Hattori, *Chem. Rev.*, 1995, **95**, 537–558.
- (a) Y. Kubota, Y. Nishizaki and Y. Sugi, *Chem. Lett.*, 2000, 998–999; (b) C. Paun, J. Barklie, P. Goodrich, H. Q. N. Gunaratne, A. McKeown, V. I. Parvulescu and C. Hardacre, *J. Mol. Catal. A*, 2007, **269**, 64–71.
- (a) M. T. Garcia, N. Gathergood and P. J. Scammells, *Green Chem.*, 2005, **7**, 9–14; (b) K. M. Docherty and C. F. Kulpa, *Green Chem.*, 2005, **7**, 185–189; (c) C. Pretti, C. Chiappe, D. Pieraccini, M. Gregori, F. Abramo, G. Monni and L. Intorre, *Green Chem.*, 2006, **8**, 238–240.
- (a) M. H. Valkenberg, C. deCastro and W. F. Hölderich, *Green Chem.*, 2002, **4**, 88–93; (b) G. S. Fonseca, J. D. Scholten and J. Dupont, *Synlett*, 2004, **9**, 1525–1528; (c) B. Gadenne, P. Hesemann and J. J. E. Moreau, *Chem. Commun.*, 2004, 1768–1769; (d) C. P. Mehnert, *Chem.–Eur. J.*, 2005, **11**, 50–56 and references therein.
- (a) N. Karbass, V. Sans, E. Garcia-Verdugo, M. I. Burguete and S. V. Luis, *Chem. Commun.*, 2006, 3095–3097; (b) P. Lozano, E. Garcia-Verdugo, R. Piamtongkam, N. Karbass, T. de Diego, M. I. Burguete, S. V. Luis and J. L. Iborra, *Adv. Synth. Catal.*, 2007, **349**, 1077–1084.
- (a) M. H. Valkenberg, C. deCastro and W. F. Hölderich, *Green Chem.*, 2002, **4**, 88–93; (b) G. S. Fonseca, J. D. Scholten and J. Dupont, *Synlett*, 2004, **9**, 1525–1528; (c) B. Gadenne, P. Hesemann and J. J. E. Moreau, *Chem. Commun.*, 2004, 1768–1769; (d) C. P. Mehnert, *Chem.–Eur. J.*, 2005, **11**, 50–56 and references therein.
- M. I. Burguete, F. Galindo, E. Garcia-Verdugo, N. Karbass and S. V. Luis, *Chem. Commun.*, 2007, **29**, 3086–3088.
- (a) U. Jas and A. Kirschning, *Chem.–Eur. J.*, 2003, **9**, 5708–5723; (b) A. Kirschning, W. Solodenko and K. Mennecke, *Chem.–Eur. J.*, 2006, **12**, 5972–5990.
- see: B. Altava, M. I. Burguete, E. Garcia-Verdugo, S. V. Luis and M. J. Vicent, *Tetrahedron*, 2001, **57**, 8675–8683.
- D. C. Sherrington, *Chem. Commun.*, 1988, 2275–2286.
- H. H. Baer, L. Urbas, in *The Chemistry of the Nitro and Nitroso Groups*, ed. H. Feuer, Wiley Interscience, New York, 1970, vol. 2.
- (a) G. Rosini, R. Ballini, M. Petrini and P. Sorrenti, *Synthesis*, 1985, 515–517; (b) B. P. Bandgar, M. B. Zirange and P. P. Wadgaonkar, *Synlett*, 1996, 149–150.
- (a) M. I. Burguete, A. Cornejo, E. Garcia-Verdugo, M. J. Gil, S. V. Luis, J. A. Mayoral, V. Martinez-Merino and M. Sokolova, *J. Org. Chem.*, 2007, **72**, 4344–4350; (b) B. Altava, M. I. Burguete, E. Garcia-Verdugo, S. V. Luis and M. J. Vicent, *Green Chem.*, 2007, **8**, 717–726.
- O. Levenspiel, *Chemical Reaction Engineering*, Wiley, New York, 3rd edn, 1999.

Oxidation of glycerol and propanediols in methanol over heterogeneous gold catalysts†

Esben Taarning, Anders Theilgaard Madsen, Jorge Mario Marchetti, Kresten Egeblad and Claus Hviid Christensen*

Received 17th September 2007, Accepted 21st December 2007

First published as an Advance Article on the web 17th January 2008

DOI: 10.1039/b714292g

Aerobic oxidation of glycerol over metal oxide supported gold nanoparticles in methanol results in the formation of dimethyl mesoxalate in selectivities up to 89% at full conversion. The oxidative esterification takes place in methanol, acting both as solvent and reactant, and in the presence of base. Thus, it constitutes a direct transformation of the glycerol by-product phase from biodiesel production or from glycerol obtained *e.g.* by fermentation. Au/TiO₂ and Au/Fe₂O₃ was found to have similar catalytic activity, whereas Au/C was inactive. 1,2-Propanediol was oxidized to methyl lactate with a selectivity of 72% at full conversion, while 1,3-propanediol yielded methyl 3-hydroxypropionate with 90% selectivity at 94% conversion. Methyl 3-hydroxy propionate can be easily converted into methyl acrylate, which is then a green polymer building block.

Introduction

The conversion of glycerol into high-value chemicals is a research area that has received tremendous attention in recent years.¹ This interest is spurred by the emergence of glycerol as an abundant renewable resource, formed as a by-product from the rapidly growing biodiesel production. Alternatively, glycerol can be obtained at relatively low cost by fermentation of glucose. Glycerol, being a highly functionalized compound, is difficult to convert selectively into useful chemical products. Recently, however, several good examples have been reported. One approach is the fermentation of glycerol to form 1,3-propanediol, which can be polymerized with terephthalic acid and used in the fibers industry.² Steam reforming of glycerol to form syn-gas coupled with a Fischer–Tropsch process to form hydrocarbon fuels is another possible approach to valorize glycerol and improve the overall efficiency of biodiesel production.³ Glycerol has recently been dehydrated over a copper-chromite catalyst to form 1-hydroxyacetone in high yields, which upon hydrogenation gives 1,2-propanediol that can be used as a replacement for ethylene glycol in anti-freeze applications.^{1,4} Dehydration over an acidic zeolite catalyst can furnish acrolein with high selectivities,⁵ thus illustrating the possibilities of producing bulk chemicals from biomass.

Here, we report that oxidation of glycerol in methanol over supported gold catalysts results in the formation of dimethyl mesoxalate in 89% selectivity at full conversion. The major by-product formed is methyl glycolate, resulting from C–C

cleavage of intermediary products. 1,2-Propanediol and 1,3-propanediol, which are both available from glycerol, are also examined as starting materials for the oxidative esterification. 1,2-Propanediol is oxidized to furnish methyl lactate with a selectivity of 72% at full conversion. Here, methyl acetate is formed as the major by-product. 1,3-Propanediol is oxidized to form methyl 3-hydroxypropionate as the major product with 90% selectivity at 94% conversion.

Selective oxidation could play a prominent role in the conversion of glycerol if the oxidizing agent used is oxygen. Kimura *et al.* have reported that aerobic oxidation of glycerol over a carbon supported Pt–Bi catalyst yields dihydroxyacetone in selectivities up to 80%.⁶ Oxidation of glycerol over Pd/C under basic conditions have been reported by Besson and co-workers to give glyceric acid with 70% selectivity at full conversion.⁷

Supported gold nanoparticles^{8,9} have been found to be excellent catalysts for the oxidation of various substrates such as CO,¹⁰ propylene,¹¹ hydrogen,¹² primary and secondary alcohols,^{13–16} aldehydes¹⁷ and even cyclohexane^{18,19} and alkenes.²⁰ Oxidation of diols and glycerol in water has also been studied extensively.^{13,21–30} The interesting finding in this research area is that under the right circumstances, Au can be more active and selective towards glyceric acid than Pd and Pt. Indeed, Hutchings and co-workers have reported glyceric acid selectivities of 100% at 56% conversion.²² Further oxidation of glyceric acid leads to formation of tartronic acid, and in some cases C–C cleavage to form glycolic acid, oxalic acid and CO₂ is observed.^{23–25} Various supports have been examined, and carbon supported catalysts appear to be of superior activity compared to metal oxide supported catalysts.^{13,26} Another parameter of crucial importance is the gold nanoparticle size.^{21,23,25} Very recently, Davis and co-workers examined the rate of glycerol oxidation using gold nanoparticles with varying sizes. Small gold nanoparticles (5 nm) were found to be much more active than larger particles (20 nm). However, higher selectivity towards glyceric acid was

Center for Sustainable and Green Chemistry, Department of Chemistry, Technical University of Denmark, Building 207, Kemitorvet, DK-2800, Lyngby, Denmark. E-mail: chc@kemi.dtu.dk; Fax: +45 4588 3136; Tel: +45 4525 2402

† This paper was published as part of the themed issue of contributions from the 3rd International Conference on Green and Sustainable Chemistry.

achieved with large sized gold nanoparticles.²⁵ The pH value of the reaction mixture is also an important reactivity parameter. Gold catalyzed oxidation of glycerol does not take place in the absence of base, and since the formation of glyceric acid will lower the pH as it is formed, it is necessary to maintain a high pH level by addition of sodium hydroxide.^{12,23} Thus, a stoichiometric amount of sodium hydroxide is required when glycerol is oxidized to glyceric acid, usually as much as four equivalents of base is used to achieve a reasonable reaction rate. Recently, it was reported that by oxidizing a primary alcohol over a gold catalyst in methanol, methyl esters are formed instead of carboxylic acids.^{27–29} In this procedure, base also promotes the catalytic activity. However, the methyl ester product does not consume base, and thus a small amount of base is capable of promoting the reaction. Since glycerol produced as a byproduct from biodiesel production is directly formed as a base-containing methanol solution, oxidation of this waste stream could offer an extremely simple route to new chemicals from biomass.

Experimental

Materials

Glycerol (>99%) was acquired from H. Struers Chemical Labs, methanol (>99.9%), 30 wt% sodium methoxide in methanol, 1,2-propanediol (>99%) and 1,3-propanediol (>99%), anisol (>99%), 1-hydroxyacetone (90%), methyl lactate (99%), methyl pyruvate (95%), methyl acrylate (>99%), and dimethyl malonate (>99%) were all acquired from Sigma-Aldrich. 5 wt% Titanyl sulfate (aqueous sulfuric acid solution) was from Fluka (highest purity). Technical air (20% O₂, 80% N₂) was from Air Liquide.

Gold catalysts, Au/C, Au/TiO₂, Au/Fe₂O₃, were supplied by the World Gold Council (WGC).³⁰

Catalyst characterisation

0.8% Au/C (X40S, type D catalyst from WGC) was prepared by the colloidal method. The average Au diameter was found to be 10.5 nm by TEM analysis and 6.7 nm with XRD.

Au/TiO₂ (type A catalyst from WGC, Lot No. #02-6) has 1.0 wt% Au and was prepared by the deposition–precipitation method. The average Au particle diameter was found to be 3.5 nm by TEM observation, with a standard deviation of 0.91 nm.

Au/Fe₂O₃ (type C catalyst from WGC, Lot No. #02-5) has 1.0 wt% Au and was prepared using the co-precipitation method. TEM observation revealed that the Au particle diameter on average is 3.6 nm, with a standard deviation of 0.65 nm.

Oxidation experiments

The oxidation experiments are performed in a 50 ml steel autoclave (MicroClave from Autoclave Engineers). The autoclave is charged with 250 mg of glycerol (2.7 mmol) and 5.1 g of methanol (159 mmol). 29 mg of 30 wt% NaOCH₃ in methanol is added (0.27 mmol) together with 30 mg of anisol (0.28 mmol, internal standard). Then the 1% Au/TiO₂ catalyst is added (0.48 g, 0.024 mmol Au) and the autoclave is sealed and pressurized to 21 bar with technical air (*ca.* 8 mmol O₂). The mixture is stirred (900 rpm) and heated to 373 K. At regular intervals, the

autoclave is cooled to 263 K, and a sample is taken out. The autoclave is then recharged with technical air, and reheated to 373 K. In this way, the time-dependencies of the oxidation of the polyols are mapped by plotting the concentrations of reactants and products to establish possible reaction routes. Without a regular refilling of the autoclave with a fresh air atmosphere, the reaction proceeds at a significantly lower rate.

Oxidations of 1,2-propanediol and 1,3-propanediol are performed analogously by using 210 mg of each, corresponding to 2.7 mmol. Furthermore, oxidation of 1,2-propanediol is performed using 0.96 g of 1% Au/TiO₂ catalyst.

Product analysis

The reaction mixtures were analyzed by GC (Agilent Technologies 6890N, the column was an HP-5 from J & W Scientific, 30 m long and a diameter of 0.32 mm, and has an inner film of 0.25 μm 5% methyl phenyl siloxane) and GC-MS (Shimadzu Spectachrom QP5000 GC-MS, the column was Supelco Equity-1 of 30 m in length, an inner diameter of 0.25 mm and an inner film of dimethyl polysiloxane).

Reference samples were used to confirm the products whenever possible. However, the oxidation products dimethyl tartronate and methyl-3-hydroxypropionate could not be obtained and identification was thus conducted on the basis of MS data.‡

Quantifiable product data was obtained from GC, and were calculated on the basis of an internal standard. The concentration change due to methanol consumption in the oxidative esterification is ignored in the calculation of product concentrations.

Hydrogen peroxide formation and decomposition was determined by absorbance measurement of the H₂O₂–titanyl complex§ at 412 nm using a Jasco V-570 UV/VIS/NIR spectrophotometer.

Results and discussion

Oxidation of glycerol

Glycerol was oxidized in a stirred batch autoclave at 373 K in the presence of 10% sodium methoxide in methanol. Au/C

‡ Methyl glycerate was generated *in situ* by dissolving sodium glycerate (>99% from Sigma-Aldrich) in methanol and adding a small excess of 18 M sulfuric acid and heating to 60 °C for one hour. Dimethyl mesoxalate is not commercially available. However dissolving commercially available diethyl mesoxalate (>95%, Sigma-Aldrich) in methanol in the presence of base affords dimethyl mesoxalate and ethanol. On basis of these procedures it was possible to acquire reference data of the retention times of methyl glycerate and dimethyl mesoxalate.

§ H₂O₂ decomposition over Au/Fe₂O₃ and Au/TiO₂ was determined by adding 0.52 g of 33% H₂O₂ to a 60 °C hot suspension containing methanol (10 ml), sodium methoxide (0.19 mmol) and gold catalyst (100 mg). Samples (0.2 ml) of the reaction mixture were centrifuged, acidified and added to a solution containing 0.025 mmol TiO(SO₄) in 2 ml sulfuric acid (5.5 M). The concentration of the formed H₂O₂–titanyl complex was determined by UV-VIS absorption and is proportional to the amount of hydrogen peroxide in the sample. After 5 minutes it was found that Au/Fe₂O₃ had decomposed 82% of the H₂O₂, while Au/TiO₂ had only decomposed 70%. This procedure was also used to identify the presence of H₂O₂ in the reaction mixture from oxidation of glycerol (H₂O₂ was not found in an unreacted sample).

has previously been reported as a highly active catalyst for oxidizing glycerol, and most reports on gold-catalyzed oxidation of glycerol use Au/C as catalyst.^{22–26,31} Oxidation of glycerol in methanol by the use of carbon supported gold nanoparticles (10.5 nm) did not result in any conversion of glycerol. The lack of reactivity for the Au/C catalyst is likely due to the large size of the gold nanoparticles since smaller gold nanoparticles (3.5 nm) on Au/TiO₂ and Au/Fe₂O₃ were found to be able to oxidize glycerol. Thus, the oxidation of glycerol was investigated by using these two metal oxide supported catalysts.

The oxidation reaction was followed by GC and the concentration of the reaction products is plotted against time (Fig. 1 and 2). When either Au/TiO₂ or Au/Fe₂O₃ was used, methyl

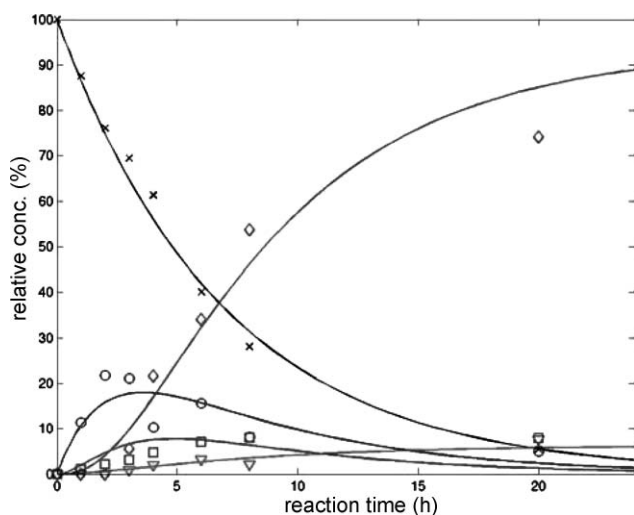


Fig. 1 Glycerol: \times —, methyl glycerate: \circ —, dimethyl tartronate: \square —, dimethyl mesoxalate: \diamond —, methyl glycolate: ∇ —. Oxidative esterification of glycerol with the use of 1% Au/TiO₂. Methanol : glycerol was 59 : 1, Au : glycerol was 1 : 112. $T = 373$ K, $p(\text{O}_2) = 5.0$ bar. 10% NaOCH₃ relative to glycerol was used.

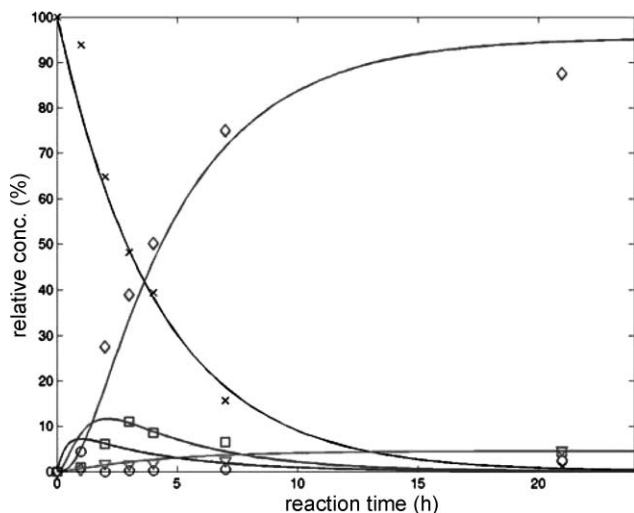


Fig. 2 Glycerol: \times —, methyl glycerate: \circ —, dimethyl tartronate: \square —, dimethyl mesoxalate: \diamond —, methyl glycolate: ∇ —. Oxidative esterification of glycerol with the use of 1% Au/Fe₂O₃. Methanol : glycerol was 59 : 1, Au : glycerol was 1 : 112. $T = 373$ K, $p(\text{O}_2) = 5.0$ bar. 10% NaOCH₃ relative to glycerol was used.

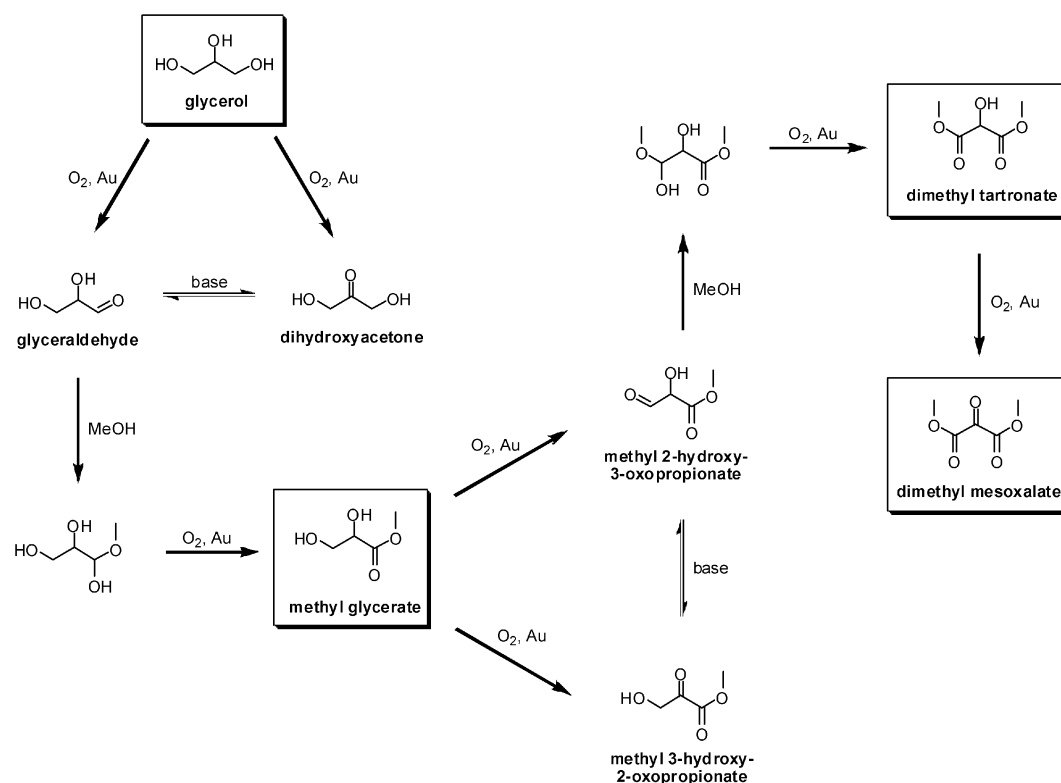
glycerate is the initially observed product. However, oxidation of glycerol must first lead to formation of dihydroxyacetone or glyceraldehyde, which are tautomers and in equilibrium under basic conditions. Thus, both intermediates can lead to methyl glycerate *via* oxidation of the glyceraldehyde hemiacetal (Scheme 1). However, none of these species were seen by GC, suggesting that they are rapidly converted into methyl glycerate. After a few hours, the concentration of methyl glycerate drops. This is caused by further conversion of methyl glycerate into dimethyl tartronate. Formation of dimethyl tartronate must be preceded by oxidation of methyl glycerate into methyl 3-hydroxy 2-oxopropionate or methyl 2-hydroxy-3-oxopropionate, which are also tautomers and in equilibrium under basic conditions. Final oxidation of dimethyl tartronate proceeds rapidly to furnish the fully oxidized dimethyl mesoxalate.

Methyl glycolate was also produced in minor quantities. This by-product results from C–C cleavage of a C3 unit during the reaction. This C–C cleavage could be thought to originate from a retro aldol reaction of methyl tartronate to form methyl 2-hydroxyacetate and dimethyl carbonate. However, dimethyl carbonate was never observed in the reaction mixture. Furthermore, it has recently been established that there is a close correlation between the formation of hydrogen peroxide and the amount of C–C cleavage observed when oxidizing glycerol in water with gold and gold–palladium particles.^{25,31} It is thus likely that the same correlation is found in methanol and that hydrogen peroxide cleaves a C–C bond in either dihydroxyacetone, methyl glycerate or dimethyl tartronate, thus forming methyl glycolate. Analysis of the reaction mixture during oxidation of glycerol in methanol established that a low concentration of hydrogen peroxide is indeed present. Hydrogen peroxide is known to form when oxidizing substrates such as CO and glycerol in water over gold catalysts.³¹ As water is inevitably present in the reaction mixture as a byproduct from the aerobic oxidation, hydrogen peroxide is likely to be formed in a similar fashion. Interestingly, methyl glycolate does not undergo further oxidation to form dimethyl oxalate. This selectivity has also been observed by Hayashi *et al.*²⁷

Oxidation of glycerol over Au/Fe₂O₃ occurs with higher rate and selectivity than over Au/TiO₂ (Fig. 2). Thus, a 50% conversion of glycerol is achieved within 3 hours. The intermediates are formed in the same order, suggesting the same reaction mechanism. However, methyl glycerate is consumed faster over Au/Fe₂O₃ than over Au/TiO₂. The final product, dimethyl mesoxalate is formed with a higher selectivity (89%) over Au/Fe₂O₃ than when using Au/TiO₂ (79%). The higher selectivity is likely attributed to the finding that the Au/Fe₂O₃ catalyst is better at decomposing hydrogen peroxide than Au/TiO₂, thereby reducing the amount of C–C cleavage induced by hydrogen peroxide.[§]

Oxidation of 1,2-propanediol

It has been reported that 1,2-propanediol is oxidized more slowly than glycerol over gold catalysts.^{21,26} We observed the same trend. However, by increasing the catalyst loading it is possible to achieve full conversion within a short time-frame (Fig. 3). Thus, after one hour, the conversion of 1,2-propanediol is 87%, and the two major products at this stage are methyl lactate and



Scheme 1 Reaction scheme for oxidative esterification of glycerol in the presence of base. Observed products are highlighted in boxes.

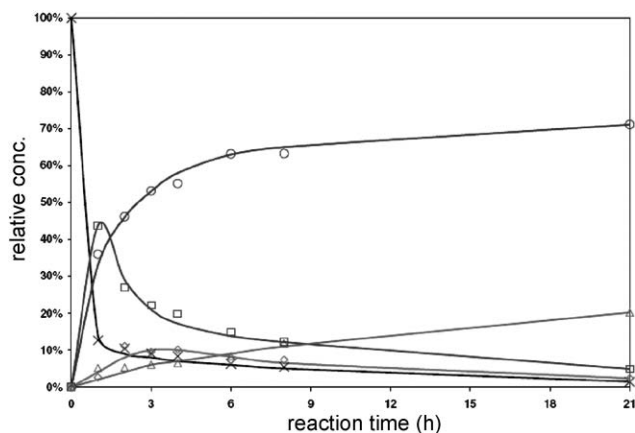


Fig. 3 1,2-Propanediol: \times —, methyl lactate: \circ —, 1-hydroxyacetone: \square —, methyl pyruvate: \diamond —, methyl acetate: Δ —. Oxidative esterification of 1,2-propanediol with the use of 1% Au/TiO₂. Methanol : 1,2-propanediol was 59 : 1, Au : 1,2-propanediol was 1 : 56. $T = 373$ K, $p(O_2) = 5.0$ bar. 10% NaOCH₃ relative to 1,2-propanediol is used.

1-hydroxyacetone, seemingly being formed at comparable rates. After 21 hours, conversion of 1,2-propanediol is >98% and the selectivity to methyl lactate is 72%. The major by-product after this period of time is methyl acetate, formed with 21% selectivity.

Prati and Rossi performed a detailed examination of the reaction pathway when oxidizing 1,2-propanediol over Au/C in water in the presence of base.¹³ They conclude that sodium lactate is stable under oxidative conditions, and that 1-hydroxyacetone

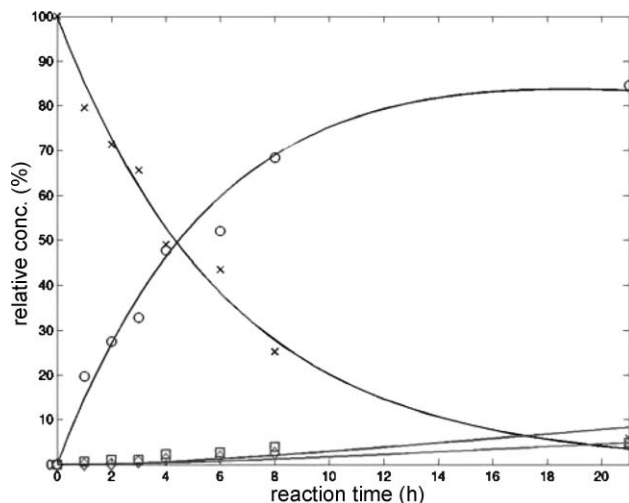
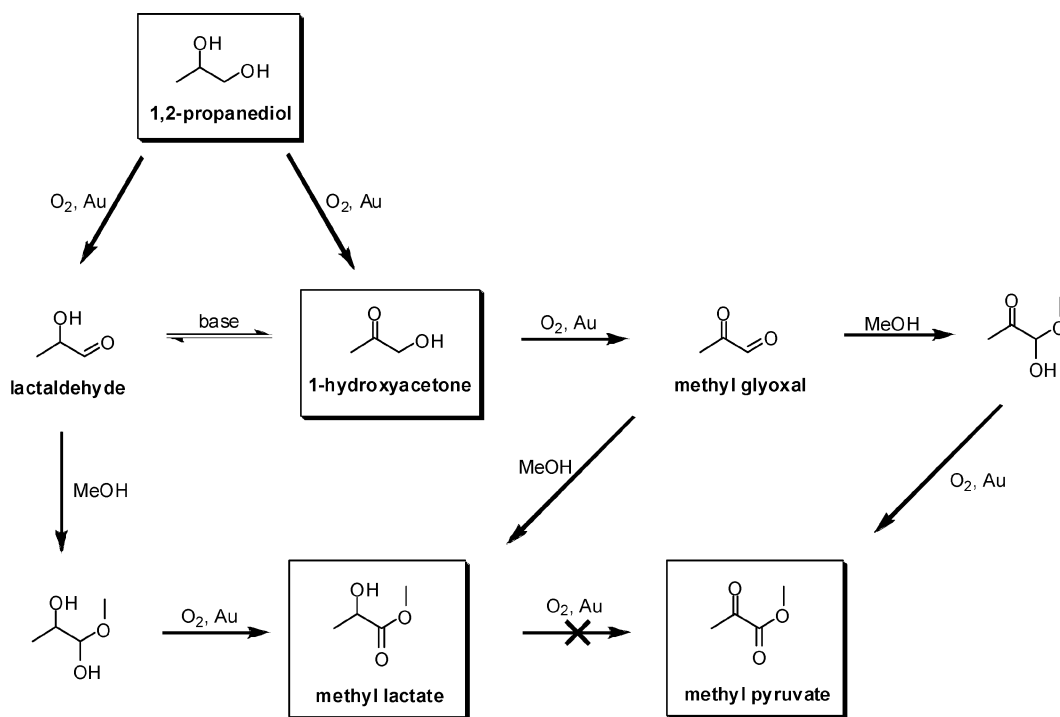


Fig. 4 1,3-Propanediol: \times —, methyl-3-hydroxypropionate: \circ —, methyl acrylate: \square —, dimethyl malonate: \diamond —. Oxidative esterification of 1,3-propanediol with the use of 1% Au/TiO₂. Methanol : 1,3-propanediol is 59 : 1, Au : 1,3-propanediol was 1 : 112. $T = 373$ K, $p(O_2) = 5.0$ bar. 10% NaOCH₃ relative to 1,3-propanediol is used.

yields sodium lactate upon oxidation. Finally, they conclude that methyl glyoxal *via* an intramolecular Cannizzaro reaction can be transformed into sodium lactate under basic conditions and that this, together with oxidation of lactaldehyde are two possible intermediates on the route from 1,2-propanediol to sodium lactate.



Scheme 2 Reaction scheme for oxidative esterification of 1,2-propanediol in the presence of base. The observed products are highlighted in boxes.

When oxidizing 1,2-propanediol in methanol, we observed no lactaldehyde, suggesting that either it is an intermediate that is rapidly oxidized into methyl lactate, or that the tautomerisation equilibrium is shifted far towards 1-hydroxyacetone. 1-Hydroxyacetone itself is consumed relatively slowly from the reaction mixture. 1-Hydroxyacetone and lactaldehyde are tautomers, and are thus in equilibrium under the basic reaction conditions (Scheme 2), hence 1-hydroxyacetone is a likely intermediate on the path to methyl lactate. To confirm the plausibility of this reaction pathway, 1-hydroxyacetone was oxidized under identical conditions to 1,2-propanediol. It was confirmed that methyl lactate was formed (46% selectivity), however large amounts of methyl pyruvate (16% selectivity) and methyl acetate (21% selectivity) were also formed at 86% conversion. The selectivity towards these two by-products was found to be greater than when the starting material is 1,2-propanediol. Oxidation of pure methyl lactate under identical conditions yielded only trace amounts of methyl pyruvate and methyl acetate. It has been reported by Sasaki and co-workers that methyl glyoxal in methanol can be converted into methyl lactate in the presence of various metal chlorides and even in the absence of catalysts.³² It therefore seems likely that hydroxyacetone can be converted into methyl lactate in two ways in methanol, either *via* tautomerisation to lactaldehyde or *via* oxidation to methyl glyoxal.

It thus seems plausible that the reaction pathway first involves oxidation of 1,2-propanediol to either lactaldehyde or 1-hydroxyacetone. Lactaldehyde is then oxidized rapidly to give exclusively methyl lactate, whereas 1-hydroxyacetone can give either methyl lactate or methyl pyruvate. This explains the higher selectivity of methyl lactate when oxidizing 1,2-propanediol than when oxidizing 1-hydroxyacetone. Based on the experimental

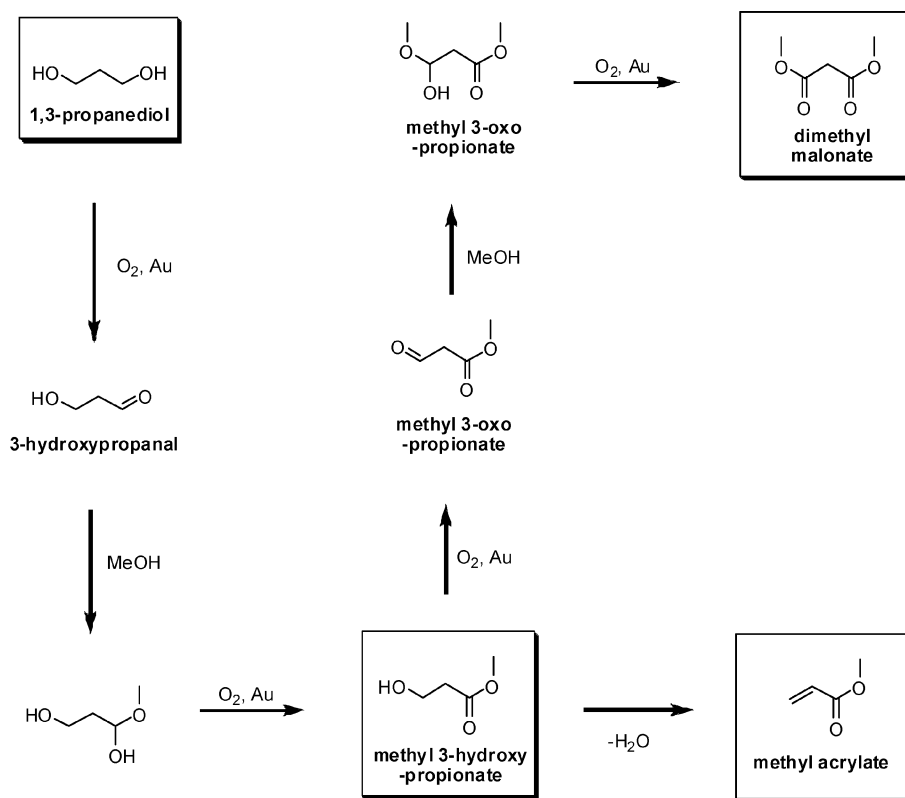
data, it seems reasonable to assume that the majority of methyl pyruvate originates from the oxidation of 1-hydroxyacetone. Methyl pyruvate then undergoes C–C cleavage to form methyl acetate. Cleavage of methyl pyruvate is likely to be the result of peroxides present, as a retro aldol reaction does not seem to be a plausible cause for this reaction.

Thus, these results are consistent with the conclusions drawn by Prati and Rossi from the oxidation of 1,2-propanediol in water.

Oxidation of 1,3-propanediol

Oxidative esterification of 1,3-propanediol in methanol over a supported gold catalyst has already been reported by Hayashi *et al.*²⁷ However, in order to compare this substrate with glycerol and 1,2-propanediol we examined the oxidative esterification for this substrate as well. We found that 1,3-propanediol is oxidized at a similar rate as glycerol (Fig. 4). Prati and Rossi have reported that diols containing two secondary alcohol groups such as 2,3-butanediol are inert towards oxidation.¹³ This points to the simple conclusion that oxidation of polyols with gold catalysts preferentially occurs at a primary alcohol group. Thus, when a substrate contains more than one primary alcohol group, it is more rapidly oxidized.

Oxidation of 1,3-propanediol results in a highly selective formation of methyl 3-hydroxypropionate, with a selectivity of 90% after 21 hours and 94% conversion. Interestingly, only small amounts of oxidation of the second alcohol functionality is taking place. This chemoselectivity indicates that the second alcohol group is influenced by the presence of a methyl ester group 3 carbon atoms away, thus rendering it more difficult to oxidize. Small amounts of oxidation do take place, however,



Scheme 3 Reaction scheme for oxidative esterification of 1,3-propanediol in the presence of base. The observed products are highlighted in boxes.

resulting in the formation of 5% dimethyl malonate. Methyl acrylate is also formed in small amounts (5%) after 21 hours, as a result of dehydration of methyl 3-hydroxypropionate (Scheme 3).

Conclusions

Gold catalyzed oxidative esterification of glycerol, 1,2-propanediol and 1,3-propanediol has been examined and found to be a possible route to important large scale chemicals such as methyl lactate and methyl acrylate. Furthermore, dimethyl mesoxalate can be obtained in high yields directly from glycerol, and potentially directly from the waste steam from biodiesel production.

The oxidation pathway from 1,2-propanediol to methyl lactate has been examined. The pathway was found to be similar to that of oxidation in water over gold catalysts by Prati and Rossi.¹³

The major by-products formed arise from C–C cleavage of C3 products and intermediates. This is likely caused by the presence of hydrogen peroxide. Indeed, using a catalyst that is efficient at breaking down hydrogen peroxide resulted in an increase of the selectivity of dimethyl mesoxalate from 79% to 89%.

The gold catalysts used in this work are significantly less active than the carbon supported gold catalysts reported for the oxidation of aqueous glycerol. A thorough comparison of the reaction rates of glycerol oxidation in water and methanol is necessary in order to draw firm conclusions on the catalytic activity in methanol.

Acknowledgements

The Center for Sustainable and Green Chemistry is sponsored by the Danish National Research Foundation.

References

- 1 M. Pagliaro, R. Ciriminna, H. Kimura, M. Rossi and C. D. Pina, *Angew. Chem. Int. Ed.*, 2007, **46**, 4434.
- 2 J. V. Kurian, in *Natural Fibers, Biopolymers, and Biocomposites*, ed. A. K. Mohanty, M. Misra and L. T. Lawrence, CRC Press LLC, Boca Raton, FL, 1st edn., 2005, pp. 497–525.
- 3 R. R. Soares, D. A. Simonetti and J. A. Dumesic, *Angew. Chem. Int. Ed.*, 2006, **45**, 3982.
- 4 C. Chiu, M. A. Dasari and G. J. Suppes, *AIChE J.*, 2006, **52**, 3543.
- 5 W. Girke, H. Klenk, D. Arntz, T. Haas and A. Neher, *Process for the production of acrolein*, US Patent 5387720, 1995; W. J.-L. Dubois, C. Duquenne, W. Hölderich and J. Kervennal, *Process for dehydrating glycerol to acrolein*, WO/2006/087084.
- 6 H. Kimura, K. Tsuto, T. Wakisaka, Y. Kazumi and Y. Inaya, *Appl. Catal. A*, 1993, **96**, 217; H. Kimura, *Appl. Catal. A*, 1993, **105**, 147.
- 7 R. Garcia, M. Besson and P. Gallezot, *Appl. Catal. A*, 1995, **127**, 165.
- 8 For recent reviews on gold catalysis and gold catalyzed oxidations see: G. C. Bond, C. Louis and D. T. Thompson, *Catalysis By Gold*, 2006, Imperial College Press, London; A. S. K. Hashmi and G. J. Hutchings, *Angew. Chem. Int. Ed.*, 2006, **45**, 7896; D. T. Thompson, *Top. Catal.*, 2006, **38**, 231; A. S. K. Hashmi, *Chem. Rev.*, 2007, **107**, 3180.
- 9 Unsupported gold nanoparticles have also been shown to be catalytically active, see: M. Comotti, C. D. Pina, R. Matarrese and M. Rossi, *Angew. Chem. Int. Ed.*, 2004, **43**, 5812.
- 10 M. Haruta, T. Kobayashi, H. Sano and N. Yamada, *Chem. Lett.*, 1987, **4**, 405; M. Haruta, N. Yamada, T. Kobayashi and S. Iilima, *J. Catal.*, 1989, **115**, 301.

- 11 B. S. Uphade, S. Tsubota, T. Hayashi and M. Haruta, *Chem. Lett.*, 1998, **12**, 1277; M. Haruta and M. Date, *Appl. Catal. A*, 2001, **222**, 427.
- 12 P. Landon, P. J. Collier, A. J. Papworth, C. J. Kiely and G. J. Hutchings, *Chem. Commun.*, 2002, 2058; P. Landon, P. J. Collier, A. F. Carley, D. Chadwick, A. J. Papworth, A. Burrows, C. J. Kiely and G. J. Hutchings, *Phys. Chem. Chem. Phys.*, 2003, **5**, 1917.
- 13 L. Prati and M. Rossi, *J. Catal.*, 1998, **176**, 552.
- 14 A. Abad, P. Concepción, A. Corma and H. García, *Angew. Chem. Int. Ed.*, 2005, **44**, 4066.
- 15 D. I. Enache, J. K. Edwards, P. Landon, B. Solsona-Espriu, A. F. Carley, A. A. Herzing, M. Watanabe, C. J. Kiely, D. W. Knight and G. J. Hutchings, *Science*, 2006, **311**, 362.
- 16 C. H. Christensen, B. Jørgensen, J. Rass-Hansen, K. Egeblad, R. Madsen, S. K. Klitgaard, S. M. Hansen, M. R. Hansen, H. C. Andersen and A. Riisager, *Angew. Chem. Int. Ed.*, 2006, **45**, 4648.
- 17 M. Comotti, C. D. Pina, R. Matarrese, M. Rossi and A. Siani, *Appl. Catal. A: General*, 2005, **291**, 204; C. Marsden, E. Taarning, D. Hansen, L. Johansen, S. K. Klitgaard, K. Egeblad and C. H. Christensen, *Green Chem.*, 2007, DOI: 10.1039/b712171g.
- 18 R. Zhao, D. Ji, G. Lv, G. Qian, L. Yan, X. Wang and J. Suo, *Chem. Commun.*, 2004, 904.
- 19 Y. Xu, P. Landon, D. Enache, A. F. Carley, M. W. Roberts and G. J. Hutchings, *Catal. Lett.*, 2005, **101**, 175.
- 20 M. D. Hughes *et al.*, *Nature*, 2005, **437**, 1132; P. Lignier, F. Morfin, S. Mangematin, L. Massin, J.-L. Rousset and V. Caps, *Chem. Commun.*, 2007, 186; P. Lignier, F. Morfin, L. Piccolo, J.-L. Rousset and V. Caps, *Catal. Today*, 2007, **122**, 284.
- 21 C. Bianchi, F. Porta, L. Prati and M. Rossi, *Top. Catal.*, 2000, **13**, 231; F. Porta, L. Prati, M. Rossi, S. Coluccia and G. Marta, *Catal. Today*, 2000, **61**, 165.
- 22 S. Carrettin, P. McMorn, P. Johnston, K. Griffin and G. J. Hutchings, *Chem. Commun.*, 2002, 696; S. Carrettin, P. McMorn, P. Johnston, K. Griffin, C. J. Kiely and G. J. Hutchings, *Phys. Chem. Chem. Phys.*, 2003, **5**, 1329.
- 23 S. Demirel-Gülen, M. Lucas and P. Claus, *Catal. Today*, 2005, **102–103**, 166.
- 24 C. L. Bianchi, P. Canton, N. Dimitratos, F. Porta and L. Prati, *Catal. Today*, 2005, **102–103**, 203.
- 25 W. C. Ketchie, Y. Fang, M. S. Wong, M. Murayama and R. J. Davis, *J. Catal.*, 2007, **250**, 94.
- 26 S. Demirel, P. Kern, M. Lucas and P. Claus, *Catal. Today*, 2007, **122**, 292; S. Demirel, K. Lehnert, M. Lucas and P. Claus, *Appl. Catal. B*, 2007, **70**, 637.
- 27 T. Hayashi, T. Inagaki, N. Itayama and H. Baba, *Catal. Today*, 2006, **117**, 210.
- 28 I. S. Nielsen, E. Taarning, K. Egeblad, R. Madsen and C. H. Christensen, *Catal. Lett.*, 2007, **116**, 35.
- 29 E. Taarning, I. S. Nielsen, K. Egeblad, R. Madsen and C. H. Christensen, *ChemSusChem*, 2008, **1**, DOI: 10.1002/cssc.200700033.
- 30 http://www.gold.org/discover/sci_indu/gold_catalysts/refcat.html.
- 31 W. C. Ketchie, M. Murayama and R. J. Davis, *J. Catal.*, 2007, **250**, 264.
- 32 Y. Hayashi and Y. Sasaki, *Chem. Commun.*, 2005, 2716.

A green, fully enzymatic procedure for amine resolution, using a lipase and a penicillin G acylase†

Hilda Ismail,‡^a Rute Madeira Lau,§^a Luuk M. van Langen,^a Fred van Rantwijk,^a Vytas K. Švedas^b and Roger A. Sheldon*^a

Received 13th September 2007, Accepted 18th December 2007

First published as an Advance Article on the web 25th January 2008

DOI: 10.1039/b714088f

A green procedure for the kinetic resolution of chiral amines *via* enzymatic acylation and deacylation has been demonstrated. The fully enzymatic approach obviates the common, waste-generating deacylation under strongly alkaline conditions. The acylating agent was (*R*)-phenylglycine propyl ester in combination with *Candida antarctica* lipase B as acylation catalyst. The enantiomerically enriched amides were subsequently deacylated in the presence of the penicillin G acylase from *Alcaligenes faecalis*. The degree of enantiomer recognition by CaLB in the acylation of aliphatic amines was unexpectedly modest, but a considerable further enantiomeric enrichment could be accomplished in the course of the subsequent enzymatic hydrolysis step.

Introduction

Enantiomerically pure amines are widely used in the fine-chemicals industry as resolving agents, chiral auxiliaries and chiral synthetic building blocks for pharmaceuticals and agrochemicals. Their industrial production *via* lipase mediated enantioselective acylation is increasing in significance compared with competing procedures,¹ such as the crystallisation of a diastereomeric salt, enantioselective reductive amination using a chiral auxiliary and enantioselective reductive amination mediated by a transaminase.

The acylating agent in lipase mediated enantioselective acylation is commonly a simple ester such as ethyl acetate or butanoate; isopropyl 2-methoxyacetate has been recommended because of its much superior reaction rate.² Under the right conditions, nearly any amine can be resolved.³ An efficient, solventless industrial process with simple downstream processing, nearly perfect from the green perspective, has been developed in recent years.¹

With regards to the subsequent deacylation of the enantiomerically enriched amide there is still much room for improvement, however. Chemical hydrolysis requires harsh reaction conditions, such as 15% NaOH in aqueous ethylene glycol at >150 °C,⁴ which give rise to a salt waste-stream and are, moreover, incompatible with sensitive functional groups. The ultimate

green solution would be a catalytic deacylation procedure under mild conditions but enzymatic amide hydrolysis⁵ is undesirably slow in general, presumably owing to the stability of the amide bond. One solution would be to employ an acylating group that is more readily removed than the commonly applied ones.⁶

We have recently demonstrated the enantioselective acylation of 1-phenylethylamine with (*R*)-phenylglycine amide in the presence of the penicillin G acylase from *Alcaligenes faecalis*,⁷ followed by a deacylation step using the same enzyme.⁸ The key to the success of the procedure is the stability of the zwitterionic (*R*)-phenylglycine hydrolysis product, which, moreover, precipitates under the reaction conditions. An additional advantage of the penicillin G acylase-catalysed hydrolysis is its high enantioselectivity.^{8,9}

We wished to extend this latter procedure to amine acylation in the presence of a lipase in anhydrous medium. Such a procedure would obviate the acyl donor hydrolysis that accompanies amine acylation in the presence of penicillin G acylase.¹⁰ An ester rather than the amide of (*R*)-phenylglycine would be preferred as the acyl donor because lipases do not react efficiently with amides. Such esters are readily prepared from (*R*)-phenylglycine, which is produced in large amounts for conversion into semisynthetic β -lactam antibiotics. *Candida antarctica* lipase B (CaLB) was an obvious choice as the acylation catalyst on account of its exquisite stability and excellent performance in the enantioselective acylation of a wide variety of amines.³ This latter characteristic is a potential advantage of acylation in the presence of a lipase rather than a penicillin G acylase, because these showed quite modest enantioselectivity with aliphatic amines.¹⁰ Hence, we have extended the scope of the reaction to include a range of 2-alkylamines (**1a–c**) as well as 1-phenylethylamine (**1d**).

Results and discussion

Acylation

Possible effects of the leaving group R² in the acyl donor (**2**, see Fig. 1) on the reaction rate were investigated in the acylation

^aLaboratory of Biocatalysis and Organic Chemistry, Department of Biotechnology, Delft University of Technology, Julianalaan 136, 2628 BL Delft, The Netherlands. E-mail: r.a.sheldon@tudelft.nl

^bFaculty of Bioengineering and Bioinformatics and Belozersky Institute of Physicochemical Biology, Lomonosov Moscow State University, Moscow 119992, Russia

† This paper was published as part of the themed issue of contributions from the 3rd International Conference on Green and Sustainable Chemistry.

‡ Present address: Department of Pharmacology, Faculty of Pharmacy, Gadjah Mada University, Yogyakarta, Indonesia.

§ Present address: DSM, Alexander Fleminglaan 1, 2613 AX Delft, The Netherlands.

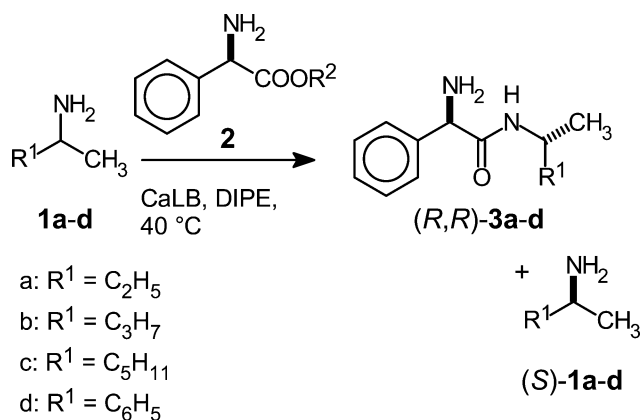


Fig. 1 Enantioselective acylation of amines **1a–d** with (*R*)-phenylglycine esters (**2**, R^2 , see text) in the presence of CaLB.

of **1c**. When comparing various short-chain alkyl esters we obtained the best results, as regards reaction rate, with the propyl ester while there was little effect on the enantiomer discrimination. No reaction was observed in the absence of enzyme. Accordingly, the propyl ester was used in all further experiments.

The time-course of the acylation reaction (Fig. 2) shows that **1d** reacted much slower than the alkylamines **1a–c**, which presumably should be ascribed to steric hindering by the aromatic ring in **1d**.

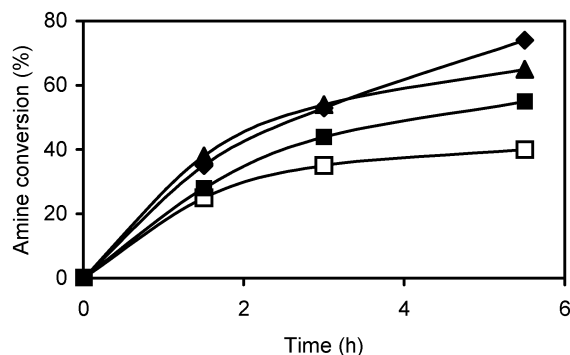


Fig. 2 Time-course of the acylation of the amines **1a–d** with (*R*)-phenylglycine propyl ester in the presence of CaLB; **1a** (◆), **1b** (▲), **1c** (■), **1d** (□).

The enantiomeric ratio (*E*) increased with the steric requirements of the amine. It did not surprise us that the enantiomer selectivity of 2-butylamine (**1a**) was modest, since this involves the discrimination between a methyl group and an

ethyl one, which is known to be problematic.³ The enantiomer discrimination of 2-pentylamine (**1b**) and 2-hexylamine (**1c**), however, also was less than would be expected on the basis of literature data, obtained with acylation by, *e.g.*, ethyl butanoate or isopropyl 2-methoxyacetate.³ The enantiomer discrimination of 1-phenylethylamine (**1d**), in contrast, was near-quantitative.

It has been proposed, on the basis of a model study, that discrimination of amine enantiomers by CaLB involves formation of a critical H-bond between the amino group in the reactant and the catalytic His.¹¹ H-bond formation between the α -amino group in **2** and the amine possibly could provide an alternative path for proton transfer and influence the enantiodiscrimination by CaLB. It is worth noting that such hydrogen bonding has been put forward in explanation of the accelerating effect of a β -oxygen atom in the acyl reagent.¹² Acyl reagent **2** is chiral and the acylation procedure is actually diastereoselective rather than enantioselective. Hence, any proton transfer by the acyl reagent as described above would be affected by its stereochemistry. The issue was addressed by performing acylations with (*S*)-phenylglycine methyl ester (see Table 1). The reactions were sluggish, in agreement with CaLB's known preference for (*R*)-phenylglycine esters,¹³ but the *E* ratios in the resolution of **1a–d** were little influenced by the stereochemistry of the acyl donor. We conclude that the enantiodiscrimination is not affected by participation of the acyl reagent in proton transfer, as well as other possibly counteracting diastereoselective effects. It would seem that the mediocre enantiomer discrimination of **1b–c** should rather be ascribed to stereoelectronic properties of the α -amino group. This issue is now the subject of further study.

Deacylation

With regards to the hydrolysis of **3a–d**, penicillin G acylase is obviously the preferred catalyst.⁸ We compared the penicillin G acylases from *E. coli* and *A. faecalis* as catalysts in the deacylation of (*R,R*)-**3c**. We found that the latter enzyme was at least three times more efficient (98% conversion in 6 h, *vs.* 89% conversion in 15 h for the *E. coli* enzyme). Although the difference is less than observed in acylation or hydrolysis reactions involving the phenylacetyl group,^{9,10} the penicillin G acylase from *A. faecalis* is the obvious choice as deacylation biocatalyst (Fig. 3).

Deacylation experiments were carried out with the amides (*R,R*)-**3a–d** at synthetically relevant concentrations (Table 2) in the presence of *A. faecalis* penicillin G acylase. The amides **3a** and **3b** had originally been obtained in a rather low diastereomeric excess (*de*), due to the modest enantiomer

Table 1 Diastereoselective acylation of the amines **1a–d** with (*R*)-phenylglycine propyl ester (**2**) and (*S*)-phenylglycine methyl ester (**4**) in the presence of CaLB^a

| Donor | (<i>R</i>)-phenylglycine propyl ester (2) | | | | (<i>S</i>)-phenylglycine methyl ester (4) | | | |
|-----------|--|-----------|-----------------------------------|----------|--|-----------|-----------------------------------|----------|
| | Time/h | Conv. (%) | ee _{amine} (% <i>S</i>) | <i>E</i> | Time/h | Conv. (%) | ee _{amine} (% <i>S</i>) | <i>E</i> |
| 1a | 3 | 50 | 19 | 1.7 | 24 | 90 | 19 | 2 |
| 1b | 3 | 53 | 55 | 5 | 24 | 58 | 66 | 5 |
| 1c | 5.5 | 52 | 73 | 11 | 24 | 50 | 80 | 21 |
| 1d | 24 | 51 | 96 | 97 | 24 | 55 | >99 | 100 |

^a Reaction conditions: **1** (0.1 M), **2** or **4** (0.2 M) and Novozym 435 (20 mg mL⁻¹) in diisopropyl ether (5 mL) at 40 °C in the presence of 4 Å molecular sieve.

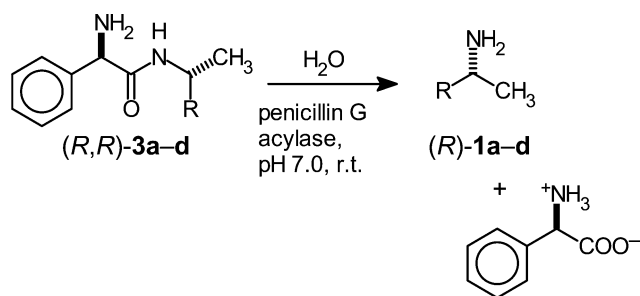


Fig. 3 Hydrolysis of (*R,R*)-**3a-d** in the presence of penicillin G acylase.

Table 2 Deacylation of **3a-d** in the presence of *A. faecalis* penicillin G acylase^a

| Amide | de ^b (%) | Time/h | Conv. (%) | ee _{amine} (% <i>R</i>) |
|---------------------------|---------------------|--------|-----------|-----------------------------------|
| (<i>R,R</i>)- 3a | 76 | 1 | 84 | 98 |
| (<i>R,R</i>)- 3b | 74 ^c | 3.5 | 91 | 91 |
| | 94 | 7 | 98 | 99 |
| (<i>R,R</i>)- 3c | 96 | 3.5 | 90 | 99 |
| (<i>R,R</i>)- 3d | 97 | 3.5 | 89 | >99 |

^a Reaction conditions: (*R,R*)-**3a-d** (0.1 M), 0.1 M phosphate buffer pH 7.0 (3 mL), *A. faecalis* penicillin G acylase CLEA (1455 BPU), rt. ^b The diastereomeric excess (de) was calculated from: $de = ([R,R] - [R,S])/([R,R] + [R,S])$. ^c Unrecrystallised amide sample.

recognition of **1a** and **1b** in the acylation step, but a simple purification, to remove the excess of acyl donor (**2**), also resulted in diastereomeric enrichment. For comparison, an unpurified sample of **3b** was also subjected to enzymatic deacylation. The penicillin G acylase that we employed in these reactions was immobilised as a cross-linked enzyme aggregate (CLEA)¹⁴ for easy recovery and reuse. Deacylation smoothly proceeded to full conversion but further enantiomeric enrichment could be accomplished upon partial hydrolysis (see Table 2).

Conclusion

Fully enzymatic kinetic resolution of chiral amines, employing CaLB and penicillin G acylase as the acylation and deacylation catalysts, respectively, has been demonstrated. In the resolution of 1-phenylethylamine, which was quite efficient, the present method avoids the accompanying hydrolysis of acyl donor due to the use of an anhydrous reaction medium. The unexpectedly low enantioselectivity in the acylation of aliphatic amines, compared with common acyl reagents, somewhat detracts from the immediate practical value of the procedure, although a considerable further enantiomeric enrichment could be accomplished in the enzymatic hydrolysis step. One more drawback of **2** is its recycling, which would require a stoichiometric amount of acid.^{15,16} Further work, towards acyl reagents that combine a high reaction rate, efficient enantiomer discrimination and are also readily cleaved enzymatically and recycled, is in progress.

Experimental section

Materials

Novozym 435 (immobilised *Candida antarctica* lipase B) was kindly donated by Novozymes (Bagsvaerd, Denmark). Chem-

icals were purchased from Sigma or Acros. Esters of (*R*)- and (*S*)-phenylglycine were obtained from the amino acids according to a published procedure.¹⁵

Penicillin G acylase from *E. coli* ATCC 11105 was kindly donated by DSM. *Acaligenes faecalis* penicillin G acylase was obtained from the fermentation of recombinant *E. coli* cells.¹⁷ A cross-linked enzyme aggregate (CLEA) was prepared by a slight variation of our published procedure.¹⁴ Semi-purified penicillin G acylase from *A. faecalis* (2000 BPU, one BPU will hydrolyze one μmol of penicillin G per min at pH 8) was dissolved in phosphate buffer pH 7. Aggregation was induced by addition of ammonium sulfate (51.6 g) under gentle stirring at 4 °C. The enzyme aggregates were crosslinked by addition of glutaraldehyde solution (25% w/v; 4 mL) then stirred at 4 °C for 60 min. The crosslinked enzyme was separated from the supernatant by centrifugation, then washed three times with phosphate buffer pH 7.0 (0.1 M). Glycine (380 mg) was added to the CLEA suspension and the mixture was left overnight under stirring. After removing the excess of glycine, the CLEA suspension was washed twice, followed by reduction of the imino bonds and any free aldehyde groups with sodium borohydride (25 mg). The CLEA suspension was washed twice with phosphate buffer pH 7.0 and stored as a suspension in phosphate buffer pH 7.0 at 4 °C.

Enzymatic reactions

Lipase catalysed acylation. (*R*)-Phenylglycine propyl ester (**2**, 1.0 mmol), amine (0.5 mmol) and 1,3-dimethoxybenzene (150 μL , internal standard) were dissolved in diisopropylether (5 mL); and 4 Å and 5 Å molecular sieves (150 mg each) were added. The reaction was started by addition of Novozyme 435 (100 mg). Samples (100 μL) were withdrawn at regular intervals, diluted with 1,2-dimethoxyethane (0.5 mL) and analysed as described below.

The reaction was stopped at 50% conversion by removal of the enzyme and molecular sieves. The unreacted amine was removed by extraction with water pH 8.5. The organic layer was dried and concentrated *in vacuo*. The excess of **2** was removed by crystallisation of the amides from hexane; yields (unoptimised): **3a**, 56%; **3b**, 30%; **3c**, 40%; **3d**, 48%.

***N*-(*R*)-phenylglyciny-2-butylamine (**3a**).** ¹H-NMR (300 MHz), (CDCl₃): δ 7.27–7.39 (5H, aromatic protons, m), δ 6.85 (1H, CONHCH, s), δ 4.48 (1H, COCHNH₂, s), δ 3.84–3.91 (1H, NHCHCH₃, m), δ 1.75 (2H, COCNH₂, s), δ 1.31–1.41 (2H, -(CH₂)₂-, m), δ 1.10 (3H, -CHCH₃, d), δ 0.84 (3H, -CH₂CH₃, t).

***N*-(*R*)-phenylglyciny-2-pentylamine (**3b**).** ¹H-NMR (300 MHz), (CDCl₃): δ 7.27–7.39 (5H, aromatic protons, m), δ 6.85 (1H, CONHCH, s), δ 4.5 (1H, COCHNH₂, s), δ 3.92–3.97 (1H, NHCHCH₃, m), δ 1.75 (2H, COCNH₂, s), δ 1.31–1.41 (4H, -(CH₂)₃-, m), δ 1.10 (3H, -CHCH₃, d), δ 0.87 (3H, -CH₂CH₃, t).

***N*-(*R*)-phenylglyciny-2-heptylamine (**3c**).** ¹H-NMR (300 MHz), (CDCl₃): δ 7.27–7.39 (5H, aromatic protons, m), δ 6.85 (1H, CONHCH, s), δ 4.5 (1H, COCHNH₂, s), δ 3.92–3.97 (1H, NHCHCH₃, m), δ 1.74 (2H, COCNH₂, s), δ 0.97–1.42 (8H, -(CH₂)₅-, m), δ 1.10 (3H, -CHCH₃, d), δ 0.9 (3H, -CH₂CH₃, t).

***N*-(*R*)-phenylglyciny-phenylethylamine (3d).** ¹H-NMR (300 MHz), (CDCl₃): δ 7.23–7.41 (10H, aromatic protons, m), δ 5.25 (1H, C₆H₅CHCH₃, m), δ 4.91 (1H, COCHNH₂, s), δ 1.74 (2H, COCNH₂, s, m), δ 1.49 (3H, CHCH₃, d).

The progress of the reactions was monitored by GC using a 0.53 mm × 50 m Varian CP Sil 5 CB column, *d*_r 0.4 μm. The oven temperature was programmed from 50 °C (1 min) to 250 °C at a rate of 10 °C min⁻¹.

The enantiomeric excess of the unconverted amines **1c** and **1d** was measured by derivatisation with trifluoroacetic anhydride followed by GC on a 0.25 mm × 30 m Astec ChiralDex β-PH column, at an oven temperature of 80 °C (**1c**) or 160 °C (**1d**). The enantiomeric excess of **1a** and **1b** was measured (after benzylation) by HPLC using a 4.6 × 250 mm 10 μm Chiracel OD column, eluent hexane–isopropyl alcohol (95 : 5, v/v) at 0.6 mL min⁻¹ with UV detection at 215 nm.

The diastereomeric purity of the amides **3a–d** was measured by HPLC on a custom-packed 8 × 100 mm 6 μm Waters Symmetry C₁₈ column contained in a Waters 8 × 10 RCM holder, eluent MeOH–H₂O (50 : 50, v/v), 1 g L⁻¹ SDS at 0.8 mL min⁻¹ pH 3.5 with UV detection at 215 nm.

Penicillin G acylase catalysed deacylation. The initial experiments were performed with **1c** (5 mg) in a 0.1 M phosphate buffer pH 7 (5 mL) at room temperature, in the presence of penicillin G acylase from *E. coli* (9.6 BPU) or *A. faecalis* (8.2 BPU). Preparative-scale reaction conditions: (*R,R*)-**3a–d** (0.1 M), 0.1 M phosphate buffer pH 7.0 (3 mL), *A. faecalis* penicillin G acylase CLEA (1455 BPU), rt. Samples were periodically withdrawn and analysed by HPLC; conversions were determined on amine formation.

The aliphatic amines **1a–c** were quantitated by mixing precise amounts of reaction mixture and a solution of 2-pentylamine (standard), followed by derivatisation during 1 min with a commercial solution of *o*-phthalaldehyde in the presence of 2-mercaptoethanol (1 mL). Analysis: HPLC on a 8 × 100 mm 6 μm Waters Symmetry C₁₈ column, eluent MeOH–H₂O 80 : 20 (v/v) at 1 mL min⁻¹, UV detection at 340 nm.

Analysis of **1d**: (*R*)-phenylglycinamide (standard) was added followed by HPLC analysis; eluent MeOH–H₂O (65 : 35, v/v), 1 g L⁻¹ SDS, 1 g L⁻¹ KH₂PO₄, pH 3.5 at 1 mL min⁻¹ with UV detection at 215 nm.

The enantiomeric excess of the aliphatic amines **1a–c** was measured as follows: the pH of the sample was brought to 11, the amine was extracted into hexane and analysed by chiral GC (see above). The enantiomeric purity of **1d** was measured by chiral HPLC on a 4 × 150 mm 5 μm Crownpack CR⁺ column, eluant aqueous 0.1 M HClO₄ pH 1.5 at 0.6 mL min⁻¹, UV detection 215 nm.

Chemical synthesis of racemic amides (reference compounds). (*R*)-phenylglycine chloride hydrochloride (11 g; 1.2 eq.) was added to a stirred solution of amine (1 eq.) in dichloromethane (50 mL) at –10 °C. The reaction mixture was allowed to stand for 2 h at –5 °C. Cold water (50 mL) was then added, the pH

adjusted to 1.5 with hydrochloride acid and the organic layer discarded. The amide was isolated from the water phase (pH 8.5) by extraction with dichloromethane. The solvent was then removed *in vacuo*, and white crystals of amide were obtained by recrystallisation in *n*-hexane.

Acknowledgements

Thanks are due to Novozymes (Bagsvaerd, Denmark) for generous donations of Novozyme 435. Financial support for H. Ismail by the QUE Project of the Faculty of Pharmacy, Gadjah Mada University, Yogyakarta, Indonesia and by the Schlumberger Foundation is gratefully acknowledged. This work was financially supported by the Netherlands Ministry of Economic Affairs (contract grant number SSC 95010) and DSM Life Science Products.

References

- G. Hieber and K. Dittrich, *Chim. Oggi*, 2001, **19**(6), 16–20.
- F. Balkenhohl, K. Dittrich, B. Hauer and W. Ladner, *J. Prakt. Chem.*, 1997, **339**, 381–384.
- F. van Rantwijk and R. A. Sheldon, *Tetrahedron*, 2004, **60**, 501–519 and references cited therein.
- K. Dittrich, F. Balkenhohl and W. Ladner, (BASF) PCT Int. Appl. WO 97/10201 [Chem. Abstr., 1997, **126**, 277259f].
- H. Smidt, A. Fisher, P. Fisher and R. D. Schmid, *Biotechnol. Tech.*, 1996, **10**, 335–338.
- T. Wagegg, M. M. Enzelberger, U. T. Bornscheuer and R. D. Schmid, *J. Biotechnol.*, 1998, **61**, 75–78.
- (a) M. Kulhánek and M. Tadra, *Folia Microbiol.*, 1968, **13**, 340–345; (b) R. M. D. Verhaert, J. M. van der Laan, J. Van Duin and W. J. Quax, *Appl. Environ. Microbiol.*, 1997, **63**, 3412–3418; (c) V. Švedas, D. Guranda, L. van Langen, F. van Rantwijk and R. Sheldon, *FEBS Lett.*, 1997, **417**, 414–418.
- D. T. Guranda, A. I. Khimiuk, L. M. van Langen, F. van Rantwijk, R. A. Sheldon and V. K. Švedas, *Tetrahedron: Asymmetry*, 2004, **15**, 2901–2906.
- D. T. Guranda, L. M. van Langen, F. van Rantwijk, R. A. Sheldon and V. K. Švedas, *Tetrahedron: Asymmetry*, 2001, **12**, 1645–1650.
- L. M. van Langen, N. H. P. Oosthoek, D. T. Guranda, F. van Rantwijk, V. K. Švedas and R. A. Sheldon, *Tetrahedron: Asymmetry*, 2000, **11**, 4593–4600.
- M. Bocola, M. T. Stubbs, C. Sottriffer, B. Hauer, T. Friedrich, K. Dittrich and G. Klebe, *Protein Eng.*, 2003, **16**, 319–322.
- M. Cammenberg, K. Hult and S. Park, *ChemBioChem*, 2006, **7**, 1745–1749.
- (a) M. C. de Zoete, A. A. Ouweland, F. van Rantwijk and R. A. Sheldon, *Recl. Trav. Chim. Pays-Bas*, 1995, **114**, 171–174; (b) M. A. Wegman, M. A. P. J. Hacking, J. Rops, P. Pereira, F. van Rantwijk and R. A. Sheldon, *Tetrahedron: Asymmetry*, 1999, **10**, 1739–1750.
- L. M. van Langen, M. H. A. Janssen, N. H. P. Oosthoek, S. R. M. Pereira, V. K. Švedas, F. van Rantwijk and R. A. Sheldon, *Biotechnol. Bioeng.*, 2002, **79**, 224–228.
- L. M. van Langen, E. de Vroom, F. van Rantwijk and R. A. Sheldon, *Green Chem.*, 2001, **3**, 316–319.
- Catalytic esterification of (*R*)-phenylglycine is known to result in racemisation, see: M. A. Wegman, J. M. Elzinga, E. Neeleman, F. van Rantwijk and R. A. Sheldon, *Green Chem.*, 2001, **3**, 61–64.
- (a) Z. Ignatova, S. Stoeva, B. Galunsky, C. Hörnle, A. Nurk, E. Piotraschke, W. Voelter and V. Kasche, *Biotechnol. Lett.*, 1998, **20**, 977–982; (b) M. Deak Peter, S. Lutz-Wahl, H. Bothe and L. Fischer, *Biotechnol. Lett.*, 2003, **25**, 397–400.

Oxidations of amines with molecular oxygen using bifunctional gold–titania catalysts

Søren K. Klitgaard, Kresten Egeblad, Uffe V. Mentzel, Andrey G. Popov, Thomas Jensen, Esben Taarning, Inger S. Nielsen and Claus Hviid Christensen*

Received 14th September 2007, Accepted 2nd January 2008

First published as an Advance Article on the web 8th February 2008

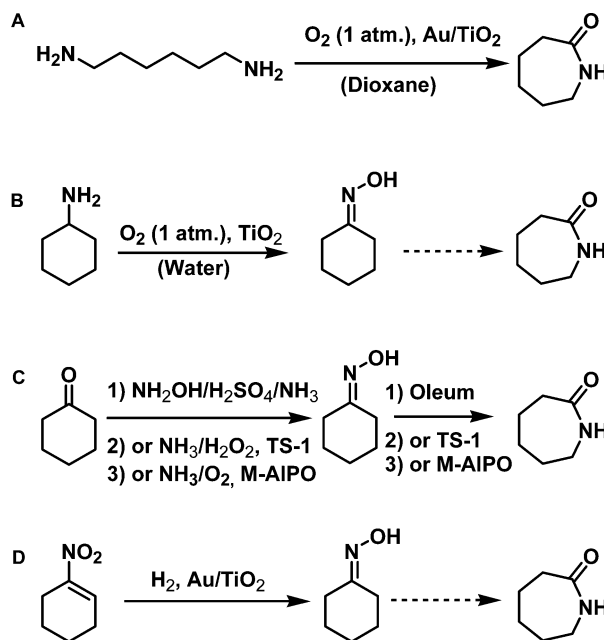
DOI: 10.1039/b714232c

Over the past decades it has become clear that supported gold nanoparticles are surprisingly active and selective catalysts for several green oxidation reactions of oxygen-containing hydrocarbons using molecular oxygen as the stoichiometric oxidant. We here report that bifunctional gold–titania catalysts can be employed to facilitate the oxidation of amines into amides with high selectivity. Furthermore, we report that pure titania is in fact itself a catalyst for the oxidation of amines with molecular oxygen under very mild conditions. We demonstrate that these new methodologies open up for two new and environmentally benign routes to caprolactam and cyclohexanone oxime, both of which are precursors for nylon-6.

Introduction

In the fine chemicals industry, as well as in traditional organic chemistry, many oxidations are being carried out using high-valent inorganic oxidants. The application of these types of reagents often containing chromium or manganese inevitably leads to the generation of huge amounts of metal waste. In recent years several new procedures have been developed wherein a catalyst is used to facilitate oxidation of alcohols employing molecular oxygen as the stoichiometric oxidant.^{1–6} In this emerging field of *green oxidation chemistry*, catalysts comprising gold nanoparticles have attained a very prominent role,⁷ since they are often surprisingly active and on some occasions exhibit different chemoselectivity than platinum metal based catalysts. Thus, from a fundamental point of view, as well as from a technical one, gold catalysis is a topic of intense scientific interest; drawing attention from a very diverse group of researchers. So far, literature reports on selective oxidations using gold catalysts have focused primarily on oxidation of alcohols to aldehydes,³ carboxylic acids⁴ or esters,^{8,9} oxidation of aldehydes to esters,¹⁰ epoxidations of olefins,^{11–13} and activation of C–H bonds in alkanes.¹⁴

Here, we report on our recent intriguing findings that gold nanoparticles supported on titania (Au–TiO₂) is a versatile and bifunctional catalyst for the oxidation of amines with molecular oxygen. To the best of our knowledge this is the first report on oxidation of amines using a heterogeneous gold catalyst. However, the fascinating feature of the chemistry reported here is not only the new application of gold catalysis but also that it opens up for the possibility of producing nylon-precursor materials from amines by oxidation with air in a heterogeneous catalytic process (Scheme 1A). Moreover, we report that cyclohexyl amine can be oxidized to cyclohexanone



Scheme 1 Methods for producing caprolactam.

oxime with molecular oxygen using TiO₂ as the catalyst in a comparatively low-temperature process (Scheme 1B).

The conventional route to the nylon-6 precursor caprolactam is a two step oximation and Beckmann rearrangement process starting from cyclohexanone (Scheme 1C, reaction path 1). First, cyclohexanone is converted into cyclohexanone oxime by reaction with hydroxyl ammonium sulfate and ammonia, and secondly, cyclohexanone oxime is converted into caprolactam by Beckmann rearrangement using oleum. Very large amounts of ammonium sulfate are generated as waste in this process. Therefore, the development of new innovative processes in which oximation is performed by reacting cyclohexanone with ammonia and hydrogen peroxide instead of using hydroxyl

Center for Sustainable and Green Chemistry, Department of Chemistry, Technical University of Denmark, Building 206, DK-2800, Lyngby, Denmark. E-mail: chc@kemi.dtu.dk; Tel: +45 4525 2402

amine, as well as substituting oleum for solid acid catalysts in the Beckmann rearrangement step, have attracted significant attention. One of these new processes (Scheme 1C, reaction path 2), which is actually already operated industrially by EniChem and Sumitomo, employs a titanium-containing zeolite (TS-1) as the oximation catalyst,¹⁵ whereas the other highly innovative process (Scheme 1C, reaction path 3) developed by Thomas and Raja employs metal doped aluminium phosphates as the catalyst.¹⁶ Very recently, yet another new process for preparing cyclohexanone oxime was reported by Corma and Serna.¹⁷ In this process (Scheme 1D), which is fundamentally different from the oximation processes, since the oxime is produced by reduction rather than oxidation, 1-nitro-1-cyclohexene is chemoselectively hydrogenated into cyclohexanone oxime facilitated by Au–TiO₂.

Experimental

All chemicals were purchased from commercial sources and used without further purification. The gold catalysts were prepared by deposition-precipitation using HAuCl₄·3H₂O (Aldrich) as the gold source.¹⁸

Oxidation of alcohol–amine mixtures

Mixtures of 1-butanol (10 mmol) and *n*-hexyl amine (10 mmol, 98%, Fluka), or neat *n*-hexyl amine (10 mmol), were charged to a 25 ml round-bottomed flask equipped with a condenser together with 0.4 g catalyst. The reactor system was connected to an O₂ cylinder and it was flushed with O₂ before being heated to 115 °C or 130 °C in an oil-bath. The reactor was maintained at the desired temperature for 20 h before being cooled to room temperature. Samples were analyzed by GC and GC-MS; the amounts of substrates and products were quantified using *n*-decane (98%, Fluka) as internal or external standard.

Oxidation of 1,6-hexanediamine

For the open flask experiments 1,6-hexanediamine (2.5 mmol, 97%, Fluka) dissolved in dioxane (10 ml) was charged to a 25 ml round-bottomed flask equipped with a condenser together with 0.4 g catalyst and a catalytic amount of water (25 μl). The reactor system was connected to an O₂ cylinder and it was flushed with O₂ before being heated to 90 °C in an oil-bath. The reactor was maintained at the desired temperature for 18 h before being cooled to room temperature. After reaction, the slurry was extracted with 10 ml CH₂Cl₂ and the extracted liquid was analyzed using GC and GC-MS; using anisole (99%, Sigma–Aldrich) as internal or external standard.

The autoclave experiments were conducted using a 325 ml stainless-steel autoclave fitted with a glass-liner as the reactor. The autoclave was charged with 1,6-hexanediamine (2.5 mmol, 97% Fluka), 0.4 g Au–TiO₂ catalyst, dioxane (10 ml) and water (25 μl). The autoclave was flushed with O₂ and charged with a pressure of 2 bar O₂ before heated to 90 °C in an oil-bath for 18 h. The product slurry was extracted with CH₂Cl₂ as described above for the open flask experiments.

Oxidation of cyclohexylamine

Cyclohexyl amine (99.5%, Fluka), TiO₂ (anatase, calcined 24 h at 500 °C) and *n*-decane, and in some experiments also water, were added to a two-necked round bottomed flask equipped with a condenser. The stirred system was flushed with O₂ and heated to different temperatures for different periods of time. The reaction was carried out under atmospheric pressure of O₂ and the reaction mixture was analyzed using GC after reaction. For the temperature series experiments, 8 g cyclohexyl amine, 2 g TiO₂ and 0.5 g H₂O were reacted for 24 h at different temperatures. For the experiments with different water contents (Fig. 3b), 8 g cyclohexyl amine, 2 g TiO₂ and different amounts of water were reacted for 24 h at 80 °C. For the time series experiment, 8 g cyclohexyl amine and 0.1 g TiO₂ were reacted at 90 °C for different periods of time.

Results and discussion

Oxidation of alcohol–amine mixtures and neat *n*-hexylamine

Our studies into the catalytic aerobic oxidation of amines were triggered by our discovery that oxidation of mixtures of *n*-hexyl amine and 1-butanol afforded different products with high selectivity when employing different gold catalysts. With 1 wt% Au–MgAl₂O₄, *N*-hexyl butanoic amide was produced, whereas application of 1 wt% Au–TiO₂ afforded *N*-hexyl hexanoic amide with surprisingly high selectivity, see Fig. 1. The product of reaction A, *N*-hexyl butanoic amide, can be easily explained and it may be formed *via* two different reaction pathways, as also discussed in the literature very recently for a different catalyst system.¹⁹ Either, butanol is oxidized to butyl butanoate, followed by aminolysis to afford the amide, or the hemiaminal of butanal and *n*-hexyl amine is oxidized directly to the amide. No attempts to verify by which reaction pathway the amide was formed were performed, partly due to the fact that these reactions are fundamentally akin entailing no oxidation state changes for the amine. However, the product of reaction B can only be explained by the amine substrate being initially oxidized in the presence of the Au–TiO₂ catalyst. In order to verify that

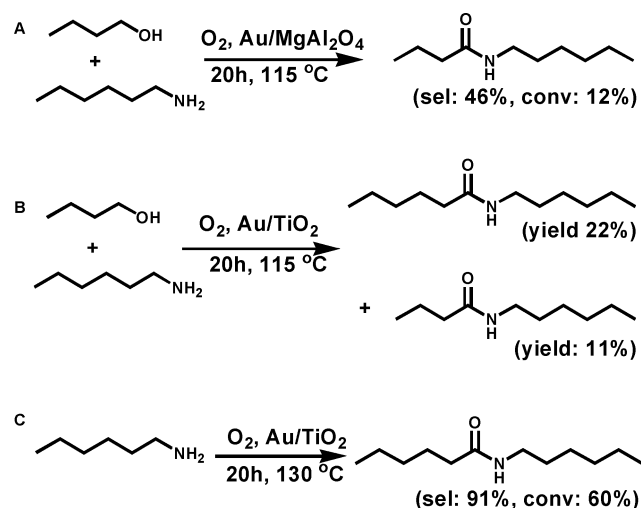


Fig. 1 Oxidation of mixtures of 1-butanol and *n*-hexyl amine using (A) Au–MgAl₂O₄ and (B) Au–TiO₂, and *n*-hexyl amine using Au–TiO₂ (C).

butanol played no role in the oxidation of *n*-hexyl amine, an experiment using neat *n*-hexyl amine as the substrate liquid was performed (Fig. 1C). Since this experiment resulted in the formation of *N*-hexyl hexanoic amide with excellent selectivity (91%), it was concluded that direct amine oxidation was in fact taking place. To the best of our knowledge this is the first observation that a heterogeneous gold catalyst can be used to facilitate the oxidation of an amine with molecular oxygen.

Oxidation of 1,6-hexanediamine

After having shown that Au–TiO₂ could be applied as a catalyst for the oxidation of *n*-hexyl amine with O₂ into *N*-hexyl hexanoic amide, we were interested in investigating if other and potentially more interesting amides could also be produced in this fashion. Specifically, we wanted to probe the reactivity of 1,6-hexanediamine, as this amine substrate could afford caprolactam upon oxidation of one of the amine functionalities. Moreover, we were interested in investigating the roles of the individual components of the Au–TiO₂ catalyst in the amine oxidation reaction. Therefore, we conducted a series of experiments with 1,6-hexanediamine as the substrate and either Au–TiO₂ or pure TiO₂ as the solid phase, as well as an experiment in which no additional solid phase was added. The results of these experiments is shown in Fig. 2.

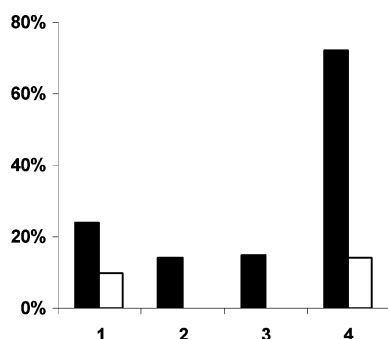


Fig. 2 Results of experiments with oxidation of 1,6-hexanediamine in open flask and in autoclave using different solid additives at 90 °C (black: conversion; white: yield). (1) Au–TiO₂ (open flask), (2) no catalyst (open flask), (3) TiO₂ (open flask), (4) Au–TiO₂ (autoclave, 2 bar O₂).

Fig. 2 shows the results of our experiments with oxidation of 1,6-hexanediamine carried out at 90 °C over 18 h. It is seen that merely heating the reaction mixture results in a small loss of 1,6-hexanediamine, but no products could be detected by GC. Since the boiling point of 1,6-hexanediamine (205 °C) is well above the reaction temperature (90 °C), the loss of substrate from the reaction mixture is most likely not due to evaporation but rather results from polymerization of the amine. Similarly, no products could be detected in GC from the experiments with pure TiO₂ added as the solid phase, proving that Au–TiO₂ is catalyzing the oxidation of these amines into amides. We also carried out experiments in autoclaves to see if increasing the O₂ pressure would also increase the caprolactam yield. In general, these experiments resulted in a toothpaste-like slurry, probably due to polymerization of both 1,6-hexanediamine and caprolactam. Instead of performing tedious isolation work on this paste, we extracted the soluble products from the solid with CH₂Cl₂ or dioxane and analyzed the liquids by GC and GC-

MS. The remaining solid might contain polymerized caprolactam, however, no attempts to quantify this were performed, since the objective of this study was merely to survey the new chemistry. As is evident from Fig. 2, increasing the O₂ pressure is not beneficial to this reaction, as the caprolactam is not increased despite higher conversion of 1,6-hexanediamine. In addition to caprolactam, the reaction mixture from the autoclave experiment also contained cycloheptanimine and azepan-2-ol, both of which might be intermediates in the formation of caprolactam. This suggests that the reaction can be tuned to give even higher yields of caprolactam. The reaction mechanism might involve peroxides when dioxane is present, as solvents in some cases have been shown to take part directly in gold-catalyzed reactions.¹³ Attempts to raise the reaction temperature to 130 °C resulted in higher conversion of the amine but with a much lower selectivity towards caprolactam.

Oxidation of cyclohexylamine

It is known that titanium catalysts can be applied to facilitate oxidation of amines to oximes with H₂O₂ as the stoichiometric oxidant.^{20–22} However, far less literature reports and patents can be found describing the application of molecular oxygen as the stoichiometric oxidant and the few known processes available either require high O₂ pressures²³ or high temperatures.²⁴ Since our process for oxidation of amines to amides functions at much milder conditions we were *a priori* compelled to also study the oxidation of amines to oximes in more detail using pure TiO₂ as the catalyst.

Fig. 3a shows the results of a series of experiments carried out to determine the optimal reaction temperature. As is evident from Fig. 3a, conversion of cyclohexyl amine under the reaction conditions proceeds more and more readily with increasing temperature up to a certain point, when it suddenly decreases dramatically. Presumably, this is due to evaporation of water from the reactor as the experiments were carried out in an open flask suggesting that water has a profound importance for the reaction. Fig. 3b shows the results of a series of experiments carried out to study the profound effect of water in the reaction. It is seen from Fig. 3b that the reaction benefits from a catalytic amount of water, and that increasing the water content of the reaction mixture has a slightly detrimental effect on the overall conversion of the cyclohexyl amine substrate. The selectivity towards the oxime in all the experiments shown in Fig. 3 is around 70%.

We tried to use less catalyst for the experiments and it turned out that when using 0.1 g of TiO₂ instead of 2 g, the addition of water is not necessary. This is illustrated in Fig. 4, where it is shown that when no water is added the reaction is much faster when using 0.1 g TiO₂ compared to 2 g. We suspect that the excess TiO₂ works as a drying agent and thereby retards the reaction.

Fig. 5 shows the result of an experiment where samples were taken out after different reaction times.²⁴ As is evident from Fig. 5, the reaction can be pushed to completion with an overall yield of cyclohexanone oxime of *ca.* 60% after *ca.* 10 days. Experiments conducted in constant darkness and using Au–TiO₂ as the catalyst gave similar results, indicating that the reaction is not photochemical and is indeed catalyzed by TiO₂.

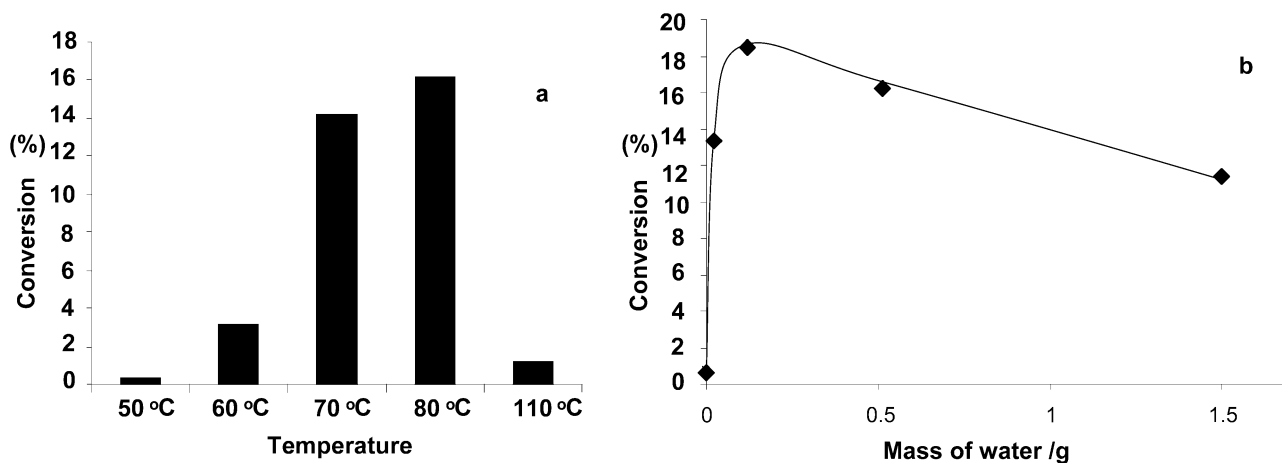


Fig. 3 Results of experiments with oxidation of cyclohexyl amine; (a) temperature series experiments, (b) experiments with different water contents.

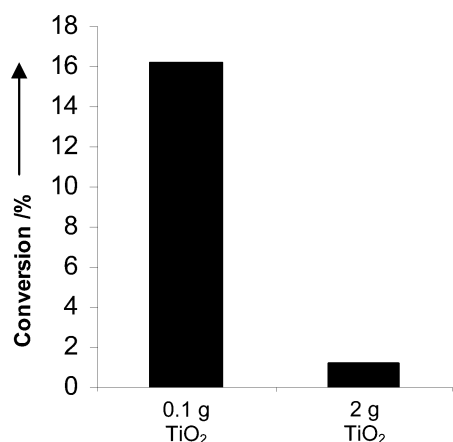


Fig. 4 Results of experiments with oxidation of cyclohexyl amine in the presence of water and with different amounts of TiO₂ catalyst.

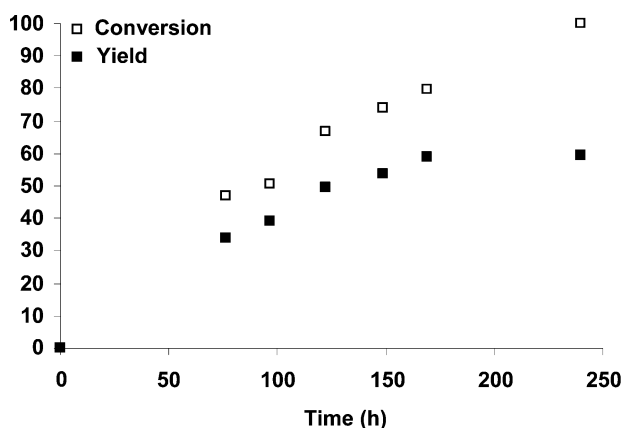


Fig. 5 Results of experiments with oxidation of cyclohexyl amine; time series experiments.

Conclusions

In conclusion, we have reported on our investigations into the oxidation of amines with molecular oxygen using Au–TiO₂ and TiO₂ as catalysts. It was found that Au–TiO₂ is capable of

catalyzing the oxidation of amines into amides. The reaction was demonstrated for *n*-hexyl amine and 1,6-hexanediamine. Using the procedure reported here, both substrates could be oxidized into amides, *N*-hexyl hexanoic amide and caprolactam, respectively. Furthermore, the procedure could be applied to carry out the oxidation of cyclohexyl amine into cyclohexanone oxime with molecular oxygen using TiO₂ as the catalyst under very mild reaction conditions. These new oxidation procedures could eventually find application as new green routes to nylon-6 precursors.

Acknowledgements

The Center for Sustainable and Green Chemistry is sponsored by the Danish National Research Foundation.

Notes and references

- G.-J. ten Brink, I. W. C. E. Arends and R. A. Sheldon, *Science*, 2000, **287**, 1636.
- K. Mori, T. Hara, T. Mizugaki, K. Ebitani and K. Kaneda, *J. Am. Chem. Soc.*, 2004, **126**, 10657.
- D. I. Enache, J. I. Edwards, P. Landon, B. Solsona-Espriu, A. F. Carley, A. A. Herzing, M. Watanabe, C. J. Kiely, D. W. Knight and G. J. Hutchings, *Science*, 2006, **311**, 362.
- A. Abad, P. Concepción, A. Corma and H. Garcia, *Angew. Chem., Int. Ed.*, 2005, **44**, 4066.
- C. H. Christensen, B. Jørgensen, J. Rass-Hansen, K. Egeblad, R. Madsen, S. K. Klitgaard, M. R. Hansen, H. C. Andersen and A. Riisager, *Angew. Chem., Int. Ed.*, 2005, **44**, 4648.
- K. Ebitani, K. Motokura, T. Mizugaki and K. Kaneda, *Angew. Chem., Int. Ed.*, 2005, **44**, 3423.
- A. S. K. Hashmi and G. J. Hutchings, *Angew. Chem., Int. Ed.*, 2006, **45**, 7896.
- T. Hayashi, T. Inagaki, N. Itayama and H. Baba, *Catal. Today*, 2006, **117**, 210.
- I. S. Nielsen, E. Taarning, K. Egeblad, R. Madsen and C. H. Christensen, *Catal. Lett.*, 2007, **116**, 35; E. Taarning, I. S. Nielsen, K. Egeblad, R. Madsen and C. H. Christensen, *ChemSusChem*, DOI: 10.1002/cssc.200700033.
- C. Marsden, E. Taarning, D. Hansen, L. Johansen, S. K. Klitgaard, K. Egeblad and C. H. Christensen, *Green Chem.*, 2008, **10**, 168, DOI: 10.1039/b712171g.
- T. Hayashi, K. Tanaka and M. Haruta, *J. Catal.*, 1998, **178**, 566.
- M. Haruta, *Appl. Catal., A*, 2001, **222**, 427.

- 13 P. Lignier, F. Morfin, L. Piccolo, J.-L. Rousset and V. Caps, *Catal. Today*, 2007, **122**, 284; P. Lignier, F. Morfin, S. Mangematin, L. Massin, J.-L. Rousset and V. Caps, *Chem. Commun.*, 2007, 186.
- 14 M. D. Hughes, Y.-J. Xu, P. Jenkins, P. McMorn, P. Landon, D. I. Enache, A. F. Carley, G. A. Attard, G. J. Hutchings, F. King, E. H. Stitt, P. Johnston, K. Griffin and C. J. Kiely, *Nature*, 2005, **437**, 1132.
- 15 H. Ichihashi, M. Ishida, A. Shiga, M. Kitamura, T. Suzuki, K. Suenobu and K. Sugita, *Catal. Surv. Asia*, 2004, **7**, 261.
- 16 J. M. Thomas and R. Raja, *Proc. Natl. Acad. Sci. U. S. A.*, 2005, **102**, 13732.
- 17 A. Corma and P. Serna, *Science*, 2006, **313**, 332.
- 18 M. Haruta, *Catal. Today*, 1997, **36**, 153.
- 19 C. Gunanathan, Y. Ben-David and D. Milstein, *Science*, 2007, **317**, 790.
- 20 J. S. Reddy and A. Sayari, *Appl. Catal., A*, 1995, **128**, 231.
- 21 R. Joseph, T. Ravindranathan and A. Sudalai, *Tetrahedron Lett.*, 1995, **36**, 1903.
- 22 S. Suresh, R. Joseph, B. Jayachandran, A. V. Pol, M. P. Vinod, A. Sudalai, H. R. Sonawane and T. Ravindranathan, *Tetrahedron Lett.*, 1995, **51**, 11305.
- 23 C. Venturello and R. D'Aloisio, *US Pat.*, 5 026 911, 1991.
- 24 A. Kaszonyi, Z. Cvengrosova and M. Hronec, *J. Mol. Catal. A: Chem.*, 2000, **160**, 393.

BINAP-Ru and -Rh catalysts covalently immobilised on silica and their repeated application in asymmetric hydrogenation†

Aidan R. McDonald,^a Christian Müller,^b Dieter Vogt,^b Gerard P. M. van Klink^a and Gerard van Koten^{*a}

Received 14th September 2007, Accepted 1st February 2008

First published as an Advance Article on the web 12th March 2008

DOI: 10.1039/b714189k

We present the facile immobilisation of a chiral diphosphine ligand, BINAP, on a silica (high pore volume, low surface area). The protected ligand has been immobilised as a phosphine oxide and deprotected on the surface to prevent side reactions of unprotected phosphines with surface silanol groups. The resulting diphosphine ligand on silica was converted to both rhodium and ruthenium complexes. The novel materials were characterised using solid-state IR-DRIFT and ²⁹Si and ³¹P CP-MAS NMR techniques as well as elemental content measurements. Ruthenium and rhodium catalysed asymmetric hydrogenation of various enamides, β-keto-esters and aromatic ketones is presented using immobilised BINAP ligands. The repeated use of the immobilised catalyst in five recycles demonstrates ‘homogeneous’ catalysis with ‘heterogeneous’ catalysts, thus reducing solvent waste, and loss of precious metal and or ligand.

Introduction

Recent years have seen a tremendous expansion in the development of immobilised homogeneous catalysts. Initial attempts at the immobilisation of asymmetric hydrogenation catalysts were aimed at improving enantioselectivity by altering reaction rates and decreasing metal-metal interactions.¹ Present work is directed towards the modern trend of cutting down on solvent use and catalyst costs. Separation of homogeneous catalysts from reaction mixtures is now key to industrial processes due to high costs of ligands and metals, and metal toxicities. From this perspective, the goal is to mimic the ease of separation of heterogeneous catalysts while keeping the high selectivity and predictability of homogeneous catalysts.

Asymmetric hydrogenation is the most widely used industrial homogeneously catalysed asymmetric reaction.² The production of a wide range of pharmaceutical and fine chemical products on a large scale relies on the asymmetric hydrogenation of precursors such as enamides, itaconates, arylketones, propenoic acids, and β-ketoesters. These hydrogenations are mediated through platinum group metal catalysed reaction with a chiral ligand bound to the metal. This chiral ligand can be diphosphine, diamine or ephedrine-type molecules which are mostly coordinated in a bidentate manner to the metal centre. Of the diphosphine ligands, the BINAP (2,2′-bis(diphenylphosphino)-1,1′-binaphthyl) ligand developed by the Noyori group has proven to give some of the highest activities and selectivities.³

As stated earlier initial attempts (1970’s) at immobilising homogeneous hydrogenation catalysts was directed towards influencing reaction kinetics so as to positively effect enantiomeric excess yields. Recent trends have seen immobilisation as a tool for ease of separation of catalyst from substrate and or product.⁴ This is mediated mostly through phase differences, with organic⁵ and inorganic polymeric⁶ supports used widely as solid state supports. We and others have shown that phase differences are not necessary to separate catalysts with dendritic systems being separated from reaction mixtures using nanofiltration membranes, or even by altering the polarity of a reaction mixture.⁷

The BINAP ligand has been immobilised in various forms using all of these techniques. Water soluble BINAP derivatives have been used in liquid biphasic systems,⁸ and ionic liquids,⁹ BINAP has been incorporated at the core of several dendritic systems,¹⁰ and both as a polymeric backbone,¹¹ as well as a functionality on a polystyrene support¹² and entrapment within polymers.¹³ Non-covalent interactions have been used to immobilise BINAP on various inorganic supports; clays,¹⁴ silica,¹⁵ and zirconium phosphonate hybrids.¹⁶ At the commencement of this work BINAP had not yet been immobilised covalently on an inorganic support, however that was achieved recently by Lin *et al.* where a mono-functionalised BINAP was covalently tethered to silica via an ethereal linker amongst others.¹⁷ Covalent immobilisation generally leads to the best results in terms of catalyst recycling.

We present here the synthesis and thorough characterisation of immobilised BINAP-Ru and -Rh complexes on silica. The protected BINAP ligand (as phosphine oxide) has been immobilised in a covalent bidentate manner to the support and subsequently converted to the diphosphine ligand. The immobilised diphosphine ligand has been applied in the rhodium and ruthenium catalysed asymmetric hydrogenation of a number of substrates showing enantioselectivity levels comparable to the parent homogeneous catalysts. The immobilised catalysts have been recycled, showing little loss in enantioselectivity over five cycles.

^aOrganic Chemistry and Catalysis, Faculty of Science, Utrecht University, Padualaan 8, 3584, CH Utrecht, The Netherlands. E-mail: g.vankoten@uu.nl; Fax: +31-30-252-3615; Tel: +31-30-253-1996

^bSchuit Institute for Inorganic Chemistry and Catalysis, Helix, STW 3.29, P.O. Box 513, 5600, MB Eindhoven, The Netherlands

† This paper was published as part of the themed issue of contributions from the 3rd International Conference on Green and Sustainable Chemistry.

Results and discussion

Synthesis

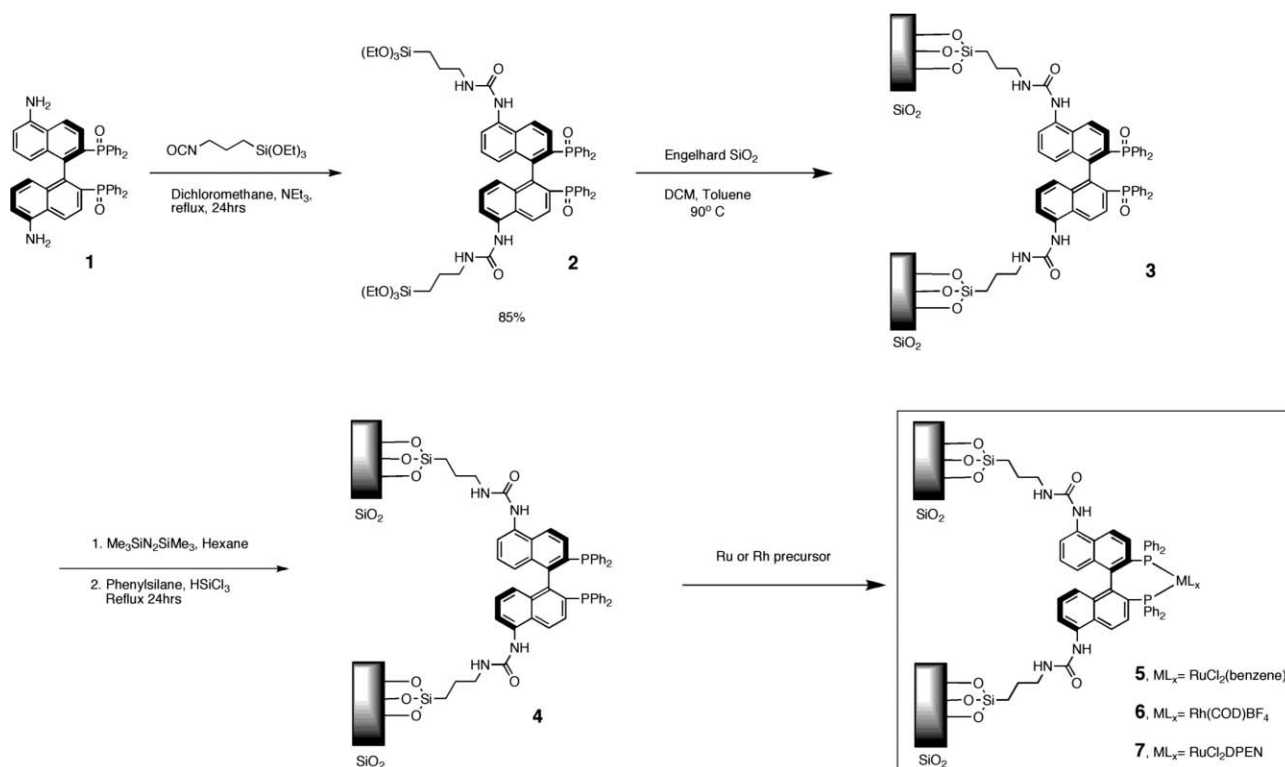
There are a number of methods for the synthesis of functionalised BINAP ligands. We have chosen one of the more straightforward methods, which is through a facile nitration of BINAP-dioxide that yields 5,5'-dinitro-BINAP-dioxide which is reduced easily to 5,5'-diamino-BINAP-dioxide.^{10b-e} This compound has been reported to be quite unreactive unless in the presence of a highly activated species, *i.e.* an acid chloride or acid anhydride. However, we have coupled it with 3-(triethoxysilyl)propyl-1-isocyanate, using a large excess of triethylamine in refluxing dichloromethane (DCM) (see scheme 1). Complete conversion to the di-ureyl compound was observed. The formed compound **2** was then reacted with silica yielding silica bound BINAP dioxide **3**. The silica used is a relatively high density material with surface area of 200m²/g and an average pore volume of 1 cm³.¹⁸ This silica was used to ensure active site accessibility and minimal mass transport effects which would be expected with highly porous silica. Because this silica is chosen we presume all phosphine groups bound to silica are available to partake in a catalytic reaction. The remaining silanol groups on **3** were capped using hexamethyldisilazane. The immobilised protected diphosphine-dioxide was reduced using trichlorosilane in phenylsilane to yield unprotected, immobilised BINAP ligand **4**. The reasons for immobilisation of the phosphine dioxide are two-fold; firstly it is easier to carry out chemistry on the dioxide, without having to worry about oxidation of the phosphine which will inevitably occur in small quantities; secondly, it has been observed that upon immobilisation of

phosphine ligands, using triethoxysilane-type linkers, an ethoxy-phosphonium cation forms quite readily when using silica surfaces.¹⁹ Complexation was mediated through various metal precursors ([RuCl₂(benzene)]₂²⁰ or [Rh(COD)₂BF₄]) yielding tethered BINAP-Ru and -Rh complexes. The introduction of other heteroligands was also possible (e.g. DPEN). Complexation resulted in stark colour changes of the silica. Material **4** is colourless, however the silica-bound ruthenium and rhodium complexes gave an orange colour in the presence of solvent. Drying of the materials showed less strong colour differences, but there was still a clear indication that the complex has been synthesised on the support. These synthetic procedures have been applied with both (*R*)- and (*S*)- enantiomers of diamino-BINAP-dioxide starting materials.

The functionalised systems **2–7** were characterised with both solution and CP-MAS solid state ¹H, ¹³C, ²⁹Si and ³¹P NMR spectroscopy, IR-DRIFT and IR-ATR spectroscopy and elemental content analysis.

Elemental analysis

Elemental content measurements gave us more insight into the effects of chemical modification on the support, and more importantly on the supported ligand or complex (Table 1). The phosphorous content of the support ligand and complexes is constant in materials **3–7** at around 0.20% of the total mass. Likewise the nitrogen loading is constant for materials **3–6**, demonstrating the stability of the ureyl linkages between the ligand and the support. In material **7** a marked increase in nitrogen content was observed as a result of the introduction



Scheme 1 Synthesis of immobilised BINAP-ruthenium and -rhodium complexes.

Table 1 Elemental content analysis^a

| Material | 3 | 4 | 5 | 6 | 7 |
|---------------------------|------|------|----------|----------|----------|
| P | 0.20 | 0.22 | 0.21 | 0.22 | 0.15 |
| C | 2.49 | 4.87 | 5.10 | 4.90 | 5.15 |
| N | 0.14 | 0.15 | 0.12 | 0.15 | 0.28 |
| M ^b | — | — | 0.20(Ru) | 0.42(Rh) | 0.17(Ru) |
| Atomic Ratio ^c | | | P/Ru | P/Rh | P/Ru |
| | | | 2:1 | 2:1 | 2:1 |

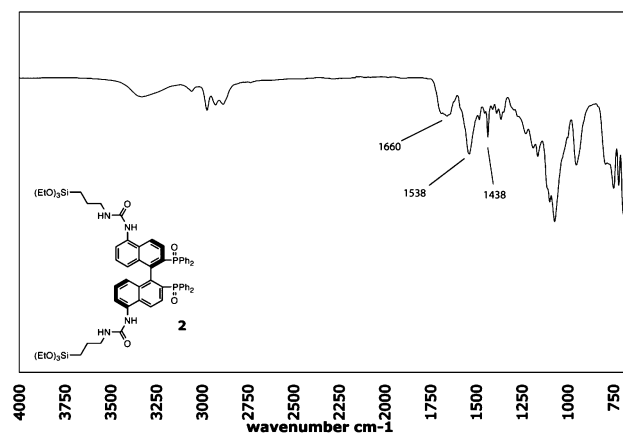
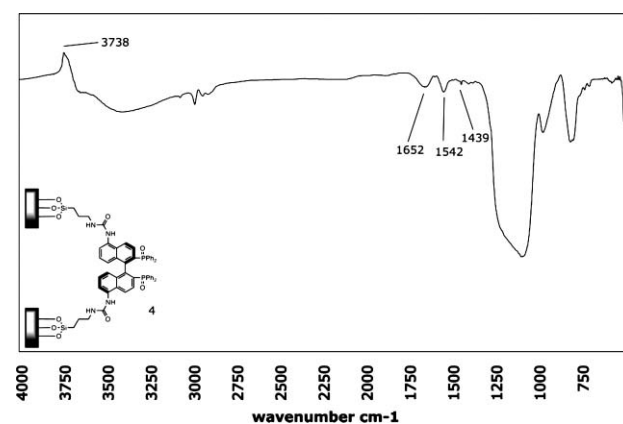
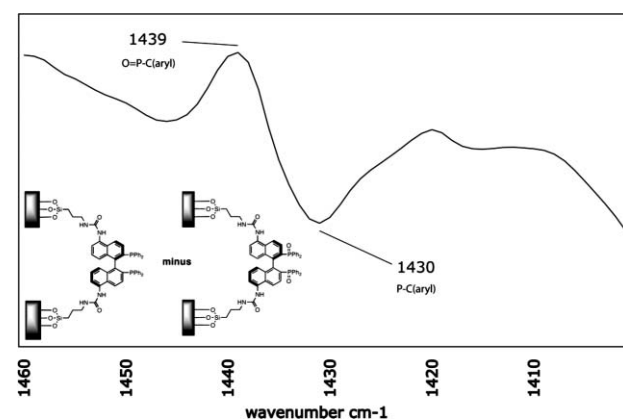
^a All values given correspond to percentage elemental content loading.
^b It must be noted the accuracy of the metal loading is greatly reduced at such low metal concentrations. ^c Approximate value.

of the DPEN co-ligand. The percentage phosphorous loading compared favourably with the carbon content in material **3** (P:C = 1:12.5), with a ratio that was comparable to that calculated for the unbound compound **2** (1:10). Similarly comparison of the phosphorous/nitrogen content in material **3** (P:N = 1:0.7) compared favourably with that of compound **2** (1:0.9). These results show that no extra carbon or nitrogen containing moieties are present in material **3**. No significant change in the P and N loadings was observed during any of the synthetic procedures carried out on the immobilised ligands, suggesting the ligand remains bound and chemically unaltered throughout. Complexation reactions yielded materials with the expected ratios of metal to phosphorous loadings. In general these results showed us that little other than the expected reactions are occurring on the functionalised silica surface. The observation that phosphorous/metal elemental content was the expected value showed us that there is only one site at which the metal is situated on the surface; between the chelating arms of the diphosphine ligand.

Infra-red analysis

The ATR-IR spectrum of **2** is shown in Fig. 1.²¹ The ureyl stretches can be observed at ~1660 and 1538 cm⁻¹ respectively. The sharp peak at 1438 cm⁻¹ is a P–C(aryl) stretch of the BINAP ligand. Using the DRIFT technique we can monitor the difference between the standard silica stretches before and after immobilisation.²² This method demonstrates that the silanol groups disappear as a result of covalent attachment of the silylpropyl- linker (of **2**) to the support. The spectrum of the starting silica is subtracted from the spectrum of **3** giving an indication of what has been ‘added’ to the silica (Fig. 2). A trough in the difference spectrum is observed at 3738 cm⁻¹ which corresponds to a clear decrease in the intensity of silanol stretches. Subsequent capping of the silanol groups with trimethylsilyl groups shows a further decrease in the number of silanol stretches and no apparent effect on the immobilised ligand (Table 2).

The conversion of tethered BINAP dioxide (**3**) to tethered BINAP (**4**) is observed with ease using DRIFT-IR. Fig. 3 is the difference spectrum between **4** and **3**. Focussing on the P–

**Fig. 1** ATR-IR of **2**.**Fig. 2** DRIFT-difference spectrum of **3** minus SiO₂.**Fig. 3** Difference spectrum of the DRIFT-spectra of **4** minus **3**.

C_(aryl) vibration, there is a clear trough where the O=P–C_(aryl) was, 1439 cm⁻¹, and a peak at 1430 cm⁻¹ (P–C_(aryl)). Obviously this is a difference spectrum, however the standard DRIFT spectrum of

Table 2 Standard IR-stretching frequencies

| Group | Si–OH | O=P–C _(aryl) | P–C _(aryl) | M–P–C _(aryl) | Ureyl |
|--|-------|-------------------------|-----------------------|-------------------------|-----------|
| Stretching frequency (cm ⁻¹) | 3740 | 1438 | 1430 | 1434 | 1660,1540 |

material **4** shows no signs of any phosphine oxide compounds. The final step in the synthesis was to incorporate metal centres in the diphosphine ligand. Monitoring the P–C_(aryl) stretch gives similar results, with the immobilised complexes showing a M–P–C_(aryl) vibration of $\sim 1435\text{ cm}^{-1}$. Fig. 4 depicts the difference spectrum of **5**/SiO₂ which shows clearly the P–C_(aryl) stretch of coordinated BINAP-Ru and also stretches corresponding to ureyl groups and a trough at $\sim 3740\text{ cm}^{-1}$ representing a decrease in the number of silanol stretches.

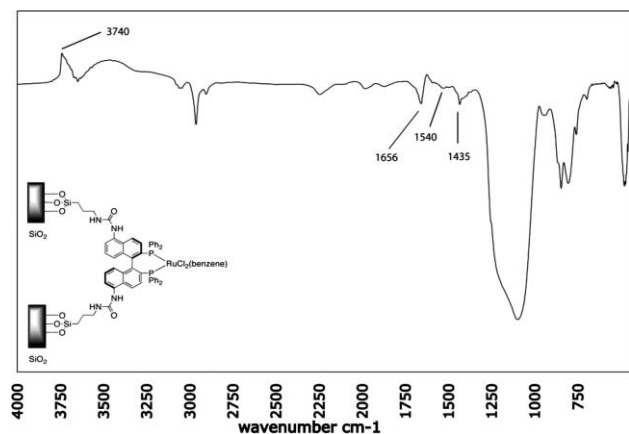


Fig. 4 DRIFT difference spectrum of **5** minus SiO₂.

NMR analysis

CP-MAS ²⁹Si NMR of the immobilised ligand (**4**) shows us several peaks that indicate different forms of silicon species (Fig. 5). Peaks at -102 (*Q*₃) and -111 ppm (*Q*₄) are characteristic

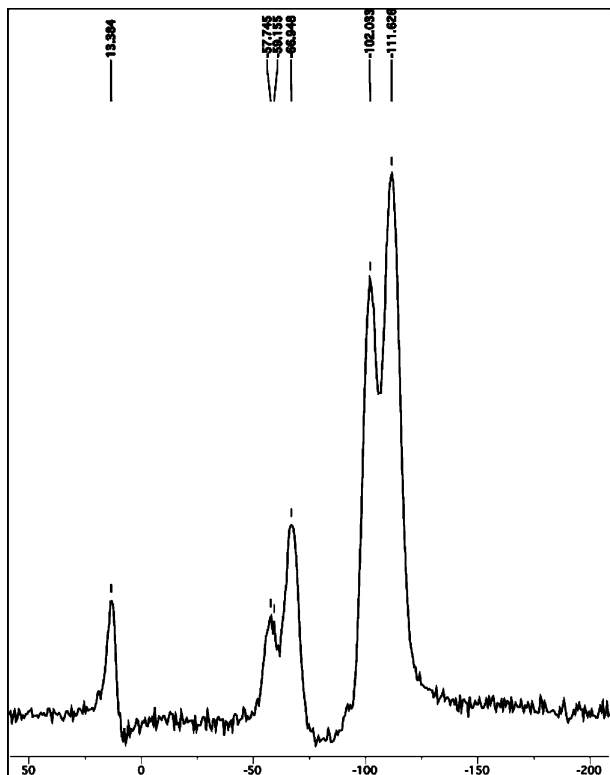


Fig. 5 ²⁹Si CP-MAS NMR spectrum of **4**.

of *Q*-type (*Si*–(*O*–)₄) silicates, which are in the bulk material. Both *Q*₃ (*Si*–(*O*–*Si*)₃(*OH*)) and *Q*₄-type (*Si*–(*O*–*Si*)₄) silicates are observed in relatively equal intensities suggesting that silanol groups are present in the bulk material. However, we believe that these silanol groups are not influential on the catalytic reaction because they are not observed in DRIFT-IR which is an analysis of the surface, where the catalyst lies. Peaks at -57 (*T*₂) and -66 ppm (*T*₃) are typical of *T*-type (*R*₁–*Si*–(*O*–)₃) silicates, that is, the silicon bound to the propyl group of **2** at the surface of the support. This is the clearest indication that the ligand is covalently bound to the support. The peak at -57 ppm is as a result of remnant ethoxide groups of **2** (*T*₂ = *R*–*Si*–(*OSi*)₂(*OEt*)) that have not reacted with surface silanol groups. While the peak at -66 ppm is *T*₃-type silicon species (*T*₃ = *R*–*Si*(*OSi*)₃). Similarly, at the surface, the single peak at 13 ppm is typical of *M*-type (*R*₃–*Si*–(*O*–)) silicates (where *R* is the methyl group of the trimethylsilyl capped silanol groups). Comparison of the ²⁹Si NMR spectra of materials **3**–**7** shows there is no difference in the silicon species of the material through the various synthetic steps that are carried out. The deprotection of phosphine oxide yielding BINAP and subsequent complexation of BINAP has no effect on the type of silicon species on the silica surface.

³¹P CP-MAS indicates that BINAP has indeed been immobilised on silica. Fig. 6 shows the NMR spectrum of immobilised ligand **5**. The peak at -15 ppm represents the reduced, unprotected phosphine. There is no sign of any phosphine oxide in the spectrum (~ 30 ppm). There is a small phosphonium-type species present on the silica surface. This is formed as a result of remnant ethoxide groups of the immobilised silane reacting with the newly formed phosphine yielding a phosphonium ion. This is

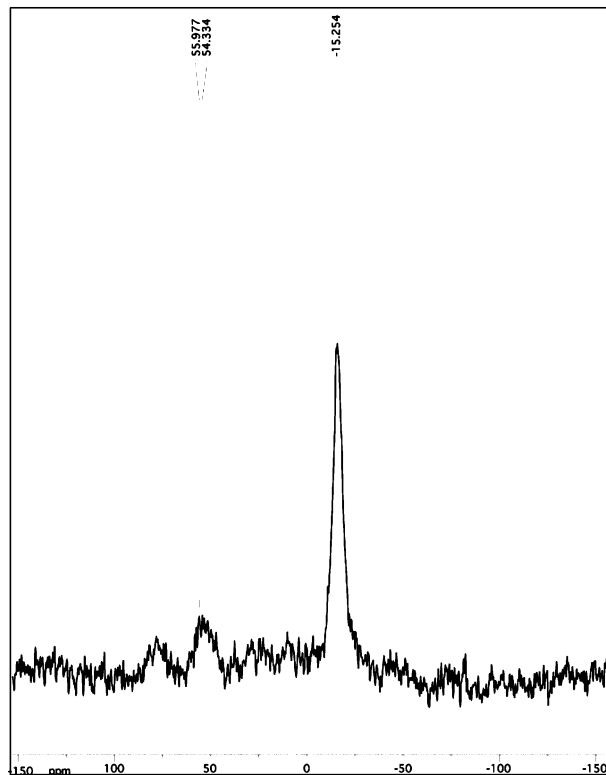


Fig. 6 ³¹P CP-MAS NMR spectrum of **4**.

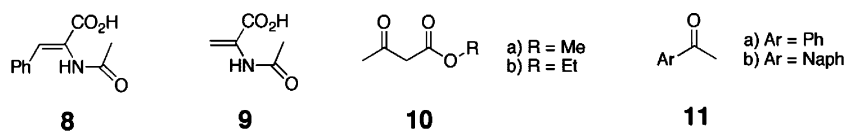


Fig. 7 Prochiral substrates for asymmetric hydrogenation.

a common occurrence when immobilising phosphines on silica, however, we believe that as a result of immobilising BINAP-dioxide and then deprotection, the extent of phosphonium formation is greatly reduced. We have ensured this problem is not a hindrance, and most phosphine ligands are available for coordination.

Catalysis

The ruthenium and rhodium catalytic materials were tested in the asymmetric hydrogenation of several substrates (Fig. 7 and 8). The use of this particular silica ensures we are only addressing catalytic sites on the silica's peripheral surface. Thus the support material is expected to have little effect on activity and selectivity as a result of mass transport limitations. In all cases, with all catalysts, complete conversion of substrate was observed. Our reaction vessels do not allow for sampling during reaction, so no accurate kinetic measurements were possible. In a separate reaction carried out elsewhere a hydrogen uptake plot showed that the heterogenised catalyst **5** shows first order reaction kinetics, as does the homogeneous catalyst, in the asymmetric hydrogenation of **10a**. The decreased reaction rate is to be expected, when using heterogenised catalysts, because you are

applying catalysts which are not in the substrate phase. We realise that accurate kinetic measurements are desirable to compare the heterogenised catalysts with their homogeneous analogues, and are busy exploring this. The *R*-isomer of immobilised BINAP has been used throughout this catalytic study.

Table 3 shows the application of catalyst **5** in the asymmetric hydrogenation of various β -ketoesters²³ and enamides²⁴ in the manner of published homogeneous systems. The heterogenised catalyst shows the same, high, enantioselectivity levels of the homogeneous catalyst. High enantiomeric excess (99% ee) was observed in the asymmetric hydrogenation of **10a** and **10b**. In the reduction of enamides the immobilised ruthenium complexes gave ee values in the 80%'s.

Rhodium catalyst **6** was also applied in the asymmetric reduction of enamides.²⁵ It also gave results which were comparable to the homogeneous system in terms of selectivity. This system was, however, not as stable as the ruthenium materials, and catalyst decomposition was observed.

Immobilised BINAP-Ru-diamine material **7** was applied in the asymmetric transfer hydrogenation of aromatic ketones acetophenone and naphthophenone.²⁶ Quantitative conversion of ketone to secondary alcohol was observed in both cases. In the case of acetophenone 25% ee was observed. Naphthophenone

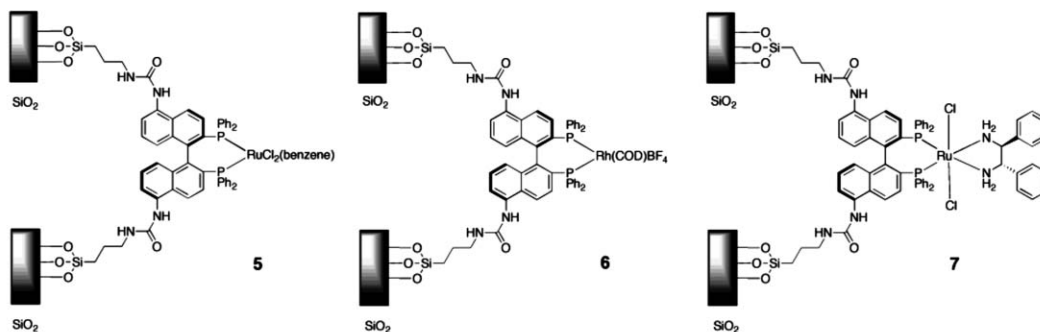


Fig. 8 Immobilised BINAP-Ru and -Rh catalysts for asymmetric hydrogenation.

Table 3 Catalytic results from immobilised BINAP-Ru/Rh asymmetric hydrogenation reactions

| Catalyst ^a | Substrate | H ₂ Pressure (bar) | Temperature (°C) | Conversion (%) ^b | ee (%) ^c |
|-----------------------|------------|-------------------------------|------------------|-----------------------------|------------------------|
| 5 | 8 | 2 | 35 | 100 | 85 (86) ^c |
| | 9 | 2 | 35 | 100 | 72 (76) ^c |
| | 10a | 40 | 50 | 100 | >99 (>99) ^c |
| | 10b | 40 | 50 | 100 | >99 (>99) ^c |
| 6 | 8 | 4 | RT | 100 | 85 (84) ^c |
| | 9 | 40 | 50 | 100 | 60 (67) ^c |
| 7 | 11a | 10 | 30 | 100 | 25 (–) ^{d, f} |
| | 11b | 10 | 30 | 100 | 95 (97) ^d |

^a See refs 23–26 for procedures on catalysis, all catalysis was carried out in a parallel autoclave system AMTEC SPR16 or a Parr 4590 micro reactor.

^b As determined by ¹H NMR and GC. ^c Measured by GC. ^d Measured by HPLC. ^e Values found with homogeneous catalyst in brackets. ^f No literature value found for this substrate.

was also converted to the corresponding secondary alcohol showing the high stereoselectivity values that are expected of these systems.

Recycling

The catalytic materials were easily separated from the substrate/product solution by either; 1) simple filtration over a glass frit and subsequent washing or; 2) removal of all liquids from the autoclave using applied pressure. The latter was found to be the easier. The autoclave could then be easily recharged with fresh substrate and the reaction could be restarted. This was demonstrated using catalyst **5** for the asymmetric hydrogenation of **10a**. The recycling process could be repeated five times with no significant loss in selectivity, and minimal losses in activity. Furthermore, the post catalysis filtrate, which was colourless, was placed in a catalyst free autoclave and fresh substrate was added. Dihydrogen pressure was applied, however no further conversion was observed. This demonstrates that no metal leaching from the silica surface is occurring. The ruthenium content (loading) of the recycled catalytic material was the same as the starting catalytic material suggesting little, if any, ruthenium leaching (Ru = 0.18%, P = 0.22%). Furthermore, the post-catalysis phosphorous content was also the same as the pre-catalysis material, demonstrating no leaching of the BINAP ligand, or any derivatives thereof from the surface (Table 4).

Table 4 Heterogenised catalyst recycling^a

| Catalyst | Cycle | 1 | 2 | 3 | 4 | 5 |
|----------|------------------------|-----|-----|-----|-----|-----|
| 5 | Yield (%) ^b | 100 | 100 | 100 | 100 | 100 |
| | ee (%) ^c | >99 | >99 | >99 | >99 | >99 |
| 6 | Yield (%) ^b | 56 | | | | |
| | ee (%) ^c | — | | | | |

^a Catalysts recycled by simple decantation of the reaction solution containing the hydrogenated product material. ^b As determined by ¹H NMR and GC. ^c Measured by GC.

As mentioned previously the rhodium systems showed catalyst decomposition. The rhodium catalytic material was recycled once post hydrogenation of enamide **8**, and showed diminished activity, but moreover, almost no enantioselectivity in the same reaction. We have not got an explanation for this, however, it does show that catalyst stability is essential when immobilising homogeneous catalysts. With rhodium complexes known sensitivity to oxygen, it is likely that some oxygen contamination has occurred resulting in complex decomposition. Furthermore, the process of recycling and subsequent washing could have adverse effects on the complex stability, that is oxidation or mechanical influences.

Conclusions

In conclusion we have synthesised and immobilised a functionalised BINAP-type ligand with a retention in chirality and in reasonably high yields. We have shown that we can carry out chemistry on the immobilised ligand without having detrimental effects on the support or the functionalised ligand. Several analytical techniques have been used to analyse these

immobilised compounds proving conclusively that we have indeed succeeded in covalently immobilising BINAP-Ru and -Rh complexes on an inorganic support. Catalytic results have shown to be conclusive in the fact that activity is down in comparison with the homogeneous system, however conversion and enantioselectivity levels are as good as if not improved upon, in comparison with the homogeneous catalyst. The catalyst is truly immobilised with the post catalysis solution showing no activity. Furthermore, the catalyst was recycled showing repeated high selectivity levels over at least five cycles.

Experimental

General information

Standard Schlenk procedures under dinitrogen were utilised throughout. Catalytic experiment preparations were carried out under argon. Reagents were used as supplied from Acros or Sigma-Aldrich. Diamino-BINAP-dioxide was prepared according to a literature procedure.²⁷ Racemic versions of catalytic products were either purchased or prepared using literature procedures.²⁸ Hydrogenation catalysis was carried out in a 50 ml Parr-4590 micro-reactor or simultaneously in the parallel autoclave system AMTEC SPR16,²⁹ equipped with pressure sensors and a mass-flow controller and suitable for monitoring and recording gas uptakes throughout the reactions. ¹H, ¹³C, and ³¹P solution NMR was carried out on a Varian Inova 300 spectrometer or a Varian Oxford AS400. CP-MAS NMR was carried out using a Bruker AV 750. Elemental analyses were performed by Dornis und Kolbe, Mikroanalytisches Laboratorium, Mülheim a. d. Ruhr, Germany. MS measurements were carried out on an Applied Biosystems Voyager DE-STR MALDI-TOF MS. Infra-Red measurements were carried out on a Perkin-Elmer SpectrumOne FT-IR Spectrometer. GC analyses were performed on a Perkin-Elmer AutosystemXL Gas Chromatograph. HPLC analyses were carried out on a Philips PU1400 liquid chromatograph with an attached PU4120 diode array detector.

5,5'-bis(3-triethoxysilylpropyl-1-ureyl)-2,2'-bis(diphenylphosphinooxide)-1,1'-binaphthyl, **2**

5,5'-bis(amino)-2,2'-bis(diphenylphosphinooxide)-1,1'-binaphthyl (0.5261 g, 0.77 mmol) was dissolved in dry CH₂Cl₂ (15 ml). A solution of NEt₃ (15 ml) containing 3-triethoxysilylpropyl-1-isocyanate (0.76 g, 3.08 mmol) was added to this, and the resulting solution was heated at reflux for 48 h. The resulting brown solution was cooled to room temperature, all solvent was removed, and the title compound was attained by recrystallisation from CH₂Cl₂/hexanes as a light brown powder. Not pristinely pure, some triethylammonium species, which we could not remove. Was used immediately in next step. Yield 60%. IR (ATR); $\nu_{\text{carbamate}}$ 1660 and 1538 cm⁻¹, $\nu_{\text{P-C(aryl)}}$ 1438 cm⁻¹. ³¹P-NMR (162 MHz, CDCl₃) 29.9. *m/z* (MALDI-ToF) 1180.38 g/mol (+H).

SiO₂-5,5'-bis(3-silylpropyl-1-ureyl)-2,2'-bis-(diphenylphosphino)-1,1'-binaphthyl, 3

5,5'-bis(triethoxy-3-silylpropyl-1-ureyl)-2,2'-bis(diphenylphosphino)-1,1'-binaphthyl (0.2149 g, 0.18 mmol) was dissolved in dry toluene (10 ml). This solution was added to 1 g of silica (BASF/Engelhard, 80 m²/g), and the resulting mixture was heated at reflux for 24 h. Hot filtration and subsequent washing with CH₂Cl₂, acetone, and finally boiling EtOH yielded a light brown powder. IR (DRIFT, difference); $\nu_{\text{SiO-H}}$ 3738 cm⁻¹ (trough), $\nu_{\text{carbamate}}$ 1652 and 1542 cm⁻¹, $\nu_{\text{P-C(aryl)}}$ 1439 cm⁻¹. ³¹P-NMR (303.6 Mhz) 30 ppm. Elem. anal. found: C 2.49, H 0.82, N 0.14, P 0.20.

Capped SiO₂-5,5'-bis(3-silylpropyl-1-ureyl)-2,2'-bis-(diphenylphosphino)-1,1'-binaphthyl, 4

Hexane (30 ml) was added to **3** with hexamethyldisilazane (1 ml, large excess) and the resulting mixture was heated at reflux for 24 h. Hot filtration and subsequent washing with CH₂Cl₂, acetone, and finally boiling EtOH yielded a light yellow powder. The resulting material was placed in phenylsilane (10 mL) and the resulting mixture was heated to reflux for 1 h. HSiCl₃ (1 ml) was added after a further 1, 3, and 16 h respectively, with continuous refluxing for a further 8 h. Hot filtration and subsequent washing with CH₂Cl₂, acetone, and finally boiling EtOH yielded an off-white powder. IR (DRIFT, difference); $\nu_{\text{SiO-H}}$ 3738 cm⁻¹ (trough), $\nu_{\text{carbamate}}$ 1652 and 1542 cm⁻¹, $\nu_{\text{P-C(aryl)}}$ 1430 cm⁻¹. ³¹P-NMR (303.6 Mhz) -15 ppm. Elem. anal. found: C 4.87, H 1.11, N 0.15, P 0.22.

Capped SiO₂-5,5'-bis(3-silylpropyl-1-ureyl)-2,2'-bis(diphenylphosphino)-1,1'-binaphthyl-ruthenium(II) dichloro(benzene), 5

Material **5** (0.26 g) was placed in freshly distilled, degassed EtOH/benzene (10 ml (9:1)). To this mixture was added [RuCl₂(benzene)]₂ (0.2 g, 0.8 mmol, excess) and the resulting mixture was stirred at 60 °C for 24 h. Hot filtration and several washings with benzene and CH₂Cl₂ yielded an orange powder. IR (DRIFT, difference); $\nu_{\text{SiO-H}}$ 3740 cm⁻¹ (trough), $\nu_{\text{carbamate}}$ 1656 and 1540 cm⁻¹, $\nu_{\text{P-C(aryl)}}$ 1435 cm⁻¹. Elem. anal. found: C 5.10, H 1.10, N 0.12, P 0.21, Ru 0.20.

Capped SiO₂-5,5'-bis(3-silylpropyl-1-ureyl)-2,2'-bis(diphenylphosphino)-1,1'-binaphthyl-rhodium(I) cyclooctadiene-tetrafluoroborate, 6

Material **5** (0.27 g) was placed in freshly distilled, degassed CH₂Cl₂ (10 ml). To this was added [Rh(COD)]₂(BF₄) (0.4 g, 0.7 mmol, excess). The resulting mixture was stirred at room temperature for 24 h. Filtration and several washings with CH₂Cl₂ yielded a yellow powder. IR (DRIFT, difference); $\nu_{\text{SiO-H}}$ 3740 cm⁻¹ (trough), $\nu_{\text{carbamate}}$ 1660 and 1548 cm⁻¹, $\nu_{\text{P-C(aryl)}}$ 1433 cm⁻¹. Elem. anal. found: C 4.90, H 1.18, N 0.15, P 0.22, Rh 0.42.

Capped SiO₂-5,5'-bis(3-silylpropyl-1-ureyl)-2,2'-bis(diphenylphosphino)-1,1'-binaphthyl-ruthenium(II) dichloro(diphenylethylenediamine), 7

Material **5** (0.2 g) was placed in freshly distilled, and degassed DMF (10 ml). To this was added [RuCl₂(benzene)]₂ (0.2 g, 0.8 mmol, excess) and the resulting was stirred at 100 °C for 1 h. This was subsequently cooled. To the resulting brown mixture DPEN (0.2 g, 0.9 mmol, excess) was added and the resulting mixture was stirred at room temperature for 24 h. Filtration followed by washing with DMF and CH₂Cl₂ yielded a yellow powder. IR (DRIFT, difference); $\nu_{\text{SiO-H}}$ 3740 cm⁻¹ (trough), $\nu_{\text{carbamate}}$ 1660 and 1548 cm⁻¹, $\nu_{\text{P-C(aryl)}}$ 1435 cm⁻¹. Elem. anal. found: C 5.15, H 0.88, N 0.28, P 0.15, Ru 0.17.

Asymmetric hydrogenation of prochiral substrates

General procedure for the catalysis experiments: Stainless steel autoclave was heated to 90 °C and flushed with argon (15 bar) four times. The reactor was subsequently cooled to room temperature and flushed with argon (4×). The atmosphere was further exchanged with hydrogen (gas exchange cycle 1) and the reactors were pressurised with hydrogen. After regulating the desired temperature and pressure they were kept constant throughout the experiment. The spin rate was 1000 rpm. The reactor was then cooled to room temperature and the autoclave contents were analysed by means of GC/NMR/HPLC analysis.

Asymmetric hydrogenation of (*Z*)- α -(acetamido)-cinnamic acid/- α -(acetamido) acrylic acid using catalyst **5**

Catalysis was carried out similar to a literature procedure.²⁴ Catalytic material **5** (0.1 g, 2×10^{-6} mol Ru) was placed in the autoclave. A 1:1 THF/EtOH mixture (30 mL) with enamide (1×10^{-4} mol, 50 equivalents) and NEt₃ (1.2×10^{-4} mol) was added to the autoclave and the reaction mixture was put under dihydrogen pressure (2 bar) for 48 h. 100% yield. Product was converted to its methyl ester for ease of separation (MeI, K₂CO₃). GC Lipodex E column (25 m \times 0.25 mm), Initial $T = 70$ °C, 10 min., then heating 2.5 °C per min. to 250 °C. For **10/11**.

Asymmetric hydrogenation of β -ketoesters using catalyst **5**

Catalysis was carried out similar to a literature procedure.²³ Catalytic material **5** (0.1 g, 2×10^{-6} mol Ru) was placed in the autoclave. β -keto-ester (2×10^{-3} mol, 1000 equivalents) was placed in MeOH (30 mL) and this solution was placed in the autoclave. The resulting mixture was put under hydrogen pressure (40 bar) for 48 h. 100% yield. Final products were reacted with acetic anhydride to produce an ester for enantiomer separation. GC Lipodex E column (25 m \times 0.25 mm).

Asymmetric hydrogenation of (*Z*)- α -(acetamido)-cinnamic acid/- α -(acetamido) acrylic acid using catalyst **6**

Catalysis was carried out similar to a literature procedure.²⁵ Enamide (4×10^{-6} mol, 150 equivalents) was dissolved in degassed ethanol (20 mL). This reaction solution was placed in the autoclave which contained catalytic material **6** (0.1 g, 4×10^{-6} mol Rh). Dihydrogen pressure (4 bar) was applied for 48 h. The reaction mixture was stirred at room temperature.

100% yield. Product was converted to its methyl ester for ease of separation (MeI, K₂CO₃). GC Lipodex E column (25 m × 0.25 mm), Initial *T* = 70 °C, 10 min., then heating 2.5 °C per min. to 250 °C. For **8/9**.

Asymmetric hydrogenation of acetophenone/naphthophenone using catalyst **7**

Catalysis was carried out similar to a literature procedure.²⁶ To 2-propanol (10 mL) was added 0.1 g of catalytic material **7** (2 × 10⁻⁶ mol Ru). Aromatic ketone (0.01 mol, 5000 equivalents) was placed in 2-propanol (20 mL) with KOH (1 mg, 2 × 10⁻⁵ mol). Both reaction mixtures were thoroughly degassed and subsequently mixed together in the autoclave. The autoclave was then heated to 28 °C and a dihydrogen pressure (10 bar) was applied for 48 h. 100% yield. HPLC; n-hexane/isopropanol 95/5. Chirasil OD. Room temperature for both phenyl and naphthyl products.

Catalyst recycling

After the time allotted to complete a certain catalytic reaction had passed, the autoclave was allowed to cool to room temperature, and the solid catalyst in the reaction solution was allowed to settle. An overpressure of argon was placed on the reaction mixture and an outlet tap was opened allowing for the removal of all liquid contents in the reaction vessel, leaving the solid catalyst behind. Extra reaction solvent was then added to the autoclave, and after stirring and allowing the mixture to settle once again, an overpressure of argon was applied. This was repeated twice. The reaction vessel, with the solid catalyst still present was then recharged with fresh solvent and substrates and could then be reapplied in catalysis.

Acknowledgements

We would like to thank Dr. Jim Brandts of BASF/Engelhard for provision of chemicals and advice. The Dutch Technology Foundation (STW, DPC-5772) are kindly acknowledged for financial support.

References

- (a) N. Takaisha, H. Imai, C. A. Bertelo and J. K. Stille, *J. Am. Chem. Soc.*, 1976, **98**, 5401–5402; (b) N. Takaishi, H. Imai, C. A. Bertelo and J. K. Stille, *J. Am. Chem. Soc.*, 1978, **100**, 264–265; (c) T. Masuda and J. K. Stille, *J. Am. Chem. Soc.*, 1978, **100**, 268–272; (d) S. J. Fritschel, J. J. H. Ackerman, T. Keyser, J. K. Stille and J. Org, *Chem.*, 1979, **44**(18), 3152; (e) W. Dumont, J.-C. Poulin, T.-P. Dang and H. B. Kagan, *J. Am. Chem. Soc.*, 1973, **95**, 8295.
- (a) H.-U. Blaser, *Chem. Commun.*, 2003, 293–296; (b) N. B. Johnson, I. C. Lennon, P. H. Moran and J. A. Ramsden, *Acc. Chem. Res.*, 2007, **40**, 1291–1299; (c) J.-P. Genet, *Pure and App. Chem.*, 2002, **74**, 77–83.
- R. Noyori and H. Takaya, *Acc. Chem. Res.*, 1990, **23**, 345–350.
- (a) D. E. De Vos, I. F. J. Vankelecom and P. A. Jacobs, *Chiral Catalyst Immobilisation and Recycling*, 2000, Wiley-VCH; (b) A. R. McDonald, R. Gossage and G. van Koten, to be submitted, review on Immobilised Homogeneous Catalysts for Asymmetric Hydrogenation.
- (a) S. J. Shuttleworth, S. M. Allin and P. K. Sharma, *Synthesis*, 1997, 1215; (b) S. J. Shuttleworth, S. M. Allin, R. D. Wilson and D. Nasturica, *Synthesis*, 2000, **8**, 1035–1074; (c) D. E. Bergbreiter, *Catal. Today*, 1998, **42**, 389–397; (d) S. Kobayashi and R. Akiyama, *Chem. Commun.*, 2003, 449–460; (e) B. Clapham, T. S. Reger and K. D. Janda, *Tetrahedron*, 2001, **57**, 4637–4662; (f) A. Akelah and D. C. Sherrington, *Chem. Rev.*, 1981, **81**, 557–587; (g) T. J. Dickerson, N. N. Reed and K. D. Janda, *Chem. Rev.*, 2002, **102**, 3325–3344; (h) P. Mastorilli and C. F. Noble, *Coord. Chem. Rev.*, 2004, **248**, 377–395; (i) D. E. Bergbreiter, *Chem. Rev.*, 2002, **101**, 3345–3384.
- C. E. Song and S. Lee, *Chem. Rev.*, 2002, **102**(10), 3495–3524.
- (a) H. P. Dijkstra, G. P. M. van Klink and G. van Koten, *Acc. Chem. Res.*, 2002, **35**, 798–810; (b) R. van Heerbeek, P. C. J. Kamer, P. W. N. M. van Leeuwen and J. N. H. Reek, *Chem. Rev.*, 2002, **102**, 3717–3756; (c) H. W. Peerlings and E. W. Meijer, *Chem. Eur. J.*, 1997, **3**(10), 1563–1570; (d) Y. Ribourbouille, G. D. Engel and L. H. Gade, *C. R. Chemie*, 2003, **6**, 1087–1096.
- (a) M. Berthod, C. Saluzzo, G. Mignani and M. Lemaire, *Tet. Asymm.*, 2004, **15**, 639–645; (b) T. Lamouille, C. Saluzzo, R. ter Halle, F. Le Guyader and M. Lemaire, *Tetrahedron Lett.*, 2001, **42**, 663–664; (c) K.-T. Wan and M. E. Davis, *Tet. Asymm.*, 1993, **4**(12), 2461–2468; (d) K. T. Wan and M. E. Davis, *J. Catal.*, 1994, **148**, 1; (e) K. T. Wan and M. E. Davis, *Nature*, 1994, **370**, 449–450; (f) K. T. Wan and M. E. Davis, *J. Catal.*, 1995, **152**, 25–30; (g) A. L. Monteiro, F. K. Zinn, R. F. de Souza and J. Dupont, *Tet. Asymm.*, 1997, **8**(2), 177–179.
- (a) M. Berthod, J.-M. Joerger, G. Mignani, M. Vaultier and M. Lemaire, *Tet. Asymm.*, 2004, **15**, 2219–2221; (b) H. L. Ngo, A. Hu and W. Lin, *Chem. Commun.*, 2003, 1912–1913; (c) A. Hu, H. L. Ngo and W. Lin, *Angew. Chem. Int. Ed.*, 2004, **43**, 2501–2504; (d) R. A. Brown, P. Pollet, E. McKoon, C. A. Eckert, C. L. Liotta and P. G. Jessop, *J. Am. Chem. Soc.*, 2001, **123**, 1254–1255.
- (a) C. Saluzzo and M. Lemaire, *Adv. Synth. Catal.*, 2002, **344**(10), 915–927; (b) G.-J. Deng, Q.-H. Fan, X.-M. Chen and G.-H. Liu, *J. Mol. Catal. A*, 2003, **193**, 21–25; (c) G.-J. Deng, Q.-H. Fan, X.-M. Chen, D.-S. Liu and A. S. C. Chan, *Chem. Commun.*, 2002, 1570–1571; (d) Q.-H. Fan, Y.-M. Chen, X.-M. Chen, D.-Z. Jiang, F. Xi and A. S. C. Chan, *Chem. Commun.*, 2000, 789–790; (e) G.-J. Deng, B. Yi, Y.-Y. Huang, W.-J. Tang, Y.-M. He and Q.-H. Fan, *Adv. Synth. Catal.*, 2004, **346**, 1440–1444.
- (a) P. Guerreiro, V. Ratovelomanana-Vidal, J.-P. Renet and P. Dellis, *Tet. Lett.*, 2001, **42**, 3423–3426; (b) C. Saluzzo, T. Lamouille, F. Le Guyader and M. Lemaire, *Tet. Asymm.*, 2002, **13**, 1141–1146; (c) H.-B. Yu, Q.-S. Hu and L. Pu, *J. Am. Chem. Soc.*, 2000, **122**, 6500–6501; (d) H.-B. Yu, Q.-S. Hu and L. Pu, *Tet. Lett.*, 2000, **41**, 1681–1685; (e) W. S. Huang, Q. S. Hu and L. Pu, *J. Org. Chem.*, 1999, **64**, 7940; (f) R. ter Halle, B. Colasson, E. Schultz, M. Spagnol and M. Lemaire, *Tet. Lett.*, 2000, **41**, 643–646; (g) M. Lemaire, R. ter Halle, E. Schulz, B. Colasson and M. Spagnol, (*Rhodia/CNRS*) *French Patent FR2789992*, 1999, *PCT: WO0049028*, 2000; (h) M. Lemaire, R. ter Halle, E. Schultz, B. Colasson and M. Spagnol, (*Rhodia/CNRS*) *French Patent FR2790477*; (i) M. Lemaire, R. ter Halle, E. Schulz, B. Colasson, M. Spagnol, C. Saluzzo and T. Lamouille, *PCT WO0052081*, 2000; (j) R. ter Halle, E. Schulz, M. Spagnol and M. Lemaire, *Synlett*, 2000, **5**, 680–682; (k) T. Ohkuma, H. Takeno, Y. Honda and R. Noyori, *Adv. Synth. Catal.*, 2001, **343**(4), 369–375; (l) Q.-H. Fan, C.-Y. Ren, C.-H. Yeung, W.-H. Hu and A. S. C. Chan, *J. Am. Chem. Soc.*, 1999, **121**, 7407–7408; (m) Q. H. Fan, C. H. Yeung, Y. C. Li and A. S. C. Chan, *Abst. Pap. Am. Chem. Soc.*, 1997, **213**, 219; (n) Q.-H. Fan, G.-J. Deng, X.-M. Chen, W.-C. Xie, D.-Z. Jiang, D.-S. Liu and A. S. C. Chan, *J. Mol. Catal. A: Chem.*, 2000, **159**, 37–43; (o) Q.-H. Fan, G.-J. Deng, C.-C. Lin and A. S. C. Chan, *Tetraheron Asymm.*, 2001, **12**, 1241–1247; (p) Q.-H. Fan, G.-H. Liu, G.-J. Deng, X.-M. Chen and A. S. C. Chan, *Tet. Lett.*, 2001, **42**, 9047–9050.
- D. J. Bayston, J. L. Fraser, M. R. Ashton, A. D. Baxter, M. E. C. Polywka and E. Moses, *J. Org. Chem.*, 1998, **63**, 3137–3140.
- (a) I. F. J. Vankelecom, D. Tas, R. F. Parton, V. Van de Vyver and P. A. Jacobs, *Angew. Chem. Int. Ed.*, 1996, **35**(12), 1346–1348; (b) R. F. Parton, I. F. J. Vankelecom, D. Tas, K. B. M. Jansen, P.-P. Knops-Gerrits and P. A. Jacobs, *J. Mol. Catal. A: Chem.*, 1996, **113**, 283–292; (c) D. Tas, C. Thoelen, I. F. J. Vankelecom and P. A. Jacobs, *Chem. Commun.*, 1997, 2323; (d) I. F. J. Vankelecom, K. A. L. Verduyze, P. E. Neys, D. W. A. Tas, K. B. M. Jansen, P.-P. Knops-Gerrits and P. A. Jacobs, *Top. Catal.*, 1998, **5**, 125–132; (e) K. De Smet, A. Pleyzier, I. F. J. Vankelecom and P. A. Jacobs, *Chem. Eur. J.*, 2003, **9**; (f) A. Kockritz, S. Bischoff, V. Morawsky, U. Prusse and K.-D. Vorlop, *J. Mol. Catal. A*, 2002, **180**, 231–243.
- (a) S. Shimazu, K. Ro, T. Sento, N. Ichikuni and T. Uematsu, *J. Mol. Catal. A*, 1996, **107**, 297–303; (b) T. Sento, S. Shimazu, N. Ichikuni and T. Uematsu, *J. Mol. Catal. A: Chem.*, 1999, **137**, 263–267.

- 15 (a) F. Gelman, D. Avnir, H. Schumann and J. Blum, *J. Mol. Cat. A*, 1999, **146**, 123–128; (b) J. Blum, D. Avnir and H. Schumann, *ChemTech.*, 1999, 32–38; (c) J. Jamis, J. R. Anderson, R. S. Dickson, E. M. Campi and W. R. Jackson, *J. Organometallic Chem.*, 2001, **627**, 37–43.
- 16 (a) A. Hu, H. L. Ngo and W. Lin, *J. Am. Chem. Soc.*, 2003, **125**, 11490–11491; (b) L-X. Dai, *Angew. Chem. Int. Ed.*, 2004, **43**, 5726–5729.
- 17 B. Kesanli and W. Lin, *Chem. Commun.*, 2004, 2284–2285.
- 18 A. R. McDonald, H. P. Dijkstra, B. M. J. M. Suijkerbuijk, M. Lutz, A. L. Spek, G. P. M. van Klink and G. van Koten, submitted for publication.
- 19 J. Sommer, Y. Yang, D. Rambow and J. Blumel, *Inorg. Chem.*, 2004, **43**, 7561–7563.
- 20 K. Mashima, K-H. Kusano, T. Ohta, R. Noyori and H. Takaya, *J. Chem. Soc. Chem. Commun.*, 1989, 1208–1210.
- 21 ATR-IR (attenuated total reflection) is a technique whereby transmission of an IR beam through a sample is measured.
- 22 DRIFT-IR (diffuse reflectance fourier transform) is a surface technique which analyses reflected IR beam from the surface/near surface of the material.
- 23 R. Noyori, T. Ohkuma and M. Kitamura, *J. Am. Chem. Soc.*, 1987, **109**, 5856–5858.
- 24 H. Kawano, T. Ikariya, Y. Ishii, M. Saburi, S. Yoshikawa, Y. Uchida and H. Kumobayashi, *J. Chem. Soc. Perkin Trans.*, 1989, 1571–1575.
- 25 A. Miyashita, A. Yasuda, H. Takaya, K. Toriumi, T. Ito, T. Souchi and R. Noyori, *J. Am. Chem. Soc.*, 1980, **102**, 7932–7934.
- 26 T. Okhuma, H. Ooka, S. Hashiguchi, T. Ikariya and R. Noyori, *J. Am. Chem. Soc.*, 1995, **117**, 2675–2676.
- 27 US Patent no. 4705895.
- 28 I. J. B. Lin, H. A. Zahalka and H. Alper, *Tet. Lett.*, 1988, **29**, 1759–1762.
- 29 www.amtec-chemnitz.de.

Choline carboxylate surfactants: biocompatible and highly soluble in water†

Regina Klein, Didier Touraud and Werner Kunz*

Received 29th November 2007, Accepted 7th February 2008

First published as an Advance Article on the web 19th February 2008

DOI: 10.1039/b718466b

With choline as a beneficial counterion of biological origin, long-chain carboxylates become water soluble at room temperature.

Introduction

Soaps have been known for over 2000 years. The oldest and most common surfactants are sodium or potassium carboxylates due to their simple preparation by neutralization of fatty acids with the respective hydroxides.¹ Nonetheless, these surfactants are restricted in their applicability by their limited solubility in water. The criterion for a surfactant's solubility is its Krafft point or Krafft temperature. It is the temperature at which the solubility of a surfactant equals the critical micellization concentration (cmc) and subsequently rises sharply.² Furthermore, it is commonly accepted to define the Krafft point of an ionic amphiphile as the clearing temperature of a 1 wt% surfactant solution, since the cmc is generally far below 1 wt%.²

While the Krafft point is still about 25 °C in the case of sodium laurate (NaC12), it is already about 45 °C for sodium myristate (NaC14) or even about 60 °C for sodium palmitate (NaC16).^{3–5} In the same manner as the Krafft point rises systematically with growing length of the hydrophobic chain, the surface activity of an amphiphile, its washing ability and its solubilising power increase.⁶ In 1972, Shinoda *et al.* pointed out that the type of the counterion markedly affects the Krafft point of a surfactant.⁷ Accordingly, Yu *et al.* found, in 1990, that a substitution of sodium in alkyl sulfates by tetrabutylammonium (TBA) considerably reduces the Krafft point, *e.g.* from 50 °C to below 23 °C in the case of octadecyl sulfate.⁸ Furthermore, Jansson *et al.* showed that replacing sodium in NaC12 by tetraalkylammonium (TAA) ions can lower the Krafft temperature (T_{Kf}) to below 0 °C.⁹ This general behavior was confirmed by Zana *et al.* who found, for example, that TBA stearate (C18) is soluble down to 0 °C, while sodium stearate (NaC18) has a Krafft point of 71 °C.^{5,10}

Obviously, substitution of the alkali counterions in soaps by quaternary ammonium ions results in a significantly increased solubility. However, this substitution simultaneously renders the systems toxicologically questionable, since simple TAA ions are potentially harmful. For instance, TAA cations act as phase

transfer catalysts and as such they can transport ions across biological membranes.^{11,12} Additionally, they can block cellular ion channels even at very low concentrations (500 μM of TBA induces a blocking of the cardiac sodium channel), whereby the blocking efficiency increases with the length of the alkyl side chains.^{13–16}

A way to benefit from the tendency of quaternary ammonium ions as counterions to reduce the Krafft points of soaps and to avoid their toxicological influence at the same time is to use a quaternary ammonium ion of biological origin, such as choline. Choline chemically refers to the cation (2-hydroxyethyl)trimethylammonium (see Fig. 1).

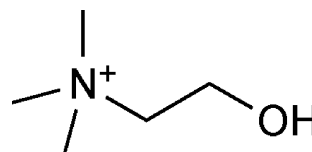


Fig. 1 Molecular structure of the choline cation.

Choline, formerly known as vitamin B₄, is present in most foods.^{17,18} In 1998, it was classified as an essential nutrient for humans.¹⁹ Choline is essential for several biological functions of the human body. For instance, it serves as a precursor for phospholipids, the constituents of biological membranes.¹⁷ Furthermore, it is a precursor for the neurotransmitter acetylcholine.²⁰ Moreover, its derivative betaine provides a source of methyl groups for protein synthesis and transmethylation reactions.²¹

Apparently, the hydroxy group of choline, in contrast to the simple TAA ions, ensures the physiological degradability. For example, it was found that for rat glioma cells, choline chloride is the least toxic amine, 5.5 times less toxic than tetramethylammonium (TMA) chloride and more than 500 hundred times less toxic than TBA chloride.²² Due to the hydroxy group, choline can, for instance, be esterified to give acetylcholine and phosphatidylcholine. Furthermore, choline can also be environmentally decomposed by microorganisms.²³

Choline carboxylates have already been described in the literature as ingredients of certain formulations, comprising, for example, cosmetic products or cryoprotectant agents for plants.^{24,25} However, there is no physicochemical characterization of these species published to date. In this communication, we report on the Krafft points and the critical micellar concentrations of choline salts of fatty acids, ranging from dodecanoic acid (C12) to octadecanoic acid (C18). Furthermore, we relate these values to the cmc's and Krafft points of the corresponding sodium, potassium and TMA carboxylates. The whole phase diagrams of these choline surfactants, established by SAXS and SANS measurements, will be presented in a forthcoming publication.

Institute of Physical and Theoretical Chemistry, University of Regensburg, 93040, Regensburg, Germany.

E-mail: Werner.Kunz@chemie.uni-regensburg.de; Fax: +49 941 943 45 32; Tel: +49 941 943 40 44

† Electronic supplementary information (ESI) available: Information regarding the synthesis, ¹H- and ¹³C-NMR, ES-MS and conductivity data of ChC_m, TMAC_m and KC_m with *m* = 12–18. See DOI: 10.1039/b718466b

Experimental data about synthesis, analysis and characterisation of choline carboxylates (ChC*m*), potassium carboxylates (KC*m*) and TMA carboxylates (TMAC*m*) with $m = 12$ –18 can be found in the ESI.†

Results and discussion

Critical micellization concentration (cmc)

In Table 1, the values of the cmc's for the investigated choline surfactants are compared with those of the related sodium and potassium carboxylates. Apparently, the cmc's of choline carboxylates are in the same order of magnitude as those of the alkali soaps. Moreover, the cmc of ChC12 coincides nearly exactly with that of TMAC12 (cmc = 25 mM),⁹ indicating that the hydroxy group of choline does not influence noticeably the micelle formation.

Furthermore, the cmc of ChC*m* decreases linearly by a factor of 4 per addition of two CH₂ groups. This feature, typical for ionic amphiphiles, can be illustrated by eqn (1), where the logarithm of the cmc is a linear function of the alkyl chain length n_c .²⁸

$$\log \text{cmc} = An_c + B \quad (1)$$

For mono-ionic surfactants, the constant A typically adopts the value 0.3,²⁹ which is in good agreement with that found for the investigated surfactants (0.29). The parameter B (1.9) is a constant for a particular ionic head at a given temperature and corresponds well to that found in the literature for potassium carboxylates (1.9).²⁹

From the values of the cmc's, it can be deduced that choline carboxylates at low concentrations generally act in the same manner as the alkali carboxylates in aqueous solutions. Since, for instance, the sodium salts are completely dissociated in dilute solution,²⁶ the choline salts can also be assumed to reveal no association of the carboxylic headgroup with the counterion choline. In contrast, the TAA salts of sulfates exhibit a pre-cmc ion-pairing.³⁰ Accordingly, the cmc values of TAA sulfates (e.g. cmc (TMA dodecyl sulfate) = 5.53 mM) are reduced in comparison to the corresponding alkali sulfates (e.g. cmc (Na dodecyl sulfate) = 8.32 mM).³⁰

Nonetheless, the most outstanding property of these choline salts is the fact that they are capable of forming micelles at room temperature even with palmitic acid (C16)—in contrast to the homologous alkali soaps, which are restricted in their solubility. As a consequence of the potential use of longer-chain surfactants, a relatively high surface tension reduction down to about 25 mN m⁻¹ for ChC16 can be obtained.³¹

Table 1 Comparison of the cmc's [mM] of choline, sodium and potassium carboxylates at 25 °C

| | Choline | Sodium | Potassium |
|-----|---------|-------------------|-------------------|
| C12 | 25.5 | 24.4 ^a | 25.5 ^b |
| C14 | 6.4 | 6.9 ^a | 6.6 ^b |
| C16 | 1.8 | — | — |

^a From ref. 26. ^b From ref. 27.

Krafft point

The Krafft point of a surfactant is the result of the interplay between two competing thermodynamic forces. One is the free energy of the solid crystalline state and the other is the free energy of the micellar solution. A strong head group interaction and a good packing in a crystal lattice contribute to the crystal's stability, which is associated with a low free energy. Consequently, the Krafft point is elevated. In turn, a low free energy of the micellar solution, promoted by e.g. the hydrophilicity of a compound, favours the solubilised state. However, the energetic state of the micellar solution varies only slightly when changing the counterion, whereas the free energy of the crystalline state may change considerably from system to system.³² Hence, the latter contribution can be considered as the main driving force in determining the solubilisation temperature.

In Fig. 2, the Krafft temperatures for ChC*m*, TMAC*m*, KC*m* and NaC*m* with $m = 12$ –18 are shown. The values, which we determined for the potassium carboxylates are generally in good agreement with those found by McBain *et al.*³³ and are in all cases 14–15 °C lower than those of the corresponding sodium salts. Concerning the TMA carboxylates, only one value of T_{K_r} has been reported so far to our knowledge, namely for TMAC12 (<0 °C) by Jansson *et al.*⁹ For the other TMA carboxylates we found the same Krafft temperatures as for the choline carboxylates within the experimental error of about 1–2 °C. Nevertheless, as can be seen from Fig. 2, the Krafft points of ChC*m* are substantially lower than those of the corresponding alkali salts. For example, T_{K_r} of ChC18 takes the value of 40 °C, while T_{K_r} of NaC18 is 71 °C and 57 °C for KC18.⁴ For palmitic acid, a reduction from 60 °C in the case of sodium and from 46 °C in the case of potassium down to 12 °C can be obtained by replacing the alkali ions by choline.⁵ Furthermore, the Krafft temperature of NaC14 and KC14 can be dropped from 45 °C and 30 °C, respectively, to 0–1 °C with choline as counterion.⁵ ChC12 is even soluble far below 0 °C (T_{K_r} (NaC12) = 25 °C, T_{K_r} (KC12) = 10 °C).⁴

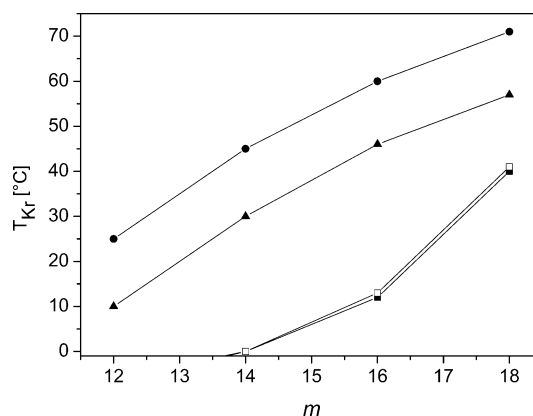


Fig. 2 Comparison of the Krafft temperatures T_{K_r} (°C) of (■) ChC*m*, (□) TMAC*m*, (▲) KC*m* and (●) NaC*m* surfactants with increasing number of carbon atoms m (values of NaC*m* with $m = 12$ taken from ref. 3, with $m = 14, 16, 18$ from ref. 4).

Obviously, the Krafft points of carboxylate surfactants decrease with increasing size of the counterion. This fact has already been reported for the homologous series of the alkali

ions and can be continued by the implementation of TAA ions.³³ As pointed out above, the micellar state of the ChCm surfactants does not differ a lot from the NaCm and KCm soaps. Thus, the reason for the pronounced T_{kr} reduction of choline carboxylates with respect to the alkali soaps must be a high free energy of the crystalline state of ChCm. Taking into account the almost equal T_{kr} values of ChCm and TMACm, the alcohol group of choline seems to have no noticeable influence, as observed similarly for the micellization process. Very probably, it is mainly the size of the bulky quaternary ammonium headgroup of choline which hinders the regular packing in a crystal lattice, rendering the solid crystalline state energetically less favourable. Consequently, the Krafft point decreases.

Conclusion

Choline carboxylate surfactants have been found to combine the characteristics of common alkali carboxylates in the low concentration regime with a substantially increased solubility. Accordingly, ChCm surfactants can be used at ambient temperature up to $m = 16$. Additionally, the investigated choline salts are produced by a straightforward synthesis with little or no heat requirement. Moreover, choline can be decomposed both in the environment and in the human body. Consequently, choline soaps, consisting exclusively of biogenic material occurring in the human body, are physiologically and environmentally harmless, and as such convenient for e.g. drug delivery systems.

Notes and references

- 1 A. Schmalstieg and G. W. Wasov, in *Handbook of Applied Surface and Colloid Chemistry*, ed. K. Holmberg, John Wiley & Sons Ltd, England, 2002, vol. 1, p 271.
- 2 R. G. Laughlin, *The Aqueous Phase Behavior of Surfactants*, Academic Press, San Diego, 1994, p 108.
- 3 J. W. McBain and W. W. Lee, *Oil Soap*, 1943, **20**, 17.
- 4 C. Madelmont and R. Perron, *Colloid Polym. Sci.*, 1976, **254**, 581.
- 5 B. Lin, A. V. McCormick, H. T. Davis and R. Strey, *J. Colloid Interface Sci.*, 2005, **291**, 543.
- 6 W. C. Preston, *J. Phys. Chem.*, 1948, **52**, 84.
- 7 K. Shinoda and H. Kunieda, *J. Phys. Chem.*, 1976, **80**, 2468.
- 8 Z.-J. Yu, X. Zhang and G. Xu, *J. Phys. Chem.*, 1990, **94**, 3675.
- 9 M. Jansson, A. Jönsson, P. Li and P. Stilbs, *Colloids Surf.*, 1991, **59**, 387.
- 10 R. Zana, *Langmuir*, 2004, **20**, 5666.
- 11 R. Moberg, F. Bokman, O. Bohman and H. O. G. Siegbahn, *J. Am. Chem. Soc.*, 1991, **113**, 3663.
- 12 T. Hrobárik, L. Vrbka and P. Jungwirth, *Biophys. Chem.*, 2006, **124**, 238.
- 13 E. Kutluay, B. Roux and L. Heginbotham, *Biophys. J.*, 2005, **88**, 1018.
- 14 V. B. Luzhkov and J. Aqvist, *FEBS Lett.*, 2001, **495**, 191.
- 15 M. E. O'Leary, R. G. Kallen and R. Horn, *J. Gen. Physiol.*, 1994, **104**, 523.
- 16 M. E. O'Leary and R. Horn, *J. Gen. Physiol.*, 1994, **104**, 507.
- 17 S. H. Zeisel and J. K. Blusztajn, *Annu. Rev. Nutr.*, 1994, **14**, 269.
- 18 J. C. Howe, J. R. Williams and J. M. Holden, *USDA Database for the Choline Content of Common Foods*, 2004, available at: <http://www.nal.usda.gov/fnic/foodcomp/Data/Choline/Choline.html>.
- 19 Food and Nutrition Board, Institute of Medicine, *Dietary Reference Intakes for Thiamin, Riboflavin, Niacin, Vitamin B₆, Folate, Vitamin B₁₂, Pantothenic Acid, Biotin, and Choline*, National Academic Press, Washington DC, 1998.
- 20 J. K. Blusztajn and R. J. Wurtman, *Science*, 1983, **221**, 614.
- 21 J. K. Blusztajn, *Science*, 1998, **281**, 794.
- 22 L. C. Mokrasch, *Mol. Cell. Biochem.*, 1990, **92**, 85.
- 23 G. J. J. Kortstee, *Arch. Mikrobiol.*, 1970, **71**, 235.
- 24 S. Nayak and V. Nayak, *US Pat.*, 6 120 779, 2000.
- 25 J. R. Geary, *US Pat.*, 5 124 061, 1992.
- 26 A. N. Campbell and G. R. Lakshminarayanan, *Can. J. Chem.*, 1965, **43**, 1729.
- 27 H. B. Klevens, *J. Colloid Sci.*, 1947, **2**, 301.
- 28 H. B. Klevens, *J. Am. Oil Chem. Soc.*, 1953, **30**, 74.
- 29 M. J. Rosen, *Surfactants and Interfacial Phenomena*, John Wiley & Sons Ltd, USA, 2nd edn, 1989; p 136.
- 30 P. Mukerjee, *Adv. Colloid Interface Sci.*, 1967, **1**, 241.
- 31 R. Klein, D. Touraud, W. Kunz, unpublished work.
- 32 B. Lindman, in *Handbook of Applied Surface and Colloid Chemistry*, ed. K. Holmberg, John Wiley & Sons Ltd, England, 2002, p 428.
- 33 J. W. McBain and W. C. Sierichs, *J. Am. Oil Chem. Soc.*, 1948, **25**, 221.

The design and synthesis of biodegradable pyridinium ionic liquids†

Jitendra R. Harjani,^a Robert D. Singer,^b M. Teresa Garcia^c and Peter J. Scammells^{*a}

Received 11th January 2008, Accepted 15th February 2008

First published as an Advance Article on the web 28th February 2008

DOI: 10.1039/b800534f

Ionic liquids with a pyridinium cation bearing an ester side chain moiety were prepared from either pyridine or nicotinic acid and their biodegradability was evaluated using the CO₂ Headspace test (ISO 14593). ILs of this type showed exceptionally high levels of biodegradation under aerobic conditions and can be classified as ‘readily biodegradable’.

Ionic liquids (ILs) are deemed greener solvent alternatives in chemical synthesis mainly because of their negligible vapor pressure, high thermal stability, low flammability and reusability in chemical applications.¹ They are also known to have an influence on the rate and selectivity of certain chemical reactions. Not surprisingly, with their numerous attributes these neoteric solvents have attracted the attention of chemists from a multitude of disciplines. In the last eight years, contributors from around the world have published more than 250 publications in this journal alone, mainly in the area of the synthesis of ILs or their use as green solvent alternatives. As research in the area of ILs continues to grow, the domain of their applications have substantially broadened. The non-volatility of ILs under operational conditions minimizes their impact on air quality during their life cycle. However, their impact on soil and water is certainly of considerable concern at the time of their disposal. Therefore, the quest to find a benign method of disposal for ILs is gaining momentum.² The evaluation of the environmental impact of ILs can, in part, be gauged by parameters such as biodegradability and toxicity.² Complete mineralization of any compound leads to non toxic CO₂ and biomass, making its disposal a safe option. Designing biodegradable chemicals is significant in that it would decrease the bioaccumulation of the parent compound and its metabolic products, reducing its toxic effects. Our interest in ILs stems from their possible use in reactions that are important in organic synthesis.³ Designing benign chemicals is acknowledged as a crucial aspect of green chemistry.^{2,4} Hence, we believe that the logical design of ILs may lead to compounds that would not just be ideal solvents

for chemical processes, but would also be safe for disposal and would therefore be sustainable. Research in this area is currently vital as ILs are likely to make a transition from academic laboratories to large scale operations where disposal of any chemical is a major concern.⁵ Enormous structural variations are possible in the ILs by changing either the cation and/or the anion. This leads us to believe that it should be possible to manipulate their chemical architecture to achieve high biodegradability.

Our initial work on the imidazolium based ILs has demonstrated that the introduction of the ester groups derived from a C₂ acid and C₄ or higher alcohol in the 3-*N*-substituent does increase their biodegradation.⁶ The *n*-octyl sulfate anion was integrated into the structure to meet the benchmark of ‘readily biodegradable’ materials.⁷ These observations clearly point toward the recalcitrance of the imidazolium core.

Although pyridinium based cationic surfactants are reported to have strong resistance towards biodegradation,⁸ some recent reports triggered our interest in them. This has led to some noteworthy results which we disclose in this communication. The amphiphilic quaternary salts based on this moiety were identified to be potential candidates for gene delivery by Engberts and Hulst.⁹ In this report, the good biodegradability and low cytotoxicity of some compounds was claimed, but the quantitative assessment of the biodegradability was lacking. Kalka *et al.* examined some cationic surface active substances based on 1-dodecylpyridinium chloride. The study concluded that these compounds are generally toxic and only partly biodegradable.¹⁰ Very recently, Docherty *et al.* reported the mineralization of 1-hexyl-3-methylpyridinium bromide and 1-octyl-3-methylpyridinium bromide after 49 and 25 days of incubation, respectively, by the DOC die-away test (OECD 301A).¹¹

We focused our attention on the ILs that were based on the ester moiety as the introduction of this group in the imidazolium based ILs improved their biodegradation probably by providing a site for an enzymatic attack.^{6,7} The CO₂ headspace test (ISO 14593)⁷ was used to evaluate the biodegradability of the ionic liquids prepared in this study. If the biodegradation level measured according to this test is higher than 60% within twenty eight days, the compound can be considered as ‘readily biodegradable’.

A simple quaternary bromide derived from pyridine and ethyl bromoacetate **1a** and the corresponding octyl sulfate based IL **1b** showed biodegradability at 87% and 89%, respectively (Fig. 1).† Here the inclusion of the octyl sulfate anion resulted in no appreciable increase in biodegradation. This is unlike our earlier observation for the imidazolium based ILs, where the octyl sulfate anion significantly increased biodegradation.⁷

^aMedicinal Chemistry and Drug Action, Monash Institute of Pharmaceutical Sciences, Monash University, Parkville, Victoria, 3052, Australia. E-mail: peter.scammells@vcp.monash.edu.au; Fax: +61 3 99039582; Tel: +61 3 9903 9542

^bDepartment of Chemistry, Saint Mary's University, Halifax, Nova Scotia, B3H 3C3, Canada

^cDepartment of Surfactant Technology, IIQAB-CSIC, Jordi Girona 18-26, 08034, Spain. E-mail: mtgbet@iiqab.csic.es; Fax: +34 93 204 5904; Tel: +34 93 400 6100

† Electronic supplementary information (ESI) available: Supplementary information on general preparation procedures. See DOI: 10.1039/b800534f

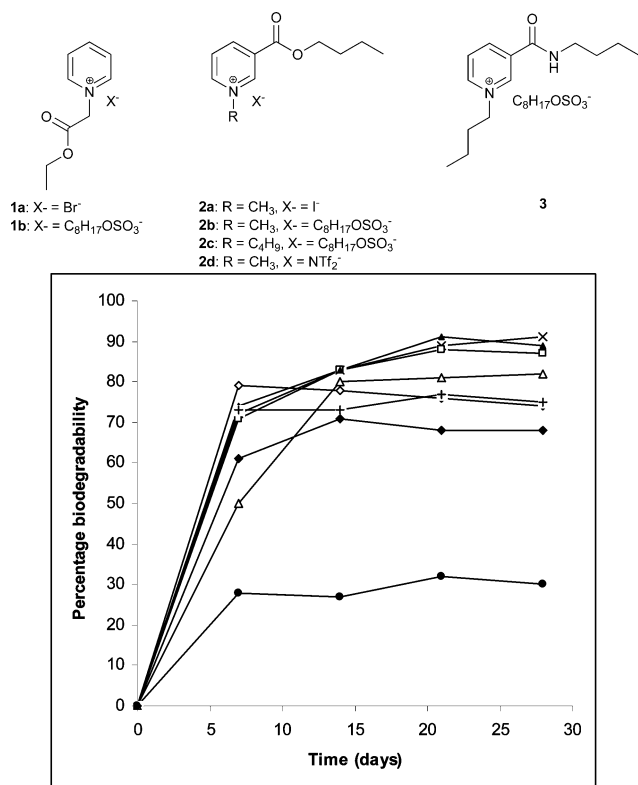


Fig. 1 Biodegradation of **1a** (□), **1b** (▲), **2a** (◇), **2b** (+), **2c** (Δ), **2d** (◆), **3** (●) and sodium dodecyl sulfate (reference compound) (×) in the CO₂ Headspace test.

Nicotinic acid, an inexpensive natural product based on pyridine, was an attractive starting material for the synthesis of pyridinium ionic liquids bearing functionality on the heterocyclic ring. Butyl nicotinate was readily obtained from nicotinic acid and was employed to derive some ILs. Its methylation with methyl iodide yielded **2a**; which upon treatment with sodium octyl sulfate yielded **2b**. Both **2a** and **2b** displayed biodegradation of 74% and 75%, respectively (Fig. 1), once again demonstrating that the high biodegradability of this class of compounds is largely dependent upon the structure of the cation. A slight increase in the biodegradability from 75% to 82% with an increase in the alkyl chain length from C₁ in **2b** to C₄ in **2c** is perhaps due to an increase in lipophilicity. Although all the above levels of biodegradation are obtained after a standard 28 day period, it is notable that the biodegradability of **1a**, **1b**, **2a** and **2b** are so high that they degrade more than 70% within the first seven days of incubation. The percentages of mineralization attained under the stringent conditions of this biodegradation test allows these pyridinium compounds (**1a**, **1b**, **2a**, **2b** and **2c**) to be classified as readily biodegradable and therefore they would be expected to degrade rapidly and completely in aerobic aquatic environments.

Compounds **1a** and **2a** are solids at room temperature with melting points higher than 100 °C; hence, these are not classified as typical ILs. However, the incorporation of a bis(triflimide) counterion afforded a compound (**2d**) which was both readily biodegradable and a liquid at room temperature.

Although the introduction of the amide group is known to improve the biodegradation of organic compounds,¹² no signifi-

cant improvement in the biodegradation was observed when this group was incorporated into the imidazolium based ILs.⁶ The nicotinamide based IL **3** was easily derived by quaternization of *N*-butyl nicotinamide with butyl iodide followed by the metathesis of the quaternary iodide using sodium octyl sulfate. The resultant IL **3** with two C₄ linear aliphatic chains and an octyl sulfate anion showed poor biodegradation at 30% after a 28 day period. Considering this as the contribution from the anion, we conclude that the presence of an amide group on the pyridinium ring does not improve biodegradation.

ILs **1b** and **2b** have comparable biodegradability to sodium dodecyl sulfate (SDS), a readily biodegradable anionic surfactant used as the reference compound in the biodegradation test. Intrigued by these preliminary results, we intend to continue exploring this class of IL further. Our main aim is to uncover the possible structural elements on the pyridinium core that are responsible for the higher biodegradation of this class of ILs. We are also interested in varying the anion relative to those commonly encountered in the ILs that would have an influence on the biodegradability. These studies can be useful in the design of ILs possessing good solvent attributes and high biodegradability. The details of this investigation will be disclosed in a subsequent full paper.

In conclusion, pyridine based ILs **1b** and **2b** and **2c** showed strikingly high levels of biodegradability over the standard 28 day period. The high biodegradation rates appear to be a characteristic of the cation and do not depend on the counter ions tested. This presents the possibility that substituted pyridinium rings lead to metabolites that are not refractory upon biodegradation. The study also demonstrates that the structural manipulation of the pyridinium skeleton may lead to ILs which are likely to possess good solvent attributes and a predisposition to biodegrade when released into an aquatic environment.

Acknowledgements

The authors thank Pfizer Global R & D, the Spanish Ministerio de Educación y Ciencia (CTQ2007–60364/PPQ) and the Australian Research Council (LX0561094) for financial support.

Notes and References

- (a) J. Dupont, R. F. de Souza and P. A. Z. Suarez, *Chem. Rev.*, 2002, **102**, 3667; (b) J. S. Wilkes, *Green Chem.*, 2002, **4**, 73; (c) P. Wasserscheid and W. Keim, *Angew. Chem., Int. Ed.*, 2000, **39**, 3772; (d) T. Welton, *Chem. Rev.*, 1999, **99**, 2071.
- (a) J. Ranke, S. Stolte, R. Störmann, J. Arning and B. Jastorff, *Chem. Rev.*, 2007, **107**, 2183; (b) R. S. Boethling, E. Sommer and D. DiFiore, *Chem. Rev.*, 2007, **107**, 2207.
- S. Bouquillon, T. Courant, D. Dean, N. Gathergood, S. Morrissey, B. Pegot, P. J. Scammells and R. D. Singer, *Aust. J. Chem.*, 2007, **60**, 843.
- (a) P. T. Anastas, J. C. Warner, *Green Chemistry: Theory and Practice*, Oxford University Press, Oxford, 1998; (b) *Benign by Design*, ed. P. T. Anastas and C. A. Farris, American Chemical Society, Washington, DC, 1994.
- (a) D. Adam, *Nature*, 2000, **407**, 938; (b) K. R. Seddon, *Nat. Mater.*, 2003, **2**, 363.
- N. Gathergood, M. T. Garcia and P. J. Scammells, *Green Chem.*, 2004, **6**, 166.
- N. Gathergood, P. J. Scammells and M. T. Garcia, *Green Chem.*, 2006, **8**, 156.

-
- 8 P. H. Howard, in *Handbook of Property Estimation Methods for Chemicals: Environmental and Health Science*, Lewis Publishers, Boca Raton, FL, 2000, ch. 12, pp. 281–310.
- 9 (a) A. Roosjen, J. Šmisterová, C. Driessen, J. T. Anders, A. Wagenaar, D. Hoekstra, R. Hulst and J. B. F. N. Engberts, *Eur. J. Org. Chem.*, 2002, 1271; (b) D. Pijper, E. Bulten, J. Šmisterová, A. Wagenaar, D. Hoekstra, J. B. F. N. Engberts and R. Hulst, *Eur. J. Org. Chem.*, 2003, 4406.
- 10 E. Grabińska-Sota and J. Kalka, *Environ. Int.*, 2003, **28**, 687.
- 11 K. M. Docherty, J. K. Dixon and C. F. Kulpa Jr., *Biodegradation*, 2007, **18**, 481.
- 12 (a) R. S. Boethling, *Designing Safer Chemicals*, ACS Symp. Ser. 640, 1996, 156; (b) P. H. Howard, R. S. Boethling, W. Stiteler, W. Meylan, J. Beauman, *Sci. Total Environ.*, 1991, 110/635; (c) R. S. Boethling, *Cationic Surfactants, Surfactant Science Series Vol. 53*, Marcel Dekker, New York, 1994, pp. 95–135.

Environmentally benign and selective reduction of nitroarenes with Fe in pressurized CO₂–H₂O medium

Ge Gao, Yuan Tao and Jingyang Jiang*

Received 13th December 2007, Accepted 16th January 2008

First published as an Advance Article on the web 18th February 2008

DOI: 10.1039/b719259b

A new method for reduction of nitroarenes employing metallic iron in pressurized CO₂–H₂O medium has been developed. *p*-Chloronitrobenzene can be reduced to the corresponding amine with a yield of 99% under the optimized conditions. The method is also applicable for the reduction of other substituted nitroarenes. After the reduction, the reaction mixture is self-neutralized on releasing of CO₂. The method is environmentally benign, easily scaled-up and applicable for the preparation of substituted anilines.

Introduction

Aromatic amines carrying chloro-, carbonyl and cyano groups are important intermediates in the synthesis of chemicals such as antioxidants, dyes, pigments, photographic, pharmaceutical and agricultural chemicals¹. Practically, aromatic amines can be produced from the corresponding nitroarenes by catalytic hydrogenation or by reduction using various reducing reagents such as iron or sulfides. The catalytic hydrogenation using molecular hydrogen is a clean and convenient method.² But when other reducible groups are present in the molecule, it is difficult to reduce the nitro group selectively in a catalytic process.³ Catalysts and reaction conditions must be carefully selected and new catalysts are still being developed for the reduction of nitroarenes carrying other reducible functionalities.^{4–6} Furthermore, the presence of highly flammable hydrogen gas poses a significant risk in catalytic processes. In such cases, the use of older, noncatalytic manufacturing processes prevails despite the large amounts of waste produced by these processes.⁷ Therefore, the development of a selective method for the reduction of nitro groups is still required.

Iron is very cheap and readily available and it is known that reduction of nitroarenes employing Fe can tolerate a variety of reducible functionalities. Traditionally, the reduction must be carried out under acidic conditions using strong acid, such as aqueous HCl.^{10–12} It is necessary to neutralize the reaction mixture with base after the reduction and hence salt formation is inevitable in the aqueous solution. Finding an alternative acid to replace the traditional acid is of importance.

Recently Poliakoff and Boix⁸ have tried the reduction of nitroarenes using a metallic reducing reagent directly in pure water at 250 °C. The yield of aniline was only 10% using iron powder under the reaction conditions. Wang *et al.*⁹ tried applying nanosized activated metallic iron powder for the reduction of nitroarenes directly in water, and good reaction yield can be achieved at 210 °C. However, the nanosized metallic iron powder is expensive.

Over the past decades, many interests have been focused on CO₂ and H₂O as environmentally benign alternatives to conventional organic solvents. Nontoxicity, low cost, abundance, and easy recycling are some of the key attributes of these two fluids.¹³ When water is mixed with CO₂, the resulting pH remains constant (~2.9) over a wide range of pressures and temperatures;^{14–16} besides, the aqueous phase is substantially buffered with CO₂. Savage *et al.* have reported the acceleration of acid-catalyzed reactions in high-temperature liquid water by the addition of carbon dioxide to the reaction medium.^{17,18} The applications of carbonic acids have been recently demonstrated in selective reduction of aldehydes to alcohols,¹⁹ synthesis of vicinal diamines,²⁰ diazotization reactions²¹ and carbonic acid-catalyzed reactions.²² There is no report of the application of carbonic acid for the reduction of nitroarenes by metallic iron.

In this work, reductions of nitroarenes employing iron in pressurized CO₂–H₂O medium are studied. Nearly quantitative yields of aromatic amines can be obtained under relatively mild reaction conditions.

Results and discussion

It is known that iron powder in acidic medium is an efficient route for the selective reduction of nitroarenes with a variety of other reducible functionalities. So the reductions of *p*-chloronitrobenzene (*p*-CNB) by iron in pressurized CO₂–H₂O medium were studied first in order to demonstrate the effect of this new protocol both in reactivity and selectivity toward the reduction of nitro group. In the reaction mixture, only *p*-chloroaniline is identified and aniline, the dechlorinated product of *p*-CNB is not found.

On the examination of reaction parameters on the reaction, the influence of CO₂ pressure on the reaction was studied first because the CO₂ pressure is the key factor affecting the system acidity. The reaction was carried out at 120 °C, and the product yields under different CO₂ pressures are shown in Fig. 1.

When no CO₂ was added to the reaction system, practically no reduction took place. With an increase of CO₂ pressure from 4.0–8.0 MPa in the system, the product yield increased drastically. The product yield was nearly 100% when the CO₂ pressure was

State Key Laboratory of Fine Chemicals, Dalian University of Technology, Dalian, 116012, China

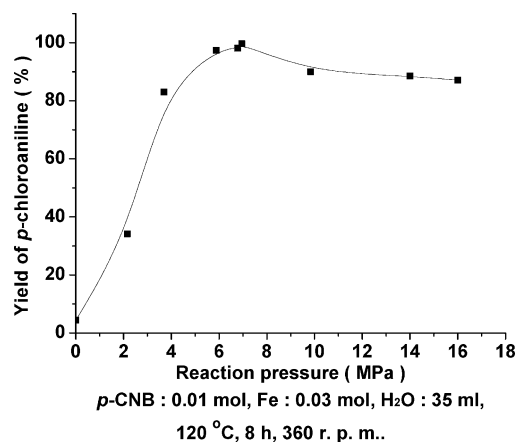


Fig. 1 The effect of reaction pressure on yield.

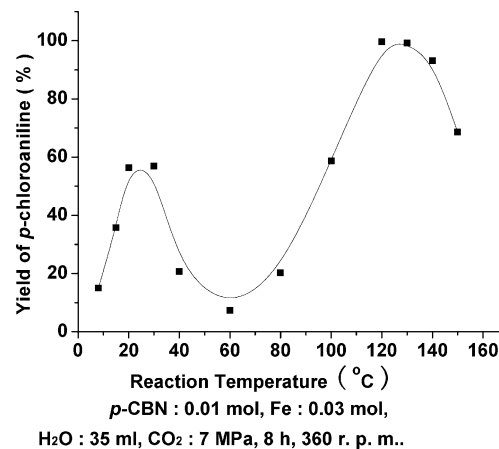


Fig. 2 The effect of reaction temperature on yield.

in the range of 6.0–8.0 MPa (also see the data in Table 1, entry 1). However, with a further increase of the CO₂ pressure to above 8.0 MPa, the product yield decreased slowly. There are probably two factors accounting for this phenomenon. First, the extracting ability of CO₂ is increasing with the increase of pressure, so more substrate is extracted into the gaseous phase and the contact between the substrate and iron powder becomes worse to a certain extent. Second, the consumption of iron through side reactions with water is increased with the increase of the acidity in the reaction medium, and the acidity is increased with the increase of CO₂ pressure. It should be noted that the molar ratio of Fe to *p*-CNB is only 3 in the reaction mixture, which is close to the theoretical amount (Fe : *p*-CNB = 2.25) for the reduction of *p*-CNB. If more Fe is added to the reaction system (Fe : *p*-CNB = 6 : 1), the product yield increased again (see the data in Table 1 entries 3 and 5).

The effects of temperature on the reaction yield were also investigated under 7.0 MPa CO₂ pressure and the results were shown in Fig. 2. It is interesting to note that when the temperature increased from 8 to 150 °C, the product yield increased to a first maximum around 30 °C, decreased to a minimum around 60 °C, increased to a second maximum (100%) around 120 °C and then decreased again. Both temperature and acidity of the system are important factors influencing the reduction of nitro group by iron. Higher temperature and higher acidity favor the reduction. In our reaction system there is a

contradiction between the temperature and the acidity, *i.e.* the acidity of the system becomes weaker with the increase of the temperature, as the solubility of CO₂ in water decreases under constant pressure. When the temperature exceeds 120 °C, the consumption of iron by side reaction with water is another unfavorable factor. This unfavorable factor can be overcome by adding an excess amount of iron to the reaction mixture (see the results in Table 1, entry 7).

Other factors, such as the stirring rate and the volume of water used in the reaction system, on product yield were also examined. The bigger the stirring rate is, the higher the product yield is. In the research work, the optimal amount of water is 35 ml for the reaction carried out in a 100 ml autoclave reactor.

Fig. 3 illustrates the influences of the ratio of iron to *p*-CNB on the product yield. It can be seen that when the ratio of iron to *p*-CNB is bigger than 4, the reduction of nitro functional group is nearly complete.

The reductions of three other nitroarenes were also tried in this system and the results are also listed in Table 1 (entries 8–10). There is no other side product beside the expected product in the reaction mixture, due to the high chemoselectivity of the reaction system.

In the reaction mixture, the product can also be extracted by pressurized CO₂ and further work on this line is under investigation. Because the reaction mixture is self-neutralized

Table 1 The reductions of nitroarenes to the corresponding aromatic amines in different reaction conditions. *Reaction conditions*: nitroarene (0.01 mol), water (35 ml), the stirring rate is 360 rpm

| Entry | Nitroarene ^a | Metal : substrate | <i>T</i> /°C | <i>p</i> /MPa | <i>t</i> /h | Products | Yield (%) ^b |
|-------|---|-------------------|--------------|---------------|-------------|--|------------------------|
| 1 | <i>p</i> -CNB | 3 : 1 | 120 | 7 | 8 | <i>p</i> -CAN | 99 |
| 2 | <i>p</i> -CNB | 3 : 1 | 120 | 14 | 8 | <i>p</i> -CAN | 89 |
| 3 | <i>p</i> -CNB | 6 : 1 | 120 | 14 | 8 | <i>p</i> -CAN | 98 |
| 4 | <i>p</i> -CNB | 3 : 1 | 120 | 16 | 8 | <i>p</i> -CAN | 87 |
| 5 | <i>p</i> -CNB | 6 : 1 | 120 | 16 | 8 | <i>p</i> -CAN | 95 |
| 6 | <i>p</i> -CNB | 3 : 1 | 150 | 7 | 8 | <i>p</i> -CAN | 68 |
| 7 | <i>p</i> -CNB | 6 : 1 | 150 | 7 | 8 | <i>p</i> -CAN | 98 |
| 8 | <i>o</i> -CNB ^c | 3 : 1 | 120 | 6 | 8 | <i>o</i> -CAN | 100 |
| 9 | <i>p</i> -NO ₂ -C ₆ H ₄ COCH ₃ ^c | 3 : 1 | 120 | 6 | 8 | <i>p</i> -NH ₂ -C ₆ H ₄ COCH ₃ | 76 |
| 10 | 1-NO ₂ AQ ^c | 3 : 1 | 120 | 6 | 8 | 1-NH ₂ AQ | 70 |

^a *o*-CNB: *o*-chloronitrobenzene, *o*-CAN: *o*-chloroaniline, 1-NO₂AQ: 1-nitroanthraquinone, 1-NH₂AQ: 1-aminoanthraquinone. ^b Determined by GC, GC-MS or LC-MS. ^c The stirring rate is 480 rpm in a high *T/p* batch reaction system.

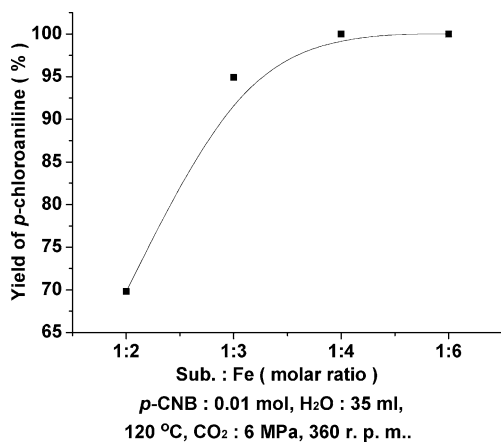


Fig. 3 The effect of the molar ratio of substrate to Fe on yield.

on releasing of CO₂, there is no salt waste accumulation in the aqueous solution. So it is fundamentally possible to eliminate the problem of salt wastes accumulation which is inevitably associated with traditional reduction processes by iron in acidic medium.

Conclusion

In conclusion, nitroarenes can be reduced to anilines with high efficiency and high chemoselectivity using iron in a pressurized CO₂-H₂O system. *p*-Chloronitrobenzene can be reduced to the corresponding amine with a yield of 99% under the optimized conditions of 7.0 MPa of CO₂ pressure, a temperature of 120 °C, Fe : *p*-CNB molar ratio of 3 : 1 and a reaction period of 8 h. The method is also applicable for the reduction of other substituted nitroarenes with high chemoselectivity.

Experimental

Nitroarenes and iron powder are commercially purchased and used without further purification. A 100 ml Parr autoclave (Parr 4842) equipment was applied and it was connected with a high pressure liquid chromatography pump (PU-1580, JASCO Co.) for supplement of CO₂. The autoclave was placed with the appropriate amount of nitroarene, iron powder and water, and then the autoclave was sealed. The reactor was flushed three times with 0.5 MPa of CO₂ and then was heated to a designated temperature and maintained at that temperature for a certain period of time. Meanwhile, CO₂ was gradually charged to the reaction system to maintain a designated pressure. The

reaction time reported in this work did not include the time required to heat or cool the system (*ca.* 15 min each). After the reaction was finished, CO₂ was released slowly. The reaction mixture was extracted thoroughly with organic solvent (toluene or ethyl acetate). The organic phase was analyzed by GC (Temp 5890 II Analyzer, capillary column, \emptyset 0.53 mm \times 50 m, SE54) for the experiments with *p*-CNB and *o*-CNB as substrate, or by GC-MS (HP 6890 GC/5973 MSD : HP-19091S-433 30 m \times 250 μ m \times 0.25 μ m), LC (Agilent 1100 series carbon-18) or LC-MS (HP 1100 LC/MSD HPLC-APCL) for other nitroarenes.

Acknowledgements

This work is supported by the National Natural Science Foundation of China (Grant No: 20476015).

References

- 1 E. L. Pitara, B. N. Zemba, J. Barbier, F. Barbot and L. Miginiac, *J. Mol. Catal. A: Chem.*, 1999, **144**, 199–206.
- 2 *Kirk-Othmer, Encyclopedia of Chemical Technology*, The Interscience Encyclopedia, Inc., Wiley, New York, NY, vol. 2, 4th edn, 1992, 426–503.
- 3 P. N. Rylander, *Catalytic Hydrogenation in Organic Synthesis*, Academic Press, New York, 1979, 122.
- 4 A. M. Tafesh and J. Weiguny, *Chem. Rev.*, 1996, **96**, 2035–2053.
- 5 R. S. Downing, P. J. Kunkeler and H. van Bekkum, *Catal. Today*, 1997, **37**, 121–136.
- 6 A. Corma and P. Serna, *Science*, 2006, **313**, 332–334.
- 7 H. U. Blaster, *Science*, 2006, **313**, 312–313.
- 8 C. Boix and M. Poliakoff, *J. Chem. Soc., Perkin Trans. 1*, 1999, 1487–1490.
- 9 L. Wang, P. H. Li, Z. T. Wu, J. C. Yan, M. Wang and Y. B. Ding, *Synthesis*, 2003, **13**, 2001–2004.
- 10 W. E. Noland, *Chem. Rev.*, 1955, **55**, 137.
- 11 A. T. Nielsen, *The Chemistry of Functional Groups; Nitronates and Nitroxides*, John Wiley, London, 1989.
- 12 H. W. Pinnick, *In Organic Reactions*, John Wiley, London, 1989, vol. 38, ch. 3.
- 13 P. G. Jessop and W. Leitner, *Chemical Synthesis Using Supercritical Fluids*, Wiley-VCH, Weinheim, 1999, 69.
- 14 K. L. Towes, R. M. Shrall and C. M. Wai, *Anal. Chem.*, 1995, **67**, 4040–4043.
- 15 A. I. Vogel, *Vogel's Textbook of Practical Organic Chemistry*, Harlow, Longman, 1989.
- 16 C. Roosen, M. Ansorge-Schumacher, T. Mang, W. Leitner and L. Greiner, *Green Chem.*, 2007, **9**, 455–458.
- 17 S. E. Hunter and P. E. Savage, *Ind. Eng. Chem. Res.*, 2003, **42**, 290–294.
- 18 S. E. Hunter, C. E. Ehrenberger and P. E. Savage, *J. Org. Chem.*, 2006, **71**, 6229–6239.
- 19 G. P. Li, H. F. Jiang and J. H. Li, *Green Chem.*, 2001, **3**, 250–251.
- 20 H. F. Jiang and X. Z. Huang, *J. Supercrit. Fluids*, 2007, **43**, 291–294.
- 21 P. Tundo, A. Loris and M. Selva, *Green Chem.*, 2007, **9**, 777–779.
- 22 C. M. Rayner, *Org. Process Res. Dev.*, 2007, **11**, 121–132.

Super absorbers from renewable feedstock by catalytic oxidation

Wolfgang A. Herrmann,^{*a} Alexandra M. J. Rost,^a Evangeline Tosh,^a Herbert Riepl^b and Fritz E. Kühn^{*a,c}

Received 6th November 2007, Accepted 22nd January 2008

First published as an Advance Article on the web 20th February 2008

DOI: 10.1039/b717134j

An improved, environmentally sound three-component system, MTO/H₂O₂/LiBr, used to prepare biodegradable oxidized starch super absorbers is reported. In contrast to previous systems (ref. 1: W. A. Herrmann, J. P. Zoller and R. W. Fischer, *J. Organomet. Chem.*, 1999, **579**, 404), a highly acidic reaction media is avoided, thus limiting product depolymerisation to a low level. This paper presents an optimized catalytic approach to make carboxy starch, which reduces overall reaction cost, and produces less harmful waste.

Introduction

For the last century the primary feedstocks for chemical industry have been crude oil and natural gas. Due to the significant growth of costs for oil, and that the current economic and environmental impact of the utilization of this resource is of concern, there exists a social and environmental pressure to develop renewable, economic and environmentally sound products which optimize use of this feedstock, and if possible replace it. A switch from non-renewable, fossil resources to renewable raw materials, such as carbohydrates derived from biomass, is a necessary step to the development of a sustainable chemical industry. Materials produced from renewable feedstocks which are biocompatible, biodegradable, CO₂-neutral and less toxic, leave a smaller “environmental footprint” than many crude oil derived products.²

One renewable feedstock material which can be exploited is starch, one of the most abundant and versatile biopolymers. Super absorbers produced from starch³ are quickly replacing synthetic polyacrylate-based super absorbents⁴ which have poor biodegradability.⁵ Examples for applications are self-tightening plastic fabrics used in concrete construction works, which make use of the pressure resulting from swelling upon contact with water, or these found in sanitary bags for infants.³ For technical applications, the use of durable polymers may be necessary, however there is an ever increasing demand for super absorbing commodity products for medicinal or sanitary applications with short product lifetime requiring a quick and safe product decomposition after use.^{3c} There is, accordingly, a clear need for a biodegradable and economical super absorber generated from starch.

Several industrial methods for the manufacture of oxidized starch are known. A common process used to oxidize starch

applies TEMPO mediated oxidation with sodium hypochlorite, which generates stoichiometric amounts of sodium chloride as waste product.⁶ An alternative method is the application of *in situ* generated nitrogen oxides which, however, produces nitric oxides and nitrogen containing salts.⁷ Finally an oxidizing system based on the catalyst methyltrioxorhenium (MTO)⁸ was reported.¹ The three-component system MTO/H₂O₂/HBr in acetic acid catalyzes the selective oxidation of the C6 hydroxy methyl group yielding the corresponding carboxylic acid.

This paper presents an optimized catalytic approach to produce carboxy starch, which reduces overall reaction cost and produces less harmful waste.

Results and discussion

There are a few limitations for the three-component system MTO/H₂O₂/HBr in acetic acid including the use of HBr as co-catalyst, acetic acid as solvent.¹ Many areas for improvement of this system still remain. Due to its multifunctionality, starch requires mild reaction conditions in polar aqueous solvents.⁹ The replacement of highly corrosive HBr by another source of bromide, *e.g.* an alkaline metal salt, which would not be as problematic and harmful as HBr is desirable.¹⁰ Lower operations costs are expected as the reaction mixture is less corrosive, and reactors, pipes and waste streams should be less damaging to the reactor which will require less up keep. The use of HBr is also undesirable as starch is not stable in the presence of strong acids, glycosidic bonds undergo hydrolysis, and therefore the ability of the resultant products to absorb water decreases.¹¹ However, the addition of bromide is necessary as it accelerates the catalytic oxidation by the factor of 1000.¹² A less acidic medium is preferred to prevent the depolymerisation of starch in an acidic medium and the subsequent loss of water absorption capacity.^{11,7c,d}

The success of a given oxidation reaction is quantified by the degree of oxidation determined by a German industrial standard DIN EN ISO 11214, which uses titration.¹³ The water absorption is distinguished by TA- (total absorbency) and CRET-values (absorbency after centrifugation) determined by a previously reported literature method.¹⁴

^aLehrstuhl für Anorganische Chemie, Department für Chemie der Technischen Universität München, Lichtenbergstrasse 4, 85747, Garching bei, München, Germany. E-mail: wolfgang.herrmann@ch.tum.de; Fax: +49 89 289 13473

^bLehrstuhl für Rohstoff- und Energietechnologie der Technischen Universität München, Petersgasse 18, 94315, Straubing, Germany

^cMolekulare Katalyse, Department für Chemie der Technischen Universität München, Lichtenbergstrasse 4, 85747, Garching bei München, Germany. E-mail: fritz.kuehn@ch.tum.de; Fax: +49 89 289 13473

Table 1 Oxidation of potato starch in the presence of alternative bromide sources with the three-component system MTO/H₂O₂/Br⁻

| Bromide | TA | CRET | Degree of oxidation (%) |
|---------|-----|------|-------------------------|
| HBr | 3.0 | 2.4 | 18.9 |
| LiBr | 6.2 | 4.5 | 12.1 |
| NaBr | 6.0 | 4.4 | 11.8 |
| KBr | 6.3 | 4.3 | 12.4 |

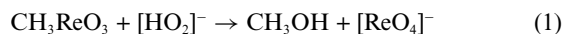
Alternative bromide sources

Alternative sources of bromide were tested as shown in Table 1.

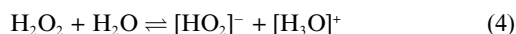
As expected, when HBr is used as co-catalyst the degree of oxidation is significantly higher than for the cases of the bromide salts. However, water absorption of the resultant product is lower because of the hydrolysis of the glycosidic bonds. All alkaline metal salts show comparable results. They achieve lower degrees of oxidation than HBr but the water absorption of resultant polymers is double. As a result, it is reasonable to propose alkaline bromides be used as a replacement for the highly corrosive HBr in the described catalytic system. The solubility in polar aqueous solvents of the alkaline bromides declines with molar mass. Therefore the use of LiBr, with the best solubility (177 g per 100 mL H₂O), is most favourable for an optimized system. However, Li ions, which are not removed at water treatment stations, have physiological effects (e.g. as antidepressants), thus this bromide source can be replaced by the economically more advantageous NaBr with a slightly lower oxidation performance.

Acidity

As described above, the application of 100% acetic acid is detrimental to water absorption of the oxidation product. A neutral medium is optimal to minimize depolymerisation. However, the stability of the catalyst decreases with increasing hydroxide concentration. In the presence of [OH]⁻, MTO and the catalytic active species (the mono- and bisperoxo complex derived from MTO), are deactivated to yield methanol and catalytic inactive perrhenate (see eqn (1)–(3)).¹⁵



In the presence of hydrogen peroxide, the deactivation occurs more readily due to the formation of the hydroperoxide anion from hydrogen peroxide present in aqueous solutions as hydroperoxide is a better nucleophile.



In this equilibrium, the concentration of hydroperoxide can be lowered by an increase of the pH of the solution and therefore the deactivation is significantly slowed (eqn (4)). Various mixtures of water and acetic acid were tested to establish optimum solvent acidity for the oxidation of starch. The results are shown in Table 2.

Using pure acetic acid as solvent, the highest degree of oxidation is achieved (12.1%). However, the water absorption of

Table 2 Oxidation of potato starch with the three-component system MTO/H₂O₂/Br⁻ using different mixtures of water and acetic acid as solvent

| Solvent | TA | CRET | Degree of oxidation (%) |
|------------------------------|-----|------|-------------------------|
| 0% HAc/100% H ₂ O | 2.9 | 2.1 | 1.3 |
| 25% HAc/75% H ₂ O | 3.3 | 2.7 | 3.4 |
| 50% HAc/50% H ₂ O | 7.1 | 5.9 | 10.3 |
| 75% HAc/25% H ₂ O | 6.4 | 5.2 | 11.6 |
| 100% HAc/0% H ₂ O | 6.2 | 4.5 | 12.1 |

the product measured by TA- and CRET-values is not optimal due to the depolymerisation of the product in acid conditions. The water absorption is highest when a 50/50% acetic acid/water mix is used. When the ratio of acid decreases, catalyst deactivation is of greater impact than product depolymerisation, and both the degree of oxidation and the water absorption are very low. The 50/50% acetic acid/water mix appears to be a good balance between catalyst stability and substrate hydrolysis.

Addition rate of hydrogen peroxide

Another way to influence the equilibrium of the formation of hydroperoxide (eqn (4)) is by the rate of hydrogen peroxide addition. When the oxidant is added slowly, its concentration is low and therefore the amount of hydroperoxide decreases in the equilibrium. The speed of addition was controlled by a pump with variable solution addition velocity (1–0.05 equiv. min⁻¹). The results are shown in Table 3.

Applying the slowest rate of H₂O₂ addition, 0.05 equiv. min⁻¹, the highest degree of oxidation and the best water absorption of the resultant product is observed. Increasing the rate leads to lower water absorption and oxidation. According to eqn (4) the concentration of the hydroperoxide ion, which is responsible for the deactivation of MTO, can be minimized by Le Chatelier's principle. Using the slowest rate of addition the total reaction time is extended from one to two hours.

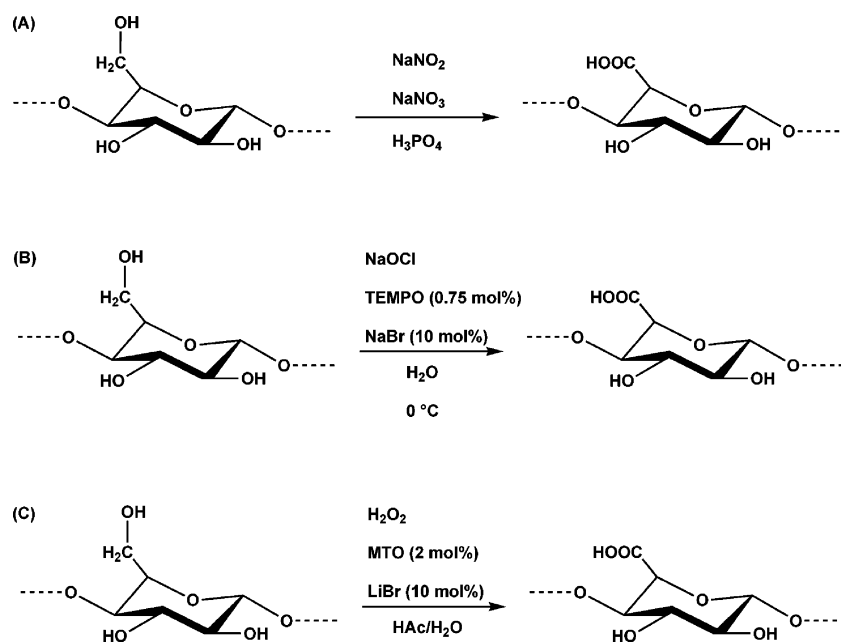
Comparison of the catalytic route with industrial methods

The oxidation of starch with the three-component system MTO/H₂O₂/Br⁻ under optimized conditions (see above) was compared with the two common industrial processes for the production of carboxy starch. The industrial processes, oxidation with *in situ* generated nitrogen oxides⁷ (A) and TEMPO mediated oxidation by sodium hypochlorite⁶ (B) along with our optimized system (C) are shown in Scheme 1.

The results of these different oxidation systems are shown in Table 4.

Table 3 Oxidation of potato starch applying various speeds of addition of hydrogen peroxide with the three-component system MTO/H₂O₂/Br⁻

| Addition speed of H ₂ O ₂ /(equiv. min ⁻¹) | TA | CRET | Degree of oxidation (%) |
|--|-----|------|-------------------------|
| 0.05 | 8.5 | 6.8 | 23.3 |
| 0.1 | 7.4 | 5.4 | 17.9 |
| 0.5 | 5.3 | 3.9 | 6.6 |
| 1 | 3.4 | 2.7 | 2.3 |



Scheme 1 Processes yielding carboxy starch: (A) oxidation with *in situ* generated nitrogen oxides;⁷ (B) TEMPO mediated oxidation by sodium hypochlorite;⁶ (C) oxidation applying the optimized three-component system $\text{MTO}/\text{H}_2\text{O}_2/\text{Br}^-$.

Table 4 Results of the oxidation of potato starch applying routes (A)–(C)

| Oxidation method | TA | CRET | Degree of oxidation (%) |
|---|-----|------|-------------------------|
| Route A: <i>in situ</i> generated nitrogen oxides | 3.7 | 2.2 | 36.8 |
| Route B: TEMPO/NaBr/NaOCl | 8.2 | 7.1 | 27.7 |
| Route C: catalytic three-component system | 8.5 | 6.8 | 23.3 |

The highest degree of oxidation, 36.8%, is achieved using *in situ* generated nitrogen oxides as an oxidant. However, the ability of water absorption of the resultant product is poor (reflected in low TA- and CRET-values) because of depolymerisation in the highly acidic reaction medium. The catalytic three-component system (C) and the oxidation process applying TEMPO and NaOCl (B) are comparable: (B) gives better yields, (C) results in a slightly better water absorption capacity.

The three-component system $\text{MTO}/\text{H}_2\text{O}_2/\text{Br}^-$ is a significantly improved alternative method for the production of super absorber compared to those currently in use. The optimized system is composed of 2 mol% MTO, 10 mol% LiBr and 300 mol% H_2O_2 with 50% acetic acid as solvent. Our efforts improve the ability of water absorption of resulting super absorbers significantly, however the degree of oxidation differs only marginally. The TA-values are increased from 3.6 to 8.5 by a factor of 2.4, the CRET-value increases from 2.4 to 6.8 by a factor 2.8 and the degree of oxidation is improved from 18.9% to 23.3%. The highly corrosive bromide source HBr is successfully replaced by less problematic LiBr. The amount of the oxidant hydrogen peroxide required is reduced from 400 mol% to 300 mol% yielding better oxidation results. A 50% acetic acid 50% water mixture was shown to be a good

compromise between the enhancing stability of the catalyst MTO and limiting the hydrolysis of the substrate starch. In addition, the solvent is more environmentally benign as a result of using less acetic acid because less base is required for the neutralization of the waste water before it is purified in the sewage treatment plant. If hydrogen peroxide is added slowly the concentration of the hydroperoxide ion decreases significantly and therefore the deactivation of the catalyst is again minimized. The optimal rate for the addition of the oxidant was found to be $0.05 \text{ equiv. min}^{-1}$.

In comparison to the two industrial methods for the manufacture of carboxy starch described above, the three-component system $\text{MTO}/\text{H}_2\text{O}_2/\text{Br}^-$ is more environmentally sound. The atom efficiency¹⁶ ($\text{AE} = M(\text{product})/M(\text{starting material}) + M(\text{stoichiometric reagents})$) of the oxidation with *in situ* generated nitrogen oxides is 56%. In spite of a high degree of oxidation of the resultant carboxy starch, the water absorption is very low (TA = 3.7, CRET = 2.2) because depolymerisation of the starch occurs under acidic conditions. The stoichiometric use of inorganic oxidants is not optimal as large amounts of nitric oxides (NO_x) and inorganic nitrogen salts are generated as waste products. The oxidation process applying TEMPO and sodium hypochlorite has a atom efficiency¹⁶ of 57%. Water absorption and degree of oxidation of the product were similar to those of products of the three-component system. However, stoichiometric amounts of sodium chloride are produced as a waste product and as a consequence of a side reaction, chlorinated starch derivatives⁶ are generated as by-products decreasing the biodegradability of the resultant material. The atom efficiency¹⁶ for the oxidation of starch applying the optimized three-component system $\text{MTO}/\text{H}_2\text{O}_2/\text{Br}^-$ is 77%. This method is selective, environmentally benign and sustainable, because no by-products occur and the green oxidant hydrogen peroxide is used resulting in water after the reaction and thereby reducing the waste.

Conclusions

A selective oxidation process for the generation of a super absorber from biomass using the key principles of green chemistry, catalysis and the utilization of renewable resources, is herein described. By balancing the social, environmental and economic impact of a variety of possible alterations to the catalytic process a balance has been met that provides an economic and environmentally more advantageous process. The selective oxidation, applying the newly developed three-component system MTO/H₂O₂/Br⁻, has been shown to be a convenient method for the manufacture of carboxy starch with mild reaction conditions that are not only environmentally sound but also cost-effective. With regard to the recently reported tin free synthesis of MTO¹⁷ the above described method is superior to the hitherto industrial important processes applying TEMPO/NaOCl⁶ or *in situ* generated nitrogen oxides.⁷ Nevertheless, many areas for optimization still remain. The amount of the rhenium catalyst used in the reaction is high, because part of it is lost by deactivation of the active Re(VII) centres as perrhenate by hydroxide ion in the aqueous reaction medium. However, the inactive perrhenate can be easily recovered.¹⁸ Thus, the valuable catalyst, which now is available by a improved, cost efficient and new synthetic route,¹⁷ can be recycled with near quantitative yields. Further efforts to improve the above described method for the manufacture of carboxy starch are currently being undertaken in our laboratories. The resulting product is advantageous compared to conventional polyacrylate-based super absorbents, and although they display lower water absorption, super absorbents made with oxidized starch are completely biodegradable.

Experimental

Soluble potato starch purchased from Sigma was used for the oxidation reactions. The oxidation catalyst MTO was prepared according to the literature.¹⁷

Oxidation of starch with the three-component system (MTO/H₂O₂/Br⁻)

Standard procedure. 3.25 g potato starch was suspended in 80 mL water. The mixture was stirred at 100 °C for 15 min and then cooled to room temperature. 80 mL acetic acid, 174 mg LiBr, 100 mg MTO and 7.0 mL H₂O₂ (35 wt%; 0.05 equiv. min⁻¹) were added. The reaction progress was monitored by colour change and regarded as being complete when the yellow reaction mixture became colourless. The oxidized starch is precipitated by the addition of 100 mL methanol. The resulting solid was separated, washed twice with a mixture of water and methanol (30/70) and dried under vacuum to constant weight. After milling the resulting solid the super absorber is obtained as a white powder.

Oxidation of starch with TEMPO and NaOCl

3.25 g potato starch was suspended in 170 mL water. The mixture was stirred at 100 °C for 15 min and then cooled to 2 °C. 24 mg TEMPO and 206 mg NaBr were added. 18.8 mL of a 13% solution of NaOCl in water was added dropwise and the pH

was maintained between 8.0 and 8.5 with 0.5 M NaOH. After a reaction time of 30 min at 2 °C, the reaction mixture was allowed to warm to room temperature. The pH was adjusted between 5.5 and 6.0 with 4 M HCl. The oxidized starch was precipitated by the addition of 50 mL of a mixture of methanol and water (70/30). The resulting solid was separated, washed twice with a mixture of water and methanol (30/70) and dried under vacuum to constant weight. After milling the resulting solid the super absorber is obtained as a white powder.

Oxidation of starch with *in situ* generated nitrogen oxides

3.25 mg potato starch was suspended in 3.5 ml H₃PO₄ (85%). After the addition of 0.26 g NaNO₂ and 2.6 g NaNO₃ the mixture was stirred for 6 h at room temperature. The oxidized starch was precipitated by the addition a mixture of methanol and water (80/20). The resulting solid was separated, washed twice with a mixture of water and methanol (30/70) and dried under vacuum to constant weight. After milling the resulting solid the super absorber is obtained as a white powder.

Determination of the water absorption ability

Degree of oxidation. The degree of oxidation was determined by the standard procedure (DIN EN ISO 11214) using titration according to a German industrial standard.¹³

5 g oxidized starch (dried to constant weight *in vacuo*; grit size < 0.8 mm) are suspended in 25 mL 0.1 M HCl. The mixture was stirred for 30 min. The solid was separated by filtration, washed several times with small portions of water, suspended in 300 mL water and stirred for 20 min at 100 °C. After the addition of phenolphthalein the hot solution is titrated with 0.1 M NaOH until the colour of the solution change to pink.

The degree of oxidation with respect to the percentage carboxyl groups present in the polymer is calculated according to the following equation (V_{NaOH} = consumption of NaOH in mL; m = initial weight of oxidized starch):

$$w_{\text{COOH}} = \frac{0.1 \times 0.045 \times 100 V_{\text{NaOH}}}{m}$$

Modified tea bag method. The water absorption of the resulting polymers was distinguished by TA (total absorbency) and CRET-values (absorbency after centrifugation) according to previously established literature methods.¹⁴

250–300 mg (m_1) of oxidized starch (dried to constant weight *in vacuo*; grit size 0.3–0.5 mm) was charged in a bag made from filter paper, which was closed with a clip. The filled bag was weighed again (m_2), immersed in 50 mL NaCl solution (0.9 wt%) for 20 min. After 3 min drain its weight was determined (m_3). The TA value is calculated according to the following equation:

$$\text{TA} = \frac{m_3 - m_2}{m_1}$$

Then the tea bag was centrifuged at 1400 rpm and reweighed (m_4). The CRET value is calculated according to the following

equitation:

$$\text{CRET} = \frac{m_4 - m_2}{m_1}$$

Acknowledgements

The authors are grateful to the Margarethe-Ammon Foundation (PhD grant for A. R.) and the Elitenetzwerk Bayern (PhD grant for E. T.).

References

- 1 W. A. Herrmann, J. P. Zoller and R. W. Fischer, *J. Organomet. Chem.*, 1999, **579**, 404.
- 2 B. E. Dale, *J. Chem. Technol. Biotechnol.*, 2003, **78**, 1093.
- 3 (a) A. de Nooy, A. C. Besemer and H. van Bekkum, *Carbohydr. Res.*, 1995, **269**, 89; (b) A. B. Sorokin, S. L. Kachkarova-Sorokina, C. Donze, C. Pinel and P. Gazelot, *Top. Catal.*, 2004, **27**, 67; (c) W. A. Herrmann, R. W. Fischer and J. P. Zoller, *WO 0061639*, 2000.
- 4 M. O. Weaver, *Stärke*, 1977, **29**, 414.
- 5 W. Ban, J. Song, D. S. Argyropoulos and L. A. Lucia, *Ind. Eng. Chem. Res.*, 2006, **45**, 627.
- 6 (a) A. C. Besemer and A. E. J. de Nooy, *WO 9507303*, 1995; (b) A. E. J. de Nooy and A. C. Besemer, *Recl. Trav. Chim. Pays-Bas*, 1994, **113**, 165.
- 7 (a) A. C. E. Besemer, A. E. J. de Nooy, NL 9301172, 1992; (b) A. E. J. de Nooy, Dissertation, Technische Universiteit Delft, 1997; (c) T. J. Painter, *Carbohydr. Res.*, 1977, **55**, 95; (d) T. J. Painter, *Carbohydr. Res.*, 1985, **140**, 61.
- 8 (a) F. E. Kühn, A. M. Santos and W. A. Herrmann, *Dalton Trans.*, 2005, 2483; (b) F. E. Kühn, A. Scherbaum and W. A. Herrmann, *J. Organomet. Chem.*, 2004, **689**, 4149; (c) W. A. Herrmann and F. E. Kühn, *Acc. Chem. Res.*, 1997, **30**, 169; (d) C. C. Romão, F. E. Kühn and W. A. Herrmann, *Chem. Rev.*, 1997, **97**, 3197; (e) W. A. Herrmann, R. W. Fischer, W. Scherer and M. U. Rauch, *Angew. Chem.*, 1992, **105**, 1209, (*Angew. Chem., Int. Ed.*, 1992, **32**, 1157); (f) W. A. Herrmann, F. E. Kühn, R. W. Fischer, W. R. Thiel and C. C. Romão, *Inorg. Chem.*, 1992, **31**, 4431; (g) W. A. Herrmann, W. Wagner, U. N. Flessner, U. Volkhardt and H. Komber, *Angew. Chem.*, 1991, **103**, 1704, (*Angew. Chem., Int. Ed.*, 1991, **30**, 1636); (h) W. A. Herrmann, R. W. Fischer and D. W. Marz, *Angew. Chem.*, 1991, **103**, 1706, (*Angew. Chem., Int. Ed.*, 1991, **30**, 1638); (i) W. A. Herrmann and M. Wang, *Angew. Chem.*, 1991, **103**, 1709, (*Angew. Chem., Int. Ed.*, 1991, **30**, 1641).
- 9 S. J. H. F. Arts, E. J. M. Mombarg, H. van Bekkum and A. Sheldon, *Synthesis*, 1997, 597.
- 10 G. Smudde, W. Bailey, B. Felker, M. George and J. Langan, *Corros. Sci.*, 1995, **37**, 1931.
- 11 (a) A. de Nooy, Dissertation, Technische Universiteit Delft, 1999; (b) B. Feuer and H.-J. Haack, *DE 19746805*, 1997.
- 12 J. H. Espenson and T. H. Zauche, *Inorg. Chem.*, 1998, **37**, 6827.
- 13 DIN Deutsches Institut für Normung e.V., *Modified starch—determination of carboxyl group content of oxidized starch*, DIN EN ISO 11214, Beuth Verlag, Berlin, 1996.
- 14 (a) G. Jonas, H. Klimmek, *DE 19645240*, 1998; (b) H. Brueggemann and K. Dahmen, *DE 19505708*, 1996; (c) H. Eschwey and L. Hackler, *DE 3720031*, 1989; (d) T. Yoshimura, R. Yoshimura, C. Seki and R. Fujioka, *Carbohydr. Polym.*, 2006, 345.
- 15 (a) J. H. Espenson, *Chem. Commun.*, 1999, 479; (b) G. Laurency, F. Lukacs, R. Roulet, W. A. Herrmann and R. W. Fischer, *Organometallics*, 1996, **15**, 848; (c) M. M. Abu-Omar, P. J. Hansen and J. H. Espenson, *J. Am. Chem. Soc.*, 1996, **118**, 4699.
- 16 (a) B. M. Trost, *Science*, 1991, **254**, 1471; (b) B. M. Trost, *Angew. Chem.*, 1995, **107**, 285, (*Angew. Chem., Int. Ed.*, 1995, **34**, 259).
- 17 (a) W. A. Herrmann, A. M. J. Rost, J. K. M. Mitterpleininger, N. Szesni, S. Sturm, R. W. Fischer and F. E. Kühn, *Angew. Chem.*, 2007, **119**, 7440, (*Angew. Chem., Int. Ed.*, 2007, **47**, 7301); (b) E. Tosh, J. K. M. Mitterpleininger, A. M. J. Rost, D. Veljanovski, W. A. Herrmann and F. E. Kühn, *Green Chem.*, 2007, **9**, 1296.
- 18 W. A. Herrmann, R. M. Kratzer and R. W. Fischer, *Angew. Chem.*, 1997, **109**, 2767, (*Angew. Chem., Int. Ed.*, 1997, **36**, 2652).

Practical oxidation of sulfides to sulfones by H₂O₂ catalysed by titanium catalyst

Walid Al-Maksoud, Stéphane Daniele* and Alexander B. Sorokin*

Received 15th November 2007, Accepted 23rd January 2008

First published as an Advance Article on the web 21st February 2008

DOI: 10.1039/b717696a

The oxidation of thianisole and other substituted arylalkyl and diaryl sulfides with aqueous H₂O₂ as the oxidant and heterogeneous TiO₂ catalyst exhibits a high selectivity affording the corresponding sulfones with 80–98% isolated yields. It should be noted that H₂O₂ provided better results as compared with *t*-BuOOH in terms of the reaction rate and yields of sulfones. The use of hydrogen peroxide and heterogeneous nanocrystalline titania catalyst is a green alternative to the traditional stoichiometric oxidation providing high yields of sulfones in one step.

Introduction

The oxidation of organosulfur compounds is of much current interest in the context of the preparation of synthetically useful sulfoxides^{1,2} and sulfones,³ as well as of the desulfurization of fuels.⁴ Because of environmental regulations limiting the sulfur content in fuel oils to the few ppm level, ultra-deep desulfurization has become an important topic of research. Dibenzothiophenes, recalcitrant in the process of catalytic hydrodesulfurization, can be oxidized to sulfoxides and/or sulfones, which can be removed from fuel by extraction or absorption using their polar properties.⁴ On the other hand, the same catalytic oxidation can be used for preparation of very important synthetic intermediates such as sulfoxides. Chiral sulfoxides are widely used in asymmetric synthesis, including important pharmaceuticals that often contain sulfinyl fragments.²

Along with sulfoxides, sulfones are also very useful building blocks for the preparation of elaborated organic structures. However, the oxidation of sulfides to sulfones is much less investigated as compared to the oxidation of sulfides to sulfoxides. Typical stoichiometric oxidants include CrO₃ in AcOH, KMnO₄, HNO₃, RuO₄, H₂O₂ in AcOH, *etc.*^{3b} Recently, stoichiometric oxidation of sulfides by sodium percarbonate and sodium perborate in the presence of solid supports (silica, alumina or amberlyst) boosted by microwave irradiation was published.⁵ Using appropriate reaction conditions (choice of oxidant, support and method of heating) it was possible to obtain preferentially sulfoxides or sulfones. Different sulfides were oxidized using dioxygen in combination with 2-methylpropanal (5 equivalents) leading to 51–78% yields of sulfones.^{3c} Addition of cobalt(II) salophen catalyst allowed the use of a 2-fold excess of aldehyde, keeping the sulfone yields in the range of 31–81%.^{3c} Binuclear [Mn^{IV}–Mn^{IV}(μ-O)₃L₂](PF₆)₂(L = 1,4,7-trimethyl-1,4,7-triazacyclononane) complex catalyzed the

oxidation of sulfides by H₃IO₆ to afford 39–99% sulfone yields.^{3d} A quantitative oxidation of PhSCH₃, PhSCH₂CH₂Cl and (PhCH₂)₂S by H₂O₂ (5.6 equivalents) was achieved in the presence of iron tetraphenylporphyrin (2.35 mol%).^{3c} A variety of electron-rich and electron-deficient sulfides were oxidized with 4 equiv. of H₃IO₆ (oxidant) and 2 mol% of CrO₃ (catalyst) to provide 90–97% yields of sulfones.^{3b} Finally, osmate-exchanged Mg–Al layered double hydroxides were shown to be efficient in aerobic oxidation of sulfides directly to sulfones.^{3a} A serious drawback of these published methods is the use of toxic oxidants and sophisticated homogeneous catalysts. Evidently, current demand for environmentally friendly processes requires the development of green oxidation methods that employ clean oxidants, such as hydrogen peroxide, and an accessible heterogeneous catalyst.

In the past decade, a considerable amount of research was dedicated to the preparation of various Ti-containing mesoporous materials and their use as catalysts in the selective oxidation of organic substrates with hydrogen peroxide or *tert*-butyl hydroperoxide (*t*-BuOOH).^{6,7} Several Ti containing catalysts were used for the oxidation of sulfides.⁸ Titanium silicate molecular sieves TS-1 and TS-2 catalyzed the oxidation of sulfides by H₂O₂ (1.2 mol equiv. to substrate) to sulfoxide–sulfone mixtures (for example, PhSOMe/PhSO₂Me = 78/22).^{8a} Ti-beta and Ti-MCM-41 were also active with *t*-BuOOH (1.1 mol equiv.) and H₂O₂ (3 mol equiv.) to give sulfoxide and sulfone in approximately 2 : 1 ratio.^{8b} Ti-beta catalyst was more active than TS-1 in oxidation of dibutylsulfide to dibutylsulfone providing 78% and 20.5% conversions, respectively.^{8c} Several titanium derivatives supported on silica were investigated for oxidation of a variety of sulfides to sulfoxides with 1 mol equiv. of *t*-BuOOH and H₂O₂, sulfones being only minor products.^{8d} Ti-containing zeolite allowed the oxidation of PhSMe and Ph₂S by H₂O₂ (1 mol equiv.) to sulfones with 70 and 38% conversions, respectively, probably because of diffusion limitation.^{8e} Polymeric Ti(IV) glycolate performed oxidation of sulfides to sulfoxides using 1 mol equiv. of *t*-BuOOH as the oxidant.^{8f} Ti-MCM-41 catalyzed formation of sulfoxides from sulfides using H₂O₂ photogenerated from benzhydrol and molecular oxygen.^{8g} Consequently, the oxidation of sulfides in the presence of Ti-based

Université Lyon 1, Institut de Recherches sur la Catalyse et l'Environnement de Lyon (IRCELYON), UMR5256, 2, Avenue A. Einstein, 69626, Villeurbanne Cedex, France. E-mail: sorokin@catalyse.cnrs.fr, stephane.daniele@ircelyon.univ-lyon1.fr; Fax: +33 472445399, +33 472445399; Tel: +33 472445337, +33 472445360

Table 1 Oxidation of the thioanisole by H₂O₂ and ^tBuOOH catalyzed by different TiO₂ catalysts at 80 °C^a

| Entry | Catalyst | Oxidant | Time/h | Conversion (%) | Sulfoxide yield (%) | Sulfone yield (%) |
|-------|------------------------------------|-------------------------------|--------|----------------|---------------------|-------------------|
| 1 | — | ^t BuOOH | 6 | 14 | 10 | 4 |
| 2 | TiO ₂ -100 | ^t BuOOH | 5 | 99 | 1 | 86 |
| 3 | TiO ₂ -400 | ^t BuOOH | 4 | 99 | 3 | 83 |
| 4 | TiO ₂ -P25 | ^t BuOOH | 4 | 65 | 9 | 46 |
| | | | 24 | 96 | 5 | 88 |
| 5 | TiO ₂ -H | ^t BuOOH | 3 | 98 | 1 | 93 |
| 6 | — | H ₂ O ₂ | 3 | 48 | 25 | 23 |
| 7 | TiO ₂ -100 | H ₂ O ₂ | 3 | 100 | 0.5 | 98 |
| 8 | TiO ₂ -400 | H ₂ O ₂ | 3 | 100 | — | 96 |
| 9 | TiO ₂ -400 ^b | H ₂ O ₂ | 3 | 100 | — | 96 |
| 10 | TiO ₂ -P25 | H ₂ O ₂ | 3 | 100 | — | 86 |
| 11 | TiO ₂ -H | H ₂ O ₂ | 2 | 100 | — | 94 |

^a Conditions: 0.4 mmol substrate, 37.4 mg catalyst, 1.2 mmol oxidant in 4 mL MeCN at 80 °C. ^b Reaction in dark.

catalysts and near equimolar amount of oxidant provides mainly sulfoxides or often the mixture of two possible products, sulfoxide and sulfone.

Recently, we have reported the preparation of nanocrystalline particles of titania at low temperature (100 °C) by a sol–gel process.⁹ The same approach was used to prepare a nanocrystalline TiO₂–iron tetrasulphophthalocyanine catalyst which demonstrated promising catalytic properties in the selective aerobic oxidation of β-isophorone to ketoisophorone.¹⁰ The combination of two catalytic sites in this material provided better product yields.

Herein, we report a practical and green method for oxidation of various sulfides by aqueous H₂O₂ and nanocrystalline titania to corresponding sulfones with high selectivity.

Results and discussion

As prepared nanocrystalline TiO₂ particles (denoted TiO₂-100, specific surface area $S_{\text{BET}} = 245 \text{ m}^2 \text{ g}^{-1}$) and calcinated samples at 400 °C (denoted TiO₂-400, $S_{\text{BET}} = 132 \text{ m}^2 \text{ g}^{-1}$) were elaborated as described previously.⁹ Such materials contain anatase (75–80%) as the main phase along with brookite, and are composed of elongated nanocrystals of 6–8 nm in length. For comparison of the catalytic activity in the oxidation of sulfides, we have also used commercially available TiO₂ catalysts such as Degussa-P25 (denoted TiO₂-P25, $S_{\text{BET}} = 55 \text{ m}^2 \text{ g}^{-1}$) and Hombikat UV 100 (denoted TiO₂-H, $S_{\text{BET}} > 250 \text{ m}^2 \text{ g}^{-1}$).

We first investigated the oxidation of thioanisole as model substrate using ^tBuOOH and H₂O₂, as oxidants. Standard conditions were 4 mL of the 0.1 M PhSMe solution and 37.4 mg

of TiO₂ at 80 °C in acetonitrile. The results are summarized in Table 1. Without any Ti catalyst, the conversions of PhSMe were 14 and 48% in the presence of ^tBuOOH and H₂O₂, respectively. In addition, both sulfoxide and sulfone products were formed. When ^tBuOOH was used as the oxidant, our as-prepared catalysts were more active than the TiO₂-P25 one, while TiO₂-H exhibited slightly better selectivity properties. We were delighted to observe that H₂O₂ provided even better results than ^tBuOOH. In addition to its environmentally benign properties, H₂O₂ is superior to ^tBuOOH in terms of reaction rate, conversion, selectivity of reaction and the yield of sulfone product. All TiO₂ catalysts provided quasi-quantitative yield of methyl phenyl sulfone. The best results were obtained by using the TiO₂-400 catalyst. For instance, the crude product easily obtained without any purification procedure, just separation of heterogeneous catalyst by filtration, and was already of high purity as indicated by its ¹H NMR spectrum (Fig. 1). Since TiO₂ is a notorious photo-catalyst, it was noteworthy that the same results were obtained in the presence and in the absence of the light (Table 1, entries 8,9) which strongly suggested the absence of photo-assisted oxidation.

We studied the influence of different reaction parameters (solvent, temperature, mass of catalyst) on the efficiency of our TiO₂-400 nanomaterial for thioanisole oxidation. The reaction was sensitive to solvent, acetonitrile being the best one. Its replacement by acetone or CH₂Cl₂ led to a decrease in sulfone yield, especially in the case of CH₂Cl₂ (Table 2). Hydrogen peroxide is known to react with MeCN to form peroxycarboximide acid *in situ*.¹¹ This is an equilibrium reaction shifted to the H₂O₂ and MeCN side, especially in the absence

Table 2 Influence of the solvent and the temperature on the oxidation of the thioanisole by H₂O₂ catalyzed by TiO₂-400

| Solvent | T/°C | Conversion (%) | Sulfoxide yield (%) | Sulfone yield (%) |
|---------------------------------|------|------------------|---------------------|-------------------|
| MeCN | 25 | 98 | 4 | 90 |
| | | 100 ^b | — | 100 ^b |
| MeCN | 40 | 100 | — | 99 |
| MeCN | 80 | 100 | — | 98 |
| Acetone | 40 | 97 | 3 | 79 |
| CH ₂ Cl ₂ | 40 | 37 | 19 | 9 |

^a Conditions: 0.4 mmol substrate, 5 mg TiO₂-400 catalyst, 1.2 mmol oxidant in 4 mL solvent; reaction time 3 h. ^b Reaction time 16 h.

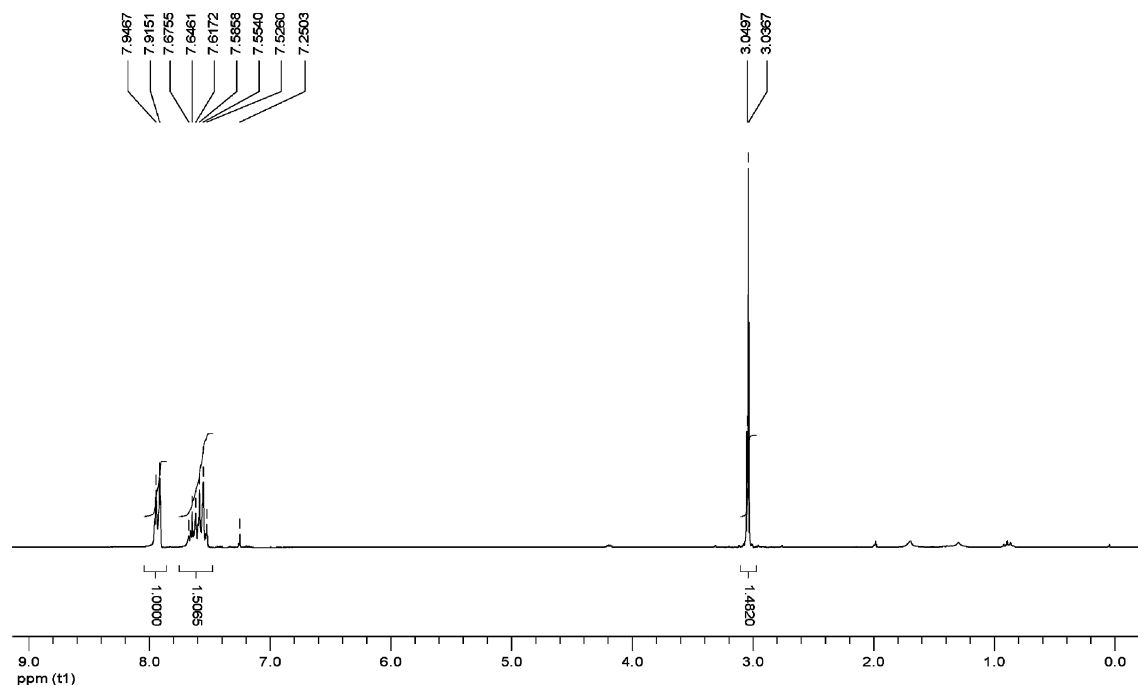


Fig. 1 ^1H NMR spectrum (CDCl_3) of the reaction mixture in oxidation of PhSMe by H_2O_2 catalyzed by TiO_2 -400; acetonitrile, 80°C , 3 h.

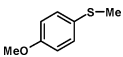
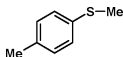
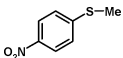
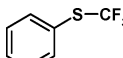
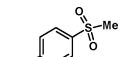
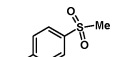
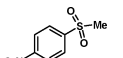
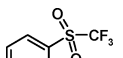
of base. Thus, only 5% of peroxide reacted with MeCN at 68°C in 24 h reaction.^{11a} Peroxycarboximidic acid is able to epoxidize olefins (Payne epoxidation)¹¹ and ketones (Baeyer–Villiger oxidation).¹² When this intermediate is involved, the reaction works only in MeCN medium.¹² In our case, possible participation of peroxycarboximidic acid should not be the principal reaction pathway because (i) no base is added to the reaction mixture, (ii) the reaction in MeCN occurs also at 25°C and (iii) other solvents, *e.g.* acetone, can be used.

The amount of the surface titanium sites accessible for catalysis was estimated as follows. Considering spherical particles of 8 nm of diameter and a surface area of 0.2 nm^2 for each external TiO_4 framework, one gram of TiO_2 -100 and TiO_2 -400 samples

led to around 2 and 1 mmol of titanium sites at the surface, respectively. The standard conditions used for the oxidation of PhSMe employed the catalyst, the substrate and the oxidant in the molar ratio 1 : 10.7 : 32.1. Interesting results have been obtained while studying the amount of solid catalyst employed for the oxidation. Remarkably, using 20, 10 or even 5 mg of TiO_2 -400 (1.25 mol% to substrate) in combination with H_2O_2 provided the complete conversion of PhSMe and the same 96–99% yield of sulfone, indicating a very good catalytic performance of the titania catalyst.

Using the optimized catalytic conditions derived from the above experiments the scope of the method has been extended to the oxidation of different sulfides including substituted aryl-alkyl and diaryl sulfides (Table 3). In all cases a high

Table 3 Oxidation of sulfides by H_2O_2 catalyzed by TiO_2 -400^a

| Substrate | Product | $T/^\circ\text{C}$ | Conversion (%) | Isolated yield (%) |
|---|---|--------------------|-------------------|--------------------|
|  |  | 40 | 100 | 99 |
|  |  | 80 | 89 | 80 |
|  |  | 40 | n.d. ^b | 83 |
|  |  | 40 | <10 | — |
| PhSPh | PhSO ₂ Ph | 80 | 90 | 81 |

^a Percent conversion and product yield were determined by ^1H NMR. Purity of the isolated products was demonstrated by ^1H NMR. ^b Not determined.

chemoselectivity toward formation of sulfones was observed. Corresponding sulfones were obtained with 80–99% isolated yields except PhSCF₃ where strong electron-withdrawing CF₃ group completely deactivated the substrate.

The possibility of recycling of the catalyst was demonstrated in the oxidation of PhSMe with 5 mg of TiO₂-400 at 40 °C. After completing the first run, new portions of the substrate and oxidant were directly added to the reaction mixture. Three successive oxidations of PhSMe showed that the catalytic activity remained high, the conversion being 100, 99 and 99%, respectively. The yields of sulfone were also consistent: 100, 96, and 93%, respectively. PhSOMe was obtained in 3 and 6% yields in run 2 and 3, respectively. The total turnover number attained was 238 cycles, showing high performance of the catalyst on re-use in continuous operation. In order to evidence the heterogeneous nature of catalytic oxidation we separated the solution by filtration at the reaction temperature as proposed by Sheldon *et al.*¹³ after 2 h reaction time. No Ti was found in solution. The detection limit of inductively coupled plasma-mass spectrometry method was estimated to be less than 0.2 ppm of Ti, which means that possible leaching of Ti into solution was less than 0.01% with respect to amount of TiO₂ used.

We attempted to perform the oxidation of PhSMe without solvent. However, after addition of 0.15 equivalents of oxidant, as 35% aqueous H₂O₂ solution, the reaction mixture was separated into organic and aqueous phases with the catalyst situated in the aqueous layer. This diminished the reaction rate and complicated the product analysis. Nevertheless, 31% conversion of PhSMe was achieved after 20 h.

The preparative oxidation of PhSMe was performed in MeCN (1.5 mL) at 4.25 mmol scale (0.5 mL) using 37.4 mg of TiO₂-400 catalyst and 9.6 mmol of H₂O₂ at 80 °C. The amount of oxidant was equal to 1.13 equiv. to substrate taking into account that 2 fold excess of H₂O₂ is necessary to convert sulfide to sulfone. Hydrogen peroxide 35% solution was added portion-wise at 0, 15, 30, 45, 60, 75, 90 and 105 min (1.2 mmol portion). The kinetics of the oxidation is presented in Fig. 2. The oxidation of PhSMe was very fast, the conversion being 99% after 1.5 h. Sulfoxide, the main product at the beginning of the oxidation, was rapidly converted to sulfone. The yield of sulfone attained 97% after 2.5 h. Remarkably, a quasi-equivalent amount of H₂O₂ oxidant was sufficient to achieve the 97% yield of sulfone, indicating a high efficiency of the oxidation.

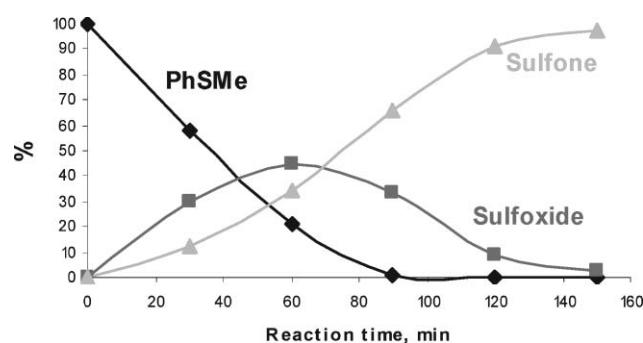


Fig. 2 Kinetics of PhSMe oxidation by H₂O₂ catalyzed by TiO₂-400. Reaction conditions: 0.5 mL PhSMe (4.25 mmol), 1.5 mL MeCN, 37.4 mg TiO₂-400, 9.6 mmol H₂O₂, 80 °C.

Experimental

General

Solvents and chemicals were purchased from Sigma–Aldrich and used without purification unless indicated. Deuterated acetonitrile-*d*₃ (99.8%) was available from Euriso-top.

Nitrogen adsorption/desorption isotherms were recorded with a Micromeritics ASAP 2010 apparatus. Metal contents were determined by an inductively coupled plasma-mass spectrometry method.

The products of oxidation were identified by NMR (AM 250 Bruker spectrometer) and GC-MS (Hewlett Packard 5973/6890 system; electron impact ionization at 70 eV, He carrier gas, 30 m × 0.25 mm crosslinked 5% PHME siloxane (0.25 μm coating) capillary column, HP-5MS) techniques. The reaction courses of PhSMe oxidation were monitored by GC (Agilent 4890D system, N₂ carrier gas, capillary column VF5-MS, 100% dimethylpolysiloxane, 30 m × 0.25 mm, 0.25 μm coating) and substrate conversions and product yields were determined using *o*-dichlorobenzene as internal standard.

Conversions and product yields of the oxidation of substituted thioanisols, phenyl trifluoromethyl sulfide and diphenyl sulfide were determined by ¹H NMR. The purity of the isolated products was checked by ¹H NMR and GC-MS.

Typical procedure for the oxidation of sulfides

To a 0.1 M solution of sulfide and 0.1 M of *o*-dichlorobenzene (internal standard) in 4 mL of solvent was added 5–37.4 mg of the TiO₂ catalyst. The reaction was started by the addition of a 35% aqueous H₂O₂ (3 equiv. to substrate) and was carried out at 25–80 °C. The reactions were followed by GC. After the reaction, the catalyst was separated by filtration, the solvent was removed in vacuum and the purity of the product was controlled by ¹H NMR.

Conclusions

A practical and green procedure for the oxidation of sulfides to sulfones was developed. These valuable synthetic intermediates have often been prepared by stoichiometric oxidation using non-environmentally benign protocols. Heterogeneous titania catalysts exhibit a high activity and a high selectivity for sulfone formation using aqueous hydrogen peroxide as the oxidant. The proposed preparatively useful catalytic method is a green alternative since it involves a green oxidant and recyclable solid catalyst. In addition to mild conditions, this procedure provides a pure sulfone product after very simple work-up: the separation of the catalyst by filtration followed by evaporation of the solvent. Both catalyst and solvent can be recycled and reused. Selective oxidation of dialkyl, alkylaryl and diaryl sulfides gives the possibility of accessing directly target sulfones, useful synthetic synthons in fine organic chemistry.

Notes and references

- (a) J.-E. Bäckvall, *Modern Oxidation Methods*, Wiley-VCH, Verlag GmbH, Weinheim, 2004; (b) A. A. Lindén, M. Johansson, N. Hermans and J.-E. Bäckvall, *J. Org. Chem.*, 2006, **71**, 3849; (c) H.

- Firouzabadi, N. Iranpoor, A. A. Jafari and E. Riazymontazer, *Adv. Synth. Catal.*, 2006, **348**, 434; (d) J. R. Lindsay Smith, J. Murray, P. H. Walton and T. R. Lowdon, *Tetrahedron Lett.*, 2006, **47**, 2005; (e) V. K. Sivasubramanian, M. Ganesan, S. Rajagopal and R. Ramataj, *J. Org. Chem.*, 2002, **67**, 1506.
- 2 (a) H. B. Kagan, and T. Luukas, in *Transition Metals for Organic Synthesis*, ed. M. Beller and C. Bolm, Wiley-VCH, Weinheim, 1998, pp. 361-373; (b) H. B. Kagan, in *Catalytic Asymmetric Synthesis*, ed. I. Ojima, 2nd edn, Wiley-VCH, New York, 2000, pp. 327-356; (c) J. Legros and C. Bolm, *Chem.-Eur. J.*, 2005, **11**, 1086; (d) Q. Zeng, H. Wang, W. Weng, W. Lin, Y. Gao, X. Huang and Y. Zhao, *New J. Chem.*, 2005, **29**, 1125; (e) K. P. Bryliakov and E. P. Talsi, *Chem.-Eur. J.*, 2007, **13**, 8045.
- 3 (a) B. M. Choudary, C. R. V. Reddy, B. V. Prakash, M. L. Kantam and B. Sreedhar, *Chem. Commun.*, 2003, 754; (b) L. Xu, J. Cheng and M. L. Trudell, *J. Org. Chem.*, 2003, **68**, 5388; (c) A. Marques, M. di Matteo and M.-F. Ruasse, *Can. J. Chem.*, 1998, **76**, 770; (d) D. H. R. Barton, W. Li and J. A. Smith, *Tetrahedron Lett.*, 1998, **39**, 7055; (e) V. Khanna, G. C. Maikap and J. Iqbal, *Tetrahedron Lett.*, 1996, **37**, 3367.
- 4 (a) V. Hulea, F. Fajula and J. Bousquet, *J. Catal.*, 2001, **198**, 179; (b) J. Palomeque, J.-M. Classens and F. Figueras, *J. Catal.*, 2002, **211**, 103; (c) F. Figueras, J. Palomeque, S. Loridant, C. Féche, N. Essayem and G. Gelbard, *J. Catal.*, 2004, **226**, 25; (d) C. Li, Z. Jiang, J. Gao, Y. Yang, S. Wang, F. Tian, F. Sun, P. Ying and C. Han, *Chem.-Eur. J.*, 2004, **10**, 2277; (e) D. Wang, E. W. Qian, H. Amano, K. Okata, A. Ishihara and T. Kabe, *Appl. Catal., A*, 2003, **253**, 91; (f) A. Chica, G. Gatti, B. Moden, L. Marchese and E. Iglesia, *Chem.-Eur. J.*, 2006, **12**, 1960.
- 5 M. V. Gómez, R. Caballero, E. Vázquez, A. Moreno, A. de la Hoz and Á. Diaz-Ortiz, *Green Chem.*, 2007, **9**, 331.
- 6 For reviews on Ti based oxidation catalyst see: (a) B. Notari, *Adv. Catal.*, 1996, **41**, 253; (b) A. Corma, *Chem. Rev.*, 1997, **97**, 2373; (c) O. A. Kholdeeva and N. N. Trukhan, *Russ. Chem. Rev.*, 2006, **75**, 411.
- 7 (a) N. N. Trukhan, V. N. Romannikov, E. A. Paukshtis, A. N. Shmakov and O. A. Kholdeeva, *J. Catal.*, 2001, **202**, 110; (b) O. A. Kholdeeva, M. S. Melgunov, A. N. Shmakov, N. N. Trukhan, V. V. Kriventsov, V. I. Zaikovskii and V. N. Romannikov, *Catal. Today*, 2004, **91-92**, 205; (c) O. A. Kholdeeva, O. V. Zalomaeva, A. N. Shmakov, M. S. Melgunov and A. B. Sorokin, *J. Catal.*, 2005, **236**, 62; (d) N. N. Trukhan, A. Yu. Derevyankin, A. N. Shmakov, E. A. Paukshtis, O. A. Kholdeeva and V. N. Romannikov, *Microporous Macroporous Mater.*, 2001, **44-45**, 603; (e) O. A. Kholdeeva, A. Yu. Derevyankin, A. N. Shmakov, N. N. Trukhan, E. A. Paukshtis, A. Tuel and V. N. Romannikov, *J. Mol. Catal. A: Chem.*, 2000, **158**, 417.
- 8 (a) R. S. Reddy, J. S. Reddy, R. Kumar and P. Kumar, *J. Chem. Soc., Chem. Commun.*, 1992, 84; (b) A. Corma, M. Iglesias and F. Sanchez, *Catal. Lett.*, 1996, **39**, 153; (c) P. Moreau, V. Hulea, S. Gomez, D. Brunel and F. Di Renzo, *Appl. Catal., A*, 1997, **155**, 253; (d) J. M. Fraile, J. I. Garcia, B. Lazaro and J. A. Mayoral, *Chem. Commun.*, 1998, 1807; (e) F. Di Renzo, S. Gomez, R. Teissier and F. Fajula, *Stud. Surf. Sci. Catal.*, 2000, **130**, 1631; (f) A. Massa, E. M. De Lorenzo and A. Scettri, *J. Mol. Catal. A: Chem.*, 2006, **250**, 27; (g) A. M. Khenkin and R. Neumann, *Catal. Lett.*, 2000, **68**, 109.
- 9 G. Goutailler, C. Guillard, S. Daniele and L. G. Hubert-Pfalzgraf, *J. Mater. Chem.*, 2003, **13**, 342.
- 10 M. Beyrhouty, A. B. Sorokin, S. Daniele and L. G. Hubert-Pfalzgraf, *New J. Chem.*, 2005, **29**, 1245.
- 11 (a) G. B. Payne, P. H. Deming and P. H. Williams, *J. Org. Chem.*, 1961, **26**, 659; (b) W. C. Frank, *Tetrahedron: Asymmetry*, 1998, **9**, 3745.
- 12 U. R. Pillai and E. Sahle-Demessie, *J. Mol. Catal. A: Chem.*, 2003, **191**, 93.
- 13 R. A. Sheldon, M. Wallau, I. W. C. E. Arends and U. Schuchardt, *Acc. Chem. Res.*, 1998, **31**, 485.

Quick and highly efficient copper-catalyzed cycloaddition of aliphatic and aryl azides with terminal alkynes “on water”

Feng Wang,^a Hua Fu,^{*a} Yuyang Jiang^{a,b} and Yufen Zhao^a

Received 21st November 2007, Accepted 16th January 2008

First published as an Advance Article on the web 25th February 2008

DOI: 10.1039/b718051a

We have developed a quick and highly efficient method for copper-catalyzed cycloaddition of water-insoluble aliphatic/aryl azides and alkynes “on water” at room temperature, the protocol uses 10 mol% CuBr as the catalyst, and 50 mol% PhSMe as the ligand.

Introduction

Selective conjugation of two functionalized fragments is highly desirable for chemists and biologists, and “click chemistry” is an effective strategy for connection of unsaturated building blocks.¹ In the past six years, the copper-catalyzed cycloadditions of azides and alkynes to triazoles² have attracted much attention, and the methods show various applications in chemical biology, organic synthesis, and materials science.³ The used copper sources come from direct addition of Cu(I) species,^{2b} or reduction of Cu(II) salts to Cu(I) salts,^{2a} oxidation of copper metal turning to give Cu(I) species,⁴ and copper nanoclusters.⁵ However, most of the reactions proceed relatively slowly, the consumption of the starting materials usually needing a longer time. Increasing reaction temperature could reduce this time, but this process is not favored for molecules containing polyfunctional groups. Recently, it has become a research focus to explore the suitable ligands for copper catalysts, the addition of ligands could greatly improve the reaction activity of the substrates, and the cycloadditions of azides with alkynes were performed at room temperature.⁶ Herein, we report a quick, efficient and general copper-catalyzed cycloaddition of water-insoluble aliphatic/aryl azides and alkynes “on water” by catalysis with a commercially available and inexpensive catalyst system (CuBr/PhSMe) at room temperature.

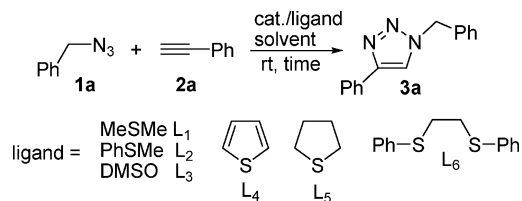
Water is the most economical and environmentally friendly solvent in the world, but chemists often choose organic solvents such as THF, toluene, tetrachloromethane, *tert*-butanol and mixed solvents in the copper-catalyzed cycloaddition of water-insoluble azides and alkynes. Herein, we want to explore the copper-catalyzed cycloaddition “on water” at room temperature. We initialized the copper-catalyzed optimum cycloaddition conditions using benzyl azide, with phenylacetylene as the model substrates, as shown in Table 1. CuBr·MeSMe is an efficient catalyst in cross-coupling reactions,^{7a} so we first attempted its catalysis by cycloaddition of water-insoluble benzyl azide and phenylacetylene “on water” at room temperature. To our

pleasure, the catalyst showed excellent activity (entry 1). Encouraged by the excellent result, several compounds containing sulfur (thioanisole, dimethyl sulfoxide, thiophene, tetrahydrothiophene and 1-(2-(phenylthio)ethylthio)benzene) (entries 2–6) were also evaluated, and thioanisole exhibited better activity than dimethyl sulfide. Copper salts (CuI, CuCl) were tested in the presence of thioanisole (entries 7 and 8), but they were inferior to CuBr. It is worthwhile to note that CuI is not a good choice for the present copper-catalyzed cycloaddition of azides with alkynes, although it is a popular catalyst in previous Cu(I)-catalyzed coupling reactions,⁷ and a possible reason is the weak dissolving power of CuI in water. We made control experiments using organic solvents (THF, CHCl₃, *tert*-butanol, mixed solvent of *tert*-butanol and water (1 : 2)), and the results showed that water was the best choice. We changed the amount of copper salt and ligand, and the results showed that more copper catalyst and ligand could shorten cycloaddition time of the substrates (entries 13–16). We tried the reaction of *p*-methylphenyl azide with phenylacetylene to test the effect of the catalyst system (CuBr/PhSMe) for aryl azides, and we found that the catalyst system was also efficient. Cycloaddition of *p*-methylphenyl azide with phenylacetylene was not observed in the absence of ligand within 2 h (entry 18).

After optimizing the process, copper-catalyzed cycloaddition of aliphatic and aryl azides with alkynes were performed under our standard conditions: CuBr as the catalyst, thioanisole as the ligand, and water as the medium, at room temperature without exclusion of air. As shown in Table 2, for all the examined substrates, experiments were carried out smoothly to completion in short reaction times, and the corresponding triazoles were obtained in excellent yields. Reaction rates depended on the aqueous solubility and states (solid and liquid) of the substrates. The substrates with good solubility in water or liquid substrates showed higher reaction rates, while the reactions for the solid and insoluble substrates were slower. For example, **2g** with good water-solubility showed a much higher rate than water-insoluble **2f** (compare entries 12 and 13). **2f** and AZT did not dissolve in water, fortunately, the coupling reaction completed under a continuous stir for 2–6 h (entries 10–13). The reactions of organic compounds in aqueous suspensions have been previously investigated.⁸ In fact, water is not a good solvent for most of the substrates examined, but it shows excellent solubility for copper salts, which is favorable for the coordination of copper(I) ion with alkyne and ligand.

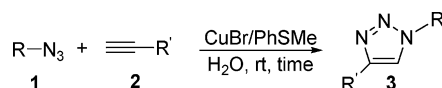
^aKey Laboratory of Bioorganic Phosphorus Chemistry and Chemical Biology (Ministry of Education), Department of Chemistry, Tsinghua University, Beijing, 100084, P. R. China.
E-mail: fuhua@mail.tsinghua.edu.cn

^bKey Laboratory of Chemical Biology (Guangdong Province), Graduate School of Shenzhen, Tsinghua University, Shenzhen, 518057, P. R. China

Table 1 Copper-catalyzed cycloaddition of benzyl azide with phenylacetylene: optimization of conditions^a

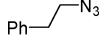
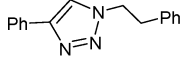
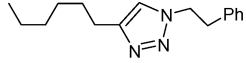
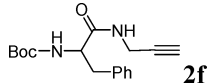
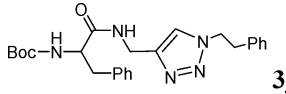
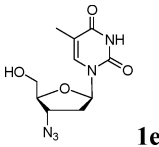
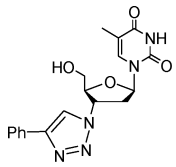
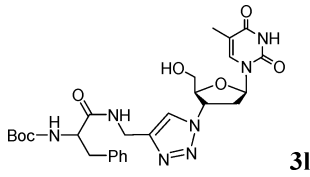
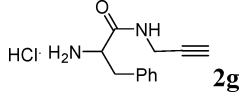
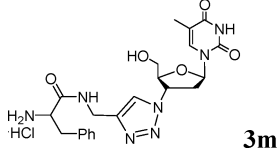
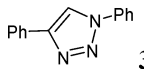
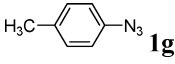
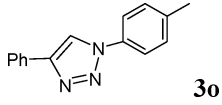
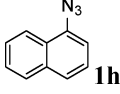
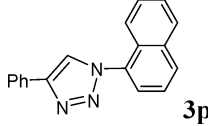
| Entry | Catalyst/ligand | Solvent | Time | Yield (%) ^b |
|-------|----------------------------|---------------------------------------|--------|------------------------|
| 1 | 5 mol% CuBr/30 mol% L_1 | H ₂ O | 7 min | 93 |
| 2 | 5 mol% CuBr/30 mol% L_2 | H ₂ O | 7 min | 96 |
| 3 | 5 mol% CuBr/30 mol% L_3 | H ₂ O | 10 min | <10 |
| 4 | 5 mol% CuBr/30 mol% L_4 | H ₂ O | 10 min | <5 |
| 5 | 5 mol% CuBr/30 mol% L_5 | H ₂ O | 10 min | 90 |
| 6 | 5 mol% CuBr/30 mol% L_6 | H ₂ O | 10 min | 92 |
| 7 | 5 mol% CuCl/30 mol% L_2 | H ₂ O | 1.5 h | 75 |
| 8 | 5 mol% CuI/30 mol% L_2 | H ₂ O | 2 h | 40 |
| 9 | 5 mol% CuBr/30 mol% L_2 | THF | 2 h | 45 |
| 10 | 5 mol% CuBr/30 mol% L_2 | CHCl ₃ | 2 h | 25 |
| 11 | 5 mol% CuBr/30 mol% L_2 | <i>t</i> -BuOH | 1 h | <5 |
| 12 | 5 mol% CuBr/30 mol% L_2 | <i>t</i> -BuOH/H ₂ O = 1/2 | 10 min | 50 |
| 13 | 2 mol% CuBr/4 mol% L_2 | H ₂ O | 1 h | 80 |
| 14 | 5 mol% CuBr/10 mol% L_2 | H ₂ O | 20 min | 95 |
| 15 | 5 mol% CuBr/50 mol% L_2 | H ₂ O | 5 min | 96 |
| 16 | 10 mol% CuBr/50 mol% L_2 | H ₂ O | 5 min | 97 |
| 17 | 10 mol% CuBr/50 mol% L_2 | H ₂ O | 20 min | 90 ^{c,d} |
| 18 | CuBr/no ligand | H ₂ O | 2 h | 0 ^c |

^a Reaction conditions: benzyl azide (0.5 mmol), phenylacetylene (0.6 mmol), solvent (1 mL). ^b Conversion yield determined by NMR using CH₃CN as the internal standard. ^c *p*-Methylphenyl azide (0.5 mmol) was used instead of benzyl azide. ^d Isolated yield.

Table 2 Copper-catalyzed cycloaddition of aliphatic and aryl azides with alkynes^a

| Entry | R-N ₃ | ≡-R' | Time | Product | Yield (%) ^b |
|-------|------------------|-----------|--------|-----------|------------------------|
| 1 | 1a | 2a | 10 min | 3a | 96 |
| 2 | 1a | 2b | 15 min | 3b | 93 |
| 3 | 1a | 2c | 30 min | 3c | 90 |
| 4 | 1a | 2d | 30 min | 3d | 97 |
| 5 | 1a | 2e | 40 min | 3e | 95 |
| 6 | 1b | 2a | 45 min | 3f | 92 |
| 7 | 1c | 2a | 40 min | 3g | 90 |

Table 2 (Contd.)

| | | $\text{R-N}_3 + \text{C}\equiv\text{C-R}' \xrightarrow[\text{H}_2\text{O, rt, time}]{\text{CuBr/PhSMe}} \text{R-N}_2\text{C(R')=N}$ | | | |
|-------|---|---|--------|--|------------------------|
| Entry | R-N ₃ | C≡C-R' | Time | Product | Yield (%) ^b |
| 8 |  1d | 2a | 20 min |  3h | 98 |
| 9 | 1d | 2d | 30 min |  3i | 95 |
| 10 | 1d |  2f | 2.5 h |  3j | 94 |
| 11 |  1e | 2a | 4.5 h |  3k | 93 |
| 12 | 1e | 2f | 6 h |  3l | 88 |
| 13 | 1e |  2g | 2 h |  3m | 96 |
| 14 | Ph-N ₃ 1f | 2a | 1 h |  3n | 82 |
| 15 |  1g | 2a | 20 min |  3o | 90 |
| 16 |  1h | 2a | 2 h |  3p | 86 |

^a Reaction conditions: azide (0.5 mmol), alkyne (0.6 mmol), CuBr (10 mol%), PhSMe (50 mol%), H₂O (1 or 2 mL). ^b Isolated yield.

In general, no significant difference of reactivity was observed for the examined reactants with varied electronic properties, electron-rich, electron-poor and/or hindered azides and alkynes, and the results show that CuBr/thioanisole is a highly efficient catalytic system for the cycloaddition of aliphatic and aryl azides with alkynes. In addition, the coupling reactions were tolerant of functional groups in the substrates, such as amide (entries 10, 12 and 13), hydroxyl (entries 11–13) and amino (entry 13).

In summary, we have developed a quick and highly efficient method for copper-catalyzed cycloaddition of water-insoluble aliphatic/aryl azides and alkynes at room temperature. The method uses commercially available and inexpensive CuBr/PhSMe as the catalyst system and economical and environmentally friendly water as the medium. Also, because it can tolerate functional groups of substrates, it has wide applications for the synthesis of various compounds containing triazole building blocks.

Experimental

All reactions were carried out at room temperature without exclusion of air. All reagents were commercially available without further purification. Flash column chromatography was performed on silica gel (200–300 mesh) and thin layer chromatography (TLC) analyses were performed on commercial silica gel plates (60 F254). ^1H and ^{13}C NMR spectra were recorded on a 300 MHz spectrometer. Chemical shifts (δ) were reported with respect to tetramethylsilane (TMS) or $\text{DMSO}-d_6$ or CD_3OD as internal standard in ppm. The following abbreviations were used to describe peak splitting patterns when appropriate: br = broad, s = singlet, d = doublet, t = triplet, q = quartet, m = multiplet. Coupling constants, J , were reported in hertz unit (Hz). Mass spectral data were acquired on a Bruker ESQUIRE-LC ion trap mass spectrometer.

Synthesis of azides

Aliphatic and aryl azides were synthesized according to the reported procedure,⁹ and AZT was commercially available.

General procedure for copper-catalyzed cycloaddition of aliphatic and aryl azides with alkynes to triazoles 3a–p

Water (2 mL for entries 10–13, 1 mL for others in Table 2), alkyne (0.6 mmol), azide (0.5 mmol), CuBr (0.05 mmol, 7.5 mg), and thioanisole (0.25 mmol, 31 mg) were added to a flask with a stir bar, and the mixture was stirred at room temperature ($\sim 25^\circ\text{C}$) without exclusion of air. After total consumption of the starting azide (determination by TLC) (see Table 2 for reaction time), the resulting solution was poured in a water/ethyl acetate mixture (except entries 11–13 in Table 2). After extraction of the aqueous phase with ethyl acetate, the combined organic phase was dried over magnesium sulfate and filtered. The solvent was removed by rotary evaporation, and the crude product was isolated on a short silica gel column to get a pure triazole. When AZT was used as the substrate, the work-up procedure is different (for entries 11–13 in Table 2). After total consumption of AZT (TLC determination), water was removed under reduced pressure, and the residue solid was dissolved in 0.5 mL of methanol. Purification on a short silica gel column provided the target product using chloroform/methanol (v/v, 15 : 1 to 1 : 1 for entries 11–13 in Table 2) or ethyl acetate/petroleum ether (v/v, 10 : 1 to 1 : 1 for others in Table 2) as eluent.

Prop-2-ynyloxymethyl-benzene (2e)¹⁰

The spectra were in agreement with those described in the literature.

Compound 2f

White solid, mp 99–100 $^\circ\text{C}$. ^1H NMR (CDCl_3 , 300 MHz) δ 7.18 (m, 5H), 6.21 (br, 1H), 5.04 (br, 1H), 4.41–4.28 (m, 1H), 3.99–3.96 (m, 2H), 3.06 (d, $J = 6.5$ Hz, 2H), 2.18 (t, $J = 2.7$ Hz, 1H), 1.40 (s, 9H). ^{13}C NMR (CDCl_3 , 75 MHz) δ 171.1, 136.6, 129.4, 128.8, 127.1, 79.1, 71.7, 38.6, 29.2, 28.4. ESI-MS m/z 341.2 $[\text{M} + \text{K}]^+$.

Compound 2g

White solid, mp 159–160 $^\circ\text{C}$. ^1H NMR (CD_3OD , 300 MHz) δ 7.37–7.26 (m, 5H), 4.04 (t, $J = 7.2$ Hz, 1H), 3.95 (d, $J = 2.4$ Hz, 2H), 3.21–3.03 (m, 2H), 2.63 (t, $J = 2.4$ Hz, 1H). ^{13}C NMR (CD_3OD , 75 MHz) δ 167.9, 134.1, 129.3, 128.8, 127.5, 78.4, 71.5, 54.4, 37.2, 28.2. ESI-MS m/z 202.3 $[\text{M} + \text{H}]^+$.

4-Phenyl-1-benzyl-1,2,3-triazole (3a)¹¹

The spectra were in agreement with those described in the literature.

4-Methylphenyl-1-benzyl-1,2,3-triazole (3b)¹²

The spectra were in agreement with those described in the literature.

4-Bromophenyl-1-benzyl-1,2,3-triazole (3c)

White solid, mp 152–153 $^\circ\text{C}$. ^1H NMR (CDCl_3 , 300 MHz) δ 7.68–7.65 (m, 3H), 7.52 (d, $J = 8.6$ Hz, 2H), 7.40–7.30 (m, 5H), 5.57 (s, 2H). ^{13}C NMR (CDCl_3 , 75 MHz) δ 147.3, 134.6, 132.0, 129.6, 129.3, 129.0, 128.2, 127.3, 122.1, 119.7, 54.4. ESI-MS m/z 314.2, 316.3 $[\text{M} + \text{H}]^+$.

4-Hexyl-1-benzyl-1,2,3-triazole (3d)

White solid, mp 47–48 $^\circ\text{C}$. ^1H NMR (CDCl_3 , 300 MHz) δ 7.39–7.30 (m, 3H), 7.26–7.23 (m, 2H), 7.17 (s, 1H), 5.48 (s, 2H), 2.67 (t, $J = 7.9$ Hz, 2H), 1.67–1.57 (m, 2H), 1.35–1.27 (m, 6H), 0.85 (t, $J = 6.5$ Hz, 3H). ^{13}C NMR (CDCl_3 , 75 MHz) δ 149.0, 135.1, 129.1, 128.7, 128.0, 120.6, 54.1, 31.6, 29.4, 29.0, 25.8, 22.6, 14.1. ESI-MS m/z 243.7 $[\text{M} + \text{H}]^+$, m/z 265.7 $[\text{M} + \text{Na}]^+$.

4-(Benzyloxymethyl)-1-benzyl-1,2,3-triazole (3e)

White solid, mp 57–58 $^\circ\text{C}$. ^1H NMR (CDCl_3 , 300 MHz) δ 7.45 (s, 1H), 7.41–7.25 (m, 10H), 5.51 (s, 2H), 4.66 (s, 2H), 4.58 (s, 2H). ^{13}C NMR (CDCl_3 , 75 MHz) δ 145.8, 137.8, 134.6, 129.2, 128.9, 128.5, 128.3, 128.0, 127.9, 122.5, 72.7, 63.8, 54.3. ESI-MS m/z 280.1 $[\text{M} + \text{H}]^+$, 302.0 $[\text{M} + \text{Na}]^+$.

4-Phenyl-1-(2-bromo-benzyl)-1,2,3-triazole (3f)¹³

The spectra were in agreement with those described in the literature.

4-Phenyl-1-(4-chloro-benzyl)-1,2,3-triazole (3g)¹⁴

The spectra were in agreement with those described in the literature.

4-Phenyl-1-phenethyl-1,2,3-triazole (3h)¹⁵

The spectra were in agreement with those described in the literature.

4-Hexyl-1-phenethyl-1,2,3-triazole (3i)

Colorless oil. ^1H NMR (CDCl_3 , 300 MHz) δ 7.32–7.19 (m, 3H), 7.08 (dd, $J = 7.6, 0.6$ Hz, 2H), 6.97 (s, 1H), 4.54 (t, $J = 7.2$ Hz, 2H), 3.18 (t, $J = 7.6$ Hz, 2H), 2.65 (t, $J = 7.6$ Hz, 2H), 1.63–1.55 (m, 2H), 1.38–1.28 (m, 6H), 0.88 (t, $J = 5.8$ Hz, 3H).

^{13}C NMR (CDCl_3 , 75 MHz) δ 148.2, 137.3, 128.8, 128.8, 127.1, 121.0, 51.6, 36.9, 31.7, 29.5, 28.9, 25.7, 22.6, 14.1. ESI-MS m/z 257.8 $[\text{M} + \text{H}]^+$, m/z 279.8 $[\text{M} + \text{Na}]^+$.

Compound 3j

White solid, mp 149–150 °C. ^1H NMR (CDCl_3 , 300 MHz) δ 7.31–7.09 (m, 1H), 6.85 (br, 1H), 5.14–5.11 (m, 1H), 4.51 (t, $J = 7.2$ Hz, 2H), 4.40 (d, $J = 5.9$ Hz, 2H), 4.36 (br, 1H), 3.17 (t, $J = 7.6$ Hz, 2H), 3.10–2.95 (m, 2H), 1.36 (s, 9H). ^{13}C NMR (CDCl_3 , 75 MHz) δ 171.5, 155.4, 144.4, 137.0, 136.7, 129.4, 128.9, 128.7, 128.6, 127.2, 126.9, 122.6, 80.2, 55.8, 51.7, 38.7, 36.8, 34.9, 28.3. ESI-MS m/z 472.2 $[\text{M} + \text{Na}]^+$, m/z 488.2 $[\text{M} + \text{K}]^+$.

3'-(4-Phenyl-1,2,3-triazol-1-yl)-2',3'-dideoxythymidine (3k)¹⁶

The spectra were in agreement with those described in the literature.

Compound 3l

White solid, mp 209–210 °C. ^1H NMR ($\text{DMSO}-d_6$, 300 MHz) δ 11.30 (s, 1H), 8.40 (t, $J = 5.5$ Hz, 1H), 7.95 (s, 1H), 7.78 (s, 1H), 7.22–7.13 (m, 5H), 6.86 (d, $J = 8.6$ Hz, 1H), 6.38 (t, $J = 6.5$ Hz, 1H), 5.34–5.29 (m, 1H), 5.24 (t, $J = 5.2$ Hz, 1H), 4.31 (d, $J = 4.5$ Hz, 2H), 4.20–4.10 (m, 2H), 3.71–3.55 (m, 2H), 2.96–2.90 (m, 1H), 2.76–2.56 (m, 3H), 1.78 (s, 3H), 1.26 (s, 9H). ^{13}C NMR ($\text{DMSO}-d_6$, 75 MHz) δ 172.2, 164.3, 155.8, 151.0, 145.6, 138.7, 136.8, 129.8, 128.5, 126.7, 123.0, 110.2, 85.0, 84.5, 79.7, 78.5, 61.3, 59.7, 56.3, 38.1, 37.7, 28.7, 12.8. ESI-MS m/z 592.3 $[\text{M} + \text{Na}]^+$.

Compound 3m

White solid, mp 171–172 °C. ^1H NMR ($\text{DMSO}-d_6$, 300 MHz) δ 8.59 (br, 1H), 8.00 (s, 1H), 7.82 (s, 1H), 7.25–7.16 (m, 5H), 6.38 (t, $J = 6.5$ Hz, 1H), 5.39–5.33 (m, 2H), 4.30–4.15 (m, 4H), 3.69–3.30 (m, 4H), 2.95 (br, 1H), 2.80–2.58 (m, 3H), 1.78 (s, 3H). ^{13}C NMR ($\text{DMSO}-d_6$, 75 MHz) δ 164.3, 151.0, 145.4, 138.3, 136.8, 129.9, 128.7, 126.9, 123.2, 110.2, 85.1, 84.5, 61.3, 59.8, 37.7, 34.7, 12.8. ESI-MS m/z 470.2 $[\text{M} + \text{H}]^+$.

4-Phenyl-1-(4-phenyl)-1,2,3-triazole (3n)¹¹

The spectra were in agreement with those described in the literature.

4-Phenyl-1-(4-methyl-phenyl)-1,2,3-triazole (3o)¹⁷

The spectra were in agreement with those described in the literature.

4-Phenyl-1-(1-naphthalenyl)-1,2,3-triazole (3p)

Oil. ^1H NMR (CDCl_3 , 300 MHz) δ 8.12 (s, 1H), 8.01–7.93 (m, 4H), 7.69 (d, $J = 8.2$ Hz, 1H), 7.60–7.52 (m, 4H), 7.47 (t, $J = 7.5$ Hz, 2H), 7.37 (t, $J = 7.2$ Hz, 1H). ^{13}C NMR (CDCl_3 , 75 MHz) δ 147.8, 134.3, 133.8, 130.5, 130.4, 129.1, 128.7, 128.5, 128.4, 128.0, 127.2, 126.0, 125.1, 123.6, 122.5. ESI-MS m/z 271.9 $[\text{M} + \text{H}]^+$, m/z 293.9 $[\text{M} + \text{Na}]^+$.

Acknowledgements

This work was supported by the National Natural Science Foundation of China (Grant No. 20472042 and 20672065), Programs for New Century Excellent Talents in University (NCET-05-0062) and Changjiang Scholars and Innovative Research Team in University (PCSIRT) (No. IRT0404) in China and the Key Subject Foundation from Beijing Department of Education (XK100030514).

References

- H. C. Kolb, M. G. Finn and K. B. Sharpless, *Angew. Chem., Int. Ed.*, 2001, **40**, 2004.
- (a) V. V. Rostovtsev, L. G. Green, V. V. Fokin and K. B. Sharpless, *Angew. Chem., Int. Ed.*, 2002, **41**, 2596; (b) C. W. Tornøe, C. Christensen and M. Meldal, *J. Org. Chem.*, 2002, **67**, 3057.
- (a) For representative applications of the Cu(I)-catalyzed azide-alkyne cycloaddition, see: Q. Wang, T. R. Chan, R. Hilgraf, V. V. Fokin, K. B. Sharpless and M. G. Finn, *J. Am. Chem. Soc.*, 2003, **125**, 3192; (b) A. E. Speers, G. C. Adam and B. F. Cravatt, *J. Am. Chem. Soc.*, 2003, **125**, 4686; (c) J. C. Anderson and P. G. Schultz, *J. Am. Chem. Soc.*, 2003, **125**, 11782; (d) A. J. Link and D. A. Tirrell, *J. Am. Chem. Soc.*, 2003, **125**, 11164; (e) J. P. Collman, N. K. Devaraj and C. E. D. Chidsey, *Langmuir*, 2004, **20**, 1051; (f) P. Wu, A. K. Feldman, A. K. Nugent, C. J. Hawker, A. Scheel, B. Voit, J. Pyun, J. M. J. Fréchet, K. B. Sharpless and V. V. Fokin, *Angew. Chem., Int. Ed.*, 2004, **43**, 3928; (g) H. C. Kolb and K. B. Sharpless, *Drug Discovery Today*, 2003, **8**, 1128; (h) Q. Wang, S. Chittaboina and H. N. Barnhill, *Lett. Org. Chem.*, 2005, **2**, 293; (i) V. D. Bock, H. Hiemstra and J. H. van Maarseveen, *Eur. J. Org. Chem.*, 2006, 51; (j) W. H. Binder and C. Kluger, *Curr. Org. Chem.*, 2006, **10**, 1791; (k) J.-F. Lutz, *Angew. Chem., Int. Ed.*, 2007, **46**, 1018; (l) P. Wu and V. V. Fokin, *Aldrichimica Acta*, 2007, **40**, 7.
- F. Himoto, T. Lovell, R. Hilgraf, V. V. Rostovtsev, L. Noodleman, K. B. Sharpless and V. V. Fokin, *J. Am. Chem. Soc.*, 2005, **127**, 210.
- (a) B. H. Lipshutz and B. R. Taft, *Angew. Chem., Int. Ed.*, 2006, **45**, 8235; (b) L. D. Pachón, J. H. van Maarseveen and G. Rothenberg, *Adv. Synth. Catal.*, 2005, **347**, 811.
- (a) W. G. Lewis, F. G. Magallon, V. V. Fokin and M. G. Finn, *J. Am. Chem. Soc.*, 2004, **126**, 9152; (b) S. Diez-González, A. Correa, L. Cavallo and S. P. Nolan, *Chem.–Eur. J.*, 2006, **12**, 7558; (c) V. O. Rodionov, S. I. Presolski, D. D. Diaz, V. V. Fokin and M. G. Finn, *J. Am. Chem. Soc.*, 2007, **129**, 12705; (d) V. O. Rodionov, S. I. Presolski, S. Gardinier, Y.-H. Lim and M. G. Finn, *J. Am. Chem. Soc.*, 2007, **129**, 12696.
- (a) For a recent review, see: S. V. Ley and A. W. Thomas, *Angew. Chem., Int. Ed.*, 2003, **42**, 5400; (b) K. Kunz, U. Scholz and D. Ganzer, *Synlett*, 2003, **15**, 2428; (c) I. P. Beletskaya and A. V. Cheprakov, *Coord. Chem. Rev.*, 2004, **248**, 2337.
- (a) S. Narayan, J. Muldoon, M. G. Finn, V. V. Fokin, H. C. Kolb and K. B. Sharpless, *Angew. Chem., Int. Ed.*, 2005, **44**, 3275; (b) J. E. Klijn and J. B. F. N. Engberts, *Nature*, 2005, **435**, 746; (c) R. N. Butler, A. G. Coyne and E. M. Moloney, *Tetrahedron Lett.*, 2007, **48**, 3501.
- Z. P. Demko and K. B. Sharpless, *Angew. Chem., Int. Ed.*, 2002, **41**, 2110.
- B. M. Trost and J. Xie, *J. Am. Chem. Soc.*, 2006, **128**, 6044.
- S. Chassaing, M. Kumarraja, A. S. S. Sido, P. Pale and J. Sommer, *Org. Lett.*, 2007, **9**, 883.
- K. R. Reddy, K. Rajgopal and M. L. Kantam, *Synlett*, 2006, **6**, 957.
- S. T. Abu-Orabi, M. A. Atfah, I. Jibril, F. M. Mari'i and A. A. S. Ali, *J. Heterocycl. Chem.*, 1989, **26**, 1461.
- Z.-X. Wang and Z.-G. Zhao, *J. Heterocycl. Chem.*, 2007, **44**, 89.
- P. Appukkuttan, W. Dehaen, V. V. Fokin and E. Van der Eycken, *Org. Lett.*, 2004, **6**, 4223.
- P. Wigerinck, A. Van Aerschot, P. Claes, J. Balzarini, E. De Clercq and P. Herdewijn, *J. Heterocycl. Chem.*, 1989, **26**, 1635.
- Z.-X. Wang and H.-L. Qin, *Chem. Commun.*, 2003, 2450.

Green chemistry metrics: a comparative evaluation of dimethyl carbonate, methyl iodide, dimethyl sulfate and methanol as methylating agents

Maurizio Selva* and Alvise Perosa

Received 12th September 2007, Accepted 22nd January 2008

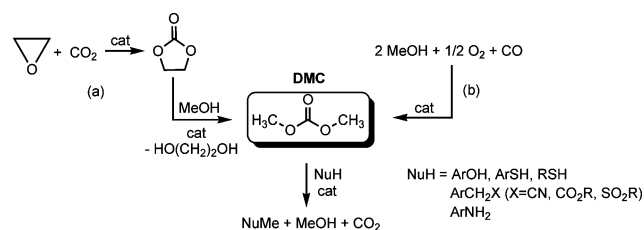
First published as an Advance Article on the web 28th February 2008

DOI: 10.1039/b713985c

The methylating efficiency of dimethyl carbonate (DMC), dimethyl sulfate (DMS), methyl iodide (MeI), and methanol (MeOH) was assessed based on atom economy and mass index. These parameters were calculated for three model reactions: the O-methylation of phenol, the mono-C-methylation of phenylacetonitrile, and the mono-N-methylation of aniline. The analysis was carried out over a total of 33 different procedures selected from the literature. Methanol and, in particular, DMC yielded very favourable mass indexes (in the range 3–6) indicating a significant decrease of the overall flow of materials (reagents, catalysts, solvents, *etc.*), thereby providing safer greener catalytic reactions with no waste.

Introduction

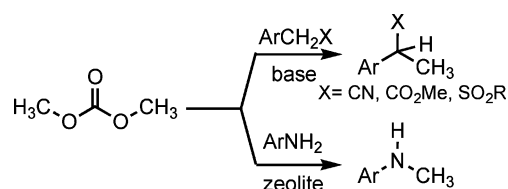
Alkylation reactions are among the key industrial/organic transformations for the production of a variety of fine and bulk chemicals.¹ In this field, particularly in the past two decades, the need for more environmentally acceptable processes has fuelled a great interest towards dialkylcarbonates (ROCO₂R) as innovative alkylating agents.² These compounds, in fact, possess physico-chemical and reactivity features which make them appealing for general synthetic applications, including, for example, the selective alkylation of amines and phenols carried out by both linear and cyclic organic carbonates.³ In addition, environmental benefits come from the (eco)toxicological profiles of dialkyl carbonates. This is especially true for the lightest term of the series, dimethyl carbonate (DMC), which is currently considered a genuine example of a green compound:^{2,4} the synergy between its non-toxicity, its good biodegradability, its clean industrial methods of synthesis (Scheme 1),⁵ and its versatile reactivity imparts to it a great potential as a reagent for the methylation of several O-, S-, C-, and N-nucleophiles.^{2,6}



Scheme 1

DMC-mediated methylations have been extensively investigated by us:⁷ the green features of these reactions have been readily recognised in the overall improvement of safety, in

their true catalytic nature, in the absence of by-products, and importantly, in the lack of added solvents. Besides, a further specific added-value is the unprecedented high selectivity (over 99%) which has been attained, for example, in the reactions of dimethyl carbonate with CH₂-active compounds and with primary aromatic amines (Scheme 2).



Scheme 2

Both these processes have been reported with the exclusive formation of the corresponding mono-C- and mono-N-methyl derivatives, while the use of classical reagents and methods always give mixtures of products of multiple C- and N-alkylations.^{7,8}

So far however, the synthetic elegance of DMC-based procedures with respect to traditional alkylation techniques, has been mostly described through conventional criteria of selectivity and yields.

An important progress of green chemistry has been the transition from general qualitative descriptions of the greenness of a process to more quantitative comparisons based on measurable metrics able to account for several aspects of a given chemical transformation, including: (i) the economic viability; (ii) the global mass flow and the waste products; (iii) the toxicological and eco-toxicological profiles of all the chemical species involved (reagents, solvents, catalysts, products).^{9–11}

In this paper, green chemistry metrics are used to compare some emblematic examples of methylation reactions carried out with four different reagents: dimethyl carbonate (MeOCO₂Me, DMC), methanol, dimethyl sulfate (MeOSO₃Me, DMS) and methyl iodide (MeI). In particular, three model transformations such as the O-methylation of phenol, the mono-C-methylation

Dipartimento di Scienze Ambientali dell'Università Ca' Foscari, Calle Larga S. Marta, 2137, Venezia, 30123, Italy. E-mail: selva@unive.it; Fax: +39 041 2348 584; Tel: +39 041 2348 687

of phenylacetonitrile, and the mono-N-methylation of aniline, have been examined.

The atom/mass balances as well as the overall flow of materials (reagents/catalysts/solvents, *etc.*) of these processes have been compared in terms of the atom economy (AE) and the mass index (MI). The reason for choosing atom economy and mass index as indicators was due mainly to their immediate connotation of the process efficiency. Other existing metrics such as effective mass yield (EMY), environmental factor (E), reaction mass efficiency (RME), carbon efficiency (CE), cost index (CI), and energy input either lacked the parameters necessary to calculate them in the literature, or are based on figures that are to some extent subjective (*e.g.* waste, non-benign reagent), and therefore hard to define.

In all cases DMC has proven to be an excellent methylating agent, often the best, among those considered.

Results and discussion

Safety and costs

A preliminary comparison of the four methylating agents was based on their chemical and toxicological properties.¹² Table 1 summarizes the figures and gives an estimation of costs of these compounds. It was readily appreciable that DMC was the only non toxic compound (it is merely classified as a flammable liquid), that could be handled without any of the precautions required for highly toxic MeI and DMS, and toxic methanol.

On the other hand, the cost of methanol was nearly 50% lower than that of DMC and DMS, and about 1/10 than that of MeI. This first set of figures indicated that methanol and DMC were both greener than MeI and DMS as far as safety and costs are concerned.

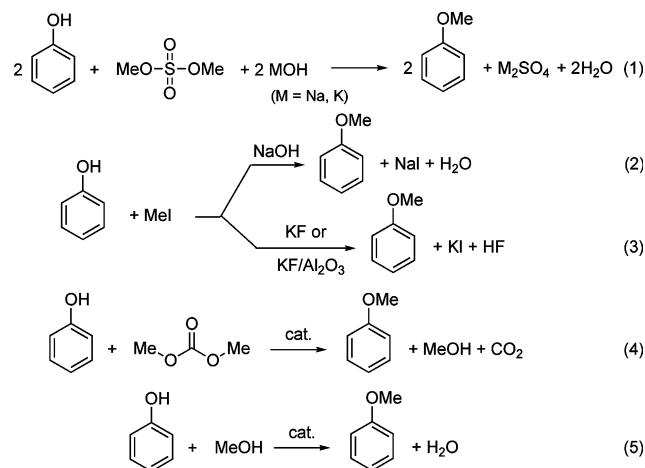
The literature sources

For the three process under investigation, the choice of bibliographic references was crucial for an objective comparison of different synthetic methods. Two major criteria were used to select examples from the literature: (i) better overall performance (yield and selectivity) of the process, and (ii) availability of the detailed description of the procedure. Nonetheless, at least

for some cited papers, authors might not have optimized experimental conditions in terms of the overall flow of materials (washing solvents, reactant's molar ratio, *etc.*).

The O-methylation reaction of phenol

The synthesis of anisole from phenol and alkylating agents such as methyl iodide and dimethyl sulfate (Williamson reaction), has been widely reported by both academic and industrial sources (Scheme 3, eqn (1), (2) and (3)).¹³ These reactions were compared to processes carried out with non toxic dimethyl carbonate and with methanol (Scheme 3, eqn (4), and (5)).



Scheme 3

Table 2 summarizes the results of thirteen different methods for the preparation of anisole.^{3,13-23}

The reactions of DMS occurred in presence of over-stoichiometric amounts of alkaline hydroxides, at $T > 60\text{ }^{\circ}\text{C}$ (processes 1–4). Under these conditions, both methyl groups of dimethyl sulfate were incorporated in the product, according to the stoichiometry of eqn (1), Scheme 3.^{14-16,23,24} In the case of MeI, basic co-reagents such as NaOH or KF were necessary (processes 5–9).²⁵

DMC-mediated processes took place over catalytic beds of potassium carbonate either as pure or supported/suspended on

Table 1 General properties of DMC, DMS, MeI and methanol

| | DMC | DMS | MeI | MeOH |
|---|----------------------------|--------------------------|--------------------|----------------------------|
| Oral acute toxicity (LD_{50} rats/ mg kg^{-1}) | 13800 | 440 | 76 | 5700 |
| Acute toxicity per contact (LD_{50} cavy/ mg kg^{-1}) | >2500 | na ^a | 110 | na |
| Acute toxicity per inhalation (LC_{50} rats/ mg l^{-1} , 4h) | 140 | 1.5 | na | 64 |
| Mutagenic properties | None | Mutagenic | Possible teratogen | na |
| Irritating properties (rabbits, eyes, skin) | None | Causes burns | Irritant to skin | Irritant to skin, eyes |
| Hazard identification | Highly flammable | Very toxic and corrosive | Very toxic | Toxic and highly flammable |
| Use of solvents | No | Yes | Yes | No |
| Waste water treatment | No | Yes | Yes | Yes/No |
| NaOH consumption | No | Yes | Yes | No |
| By-products ^b | MeOH, CO_2 | NaSO_4Me | NaI | H_2O |
| Thermodynamic | Not or slightly exothermic | Exothermic | Exothermic | |
| Cost/ € L^{-1} | ~30 | ~30 | ≥ 120 | 15–20 |

^a na: not available. ^b By-products defined for methylation processes.

Table 2 The evaluation of atom economy (AE,%) for the *O*-methylation of phenol

| Process number | Alkylating agent | Base | Operating mode | T/°C | Anisole yield (%) | AE (%) | Ref. | |
|----------------|---------------------------|---|--------------------|------|--------------------|--------|------|----|
| 1 | DMS | NaOH | Batch | 100 | 55 ^a | 55 | 14 | |
| 2 | | NaOH | | 100 | 74 ^a | | 15 | |
| 3 | | NaOH | | 100 | 72–75 ^a | | 16 | |
| 4 | MeI | KOH | Batch | 65 | 97 ^a | 51 | 17 | |
| 5 | | NaOH | | 25 | 90 ^a | | 18 | |
| 6 | | NaOH | | 60 | 97 ^a | | 19 | |
| 7 | | KF | | 25 | 88 ^a | | 35 | 20 |
| 8 | | KF/Al ₂ O ₃ | | 25 | 95 ^b | | 21 | |
| 9 | DMC | KF/Al ₂ O ₃ | c.-f. ^d | 25 | 100 ^b | 59 | 22 | |
| 10 | | K ₂ CO ₃ ^e | | 180 | 100 ^a | | 3a | |
| 11 | | K ₂ CO ₃ ^e | | 200 | 100 ^a | | 3d | |
| 12 | | K ₂ CO ₃ | | 160 | 92 ^a | | 23 | |
| 13 | MeOH/PhCO ₂ Me | NaOH | Batch | 320 | 42 ^e | 86 | 13b | |

^a Isolated yields. ^b Yield determined by GLC. ^c K₂CO₃ was coated/suspended with/in PEG 1500-6000. ^d Continuous-flow conditions. ^e The yield was evaluated at a conversion of 44%.

PEGs (polyethylene glycols). Although high temperatures (160–200 °C) were necessary, the base could be recycled indefinitely both under continuous-flow (c.-f.) and batch conditions (processes 10–12). Finally, a recent example of catalytic Williamson ether synthesis (CWES) was examined, by which anisole was prepared at a very high temperature (320 °C), from the reaction of phenol, methanol, benzoic acid, and NaOH (process 13). This environmentally benign CWES method, whose formal stoichiometry is described by eqn (5), Scheme 3, worked at a moderate conversion (44%), with an overall yield of 42% on the desired methyl ether.

The overall set of alkylation methods was initially evaluated through atom economy (AE, %: eqn (6)), which represents the mass-balance of a process related to its stoichiometric equation, *i.e.* the percentage of atoms of the reagent which end up in the product.¹¹

$$AE = \frac{MW \text{ (g mol}^{-1}\text{) product}}{\sum MW \text{ (g mol}^{-1}\text{) of all reagents used}} \times 100 \quad (6)$$

According to eqn (5) of Scheme 3, procedures mediated by MeOH allowed the best AE (86%, process 13). The reactions of DMS and DMC offered comparable values of AE (55–59%, processes 1–3 and 10–12, respectively). In fact, notwithstanding the non-catalytic nature of processes 1–3 (eqn (1), Scheme 3), both methyl groups of dimethyl sulfate ended up in the final product. The consumption of bases and most of all, the release of iodide salts, accounted for the poor AE in the case of MeI (35–39%, processes 5–9). However, by its intrinsic definition, the atom economy did not suffice to identify the cleaner (greener) process.

In order to include the chemical yield and the selectivity towards the desired product, as well as the mass of all reagents, solvents, catalysts, *etc.*, used in the examined reactions, a more all-encompassing metric, the mass index (MI or S⁻¹), was considered (eqn (7)).²⁶

$$MI = S^{-1} = \frac{\sum \text{reagents} + \text{catalysts} + \text{solvents} + \text{etc. (kg)}}{\text{Desired product (kg)}} \quad (7)$$

The overall flows of materials necessary for the calculation of MI, were taken from ref. 7b and 8–18.

Table 3 details the weight amounts of reagents, reaction auxiliaries (catalysts, solvents, co-reagents), and the desired product involved in processes 1–13.

The MI was initially evaluated only for the actual methylation reaction step. In some cases (processes 1–4 and 6), two values (a and b) of the mass index are indicated (Table 3): the first (a) included the mass of water used as the solvent and for workup, while the second (b) did not.²⁷ The comparison based on this metric showed that: (i) methyl iodide was the least efficient reagent (MI of 21–88, processes 6–9). The presence of iodine in the exhausted salt reasonably accounted for this result. (ii) Dimethyl sulfate (DMS) and dimethyl carbonate (DMC) afforded similar MI values (2.5 to 3.9, processes 1–3 and 10, 12), only on the condition that water was excluded from the mass balance. Otherwise, the mass index of reactions with DMC was, on average, 4 to 8 times lower than that of DMS mediated procedures (14 to 31, processes 1–2 and 4); (iii) the use of MeOH did not significantly improve the MI (2.9, process 13).

To further refine this mass analysis the reaction work-up had to be considered as well, by including all the solvents used for washes and extractions. Due to the lack of detailed experimental descriptions, the evaluation of MI for both the reaction and purification steps was possible only in a limited number of the examined processes. In particular, ref. 14–16, 3 and 23 allowed comparison of methods 1–3 and 10–12. In the reactions carried out with DMS, the extraction of anisole required extra solvents such as diethyl ether (150 mL, proc. 1–2), and benzene (200 mL, proc. 3), and CaCl₂ (10 g) as the drying agent. In the case of DMC, the c.-f. methods (proc. 10–11), did not involve additional materials, while the batch reaction consumed diethyl ether (20 mL, proc. 12) for the filtration/washing of the catalyst.²⁸ The comparison of the corresponding MI is summarized in Table 4.

This second approach confirmed that if water was excluded from the mass analysis, the flows of materials involved in processes mediated by DMS and DMC were comparable.

Except for process 1, mass indexes ranged from 3.0 to 6.2; in particular, for processes 3 and 10, the corresponding MI were 3 (DMS) and 3.5 (DMC). These data clearly indicated that the non toxic DMC was not only a safer replacement of DMS, but under suitable experimental conditions, the two alkylating agents were synthetically equivalent in terms of amounts of reactants and reaction auxiliaries involved.

Table 3 Overall flow of materials involved in processes of Scheme 3. The evaluation of mass index

| Process | Phenol/g | Alkylating agent (g used) | Base (g used) | Solvents ^a (g used) | Anisole (g used) | Others ^b (g used) | MI ^c | Ref. |
|---------|----------|---------------------------|---|-----------------------------------|------------------|------------------------------|--------------------|------|
| 1 | 18.8 | DMS (12.6) | NaOH (15) | H ₂ O (328.8) | 11.9 | — | (a) 31.5; (b) 3.9 | 14 |
| 2 | 47.0 | DMS (63.0) | NaOH (21) | H ₂ O (400) | 40 | — | (a) 13.2; (b) 3.3 | 15 |
| 3 | 470.0 | DMS (315.0) | NaOH (200) | H ₂ O (1000) | 388 | — | (a) 5.1; (b) 2.5 | 16 |
| 4 | 6.6 | DMS (8.8) | KOH (14) | H ₂ O (2) Dioxane (72) | 7.4 | — | (a) 14.0; (b) 13.7 | 17 |
| 5 | 0.94 | MeI (2.5) | NaOH (1.6) | DMSO (20) | 0.98 | — | 25.6 | 18 |
| 6 | 9.4 | MeI (15.1) | NaOH (200) | H ₂ O (1000) | 10.5 | CTMAB (3.2) | (a) 117; (b) 21.4 | 19 |
| 7 | 0.94 | MeI (1.26) | KF (1.74) | MeCN (20) | 0.95 | — | 25.2 | 20 |
| 8 | 0.41 | MeI (0.68) | KF/Al ₂ O ₃ (3.3) | MeCN (5.1) | 0.45 | — | 21.0 | 21 |
| 9 | 0.05 | MeI (0.2) | KF/Al ₂ O ₃ (0.4) | MeCN (4.4) | 0.057 | — | 88.6 | 22 |
| 10 | 94 | DMC (180) | K ₂ CO ₃ (95) | — | 108.0 | PEG 6000 (5) | 3.5 | 3a |
| 11 | 73.5 | DMC (76.5) | K ₂ CO ₃ (6) | — | 84.5 | PEG 1000 (300) | 5.4 | 3d |
| 12 | 10 | DMC (25) | K ₂ CO ₃ (4) | — | 10.6 | — | 3.7 | 23 |
| 13 | 213.4 | MeOH (70.4) | NaOH (3.2) | — | 102.9 | PhCO ₂ H (8.5) | 2.9 | 13b |

^a Overall amounts of solvents used as reaction media. ^b Additional reagents/catalysts. ^c (a) including water, (b) not including water.

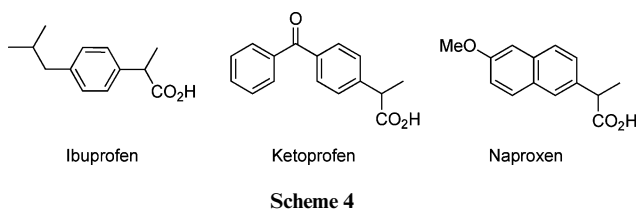
Table 4 The mass index evaluated for both reaction and work-up steps of the synthesis of anisole

| Process | Alkylating Agent | MI ^a | | Ref. |
|---------|------------------|-----------------|---------------------|------|
| | | Reaction | Reaction and workup | |
| 1 | DMS | 3.9 | 13.5 | 14 |
| 2 | | 3.3 | 6.2 | 15 |
| 3 | | 2.5 | 3.0 | 16 |
| 10 | DMC | 3.5 | 3.5 | 3a |
| 11 | | 5.4 | 5.4 | 3d |
| 12 | | 3.7 | 5.0 | 23 |

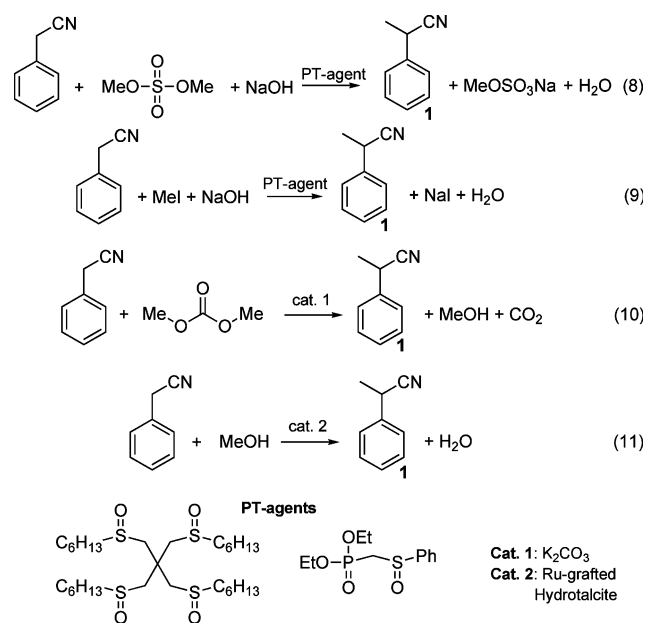
^a Water was always excluded from the mass-flow calculation.

The selective mono-C-methylation reaction of phenylacetoneitrile

In the past thirty years, the selective mono-C-methylation of arylacetic acid derivatives (arylacetonitriles and arylacetate esters) has been used for the synthesis of non steroidal analgesics belonging to the class of 2-arylpropionic (hydratropic) acids.^{2b,29} Ibuprofen, Ketoprofen, and Naproxen are well-known commercial examples (Scheme 4).



However, in the case of methylene active compounds, conventional methylation procedures with methyl halides or dimethyl sulfate, were often not satisfactory since competitive bis-C-alkylation reactions took over even at moderate conversions. The mono-methyl selectivity could be improved using phase-transfer (PT) catalysis. However, costly and not readily available PT-agents were necessary, and sizeable amounts of highly polluted water streams were generated. Scheme 5 (eqn (8) and (9))³⁰ and Table 5 (processes 14–18) report specific examples of the mono-methylation of phenylacetoneitrile with MeI and DMS, to prepare 2-phenylpropionitrile (**1**).^{31–35}



The use of dimethylcarbonate procured a major enhancement of both selectivity and process safety. In fact, in the presence of solid green catalysts (e.g. alkaline carbonates and zeolites), the reactions of a number of arylaceto-esters and -nitriles with DMC, gave the corresponding mono-C-methyl derivatives in up to 99% yield and selectivity.^{2b,7,36} Moreover, neither additional solvents nor treatment of waste effluents were required. Scheme 5 (eqn (10)) and Table 5 detail the case of phenylacetoneitrile by considering both continuous-flow and batch operating modes (processes 20 and 21, respectively).^{7a,e,37}

Finally, Table 5 also includes a recent report on the use of methanol for the methylation of phenylacetoneitrile carried out over a Ru-grafted hydrotalcite catalyst (process 22, eqn (11)).³⁸

Methylations with DMC and MeOH were highly atom economic (63–88%, processes 20–21 and 22) with respect to those mediated by MeI and DMS (44–46%, processes 14–18). In fact, the latter required one equivalent of base, thereby forming

Table 5 The evaluation of atom economy (AE,%) and mass index for the mono-*C*-methylation of phenylacetoneitrile

| Process number | Alkylating agent | Base | O. M. ^a | T/°C | Prod. 1 yield (%) | AE (%) | MI | Ref. |
|----------------|------------------|---|--------------------|------|-------------------|--------|----------|--------------------|
| 14 | MeI | NaNH ₂ | Batch | 80 | 74 ^b | 44 | 5.8 | 31 |
| 15 | | NaOH | Batch | rt | 92 ^b | 44 | 4.1 | 32 |
| 16 | | NaOH | Batch | rt | 66 ^b | 44 | 9.7 | 33 |
| 17 | | NaOH | Batch | rt | 83 ^b | 44 | 6.4 | 34 |
| 18 | DMS | K ₂ CO ₃ | Batch | rt | 82 ^b | 46 | 21.6 | 35 |
| 20 | DMC | K ₂ CO ₃ ^d | c.-f. ^e | 180 | 98 ^b | 63 | 3.7 | 36 |
| 21 | | K ₂ CO ₃ | Batch | 180 | 98 ^c | 63 | 8.2–11.9 | 7a,37 ^f |
| 22 | MeOH | none | Batch | 180 | 65 ^b | 88 | 21.5 | 38 |

^aO. M.: operating mode. ^bYield determined by GLC. ^cIsolated yields. ^dK₂CO₃ was coated/suspended with/in PEG 6000. ^eContinuous-flow conditions. ^fThe range of mass index depends on the DMC:substrate molar ratio (from 18:1 to 10:1) reported in ref. 7a and 37.

one equivalent of an inorganic salt as by-product (eqn (8) and (9), Scheme 5).

Experimental details of ref. 31–35 were not sufficient to estimate the mass flow of both reaction and work-up steps of processes 14–18. Therefore, the evaluation of MI was limited only to the methylation step of Scheme 5. Comparable mass indexes were calculated for MeI and DMC (4.1–9.7: processes 14–17; 3.7–11.9: processes 20–22). However, for MeI: (i) water had to be carefully excluded from the mass balance, and (ii) all PT-agents (processes 15–17) had to be considered as genuine catalysts, for which a quantitative recovery and reuse was possible.³⁹

In the case of process 22, despite the high atom economy, the MI was penalized by the excess of MeOH with respect to the substrate (a molar ratio MeOH/PhCH₂CN of ~50 was used).³⁸

Table 5 leads to conclusions similar to those mentioned above for the synthesis of anisole. In the methylation of phenylacetoneitrile and of related CH₂-active compounds, the non toxic DMC allowed a higher mono-*C*-methyl selectivity, and proved to be equivalent to or better than DMS and MeI, in terms of both AE and MI.

The selective mono-*N*-methylation reaction of aniline

The methylation of primary aromatic amines with methyl halides and dimethyl sulfate is even less selective than that of CH₂-active compounds. These reactions lead to mixtures of mono- and bis-*N*-methyl amines along with the corresponding trimethylanilinium salts.⁸

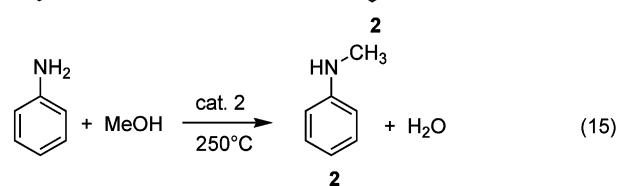
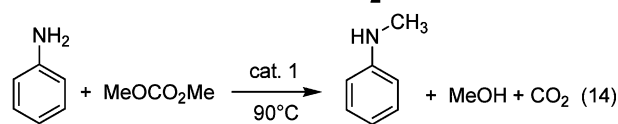
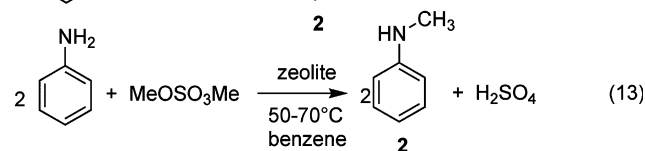
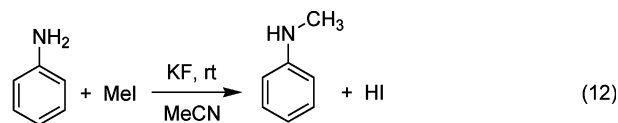
Therefore, the selective syntheses of mono-*N*-methyl anilines are mostly indirect multi-step procedures^{8,40} that are inherently inefficient, especially from a green chemistry perspective.⁹

These drawbacks can be overcome by using green alkylating agents such as dialkyl carbonates, in the presence of zeolites. Such methods not only make use of safer reagents and catalysts, but are also experimentally straightforward.

For example, in presence of alkali metal exchanged faujasites, a variety of anilines, even deactivated by both steric or electronic effects, reacted with dimethyl carbonate or methyl alkyl carbonates (ROCO₂Me, R = MeO(CH₂CH₂O)_{*n*}, *n* ≥ 2) to produce the corresponding mono-*N*-methyl anilines with up to 98% selectivity (Scheme 2) at quantitative conversions.^{7,41} Likewise, the use of methanol with different heterogeneous catalysts (V-, Cs-P-oxides, and Mg-phosphates) was reported to induce the selective formation of *N*-methyl aromatic amines;⁴² though,

under such conditions, the high reaction temperature (up to 500 °C) demanded gas-phase operations in continuous-flow. A modest conversion (not over 15–25% per pass) was compulsory to control the final selectivity.

In Table 6, the model mono-*N*-methylation of aniline is compared using the title methylating agents under different conditions (Scheme 6).^{20,40,43–50}



cat. 1: zeolites, V-AlPO₄, K₂CO₃

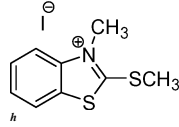
cat. 2: V-AlPO₄, Cs-P-Si oxide, Mg₃(PO₄)₂

Scheme 6

The choice of the reactions, and of the related references, was dictated by the possibility of calculating the mass index with sufficient uniformity.

The reaction of methanol showed the best atom economy, as almost 50% of the mass of the alcohol ended up in the product. For the other methylating agents, the trend of AE was different with respect to O- and C-alkylations (Tables 2 and 5): in particular, DMS afforded higher AE than DMC, followed by methyl iodide. The catalytic nature of processes 23–25, which represented rare examples where both DMS and MeI were used for a direct synthesis of mono-*N*-methyl aniline, accounted for this result.⁵¹ Notwithstanding the reasonably good AE, procedures based on methyl iodide (eqn (12), Scheme 6), and more so on DMS (eqn (13), Scheme 6), offered moderate

Table 6 The evaluation of atom economy (AE) and mass index (MI) for the mono-*N*-methylation of aniline

| Process number | Methylating agent | Catalyst | O.M. ^a | <i>T</i> /°C | Prod. 2 Yield (%) | AE (%) | MI | Ref. |
|----------------|-------------------------------------|---|--------------------|--------------|-------------------|--------|---------------------|------|
| 23 | MeI | KF | Batch | 25 | 67 ^b | 46 | 27.9 ^f | 20 |
| 24 | DMS | Zeolite K-X | Batch | 79 | 55 ^c | 69 | 126 ^a | 43 |
| 25 | DMS | Zeolite K-Y | Batch | 50 | 58 ^c | 69 | 480 ^f | 44 |
| 26 | DMC | Zeolite Na-Y | Batch | 90 | 93 ^b | 59 | 6.3 | 45 |
| 27 | DMC | V–AlPO ₄ | c.-f. ^e | 250 | 39 ^c | 59 | 5.3 ^{f,g} | 46 |
| 28 | DMC | K ₂ CO ₃ ^d | c.-f. ^e | 180 | 41 ^c | 59 | 51.2 ^g | 47 |
| 29 | MeOH | V–AlPO ₄ | c.-f. ^e | 250 | 32 ^c | 86 | 3.4 ^{f,g} | 46 |
| 30 | MeOH | Mg ₃ (PO ₄) ₂ | c.-f. ^e | 500 | 24 ^c | 86 | 10.2 ^{f,g} | 48 |
| 31 | MeOH | Cs–P–Si oxide | c.-f. ^e | 300 | 14 ^c | 86 | 58.2 ^{f,g} | 49 |
| 32 | TosCH ₃ |  | batch (3 steps) | 25–100 | 88 ^b | 14 | 774 | 40 |
| 33 | (CH ₃ O) ₃ CH | H ₂ SO ₄ | Batch (2 steps) | 180 | 44 ^b | 54 | 15.9 | 50 |

^a O.M.: operating mode. ^b Isolated yields. ^c Yield determined by GLC. ^d K₂CO₃ was coated with PEG 6000. ^e Continuous-flow conditions. ^f Does not include workup. ^g For convenience of comparison, the MI was normalized for 1h of c.-f. operation. ^h 3-methyl-2-methylthiothiazolium iodide was used as a stoichiometric reagent.

yields (58–67%) and required large amounts of added materials (excess of reagents and solvents), that raised significantly the corresponding MI (27.9, 126, and 480). Plus, they suffered from laborious workup procedures, whose overall mass flow was not exactly quantifiable, that would have multiplied MI by a factor of at least 3. Not to mention the toxicity of both the methylating reagents.

The methylations using DMC were effective both in batch and in c.-f. conditions, in the presence of zeolites and V–AlPO₄ catalysts (processes 26 and 27). These procedures showed extremely good MIs of 6.3 and 5.3, respectively. In particular, a good example was process 26, reported here for the first time as an optimization of a previous procedure:⁴⁵ it worked at 90 °C, and gave the product (**2**) in a 93% isolated yield. At 250 °C, instead, in the c.-f. system 27, a high mono-*N*-methyl selectivity was possible only by operating with low conversions which resulted in low yields per pass (39%). The MI would improve by recycling the feed.⁵² Process 28 was also considered among c.-f. methods mediated by DMC. In this case, the use of K₂CO₃ as catalyst allowed only a 41% yield of mono-*N*-methyl aniline even in the presence of a relatively large molar excess of dimethyl carbonate (4 with respect to aniline), that resulted in a poor MI of 51.2.

The methylation of aniline with MeOH was highly efficient in the gas phase (250–500 °C) under c.-f. conditions.⁵³ An excellent MI of 3.4 was calculated with V–AlPO₄ as the catalyst (process 29). The overall reaction effectiveness decreased considerably with other catalytic systems: in fact, the mono-*N*-methyl selectivity was of only 78% over Mg-phosphates (process 30), while the reaction catalysed by mixed oxides required large volumes of methanol (PhNH₂ : MeOH in a 1 : 20 molar ratio; process 31). The corresponding MIs were of 10.2 and 58.2, respectively.

In Table 6, two more examples were considered in which batch multistep methods and different methylating agents were involved. Process 32 was based on toluene *p*-sulfonate and it represented a very elegant and high yielding procedure for the mono-*N*-methylation of a number of amines. The large number

of steps and of reagents, along with the fact that the reaction was stoichiometric rather than catalytic, provided for the low atom economy (14%) and the staggering mass index (774). This represents a perfect example of a high yielding laboratory method (overall yield = 88%) that will hardly be used on large scale, and was inserted mainly for comparison.

The second method, process 33, used trimethylorthoformate in presence of catalytic amounts of H₂SO₄. This was a procedure published in *Organic Syntheses*, whose values of AE (54%) and MI (15.9, including workup) could be calculated reliably and were competitive. However, it required two steps, and the isolation of *N*-methylformanilide as an intermediate.

Conclusions

The synthesis of anisole, of 2-phenylpropionitrile, and of mono-*N*-methyl aniline, representative of industrial processes for the production of pharmaceuticals, fragrances, dyestuffs, and cosmetics, were used to compare the methylating efficiency of dimethyl carbonate, dimethyl sulfate, methyl iodide and methanol.

Atom economy and mass index were calculated for 33 different procedures. The results are summarized in Fig. 1, where the best values of AE and MI are plotted for each methylating agent and for each of the tested reactions.

The atom economy generally follows the trend: MeOH >> DMC ≥ DMS > MeI (Fig. 1, left). Two factors account for this behaviour: (i) for methanol, 47% of its mass is incorporated in the final products, more than twice as much as the other reagents (DMC 16%, DMS 12%, or 24% when both methyl groups are incorporated, MeI 11%); (ii) methanol and DMC require catalytic base or zeolites, as opposed to DMS and MeI.

MeOH and DMC offer similar low values of MI (on average, in the range of 3–5.5), better than those achievable with DMS and MeI (Fig. 1, right).

This analysis is, of course, far from being exhaustive. For example, the energy input and the cost index of each process

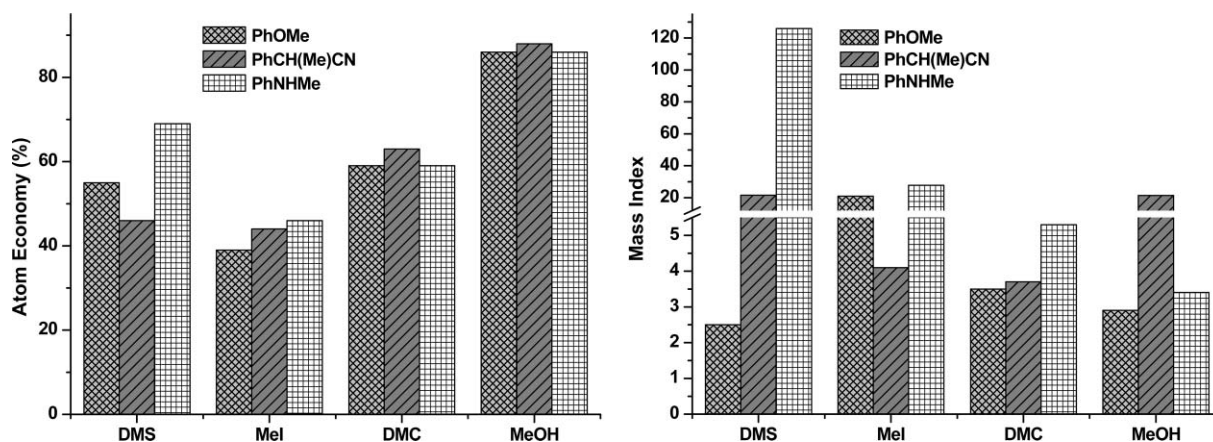


Fig. 1 The atom economy (right) and the mass index (left) for the reaction of phenol, phenylacetonitrile, and aniline with different methylating agents.

as well as eco-toxicological metrics^{3d} were not examined. This, however, is beyond the scope of this work.

The conclusion is that the favourable AE and MI of methylation processes mediated by dimethyl carbonate and methyl alcohol, inherently reflect the greenness of these reactions, attained by avoiding wastes and by-products, by avoiding additional solvents and derivatization sequences, by the catalytic use of base or solid catalysts, and thanks to the ease of workup (if any). Additional factors make the use of DMC favourable with respect to MeOH: (i) DMC is non toxic; (ii) it is active at lower temperatures than methanol; (iii) usually, DMC operates with simple catalytic systems that can be recycled indefinitely.⁵⁴ MeOH, on the other hand, often requires catalysts prepared *ad hoc*, the synthesis of which should perhaps be included in the calculations of the mass balance, along with an evaluation of their lifetime.

Acknowledgements

MUR (Italian Ministry of University and Research) is gratefully acknowledged for financial support.

References

- (a) K. Weissermel, H.-J. Arpe, in *Industrial Organic Chemistry*, Wiley-VCH, Weinheim, 2003; (b) A. Kleemann, J. Engel, B. Kutschner and D. Reichert, in *Pharmaceutical Substances: Syntheses, Patents, Applications*, Thieme, Stuttgart, New York, 2001.
- (a) A.-A. Shaik and S. Sivaram, *Chem. Rev.*, 1996, **96**, 951–976; (b) P. Tundo and M. Selva, *Acc. Chem. Res.*, 2002, **35**, 706–716.
- (a) P. Tundo, F. Trotta, G. Moraglio and F. Ligorati, *Ind. Eng. Chem. Res.*, 1988, **27**, 1565–1571; (b) H. Dressler, *US Pat* 5059723, October 22, 1991; (c) M. Selva and P. Tundo, *Chemtech.*, 1995, **25**(5), 31–35; (d) Y. Ono, *Appl. Catal. A: General*, 1997, **155**, 133–166; (e) A. Bomben, M. Selva, P. Tundo and L. Valli, *Ind. Eng. Chem. Res.*, 1999, **38**, 2075–2079; (f) A. Perosa, M. Selva, P. Tundo and F. Zordan, *Synlett*, 2000, **1**, 272–274; (g) M. Selva, P. Tundo and A. Perosa, *J. Org. Chem.*, 2001, **66**, 677–680; (h) S. Udayakumar, A. Pandurangan and P. K. Sinha, *Appl. Catal. A: General*, 2004, **272**, 267–279; (i) A. B. Shivarkar, S. P. Gupte and R. V. Chaudari, *Synlett*, 2006, **9**, 1374–1376; (j) M. Selva, P. Tundo, *Eur. Pat.* 1431274, August 15, 2007.
- (a) A.-A. Shaik and S. Sivaram, *Ind. Eng. Chem. Res.*, 1992, **31**, 1167–1170; (b) F. Rivetti, U. Romano and D. Delledonne, in *Green Chemistry: Designing Chemistry for the Environment*, ed. P. T. Anastas and T. C. Williamson, ACS symposium series 626, Washington DC, 1996, ch. 6; (c) M. A. Pacheco and C. L. Marshall, *Energy Fuels*, 1997, **11**, 2–29; (d) D. Delledonne, F. Rivetti and U. Romano, *Appl. Catal. A: Gen.*, 2001, **221**, 241; (e) P. De Filippis, M. Scarsella, C. Borgianni and F. Pochetti, *Energy Fuels*, 2006, **20**, 17–20.
- In path (a) of Scheme 1, ethylene carbonate serves as the building block for the CO₂ fragment of DMC. Although, the reaction itself has a modest atom economy, the overall reaction efficiency should consider that the co-product ethylene glycol is also a highly valuable compound.
- (a) M. Massi Mauri, U. Romano, R. Tesi and P. Rebora, *Ind. Eng. Chem. Prod. Res. Dev.*, 1980, **19**, 396–402; (b) B. M. Bhanage, S.-I. Fujita, Y. Ikushina and M. Arai, *Appl. Catal. A: General*, 2001, **219**, 259–266.
- (a) M. Selva, C. A. Marques and P. Tundo, *J. Chem. Soc., Perkin Trans. 1*, 1994, 1323–1328; (b) M. Selva, A. Bomben, P. Tundo and C. A. Marques, *Tetrahedron*, 1995, **51**(42), 11573–11580; (c) M. Selva, A. Bomben and P. Tundo, *J. Chem. Soc., Perkin Trans. 1*, 1997, 1041–1045; (d) P. Tundo, M. Selva and A. Bomben, *Org. Synth.*, 1999, **76**, 169–177; (e) M. Selva, P. Tundo, A. Perosa and S. Memoli, *J. Org. Chem.*, 2002, **67**, 1071–1077; (f) M. Selva, P. Tundo and A. Perosa, *J. Org. Chem.*, 2003, **68**, 7374–7378; (g) M. Selva and P. Tundo, *J. Org. Chem.*, 2006, **71**, 1464–1470; (h) M. Selva, P. Tundo, D. Brunelli and A. Perosa, *Green Chem.*, 2007, **9**, 463–468.
- J. March, in *Advanced Organic Chemistry, Reactions, Mechanisms and Structure*, J. Wiley & Sons, Inc., New York, 4th edn, 1992.
- (a) P. T. Anastas, T. C. Williamson, In *Green Chemistry, Frontiers in Benign Chemical Syntheses and Processes*, ed. P. T. Anastas, T. C. Williamson, Oxford University Press, Oxford, 1998; (b) P. T. Anastas, J. C. Warner, In *Green Chemistry Theory and Practice*, Oxford University Press, 1998.
- J. L. Tucker, *Org. Process Res. Dev.*, 2006, **10**, 315–319.
- (a) N. Winterton, *Green Chem.*, 2001, **3**, G73–G75; (b) A. D. Curzons, D. J. C. Constable, D. N. Mortimer and V. L. Cunningham, *Green Chem.*, 2001, **3**, 1–6; (c) A. D. Curzons, D. J. C. Constable and V. L. Cunningham, *Green Chem.*, 2002, **4**, 521–527; (d) M. Eissen and J. Metzger, *Chem.–Eur. J.*, 2002, **8**, 3581–3585; (e) M. Eissen, K. Hungerbühler, S. Dirks and J. Metzger, *Green Chem.*, 2003, **5**, G25–G27; (f) M. Eissen, R. Mazur, H.-G. Quebbemann and K.-H. Pennemann, *Helv. Chim. Acta*, 2004, **87**, 524–535.
- Data were taken from: (a) ref. 4b; (b) MSDS on <http://www.sigmaaldrich.com>.
- (a) Kirk-Othmer, *Encyclopedia of Chemical Technology* 1983, 3rd edn, vol. 22, pp. 236–250; (b) E. Fuhrmann and J. Talbiersky, *Org. Process Res. Dev.*, 2005, **9**, 206–211.
- (a) H. R. Lewis, S. Shaffer, W. Trieschmann and H. Cogan, *Ind. Eng. Chem.*, 1930, **22**, 34–36.
- A. I. Vogel, A. R. Tatchell, B. S. Furnis and A. J. Hannaford, *Vogel's Textbook of Practical Organic Chemistry*, Longman, UK, 4th edn, 1988.
- G. S. Hiers, F. D. Hager, *Org. Synth. Coll. Vol. I*, Wiley, New York, 1932, pp. 58–60.
- D. Achet, D. Rocrelle, I. Murengezi, M. Delmas and A. Gaset, *Synthesis*, 1986, 642.

- 18 N. J. Hales, H. Heaney, J. H. Hollinshead and S. V. Ley, *Tetrahedron*, 1995, **51**, 7741–7754.
- 19 B. Jurić, *Tetrahedron*, 1988, **44**, 6677–6680.
- 20 N. Ishikawa, T. Kitazume and M. Nakabayashi, *Chem. Lett.*, 1980, 1089–1090.
- 21 T. Ando, J. Yamawaki, T. Kawate, S. Sumi and T. Hanafusa, *Bull. Chem. Soc. Jpn.*, 1982, **55**, 2504–2507.
- 22 T. Ando, S. J. Brown, J. H. Clark, D. G. Cork, T. Hanafusa, J. Ichihara, J. M. Miller and M. S. Robertson, *J. Chem. Soc. Perkin Trans. 2*, 1986, 1133–1139.
- 23 Process 12 was carried out by modifying a procedure previously reported by us: M. Selva, F. Trotta and P. Tundo, *J. Chem. Soc. Perkin Trans. 2*, 1992, **4**, 519–522. In particular: phenol (10 g, 106 mmol), DMC (25 g, 288 mmol), and K_2CO_3 (4 g, 29 mmol) were charged in a 90 mL stainless-steel autoclave. The reactor was purged (vacuum– N_2 cycles), and heated at 160 °C, while the mixture was magnetically stirred. After 15 hours, the autoclave was cooled to room temperature, the solid base was removed by vacuum filtration, and the resulting solution stripped of residual MeOH/DMC by rotary evaporation to yield pure anisole in 92% yield.
- 24 G. H. Green and J. Kenyon, *J. Chem. Soc.*, 1950, 1589–1596.
- 25 In presence of KF, the alkylation reaction released HF (eqn (3), Scheme 3) which, in turn, reacted with the basic alumina surface to produce K_3AlF_6 (ref. 14). Although this reaction modified the support, it had no effects on the overall methylation stoichiometry.
- 26 As reported in ref. 3, the MI is expressed as the ratio of all raw materials [kg] to the product [kg]. From both environmental and synthetic standpoints, the lower the MI, the better the process is. In the ideal situation, MI would approach 1.
- 27 Stemming from the fact that water is an intrinsically safe solvent and it is often used in large amounts, some authors tend to exclude it from mass calculations to not skew mass data (see ref. 3). However, in the present study, water streams are highly polluted by toxic alkylating agents (DMS and MeI).
- 28 In the c.-f. methylations mediated by DMC, a mixture of anisole and MeOH was collected at the outlet of both plug-flow and CSTR reactors. Only a final distillation step was necessary to recover the pure product.
- 29 J.-P. Rieu, A. Boucherle, H. Cousse and G. Mouzin, *Tetrahedron*, 1986, **42**, 4095–4131.
- 30 Since only one methyl group of DMS reacted with phenylacetone at ambient temperature, stoichiometric coefficients and the co-product salt ($NaOSO_3Me$) of eqn (8), Scheme 5 were different than those of the corresponding reaction with phenol (eqn (1), Scheme 3).
- 31 R. W. Hartmann and C. Batzl, *J. Med. Chem.*, 1986, **29**, 1362–1369.
- 32 (a) H. Fujihara, K. Imaoka and N. Furukawa, *J. Chem. Soc., Perkin Trans. 1*, 1986, 333–336; (b) N. Furukawa, K. Imaoka, H. Fujihara and S. Oae, *Chem. Lett.*, 1982, 1421–1424.
- 33 (a) C. M. Starks, C. Liotta, in *Phase Transfer Catalysis Principles and Techniques*, Academic Press Inc., London, 1978; (b) M. Mikołajczyk, S. Grzejszczak, A. Zaroski, F. Montanari and M. Cinquini, *Tetrahedron Lett.*, 1975, 3757–3760.
- 34 N. Furukawa, S. Ogawa, T. Kawai and S. Oae, *J. Chem. Soc., Perkin Trans. 1*, 1984, 1833–1838.
- 35 V. L. K. Valli, G. V. M. Sarma and B. M. Choudary, *Indian J. Chem., Sect. B: Org. Chem. Incl. Med. Chem.*, 1990, **29B**, 481–482.
- 36 P. Tundo, F. Trotta and G. Moraglio, *J. Chem. Soc., Perkin Trans. 1*, 1989, 1070–1071.
- 37 P. Tundo, P. Loosen, M. Selva, *Eur. Pat.* 0525 506B1, May 01, 1996 and *US Pat.* 5278333, January 10, 1994.
- 38 K. Motokura, D. Nishimura, K. Mori, T. Mizugaki, K. Ebitani and K. Kaneda, *J. Am. Chem. Soc.*, 2004, **126**, 5662–5663.
- 39 It is well known that, under phase-transfer catalysis conditions, the partitioning of PT-agents between an organic and an aqueous phase, does not allow the full recovery and restoration of the catalyst, after each reaction (see ref. 30).
- 40 A. R. Katritzky, M. Drewniak and J. M. Aurrecochea, *J. Chem. Soc., Perkin Trans. 1*, 1987, 2539–2541.
- 41 (a) Z.-H. Fu and Y. Ono, *Catal. Lett.*, 1992, **18**, 59–63; (b) M. Selva, P. Tundo and A. Perosa, *J. Org. Chem.*, 2001, **66**, 677–680; (c) M. Selva, P. Tundo and A. Perosa, *J. Org. Chem.*, 2002, **67**, 9238–9247; (d) M. Selva, P. Tundo and T. Foccardi, *J. Org. Chem.*, 2005, **70**, 2476–2485.
- 42 (a) P. Y. Chen, S. J. Chu, M. G. Chen, N. S. Chung, W. C. Lin, *US Pat.* 4801752, January 31, 1989; (b) F. M. Bautista, J. M. Campelo, A. Garcia, D. Luna, J. M. Marinas, A. A. Romero and M. R. Urbano, *J. Catal.*, 1997, **172**, 103–109; (c) M. Vijayaraj and C. S. Gopinath, *J. Catal.*, 2006, **241**, 83–95; (d) M. Vijayaraj and C. S. Gopinath, *Appl. Catal. A: General*, 2007, **320**, 64–68.
- 43 M. Onaka, K. Ishikawa and Y. Izumi, *Chem. Lett.*, 1982, 1783–1786.
- 44 M. Onaka, A. Umezono, M. Kawai and Y. Izumi, *J. Chem. Soc., Chem. Commun.*, 1985, 1202–1203.
- 45 Process 26 was carried out by modifying the experimental procedure reported in the ref. 7c. In particular: aniline (2 g, 21.5 mmol), DMC (4 g, 44.4 mmol), and a faujasite NaY (2.4 g, from Aldrich) were charged in a 25 mL round bottomed flask fitted with a reflux condenser. After three vacuum– N_2 cycles, the mixture was magnetically stirred and heated at 90 °C under nitrogen for 5 hours. After cooling to room temperature, the zeolite was removed by vacuum filtration, and the resulting solution stripped of residual DMC by rotary evaporation to yield pure product (2) in 93% yield.
- 46 N. Nagaraju and G. Kuriakose, *New J. Chem.*, 2003, **27**, 765–768.
- 47 F. Trotta, P. Tundo and G. Moraglio, *J. Org. Chem.*, 1987, **52**, 1300–1304.
- 48 M. A. Aramendia, V. Borau, C. Jimenez, J. M. Marinas and F. J. Romero, *Appl. Catal. A: General*, 1999, **183**, 73–80.
- 49 T. Oku, Y. Arita, H. Tsuneki and T. Ikariya, *J. Am. Chem. Soc.*, 2004, **126**, 7368–7377.
- 50 R. M. Roberts and P. J. Vogt, *Org. Synth.*, 1963, **4**, 420–422.
- 51 It should be noted that co-products of reactions (12) and (13) were HI and H_2SO_4 . The release of both these acids should be expected to affect the catalytic activity of KF and zeolites (KX and NaX).
- 52 Recycling of the feed was not mentioned by the authors of ref. 44 (process 27).
- 53 At high temperatures, batch reactions with MeOH proceed under high autogenous pressures. For instance, at 320 bar, a volume of 90 mL of methyl alcohol generates 60 bar of pressure (see ref. 9b). Therefore, c.-f. methods are always recommended with volatile alcohols, to avoid hazardous conditions.
- 54 The formation of the toxic methanol as a co-product of DMC-mediated methylations (Scheme 3, 4 and 6), might somewhat mitigate the environmental benefits of DMC. Methanol is usually isolated (and disposed) by filtration/distillation, under conditions which are more controlled (and safer) than those used for the reactions. A thorough assessment of this problem should however, be carried out by toxicological metrics, not pertinent to this work.

Solvent-free synthesis of substituted ureas from CO₂ and amines with a functional ionic liquid as the catalyst

Tao Jiang,* Xiumin Ma, Yinxi Zhou, Shuguang Liang, Jicheng Zhang and Buxing Han*

Received 19th November 2007, Accepted 11th February 2008

First published as an Advance Article on the web 29th February 2008

DOI: 10.1039/b717868a

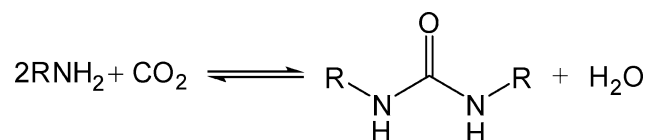
The synthesis of disubstituted ureas from amines and CO₂ were carried out using a basic ionic liquid (IL) 1-*n*-butyl-3-methyl imidazolium hydroxide ([Bmim]OH) as the catalyst. The effects of reaction time, amount of [Bmim]OH, reaction temperature, pressure, and solvent on yields of the products were investigated. The results indicated that aliphatic amines, cyclohexylamine, and benzylamine could be converted to the corresponding ureas selectively in moderate yields under solvent-free conditions without using any dehydrating reagent. The IL could be reused after a simple separation procedure.

Introduction

Chemistry is facing increasing pressure from environmental concerns. Many conventional chemical processes use large amounts of toxic reactants and/or volatile solvents. Replacement of these hazardous reagents in chemical processes is one of the main goals of green chemistry. It is well known that isocyanates, carbamates, and 1,3-disubstituted ureas are important N-containing chemical products. 1,3-Disubstituted ureas are useful chemical intermediates in the synthesis of pharmaceuticals, agricultural chemicals, and in dye chemistry.¹ They are also used as antioxidants in gasoline and additives in plastics.

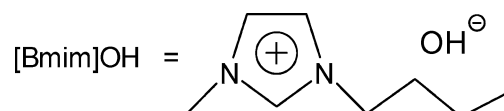
1,3-Disubstituted ureas are generally synthesized by the phosgenation of amine, which uses highly toxic phosgene. Some non-phosgene-based manufacturing processes have been developed to avoid use of phosgene. Oxidative carbonylation of amines with CO is one of the alternative routes. Metal catalysts, including Au,² Pd,³ and W⁴ *etc.*, have been extensively utilized in this process. But aside from the toxicity of CO, there exists the risk of explosive of the mixture of CO and O₂. Another phosgene-free route is the use of dimethyl carbonate or dimethyl sulfate.^{5,6} But these methylating reagents are relatively expensive. In recent years, the utilization of CO₂ has attracted much attention because it is a renewable, cheap, safe, abundant, and non-toxic carbon resource. Direct synthesis of substituted ureas from amines and CO₂ has also been reported (Scheme 1), and different catalysts, such as RuCl₃·H₂O/Bu₃P⁷ and Ph₃SbO/P₄S₁₀⁸ can be used. Water is the only byproduct in this process. Addition of dehydrating agents such as POCl₃, propargyl alcohols,⁷ Me₃NSO₃,⁹ diorganophosphites,¹⁰ and carbodiimide¹¹ can increase the yields of target products because this is a reversible reaction.¹² Vos and coworkers prepared symmetrical and asymmetrical urea

derivatives in good yields from CO₂ and amines using Cs⁺ base catalysts and *N*-methylpyrrolidone as the solvent without dehydrating agent.¹²



Scheme 1 Carbonylation of amines with CO₂.

In recent years, ionic liquids (ILs) have attracted much attention due to their special properties, such as almost undetectable vapor pressure, wide liquid temperature range, excellent chemical stability, high thermal stability, and strong solvent power for a wide range of organic, inorganic, and polymeric molecules. Some ILs have been successfully used as the media in many chemical reactions.^{13,14} Deng *et al.* reported the synthesis of substituted ureas from CO₂ and primary amines using CsOH as the catalyst in ILs [Bmim]BF₄, [Bmim]PF₆, [Bmim]Cl, and [Cmim]Cl,¹⁵ and excellent coupling of reaction and separation was realized using the CsOH/IL system. Many functional ILs have also been synthesized and utilized as catalysts for different reactions, such as Henry reaction,¹⁶ and direct Aldol reaction,^{17,18} Mannich reaction,¹⁹ synthesis of tocopherol,²⁰ and esterification.^{21–24} Recently, Ranu and coworkers²⁵ reported a basic IL, 1-*n*-butyl-3-methyl imidazolium hydroxide [Bmim]OH (Scheme 2). This IL has been used to catalyze Michael addition^{26,27} and Knoevenagel condensation.²⁸



Scheme 2 Structure of 1-*n*-butyl-3-methyl imidazolium hydroxide [Bmim]OH.

Clearly, synthesis of 1,3-disubstituted ureas by carbonylation of amines with CO₂ using cheaper and recyclable catalysts at solvent-free condition is desirable and challenging. In this work,

Beijing National Laboratory for Molecular Sciences (BNLMS), Centre for Molecular Science, Institute of Chemistry, Chinese Academy of Sciences, Beijing, 100080, China.
E-mail: Jiangt@iccas.ac.cn, Hanbx@iccas.ac.cn; Fax: +86 10 62562821; Tel: +86 10 62562821

Table 1 Effect of reaction time on the reaction of *n*-butylamine with CO₂^a

| Entry | Catalyst (mol%) | Reaction time/h | Isolated yields (%) |
|-------|-----------------|-----------------|---------------------|
| 1 | 5 | 11 | 36.7 |
| 2 | 5 | 19 | 42.8 |
| 3 | 5 | 24 | 52.3 |
| 4 | 10 | 8 | 52.4 |
| 5 | 10 | 15 | 53.5 |
| 6 | 10 | 19 | 54.4 |
| 7 | 10 | 24 | 54.4 |

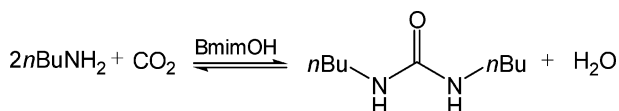
^a Conditions: 5 mmol of *n*-butylamine, pressure 5.5 MPa, temperature 170 °C, solvent-free. The yield was determined by the mol of product and *n*-butylamine.

we explored the catalytic performance of [Bmim]OH for these kinds of reactions. It was discovered that 1,3-disubstituted ureas could be synthesized in reasonable yield and very high selectivity using the IL as the catalyst without using any dehydrating agent under solvent-free conditions. Different amines including aliphatic amines, cyclohexylamine, and benzylamine can be converted to the corresponding ureas. The recovery of the catalyst and separation of products are easy.

Results and discussion

Effects of reaction time

The reaction of *n*-butylamine with CO₂ was used as a model reaction (Scheme 3) to investigate the catalytic performance of [Bmim]OH. Table 1 lists the effect of reaction time on the reaction. The reaction between amines and CO₂ can be

**Scheme 3** Synthesis of *N,N'*-dibutyl urea from *n*-butylamine and CO₂.

performed without any dehydrating agents and solvents. With the increasing reaction time, the yield of *N,N'*-dibutyl urea increased. When the amount of [Bmim]OH was 10 mol%, the yield of the product did not increase with the reaction time after 19 h (Table 1, entries 4–7). Byproduct was not detected in the reaction. Therefore, other experiments were performed for 19 h in the following research.

Effects of other conditions

The effect of temperature on the yield can be seen from Table 2. It was shown that a suitable temperature is required for the reaction to reach a reasonable conversion (Table 2, entries 1–5). At low temperatures the reaction rate was slow. At 170 °C, the yield reached a maximum, *i.e.* 55.1%. When the temperature was increased to 190 °C, the yield decreased because the reaction is exothermic,¹² and was shifted towards the left with increasing temperature. The yield increased from 42.8% to 55.1% when the amount of [Bmim]OH increased from 5 mol% to 15 mol%, but did not change noticeably as the amount was increased further (Table 2, entries 6–9).

The phase behavior of the reaction system containing CO₂, *n*-butylamine and [Bmim]OH was observed in a high-pressure view cell at 170 °C and 1.5–12.5 MPa (the volume ratio of the chemicals to the view cell was the same as that in the reaction system). There were two phases in the system in the entire pressure range studied, indicating that the variation of CO₂ pressure did not affect the phase behavior of the reaction system. The effect of CO₂ pressure on the yield was investigated in the range of 1.5–12.5 MPa at 170 °C (Table 2, entries 10–17). The yield of *N,N'*-dibutyl urea increased with the increasing pressure up to 12.5 MPa. But the yield was more sensitive to pressure up to 4.5 MPa, and the effect of pressure on the yield was much smaller at the higher pressure. The main reason is that at lower pressure, an increase in pressure enhances the reaction rate because CO₂ is a reactant and the solubility of CO₂ in the reaction phase increases with increasing pressure. When the

Table 2 Effect of other conditions on the reaction of *n*-butylamine with CO₂^a

| Entry | Catalyst (mol%) | Temperature/°C | Pressure/MPa | Isolated yields (%) |
|-----------------|-----------------|----------------|--------------|---------------------|
| 1 | 15 | 150 | 5.5 | 35.3 |
| 2 | 15 | 160 | 5.5 | 47.0 |
| 3 | 15 | 170 | 5.5 | 55.1 |
| 4 | 15 | 180 | 5.5 | 50.0 |
| 5 | 15 | 190 | 5.5 | 39.5 |
| 6 | 5 | 170 | 5.5 | 42.8 |
| 7 | 10 | 170 | 5.5 | 54.4 |
| 8 | 15 | 170 | 5.5 | 55.1 |
| 9 | 20 | 170 | 5.5 | 55.6 |
| 10 | 15 | 170 | 1.5 | 25.1 |
| 11 | 15 | 170 | 2.5 | 33.0 |
| 12 | 15 | 170 | 3.5 | 48.6 |
| 13 | 15 | 170 | 4.5 | 54.2 |
| 14 | 15 | 170 | 5.5 | 55.1 |
| 15 | 15 | 170 | 7.5 | 55.4 |
| 16 | 15 | 170 | 10.0 | 57.4 |
| 17 | 15 | 170 | 12.5 | 58.6 |
| 18 ^b | 15 | 170 | 5.5 | 52.8 |

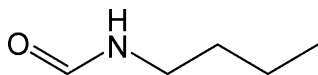
^a Conditions: 5 mmol of *n*-butylamine, reaction time 19 h, solvent-free. The yield was determined by the mol of product and *n*-butylamine. ^b Resued for the second time of [Bmim]OH in entry 14.

pressure is higher than 4.5 MPa, the concentration of CO₂ in the reaction phase is high enough, and therefore, the effect of pressure on the yield is very limited at the higher pressure.

The recycling of [Bmim]OH was performed with the catalyst used in entry 14. The results showed that similar yield of *N,N'*-dibutyl urea could be obtained in the second reuse (Table 2, entries 14 and 18). The used [Bmim]OH was characterized using NMR, and it was shown that the structure of the used [Bmim]OH was the same as the original one.

Carbonylation in different solvents

The reaction of *n*-butylamine and CO₂ was conducted in several organic solvents at 5.5 MPa, and the results are presented in Table 3. The yield of 1,3-dibutyl urea was 55.1% in solvent-free condition (Table 3, entry 1). The yield of the product in NMP or *N*-methylpyrrole was a little higher than that in solvent-free condition (Table 3, entries 2 and 3). But the yield in pyridine was similar to that in solvent-free condition (Table 3, entry 4). The yields in THF or DMF were relatively low (Table 3, entries 5 and 6). In other solvents, the reaction did not occur obviously (Table 3, entries 7–10). We analyzed the by-products of the reactions in different solvents with GC-MS, and the selectivities are presented in Table 3. As shown in Table 3, in solvent-free condition or in NMP, *N*-methylpyrrole and pyridine, the by-product was not detectable, while in THF and DMF, there was a by-product, the structure of which is given in Scheme 4. The results in Table 3 indicate that the properties of solvents affect both the yields and selectivity, and in the basic solvents both yield and selectivity are higher. The solvent effect is a very important issue but quite complex. At present, we do not have complete explanation for these observations.

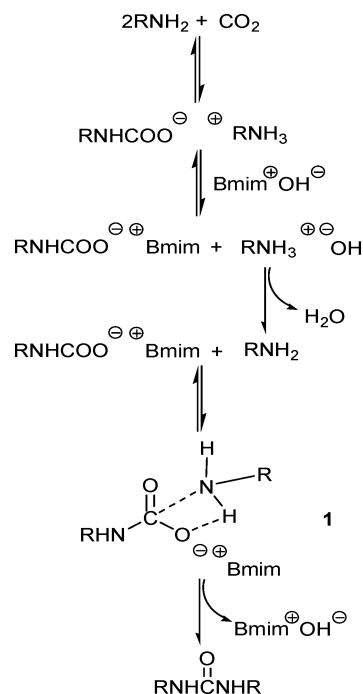


Scheme 4 By-product in reactions of *n*-butylamine in THF or DMF.

Synthesis of disubstituted ureas from different amines

The reactions of some other amines with CO₂ were also conducted at solvent-free condition and in NMP, and the results are given in Table 4. In solvent-free conditions, the linear amines

(Table 4, entries 2–4) showed better reactivity than branched amine (Table 4, entry 1). With benzylamine as the reactant, the yield was 46.1% (Table 4, entry 6). Cyclohexylamine exhibited similar activity as benzylamine with a yield of 47.9%. No product could be detected when aniline was used as the reactant (Table 4, entry 7). The inactivity of aniline for this reaction may result from its molecular structure. The π -bond in the aniline molecule strongly affects the electronic property of NH₂ group compared with the case of linear amines. In addition, the basicity of aromatic amines is generally much weaker than that of aliphatic amine. The pK_a value of aniline is 10⁶ times smaller than that of aliphatic amine.²⁹ Moreover, it is easy to understand the reason according to the reaction mechanism. From the proposed reaction mechanism (Scheme 5), the first step of the reaction is the formation of carbamic acid from –NH₂ and CO₂. Our experiments showed that *n*-butylamine can form a white solid upon contacting CO₂ at ambient temperature and pressure, while



Scheme 5 The possible reaction mechanism.

Table 3 Synthesis of 1,3-dibutyl urea from *n*-butylamine and CO₂ in different solvents at 5.5 MPa^a

| Entry | Solvents | Temperature/°C | Yields (%) | Selectivity (%) |
|-------|------------------------------------|----------------|------------|-----------------|
| 1 | Solvent-free | 170 | 55.1 | >99 |
| 2 | <i>N</i> -Methylpyrrolidone(NMP) | 170 | 59.1 | >99 |
| 3 | <i>N</i> -Methylpyrrole | 170 | 59.5 | >99 |
| 4 | Pyridine | 170 | 55.4 | >99 |
| 5 | Tetrahydrofuran(THF) | 170 | 39.5 | 95 |
| 6 | <i>N,N</i> -Dimethylformamide(DMF) | 170 | 30.9 | 82 |
| 7 | Acetonitrile(CH ₃ CN) | 170 | 1.2 | — |
| 8 | <i>N,N</i> -Dimethylacetamide(DMA) | 170 | 0 | — |
| 9 | Dimethylsulfoxide(DMSO) | 170 | 0 | — |
| 10 | <i>n</i> -Decane | 170 | 0 | — |

^a Conditions: 5 mmol of *n*-butylamine, 1.0 mL solvent, reaction time 19 h, 15 mol% [Bmim]OH. The yield was determined by the moles of product and *n*-butylamine.

Table 4 Synthesis of disubstituted ureas with different amines with or without solvents^a

| Entry | Amines | Products | Isolated yields (%) | |
|-------|----------------------|----------|---------------------|------------------|
| | | | Solvent-free | NMP ^b |
| 1 | <i>i</i> -Propyl | | 10.3 | — |
| 2 | <i>n</i> -Butyl | | 55.1 | 59.1 |
| 3 | <i>n</i> -Octyl | | 51.5 | 57.0 |
| 4 | Dodecyl | | 57.7 | 64.1 |
| 5 | Cyclohexyl | | 47.9 | 50.1 |
| 6 | Benzyl | | 46.1 | 66.3 |
| 7 | Aniline | | 0 | — |
| 8 | Di- <i>n</i> -butyl | — | No reaction | — |
| 9 | Tri- <i>n</i> -butyl | — | No reaction | — |

^a Conditions: 5 mmol of amine, pressure 5.5 MPa, temperature 170 °C, reaction time 19 h; 15 mol% [Bmim]OH. The yield was determined by the mol of product and amine. ^b 1.0 mL NMP was used in each reaction.

no reaction was observed with aniline. All these observations can explain the low activity of aniline. Di-*n*-butyl amine and tri-*n*-butyl amine were also tested as the reactants, but no reaction occurred in either case (Table 4, entries 8 and 9). Generally, the yields of the products in NMP were slightly higher than those in solvent-free conditions. No byproducts were detected in the reactions.

Reaction mechanism

It is known that [Bmin]OH is a basic IL and CO₂ may have strong interaction with [Bmin]OH. To explore the possible effect of CO₂ on [Bmin]OH, [Bmin]OH was heated in a stainless steel reactor for 19 h at 170 °C and 5.5 MPa CO₂. After decreasing the temperature and releasing CO₂, the treated [Bmin]OH was characterized with ¹H NMR and ¹³C NMR. The results indicated that [Bmin]OH remained its structure after being treated. Therefore, we can deduce that [Bmin]OH may complete a catalytic cycle while retaining its structure. In this work, we proposed a possible reaction mechanism as shown in Scheme 5. The mechanism of the reaction can be explained as follow. First, the amine easily forms the corresponding carbamic acid upon the introduction of CO₂. It is known that this step

occurs almost spontaneously even at room temperature and atmospheric pressure,³⁰ but its further transformation into ureas generally requires quite drastic conditions, or the presence of stoichiometric amount of base.¹² As the temperature increases, the ion exchange reaction takes place between the carbamic acid and [Bmin]OH. As a result, the carbamate anion is activated by the 1-butyl-3-methyl imidazolium ion [Bmin]⁺ and the ammonium cation is reduced to amine in the presence of hydroxyl, along with the formation of H₂O. Compared with the ammonium cation RNH₃⁺, amine RNH₂ can react more easily with carbamate ion to form **1** and transform further into urea, because the N atom in RNH₂ is at the vertex of the tetrahedral RNH₂, while in RNH₃⁺ it is located in the centre of the tetrahedral RNH₃⁺. At the same time, [Bmim]OH is regenerated to complete the catalytic reaction cycle.

Conclusion

In summary, basic IL [Bmim]OH is an efficient catalyst for the synthesis of disubstituted ureas from amines and CO₂ without any dehydrating agents. Different kinds of amines can be converted into the corresponding ureas with moderate yields and high selectivity in solvent-free conditions. The utilization of

organic solvents does not improve the yield of the carbonylation significantly. This process is advantageous because the catalyst is cheaper, the reaction can be conducted in solvent-free conditions and the separation of products is easy.

Experimental

Chemicals

CO₂ was purchased from Beijing Analytical Instrument Factory with a purity of 99.995%. *i*-Propylamine, *n*-butylamine, *n*-octylamine, benzylamine and aniline were A.R. grade and produced by Beijing Chemical Reagents Company. Other amines were purchased from Sinopharm Chemical Reagent Co., Ltd. All chemicals were used as received. IL [Bmim]OH was prepared using the procedures reported in literature.^{25,31}

Chemical reactions

All the reactions were conducted in a stainless steel reactor of 6 mL with a magnetic stirrer in batch mode. An air bath was used to heat the reactor and its temperature was controlled by a PID temperature controller (model SX/A-1, Beijing Tianchen Electronic Company). The temperature fluctuation of the constant temperature air bath was ± 0.1 °C. Typical procedures to conduct chemical reactions were as follows: 5 mmol of *n*-butylamine (374 mg), 0.75 mmol of [Bmim]OH (117 mg) and 1.0 mL of solvent (if used in the reaction) were charged in the reactor. The reactor was sealed and heated to a desired temperature. After the temperature of the reactor was steady, CO₂ was pumped into the reactor to desired pressure at the reaction temperature. After a suitable period, the reactor was cooled and carefully depressurized. 5 mL of water was mixed with the reaction mixture to precipitate the product, which was collected by filtration. The product was washed using ethyl ether, dried and identified by GC-MS (Shimadzu GCMS-QP2010). The mass of the product was determined by a balance (accurate to 0.1 mg). The yield of product was calculated using the molar ratio of product to amine. The [Bmim]OH in the filtrate was recovered by removing water under vacuum. The recovered [Bmim]OH was used directly. [Bmim]OH was characterized with a Bruker 400 MHz spectrometer.

Spectroscopic data for the synthesized urea derivatives

***N,N'*-Di(*i*-propyl) urea.** GC-MS, *m/z*: 44 (100%), 58 (25), 87 (5), 129 (10), 144 (14).

***N,N'*-Dibutyl urea.** GC-MS, *m/z*: 30 (100%), 44 (20), 57 (6), 74 (5), 87 (4), 101 (5), 129 (4), 143 (2), 157 (1), 172 (6).

***N,N'*-Dioctyl urea.** GC-MS, *m/z*: 30 (100%), 44 (30), 57 (10), 71 (5), 86 (5), 101 (6), 115 (4), 130 (10), 143 (3), 156 (10), 173 (3), 186 (7), 199 (3), 213 (12), 227 (13), 241 (8), 255 (8), 269 (2), 284 (18).

***N,N'*-Didodecyl urea.** GC-MS, *m/z*: 30 (100%), 44 (30), 57 (20), 71 (8), 86 (6), 100 (5), 115 (4), 129 (4), 143 (3), 157 (3), 171 (3), 186 (15), 199 (3), 212 (17), 229 (9), 242 (10), 255 (5), 269 (12), 283 (14), 297 (14), 311 (12), 325 (11), 339 (11), 353 (10), 367 (10), 381 (3), 396 (45).

***N,N'*-Dibenzyl urea.** GC-MS, *m/z*: 28 (10%), 51 (7), 65 (20), 79 (25), 91 (55), 106 (100), 149 (25), 164 (1), 206 (1), 240 (33).


***N,N'*-Dicyclohexyl urea.** GC-MS, *m/z*: 41 (18%), 56 (100), 70 (18), 99 (36), 143 (22), 224 (20).

Acknowledgements

The authors wish to thank the financial supports from National Natural Science Foundation of China (20773144) and National Key Basic Research Project of China (2006CB202504).

References

- 1 F. Bigi, R. Maggi and G. Sartori, *Green Chem.*, 2000, **2**, 140, and references cited therein.
- 2 F. Shi and Y. Deng, *Chem. Commun.*, 2001, 432.
- 3 G. Bartolo, G. Salerno, R. Mancuso and M. Costa, *J. Org. Chem.*, 2004, **69**, 4741.
- 4 J. E. McCusker, A. D. Main, K. S. Johnson, C. A. Grasso and L. McElwee-White, *J. Org. Chem.*, 2000, **65**, 5216.
- 5 N. Nagaraju and G. Kuriakose, *Green Chem.*, 2002, **4**, 269.
- 6 Q.-F. Li, J.-W. Wang, W.-S. Dong, M.-Q. Kang, X.-K. Wang and S.-Y. Peng, *J. Mol. Catal. A: Chem.*, 2004, **212**, 99.
- 7 J. Fournier, C. Bruneau, P. H. Dixneuf and S. Lécolier, *J. Org. Chem.*, 1991, **56**, 4456.
- 8 R. Nomura, Y. Hasegawa, M. Ishimoto, T. Toyosaki and H. Matsuda, *J. Org. Chem.*, 1992, **57**, 7339.
- 9 C. F. Cooper and S. J. Falcone, *Synth. Commun.*, 1995, **25**, 2467.
- 10 N. Yamazaki, F. Higashi and T. Iguchi, *Tetrahedron Lett.*, 1974, **13**, 1191.
- 11 H. Ogura, K. Takeda, R. Tokue and T. Kobayashi, *Synthesis*, 1978, 394.
- 12 A. Ion, V. Parvulescu, P. Jacobsa and D. De Vos, *Green Chem.*, 2007, **9**, 158.
- 13 T. Welton, *Coordin. Chem. Rev.*, 2004, **248**, 2459.
- 14 J. Dupont, R. F. de Souza and P. A. Z. Suarez, *Chem. Rev.*, 2002, **102**, 3667.
- 15 F. Shi, Y. Q. Deng, T. L. SiMa, J. J. Peng, Y. L. Gu and B. T. Qiao, *Angew. Chem., Int. Ed.*, 2003, **42**, 3257.
- 16 T. Jiang, H. Gao, B. X. Han, G. Zhao, Y. Chang, W. Wu, L. Gao and G. Yang, *Tetrahedron Lett.*, 2004, **45**, 2699.
- 17 A. L. Zhu, T. Jiang, D. Wang, B. X. Han, L. Liu, J. Huang, J. C. Zhang and D. H. Sun, *Green Chem.*, 2005, **7**, 514.
- 18 A. L. Zhu, T. Jiang, B. X. Han, J. Huang, J. C. Zhang and X. M. Ma, *New J. Chem.*, 2006, **30**, 736.
- 19 G. Y. Zhao, T. Jiang, B. X. Han, Y. H. Chang, H. X. Gao, J. Huang and D. H. Sun, *Green Chem.*, 2004, **6**, 75.
- 20 H. Xing, T. Wang, Z. Zhou and Y. Dai, *Synth. Commun.*, 2006, **36**, 2433.
- 21 H. P. Nguyen, S. Znifche and M. Baboulene, *Synth. Commun.*, 2004, **34**, 2085.
- 22 A. C. Cole, J. L. Jensen, I. Ntai, K. L. T. Tran, K. J. Weaver, D. C. Forbes and J. H. Davis, Jr., *J. Am. Chem. Soc.*, 2002, **124**, 5962.
- 23 H. Zhu, F. Yang, J. Tang and M. He, *Green Chem.*, 2003, **5**, 38.
- 24 J. Z. Gui, X. H. Cong, D. Liu, X. T. Zhang, Z. D. Hu and Z. L. Sun, *Catal. Commun.*, 2004, **5**, 473.
- 25 B. C. Ranu and S. Banerjee, *Org. Lett.*, 2005, **7**, 3049.
- 26 B. C. Ranu, S. Banerjee and R. Jana, *Tetrahedron*, 2007, **63**, 776.
- 27 J.-M. Xu, Q. Wu, Q.-Y. Zhang, F. Zhang and X.-F. Lin, *Eur. J. Org. Chem.*, 2007, 1798.
- 28 B. C. Ranu and R. Jana, *Eur. J. Org. Chem.*, 2006, 3767.
- 29 T. Baba, A. Kobayashi, T. Yamauchi, H. Tanaka, S. Aso, M. Inomata and Y. Kawanami, *Catal. Lett.*, 2002, **82**(3–4), 193, and the literatures cited therein.
- 30 E. M. Hampe and D. M. Rudkevich, *Tetrahedron*, 2003, **59**, 9619.
- 31 C. P. Mehnert, N. C. Dispenziere and R. A. Cook, *Chem. Commun.*, 2002, **15**, 1610.



2ND EUCHEMS CHEMISTRY CONGRESS

2008 SEPTEMBER 16 - 20
TORINO, ITALY

CHEMISTRY: THE GLOBAL SCIENCE

PLENARY LECTURES BY

Peter AGRE (Baltimore, USA)
Avelino CORMA (Valencia, Spain)
Jean M.J. FRÉCHET (Berkeley, USA)
Robert H. GRUBBS (Pasadena, USA)
Kyriacos C. NICOLAOU (La Jolla, USA)
Martyn POLIAKOFF (Nottingham, UK)
K. Barry SHARPLESS (La Jolla, USA)

KEYNOTE LECTURES BY

Varinder AGGARWAL (Bristol, UK)
Lucia BIANCI (Florence, IT)
Matthias BELLER (Rostock, DE)
Richard CATLOW (London, UK)
Ken CAULTON (Bloomington, USA)
Fritz FRIMMEL (Karlsruhe, DE)
Dante GATTESCHI (Florence, IT)
Jana HAJŠLOVA (Prague, CZ)
Dino MORAS (Illkirch, FR)
Ulrich STIMMING (Munich, DE)
Philip TAYLOR (Geel, BE)
Jun-ichi YOSHIDA (Kyoto, JP)

SCIENTIFIC COMMITTEE

Chair **Hartmut MICHEL** (DE)
Co-chair **Igor TKATCHENKO** (FR)

ORGANISING COMMITTEE

Chair **Giovanni NATILE** (IT)
Co-chair **Francesco DE ANGELIS** (IT)

LOCAL ORGANISING COMMITTEE

Chair **Lorenza OPERTI** (IT)
Co-chair **Salvatore COLUCCIA** (IT)

Special topic symposia:

ADVANCES IN SYNTHESIS

- Organic Catalysis
- Radical Reactivity in Transition Metal Chemistry
- Reactions under Novel Conditions

ADVANCES IN UNDERSTANDING

- Chemical Measurement Quality: Societal Impact
- Cutting Edge Chemistry with Computers
- Food Analysis: Pushing Detection Limits down to Nothing

CHEMISTRY AND LIFE SCIENCES

- Biomolecular Interactions and Mechanisms
- Drug Targeting and Delivery
- Metal Homeostasis

ENERGY AND INDUSTRY

- Biorefineries and Biotechnologies
- Energy Production & Storage
- New Trends for Agrochemicals

ENVIRONMENT

- Greening Chemistry
- Greenhouse Gases
- Water Pollutants

MATERIALS AND DEVICES

- Branched Polymers - Smart Functional Materials
- Nanomaterials
- Porous Materials

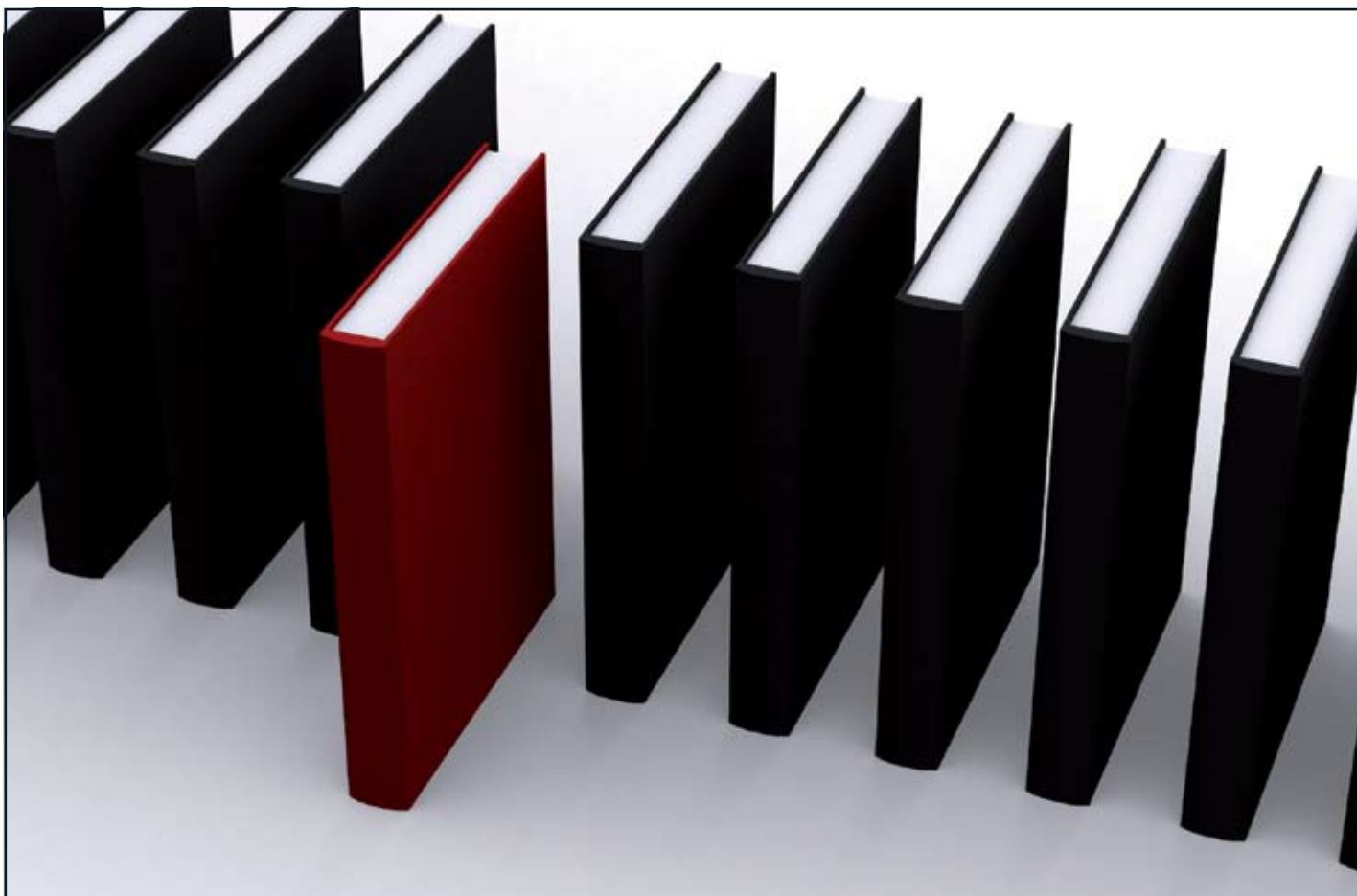
cci ORGANISING SECRETARIAT

Centro Congressi Internazionale s.r.l. - Corso Bramante 58/9 10126 Torino - I
tel +39 011.2446911 fax +39 011.2446900/44 - info@euchems-torino2008.it

www.euchems-torino2008.it

*EuCheMS, the European Association for Chemical and Molecular Sciences incorporates
50 member societies which in total represent some
150.000 individual chemists in academia, industry and government in over
35 countries across Europe.





'Green Chemistry book of choice'



Why not take advantage of free book chapters from the RSC? Through our '*Green Chemistry* book of choice' scheme *Green Chemistry* will regularly highlight a book from the RSC eBook Collection relevant to your research interests. Read the latest chapter today by visiting the *Green Chemistry* website.

The RSC eBook Collection offers:

- Over 900 new and existing books
- Fully searchable
- Unlimited access

Why not take a look today? Go online to find out more!

RSC Publishing

www.rsc.org/greenchem

Registered Charity Number 207890

GORDON RESEARCH CONFERENCES



Gordon Research Conference on Green Chemistry

August 3-8, 2008
Bates College, Lewiston, ME

Chairs:
James E. Hutchison & Janet L. Scott

<http://www.grc.org/programs.aspx?year=2008&program=green>

Green chemistry: applying innovation to the design and realisation of chemical products and processes with reduced environmental impact, maximum energy-efficiency and the least possible intrinsic hazard. This focus includes design for inherent safety for human health and the environment.



SESSION TOPICS & SPEAKERS

- **Design of Greener Chemicals and Nanoparticles**
(Paul Anastas / Robert Tanguay)
- **Bio-Based and Bio-Inspired Products**
(Richard Wool / Angela Belcher / Yonas C. Gebre)
- **Using Technology in Greener Routes to Complex Molecular Targets**
(Steven Ley)
- **Additive Processing & sc-Fluids for High Performance Materials**
(Douglas Keszler / Steven Howdle)
- **Catalysis for Activation of Small Molecules and in Organic Synthesis**
(Shu Kobayashi / Karen Goldberg / Walter Leitner)
- **Bio-Based Processing and Catalysis**
(Laura Babcock / Roger Sheldon)
- **Future Fuels - Some Possibilities**
(Jeremy Tomkinson / Arno de Klerk)
- **Green Chemistry Advances in Organic Chemistry**
(Paul Wender / Michael Krische)
- **Clean Stereoselective Chemical Transformations**
(Miguel Garcia-Garibay)

Visit the frontiers of science... attend a GRC! www.grc.org